

**West African Monsoonal Rainfall
and Intense Hurricane Associations**

by
Christopher W. Landsea

William M. Gray, P.I.

Department of Atmospheric Science
Colorado State University
Fort Collins, Colorado

NSF ATM-8814373
NOAA NA16RC116-01
NOAA NA85RAH05045 AMEND 2



**Department of
Atmospheric Science**

Paper No. 484

WEST AFRICAN MONSOONAL RAINFALL AND INTENSE HURRICANE
ASSOCIATIONS

By
Christopher W. Landsea

Department of Atmospheric Science
Colorado State University
Fort Collins, CO 80523

October 7, 1991

Atmospheric Science Paper No. 484

ABSTRACT

Atlantic basin tropical cyclone variability is examined in relation to monsoonal rainfall over West Africa. Variations in the incidence of intense hurricanes are of the most interest in that they account for over three quarters of U.S. tropical cyclone spawned destruction and their frequency has shown a large downward trend during the last few decades. It is these storms, the Saffir-Simpson Category 3, 4, and 5 hurricanes, which also have the strongest association with Western Sahel June to September rainfall.

Besides the concurrent hurricane-rainfall relationship, two strong predictive signals for seasonal hurricane activity were observed in the West African rainfall. In the first, rainfall anomalies along the Gulf of Guinea in the previous year August to November are shown to correlate with tropical cyclone activity and Sahelian rainfall in the following season. In the second, the early season Western Sahel rainfall, in the months of June and July, correlated highly with subsequent (August to October) tropical cyclone activity and with the remaining Sahel rainfall. These two predictors were optimally combined to produce the best forecast scheme for intense Atlantic hurricane activity.

The associations were tested using two sources of independent data, which verified most conclusions reached.

The fact that the Sahel periodically experiences multidecadal wet and dry regimes leads to the conclusion that the current drought is likely a temporary condition which may end in the near future. If this is correct, then the numbers of intense hurricanes that can threaten the Caribbean islands and the U.S. East Coast/Florida will almost assuredly go up by a factor of four or five.

TABLE OF CONTENTS

1 INTRODUCTION	1
1.1 Terminology and Statistical Methods	2
1.1.1 Tropical Cyclones	2
1.1.2 African Rainfall	5
1.2 Overview of Previous Research	6
2 DATA	9
2.1 Tropical Cyclone Data	9
2.1.1 Best Track Data	9
2.1.2 Landfalling Storms	11
2.1.3 Damage Information	12
2.1.4 Genesis Data	13
2.2 African Rainfall Data	13
2.3 Atlantic Basin Sea Level Pressures, 200mb Winds, and Stratospheric Winds . .	15
2.4 Equatorial East Pacific Sea Surface Temperatures	16
2.5 Analysis Starting Point	17
3 TROPICAL CYCLONE VARIABILITY	18
3.1 Intraseasonal Variability	18
3.1.1 Daily Variability	18
3.1.2 Monthly Variability	31
3.2 Interseasonal Variability	32
3.2.1 Basinwide Tropical Cyclones	33
3.2.2 U.S. Landfalling Tropical Cyclones	45
3.2.3 Tropical Cyclone Spawned U.S. Damage	55
3.2.4 Ranking of Tropical Cyclone Activity	62
3.2.5 Overestimation of Intense Hurricanes and Removal of Bias	66
3.2.6 African Easterly Wave Genesis Variability Versus Tropical Cyclone Intensity	69
4 AFRICAN RAINFALL VARIABILITY	74
4.1 Lamb Index	74
4.2 The Annual Cycle	79
4.3 Correlation with Current Year Tropical Cyclones	85
4.4 Correlation with Following Year Tropical Cyclones	90

5	“SEEDLING” RAINFALL INDEX	96
5.1	June to September African Rainfall	96
5.2	Active Versus Calm Tropical Cyclone Seasons	98
5.3	Single Station Example: Dakar, Senegal	101
5.4	Development of the June to September Seedling Index	101
5.5	Correlation with Tropical Cyclones	110
5.6	Correlation with Other Tropical Cyclone Associated Factors	113
5.7	Threshold Values of Rainfall	116
5.8	Ranking of “Seedling” Index Rainfall Values	119
5.9	Wet Versus Dry Seasons	120
5.9.1	Geographic Rainfall Variations	121
5.9.2	Tropical Cyclone Variability	123
5.9.3	Easterly Wave Genesis Variations	127
5.10	Persistence of Rainfall	130
5.11	August to September “Seedling” Index Subset	131
6	GULF OF GUINEA RAINFALL INDEX	134
6.1	August to November Gulf of Guinea Rainfall	134
6.2	Development of the Gulf of Guinea Rainfall Index	136
6.3	Correlation with Tropical Cyclones	143
6.4	Correlation with Seedling Index	147
7	JUNE TO JULY WESTERN SAHEL RAINFALL INDEX	151
7.1	June to July Western Sahel Rainfall	151
7.2	Development of the June to July Rainfall Index	156
7.3	Correlation with Tropical Cyclones	158
7.4	Correlation with Seedling Index	162
7.5	Correlation with Gulf of Guinea Index	163
8	EARLY SEASON COMBINATION RAINFALL INDEX	167
8.1	Development of the Index	167
8.2	Correlation with Tropical Cyclones	169
8.3	Correlation with Seedling Index	174
9	INDEPENDENT VERIFICATION	176
9.1	Use of 1990 Data	176
9.1.1	1989 August to November Gulf of Guinea Rainfall	177
9.1.2	1990 June to July Western Sahel Rainfall	179
9.1.3	1990 Early Season Combination Index	181
9.1.4	Verification of Forecasts	182
9.2	Use of 1920’s to 1940’s Data	190
9.2.1	U.S. Landfalling Tropical Cyclones	191
9.2.2	June to September Seedling Index	192
9.2.3	August to November Gulf of Guinea Rainfall Index	195
9.2.4	June to July Western Sahel Rainfall Index	198
10	SUMMARY AND FUTURE RESEARCH POSSIBILITIES	205

REFERENCES	219
A AFRICAN RAINFALL STATION: BACKGROUND	226
B REVISED RAINFALL INDICES	241

LIST OF SYMBOLS AND ACRONYMS

LIST OF ACRONYMS

AOC = Aircraft Operations Center

AID = Agency for International Development

AVHRR = Advanced Very High Resolution Radiometer

CAC = Climate Analysis Center

ECMWF = European Centre for Medium Range Weather Forecasts

EN = El Niño

EOF = Empirical Orthogonal Function

GTS = Global Telecommunication System

H = Hurricane

HDP = Hurricane Destruction Potential

HURDAT = Hurricane Data Tape

IH = Intense Hurricanes (Cat. 3-4-5)

ITCZ = Intertropical Convergence Zone

MCDW = Monthly Climatic Data for the World

NCAR = National Center for Atmospheric Research

NCDC = National Climate Diagnostics Center

NHC = National Hurricane Center

NHOP = National Hurricane Operations Plan

NMC = National Meteorological Center

NOAA = National Oceanic and Atmospheric Administration

NS = Named Storms (e.g. tropical storms and hurricanes)

NWS = National Weather Service

QBO = Quasi Biennial Oscillation of Stratospheric Wind

SLPA = Sea Level Pressure Anomalies

SST = Sea Surface Temperature

TS = Tropical Storm

US = United States of America

USWB = United States Weather Bureau (now is National Weather Service)

WH = Weak Hurricanes (Cat. 1-2)

WMO = World Meteorological Organization

WMSSC = World Monthly Surface Station Climatology

ZWA = Zonal Wind Anomalies

Chapter 1

INTRODUCTION

“Squalls out on the Gulf Stream,

Big storm is coming soon...”

Jimmy Buffett, 1974

Trying to Reason with Hurricane Season

The anticipation of hurricanes apparent in Mr. Buffett’s songwriting mirrors the dire warnings broadcasted from the National Hurricane Center during the 1970’s. The rapid increase in US coastal development and populations gave great concern to Dr. Neil Frank, the NHC director at the time, that the U.S. might be headed for a hurricane disaster, especially in Florida. Instead, what happened was that no intense hurricanes made landfall along the eastern seaboard, from the Florida peninsula to Maine, during the late 1960’s through the early 1980’s. Was the National Hurricane Center crying wolf to increase public awareness unduly?

One would not think so in view of the frequency with which major hurricanes hit the U.S. East Coast in earlier years. From the late 1940’s through the mid-1960’s, the East Coast received an intense hurricane strike more than once every two years. What then was the cause of these large multidecadal swings of hurricane activity?

What occurred simultaneously with the decrease of intense hurricane activity in the Atlantic basin was a severe drought in Africa’s Sahel region. Not realized at the time was how strongly year to year fluctuations in intense hurricane activity relate to concurrent seasonal amounts of rainfall in the Sahel. Although this association does not explain why large decadal variations in intense hurricane activity have occurred, it may bring us closer to an understanding of the seasonal controls on hurricane formation and intensification.

That a West African rainfall-hurricane relationship exists should not be so surprising since tropical easterly waves, the same disturbances that bring much of the rain to the Sahel, are often the genesis points for Atlantic tropical cyclones. What is surprising is the strength of the concurrent correlations and the possibility of having useful predictive signals for both the hurricane activity and the Sahel rainfall. Two predictors are available: one by December 1 of the prior year—near the end of the previous year’s rainy season, and the other by August 1 of the current year—before the main part of the rainy season and before intense Atlantic basin hurricanes begin to form.

The remainder of this chapter attempts to define terminology, describe the statistical methods employed, and give a brief overview of research previously accomplished in this area. Chapter 2 describes the various data sets acquired for this research and credits the data sources. Chapters 3 and 4 document the tropical cyclone and African rainfall variability, respectively. Chapter 5, 6, 7, and 8 look at four indices created to focus on certain aspects of variability seen in the African rainfall data. Chapter 9 employs two statistical methods for testing the earlier conclusions using independent data sets. Finally, Chapter 10 highlights the main points of the research and suggests where future studies may lead.

1.1 Terminology and Statistical Methods

1.1.1 Tropical Cyclones

Confusion can arise when discussing various characteristics of tropical cyclones. The United States (U.S.) Department of Commerce’s National Oceanic and Atmospheric Administration (NOAA) (1977) technically defines **tropical cyclones** as nonfrontal low pressure synoptic-scale systems that develop over tropical or subtropical waters and have a definite organized circulation. There are two additional requirements which should be added: these cyclones must have a tropospheric inner core structure which is warmer than the environment (i.e. a “warm-core”) and the maximum intensity of tangential winds should be located in the lower troposphere.

The tropical cyclone designation is a broad term under which various strength systems are divided into:

Tropical Depression...Maximum sustained surface wind speed (1 min mean) $< 18ms^{-1}$.

Tropical Storm...Wind speed 18 to $< 33ms^{-1}$.

Hurricane...Wind speed at least $33ms^{-1}$.

Often the term “tropical storm” is used to refer to **any** cyclone of tropical storm or hurricane strength. This type of imprecise reference will be avoided. Tropical storms and hurricanes will be collectively referred to as **named storms** [in deference to the fact that since 1950, all tropical cyclones that were of at least tropical storm force were given a name for identification (Neumann *et al.*, 1987), though, some cyclones were determined to be of tropical storm strength after the fact and thus lack a formal name].

Hurricane status can be further stratified by the severity of the cyclone. The Saffir/Simpson (Simpson, 1974) Hurricane Scale provides a measure of intensity ranging from a Category 1 (Minimal) to Category 5 (Catastrophic). Table 1.1 summarizes the delineation of strength and effect. For purposes of this study, it became instructive to consider the Saffir/Simpson Category 3, 4, and 5 cyclones collectively as **intense or major hurricanes**.

Table 1.1: Maximum sustained wind speed, minimum surface pressure, storm surge, and general damaging effects for the various Saffir/Simpson Hurricane Scale values.

Saffir/ Simpson Category	Maximum Sustained Wind Speed (ms^{-1})	Minimum Surface Pressure (mb)	Storm Surge (m)	Potential Damaging Effects
1	33 to 42	≥ 980	1.0 to 1.7	Minimal
2	43 to 49	979 to 965	1.8 to 2.6	Moderate
3	50 to 58	964 to 945	2.7 to 3.8	Extensive
4	59 to 69	944 to 920	3.9 to 5.6	Extreme
5	> 69	< 920	> 5.6	Catastrophic

Occasionally, cyclones which develop over subtropical water contain characteristics of both tropical and extratropical nature. Although their existence was suspected for many years, these hybrid cyclones were only confirmed with the advent of continuous daytime satellite coverage (Simpson and Pelissier, 1971; Spiegler, 1971). The formal definition (U.S. Department of Commerce, 1977) of the **subtropical cyclone** is a nonfrontal low pressure system composed of a baroclinic (cold-core) circulation that develops over subtropical water. Note that these systems can often evolve into purely tropical (warm core) systems.

One method of objectively delineating the amount of seasonal tropical cyclone activity is through the duration of each storm. Dunn and Staff (1965) first used the concept of number of **hurricane days**. The seasonal total of hurricane days is the number of days in which hurricanes existed (two simultaneous hurricanes count as two days). However, their calculations and similar ones made by Gray (1984a) count a full hurricane day even if the cyclone was of hurricane strength for just six hours of that 24 hour period. The computations for this present report count days in one quarter increments (six hour periods). This refinement will reduce somewhat the numbers obtained by earlier studies. Similar calculations have been performed for **intense hurricane days** and **named storm days**.

Another way to consider tropical cyclone variability on a seasonal basis is through Gray's (1987) **Hurricane Destruction Potential** or **HDP** which gives a combined measure of both the intensity and duration of hurricanes. *HDP* is defined as the sum of the sustained wind speed (in knots) squared for every six hours that the cyclone is of at least hurricane strength (65 kt or 33 ms^{-1}). *HDP* reflects the fact that hurricane damage is more related to the square of their wind speed (i.e. a proxy of the summed kinetic energy of the cyclone's winds) than to direct measure of the wind. Both intense hurricane days and *HDP* are used extensively as measures of seasonal activity in this report.

The **tropical disturbance** is defined in the National Hurricane Operations Plan (U.S. Department of Commerce, 1990a) as:

A discrete tropical weather system of apparently organized convection - generally 100 to 300 mi in diameter—originating in the tropics or subtropics,

having a nonfrontal migratory character, and maintaining its identity for 24 hr or more. It may or may not be associated with a detectable perturbation of the wind field.

Tropical disturbances are the predecessors of tropical cyclones, though not all tropical disturbances develop into tropical cyclones. Indeed, it is still deemed fairly accurate today that as Simpson *et al.* (1968) said, “perhaps nine out of 10 (tropical disturbances)...remain benign rain-producing systems.”

1.1.2 African Rainfall

The Sahel lies approximately between 11 and 20°N in Africa. This area separates the hyperarid Sahara desert to the north from the tropical rainforests along the Gulf of Guinea to the south. Only during a few months in the summer and early fall does the Sahel receive substantial precipitation accompanying the annual migration of the Intertropical Convergence Zone (ITCZ) as it reaches its northernmost position at that time. Over Africa, the ITCZ takes the form of low level southwesterlies (monsoonal flow) to the south which converge with low level northeasterlies to the north. An excellent qualitative overview of West African meteorology is given by Hayward and Oguntoyinbo (1987). For this study, African rainfall refers to any form of precipitation. However, since temperatures in the Sahel range from 15 to 45°C the only non-rain precipitation possible is hail, that occurring only infrequently.

The primary statistical method used for analyzing rainfall variations is the area-average normalization procedure developed by Kraus (1977). To examine regional aspects of rainfall variation, Kraus hoped to combine multiple stations together without inducing a bias toward any station or subgroup of stations. The use of simple percentages from the long term mean precipitation for a group of stations will tend to favor the drier stations that will typically experience huge percentage variations of rainfall. Conversely, using mean absolute deviations would bias the values toward stations with higher average rainfall. To avoid either of these problems, Kraus used a normalization of rainfall based upon the mean and standard deviation at each station. This method is currently the standard used by several researchers studying Sahel rainfall variability (Hastenrath, 1990;

Lamb *et al.*, 1990; Nicholson, 1986; and Shinoda, 1989) as well as by the U.S. Climate Analysis Center (CAC) (U.S. Department of Commerce, 1990c) in their real-time analysis of U.S. and worldwide precipitation patterns.

Using the following definition of mean, \bar{r}_i , and variance, σ_i^2 at station i ,

$$\bar{r}_i = \frac{1}{J_i} \sum_j r_{ij}$$

$$\sigma_i^2 = \frac{1}{J_i - 1} \sum_j (r_{ij}^2 - \bar{r}_i^2)$$

where

r_{ij} is the period rainfall at station i during year j and

J_i is the number of years of data station i contains,

The normalization for station i in year j is

$$x_{ij} = (r_{ij} - \bar{r}_i) / \sigma_i$$

which indicates the number of standard deviations (ie., a normalized Z-score) the rainfall departure is for a particular year.

The resulting regionally averaged Index value of x_{ij} for the year j is defined as

$$a_j = \frac{1}{I_j} \sum_i x_{ij}$$

where I_j is the number of stations in the region available in year j .

The formulation of this Index value is very useful in marginally available data areas because one is not dependent on having every station with every data point.

1.2 Overview of Previous Research

Mechanisms of rainfall variability in the African Sahel received little attention until the severe drought of 1972 and 1973, the magnitude of which caused widespread crop failure and the deaths of thousands of people. Since that time, a variety of studies, both

in observational and numerical modeling methods [see excellent review by Hastenrath (1988)], have been employed for the analysis and prediction of Sahelian rainfall.

In contrast, seasonal Atlantic basin tropical cyclone variability has intrigued researchers for almost a century. Garriott (1906) attempted to relate the exceptional high hurricane activity of September 1906 to the Atlantic basin surface pressure fluctuations. Since then many researchers have also attempted to correlate the tropical cyclone frequencies and intensities to sea surface temperature anomalies (Ray, 1935), general circulation patterns (Namias, 1955; Ballenzweig, 1958), as well as surface pressure variations (Shapiro, 1982).

In the early 1980's, Gray (1984c, 1984d) identified strong seasonal relationships between tropical cyclone activity and El Niño (EN), the phase and time change of the stratospheric Quasi-Biennial Oscillation (QBO), and sea level pressure anomalies of the Caribbean basin (SLPA). Gray has since modified the forecast scheme (Gray, 1989b, 1989c) to include 200 mb Caribbean zonal wind anomalies (ZWA) while discounting the use of the time change of the QBO phase. Yearly forecasts and verifications have been issued since 1984. Some skill in the seasonal predictions has been shown (Gray, 1990d).

A strong interrelationship between seasonal tropical cyclone activity in the Atlantic basin and rainfall amounts in the Sahel had not been realized or even speculated on in the literature until very recently. This is somewhat surprising in that the same systems which contribute to Sahel rainfall often serve as the genesis points for tropical cyclones (Riehl, 1945). These, of course, are the easterly waves.

The first suggestion of a possible connection between Sahel rainfall and tropical cyclones variability appears in class notes from Carlson and Lee (1978). They speculated that "the severe drought conditions" over the African Sahel could be associated with "the diminution of hurricane activity" in the Atlantic basin. Apparently though, they did not pursue this further.

Gray (1987) revived the hypothesis when he noted similarities between his seasonal measure of hurricane intensity and duration, HDP, and the strong downward trend of Sahel

rainfall, which continued into the 1980's. However, it took a failed seasonal forecast in 1989 (where Gray then attributed his underestimation of hurricane activity to conditions associated with increased rainfall in the Sahel) to stress the importance of the tropical cyclone–Sahel rainfall relationship (Gray, 1989d). Thus, a significant forecasting failure led to this investigation of the Atlantic tropical cyclone–West African rainfall association.

Chapter 2

DATA

2.1 Tropical Cyclone Data

2.1.1 Best Track Data

The accepted positions and intensities (sustained wind speed and minimum surface pressure) of all Atlantic basin tropical cyclones of at least tropical storm strength have been archived and are continually being updated by the National Hurricane Center (NHC) in Miami, Florida. The “Atlantic basin” is defined as the tropical and subtropical regions north of the equator in the Atlantic Ocean, the Caribbean Sea, and the Gulf of Mexico. This data set extends from 1886 to 1990 and is described in detail by Jarvinen *et al.* (1984). This “Best Track” data set is composed of the “best” estimate of positions and intensities in a post-analysis of all available data. Also termed “HURDAT” (for HURricane DATA), these data have been used extensively by Prof. W. M. Gray’s Tropical Meteorology Project at Colorado State University in the rawinsonde compositing studies (Gray, 1981), and more recently, in seasonal forecasting research (Gray, 1984a, 1984b, 1990c).

There are, of course, many caveats to be considered when using this data set; the main one being reliability of the data, especially in the late 1800’s and early 1900’s. The observational platforms used to monitor tropical cyclones have, for the most part, improved immensely during the last 100 years. During the nineteenth century and earlier, observations of cyclones were limited to reports of landfalling storms and to the occasional ship that survived an encounter with a cyclone. In 1905, shipboard weather reports became available in real-time with the advent of the wireless telegraph (Neumann, *et al.* 1987). Aircraft reconnaissance flights provided the next major improvement in tropical cyclone detection. The U.S. Air Force and Navy began the practice of routine flights into

tropical storms and hurricanes in 1944. Currently, the Air Force fleet of WC-130 aircraft is supplemented by the two Orion P3's, operated by NOAA's Aircraft Operations Center (AOC) (US Department of Commerce, 1990a). However, the most relied upon tools for tropical cyclone detection and monitoring are the meteorological satellites, both geostationary (GOES-7 and METEOSAT) and polar orbiters (NOAA-10, NOAA-11, DMSP F-8, and DMSP F-9). These satellites and their predecessors have been monitoring the Atlantic basin continuously since 1966. Thus, the question arises: What year should one begin with for reliable statistics on Atlantic basin tropical cyclones - especially the intense hurricanes?

Neumann *et al.* (1987) suggest that without the relatively recent additions of aircraft reconnaissance and weather satellites "there is a chance...that weaker, short duration storms could have gone completely undetected." Forecaster Grady Norton (1953a) went even further in his summary of the 1952 hurricane season: "Two of (the tropical cyclones) would probably not have been discovered had it not been for the long arm of aircraft reconnaissance because they remained over the Atlantic far to the east of the Lesser Antilles during their short life spans." Note that both of these storms (Dog and Easy) are described as reaching hurricane strength, albeit briefly.

In general, the present report follows Neumann's recommendation to use statistics based on data since the mid-1940's, when organized aircraft reconnaissance began, since this "probably best represents Atlantic tropical cyclone frequencies". The same logic follows for the day-to-day assessment of the intensity of individual storms because, in the earlier period, "storms that were detected could have been misclassified as to intensity."

Another consideration in using tropical cyclone frequency and intensity data is the subjectivity inherent in the categorization. Cyclones do not hang a sign on themselves saying that they are a 50 ms^{-1} storm. Satellite observations used in tropical cyclone intensity estimations are pattern recognition and other empirical methods that do not directly measure storm winds (Dvorak, 1977, 1984). Aircraft reconnaissance can typically obtain maximum wind speeds at flight level (usually 850 or 700mb), but these are instantaneous

values and do not necessarily represent what is occurring at the surface. In section 3.2.5, corrections are needed for a small bias in the Best Track data which seemed to stem from overestimating the surface winds in relation to observed minimum surface pressure in the earlier reconnaissance years. This error possibly arose due to the use of flight level winds as the surface winds without any alteration. The lack of absolute data allows for interpretations that may or may not truly reflect what occurred. Thus, some storms that were classified as minimum hurricanes (35 to 40 ms^{-1}) may have actually been only of strong tropical storm strength (30 ms^{-1}) or vice versa. This also applies to all Saffir/Simpson hurricane categories (Simpson, 1974).

Also, as mentioned in Chapter 1, the subtropical cyclone category has been created recently to accommodate storms that appear to contain both tropical cyclone and mid-latitude storm characteristics. This procedural detail creates some problems in studying frequency variation in tropical cyclones. Obviously, these storms were present before they were formally identified as such beginning in 1968 (Hebert and Poteat, 1975). As Neumann *et al.* (1987) states,

In earlier years, subtropical systems were not formally recognized and, in most cases, they were designated as tropical systems. Consequently, failure to include these systems could alter the tropical cyclone climatology for the years following the introduction of the subtropical concept.

Thus, in much of this report, we include those systems that were subtropical storms throughout their lifetime when drawing conclusions about named storm frequency.

2.1.2 Landfalling Storms

Tropical cyclones that have affected the United States mainland have a longer period of reliable concerning their frequency and intensity because of the large coastal populations along the Gulf of Mexico and Atlantic Ocean. It is unlikely that any tropical storms or hurricanes crossed the coastline unnoticed since the turn of the century. Hebert and Taylor (1975) performed a Saffir/Simpson categorization of all U.S. landfalling hurricanes from 1900 to 1974. They based this categorization primarily on minimum central pressures of the storm at time of landfall. Neumann *et al.* (1987) also analyzed 1899 and 1975 through

1986. This paper further extends the analysis to 1990 using NHC's end of the season write-ups (Case and Gerrish, 1988; Lawrence and Gross, 1989; and Case and Mayfield, 1990) and the preliminary summary for 1990 (H.P. Gerrish, 1990, personal communication).

Besides the various categories of landfalling hurricanes, this report also makes use of tropical storms that affected the US. Information on the latter was gleaned from Neumann *et al.*'s (1987) reference book. Again, since only cyclones that caused tropical storm conditions over the US are considered, it is unlikely that many were missed since 1899, the furthest back period being considered.

One final note regarding landfalling storms is the fact that, since 1968, some cyclones that may previously have been considered tropical cyclones have been designated the name "subtropical storm". Occasionally, these storms do make landfall and cause some appreciable damage as, for example, the 18-20 June 1982 subtropical storm that struck the southeast U.S. and caused ten million dollars damage (Clark, 1983). Inclusion of these storms when analyzing landfalling tropical storms has been attempted.

2.1.3 Damage Information

The main forecasting concern regarding tropical cyclones is for the destructive forces that these storms can unleash. Jarrell (1987) reported on a survey of the International Workshop on Tropical Cyclones participants in 1985. He found that the "most critical factors for tropical cyclone warnings" were hurricane-force winds, storm surge, flood rains, and rough seas and that "the associated storm surge and flooding from heavy rain...cause the greatest loss of lives and destruction to property." In the belief that some of this research may be applicable in understanding variability in tropical cyclone spawned damage in the Gulf of Mexico and Atlantic Ocean coastal regions of the US, statistics on damage were obtained from the yearly summaries in the Monthly Weather Review.

The following papers, listed chronologically, were referenced for the damage statistics: Zoch, 1949; Norton, 1951, 1952, 1953a, 1953b; Davis, 1954; Dunn *et al.*, 1955, 1956; Moore and USWB Staff, 1957; USWB Staff, 1958; Dunn and USWB Staff, 1959, 1962, 1963, 1964, 1965; Dunn, 1961; Sugg, 1966, 1967; Sugg and Pelissier, 1968; Sugg and Hebert, 1969;

Simpson *et al.*, 1970; Simpson and Pelissier, 1971; Simpson and Hope, 1972; Simpson and Hebert, 1973; Hebert and Frank, 1974; Hope, 1975; Hebert, 1976; Lawrence, 1977, 1978, 1979, 1987; Hebert, 1980; Lawrence and Pelissier, 1981, 1982; Clark, 1983; Case and Gerrish, 1984, 1988; Lawrence and Clark, 1985; Case, 1986; Lawrence and Gross, 1989; and Case and Mayfield, 1990.

2.1.4 Genesis Data

Recently, Avila and Clark (1989) revived an annual summary series in the Monthly Weather Review: Atlantic basin tropical disturbances. The article is a companion paper to the annual summary of Atlantic Basin tropical cyclones (see original paper by Simpson *et al.* (1968)). Since 1967, when satellite analysis made it possible, these papers have attempted to report on the origins of tropical cyclogenesis and the numbers and varieties of tropical disturbances. L.A. Avila of NHC provided a detailed list of the origins of all Atlantic basin tropical cyclones of at least tropical storms strength from 1967 to 1990.

2.2 African Rainfall Data

Our current analysis of rainfall has emphasized monthly and multi-month data combinations. We are fortunate in being able to locate several data sets which were painstakingly merged together. The main data base for African rainfall is the “World Monthly Surface Station Climatology” (WMSSC) managed by W.M.L. Spangler and R.L. Jenne at the National Center for Atmospheric Research (NCAR). Though WMSSC provides global surface data (precipitation, temperatures, surface pressures, sea level pressures, and others), we focused primarily on precipitation data over Africa. The data collection which extends from the mid-1800’s to 1988, is due largely to the efforts of Prof. S.E. Nicholson of Florida State University who provided additional historical data. Including stations located on nearby islands (Azores, Canary, Madeira, Seychelles, and Madagascar), the WMSSC data set has 584 African stations with rainfall information. The Monthly Climatic Data for the World (MCDW) by the National Climatic Data Center (NCDC, 1989, 1990) has provided an offi-

cial monthly updating for the same stations through December 1990. The data presented in MCDW is essentially what will be used in the next updating of WMSSC.

A second data set which is complimentary to the WMSSC information was supplied to us by G. Farmer of the World Meteorological Organization's (WMO) Agency for International Development (AID)/Fews Project in Washington, D.C. This data provided us with additional information on 36 WMSSC stations and data on 75 agricultural raingages that have been available since 1951. These stations are all in the Sahel region, from Senegal in the west to Chad in the east. In general, the quality of the 36 stations that overlapped with the WMSSC stations was higher for the AID stations (e.g. less rounding to the nearest 10 mm, less missing data, fewer unreasonable outliers). Therefore, in combining the data sets together, we chose the AID data as more reliable in cases where there was a 3 mm or greater difference between WMSSC and AID for monthly rainfall amounts.

P.J. Lamb also provided us with data for the 20 stations used in his index of Sahel rainfall (herein referred to as the "Lamb Index"). Lamb has used this data in connection with his research into the underlying physical mechanisms for Sahel drought (Lamb, 1982) as well as in a real-time monitoring of the Sahel in conjunction with CAC (Lamb *et al.*, 1990). The Lamb data were very similar in quality to WMSSC yet provided information for several stations which had missing data. Accordingly, we used Lamb's data to fill in gaps but assigned it lower priority than WMSSC and AID data where duplications occurred.

The final data addition that was used for this study included more recent data provided us by D. Miskus and R.J. Tinker of CAC. CAC provided us with their best estimates of monthly rainfall as inferred from daily reports on the Global Telecommunications System (GTS). This information provided us excellent preliminary data that temporarily filled gaps until updated reports were received from NCDC. Miskus and Tinker have also been very generous in providing data in real-time which enabled us to monitor the Sahel as it now relates to Prof. W.M. Gray's (1990a, 1990b, 1990d) seasonal hurricane forecasts. Since these are estimates (and can be somewhat erroneous due to missing and mistaken

reports), these data are only used in absence of any other information (i.e. WMSSC, AID, and Lamb).

In summary, the data sets used in this report in relative order of priority are as follows:

Highest Priority	AID Data
	WMSSC and MCDW Data
	Lamb Data
Lowest Priority	CAC Estimated Data

Information is currently being incorporated into the monthly rainfall data base from two different sources. First, with assistance from Y.R. Adebayo at Kenyatta University, Nairobi, Kenya, we received Nigerian monthly rainfall data from E.O. Oladipo of Ahmadu Bello University in Zaria, Nigeria. In recent years Nigeria has been a difficult country to receive data from. Prof. Oladipo has graciously provided us with rainfall information for 13 stations from 1970 to 1988. Secondly, we are adding historical CAC estimated data (extending back to 1960) where gaps exist in the official record. Again this estimate based data will only be used where no other data are available. Appendix 2 provides a reanalysis of data presented in the following chapters, including this newly available Nigeria and historical CAC data.

2.3 Atlantic Basin Sea Level Pressures, 200mb Winds, and Stratospheric Winds

Gray (1984a, 1984b) has previously shown strong predictive and concurrent associations for seasonal tropical cyclone activity. These predictors include Caribbean Basin sea level pressures, 200 mb zonal winds, and the stratospheric QBO phase. Data collected for prior tropical cyclone studies have also been studied for relationships with West Sahel rainfall.

Data going back to 1949 (due to limitations in stratospheric observations) were collected from a variety of sources. The primary sources for historical data were the World Weather Records and Monthly Climatic Data for the World (US Department of Commerce, 1959, 1966, 1982, 1971-1983).

Data for 1949 to 1989 were obtained for the following stations:

San Juan, Puerto Rico, U.S.	18.29N	66.08W	1
Kingston, Jamaica	17.58N	76.48W	2
Bridgetown, Barbados	13.06N	59.37W	123
Willemstad, Curacao	12.12N	68.56W	123
Port of Spain, Trinidad and Tobago	10.38N	61.31W	123
Balboa, Panama	8.57N	79.33W	23
Cayenne, French Guiana	4.55N	52.18W	1

where the numbers on the far right denote data for:

1. Sea level pressures (April to October)
2. 200mb zonal winds (April to October)
3. Stratospheric zonal winds (April to October)

Data since 1983 was supplemented by analysis made at the Colorado State University Weather Laboratory and by reports from C. McAdie and the late A. Pike of NHC. J. Angell of NOAA also provided a portion of our stratospheric wind information.

2.4 Equatorial East Pacific Sea Surface Temperatures

Another factor which Gray (1984a) showed to be related to the incidence of Atlantic Basin tropical cyclones was the presence or absence of El Niño conditions. To further explore relationships among tropical cyclones, West Sahel rainfall and the El Niño phenomena, we used an extended rendering of Wright's (1984) Sea Surface Temperature (SST) Index. Wright's index of sea surface temperature anomalies in the equatorial east and central Pacific Ocean extends from 1950 to 1983. We have taken a three month August to October average of the anomalies corresponding to the most active months of the Atlantic basin hurricane season. To extend Wright's index backwards to 1949, we did an empirical fit with Weare's (1986) El Niño Index. Weare, who used empirical orthogonal functions (EOF) of the Pacific Ocean SSTs to define his index, showed that his index had a correlation of 0.92 with Wright's index. To extend the index forward, up to 1989, we did a similar empirical fit using SST anomalies reported in the Climate Diagnostics Bulletin (US Department of Commerce, 1990b) for their Nino-3 region as this area best corresponds to the area and time series appearing in Wright's index.

2.5 Analysis Starting Point

The original motivation for this study arose from the failure of W.M. Gray's seasonal tropical cyclone forecast for 1989 (Gray, 1989a, 1989b, 1989c). Gray attributed his underestimation of seasonal tropical cyclone activity to the above average rainfall amounts which occurred in the Western Sahel that year. The author undertook this study with the purpose of identifying, documenting, and better understanding the concurrent and predictive relationships so as to improve Gray's forecast system.

Naturally, the beginning point in the analysis of rainfall was chosen to correspond to the first year used in Gray's studies, 1949. Gray's analysis has been limited to that date because of the lack of prior equatorial stratospheric data; stratospheric data being essential due to the strong relationship between the QBO and Atlantic basin tropical cyclones (Gray, 1984a; Shapiro, 1989). This starting point also agrees well with Neumann *et al.*'s (1987) assessment (mentioned earlier) that accurate quantitative climatological studies on Atlantic basin tropical cyclones are possible utilizing data since the mid 1940's.

Though the earlier tropical cyclone data are suspect, an independent verification of the relationships found for the time period 1949 to 1989 is attempted (in Chapter 9) using data from 1922 to 1948. Less degradation is seen in the rainfall data

Chapter 3

TROPICAL CYCLONE VARIABILITY

Neumann *et al.* (1987) present an extensive climatology of Atlantic basin tropical cyclones. This is the most complete and up-to-date reference for the basin. However, what is stressed in this research but not explicitly treated by Neumann *et al.* (1987) is the variability of intense hurricanes; those with a maximum sustained wind speed of at least 50 ms^{-1} . These storms account for the majority of tropical cyclone spawned destruction even though they are much less numerous than the weaker storms. In addition, intense hurricanes also have the largest variability in the intraseasonal, interannual and multidecadal time scales.

3.1 Intraseasonal Variability

3.1.1 Daily Variability

Atlantic basin tropical cyclones show a very pronounced annual cycle of frequency and intensity. These intraseasonal variations are accompanied by systematic changes in the locations where tropical cyclones are likely to form. To observe frequency differences on an intraseasonal basis, we must use the longest available record because of the relative sparse occurrence in contrast to, say, the northwest Pacific basin. The entire best track data set extending from 1886 to 1989 has been utilized. The data from the late 1800's to the mid 1900's will, as noted in Chapter 2, be incomplete in that a few storms have been inadvertently left out simply because they were not observed (i.e. short lifetimes over the open ocean). However, it is likely that there is no systematic intraseasonal bias in the missed storms.

Neumann *et al.* (1987) provided an analysis of intraseasonal variation of named storms and hurricanes (Fig. 3.1). Events prior to May 1 are negligible and are not shown. Note also the use of a nine day running mean to smooth the data. The same averaging procedure has been used in analysis presented here. Neumann, *et al.*'s analyses recorded a full named storm or hurricane day, even when only a single entry was observed (equivalent to six hours in the Best Track file). Keeping track of quarter day or six hour increments will tend to reduce the overrepresentation of storms that had short lifetimes.

As our analysis also extends the data out to 1989, Figs. 3.2 and 3.3 are the expanded equivalent of Neumann's analysis (i.e., Fig. 3.1). Qualitatively, it appears that this analysis shows sharper frequency peaks than Neumann's figures. Comparing (as ratios) the nine day running mean for the named storms on September 11 (Julian day 254) to June 16 (Julian day 167) for Neumann's figure gives a ratio of 7.5 to 1 while the one presented in Fig. 3.2 has a ratio of 8.5 to 1. Again this is due to differences in counting procedure that is accentuated by early season storms having, in general, shorter lifetimes.

Regardless, all these figures show a primary maximum of occurrence around mid September (Julian days 250-260), a secondary maximum in mid October (Julian days 285-295), and minor maximum in mid to late June (Julian days 165-180). The mid September maximum corresponds to the annual maximum area of warm SSTs and of low vertical shear (Gray, 1975) where easterly waves generally provide most of the genesis points for tropical cyclones in the Atlantic, Caribbean, and Gulf of Mexico. The mid October maximum in Figs. 3.1-3.3 is due to a combination of easterly wave spawned storms plus storms which form in the western Caribbean from stationary cold fronts, from upper tropospheric cutoff lows, and from an extension of the eastern Pacific monsoon. The June storms are primarily Gulf of Mexico and northwestern Caribbean spawned systems (stationary cold fronts and upper tropospheric cutoff lows).

The annual cycle of intense hurricanes is shown in Fig. 3.4. The unsmoothed data in the top panel show more noise than do the corresponding data in Figs. 3.2 and 3.3. This difference occurs because intense hurricanes are comparatively infrequent events, averaging

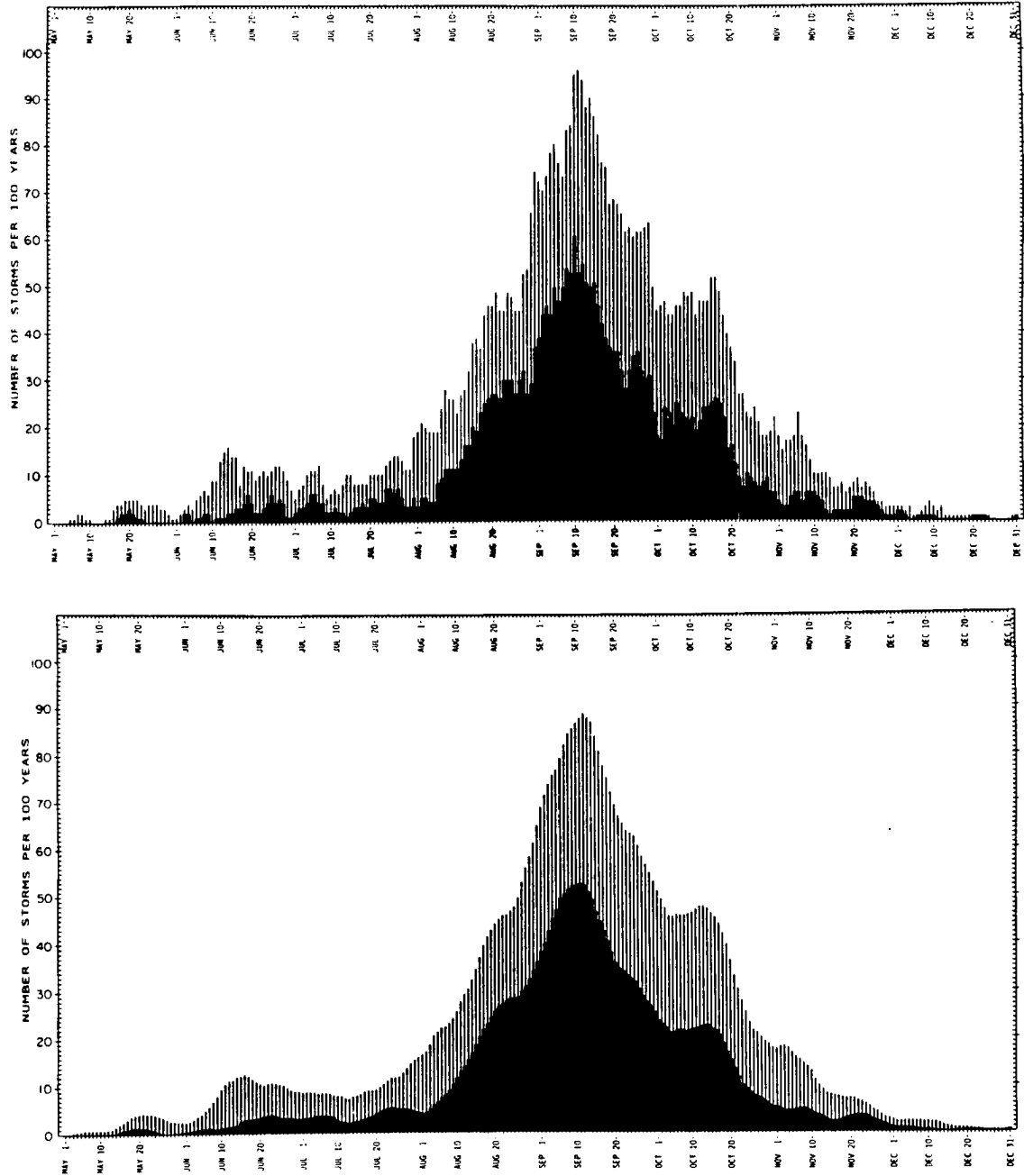


Figure 3.1: Intraseasonal variation in frequency of named storms (vertical lines) and hurricanes (solid area). Bottom panel is the same data with a nine day running average applied. Based on data from 1886-1986 (from Neumann *et al.*, 1987).

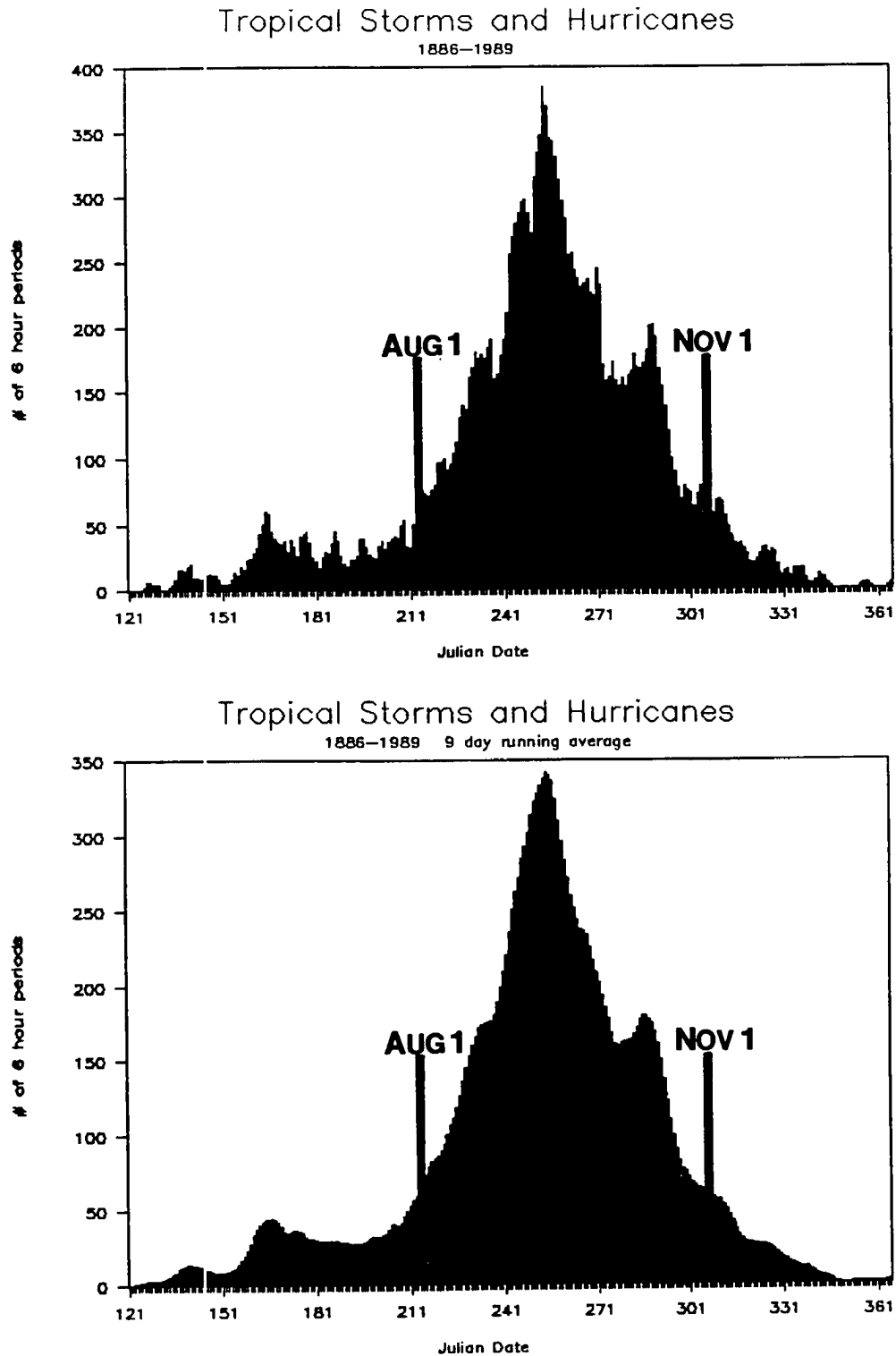


Figure 3.2: Intraseasonal variation of named storms (tropical storms and hurricanes). Bottom panel uses a nine day running average. Julian day 121 is May 1.

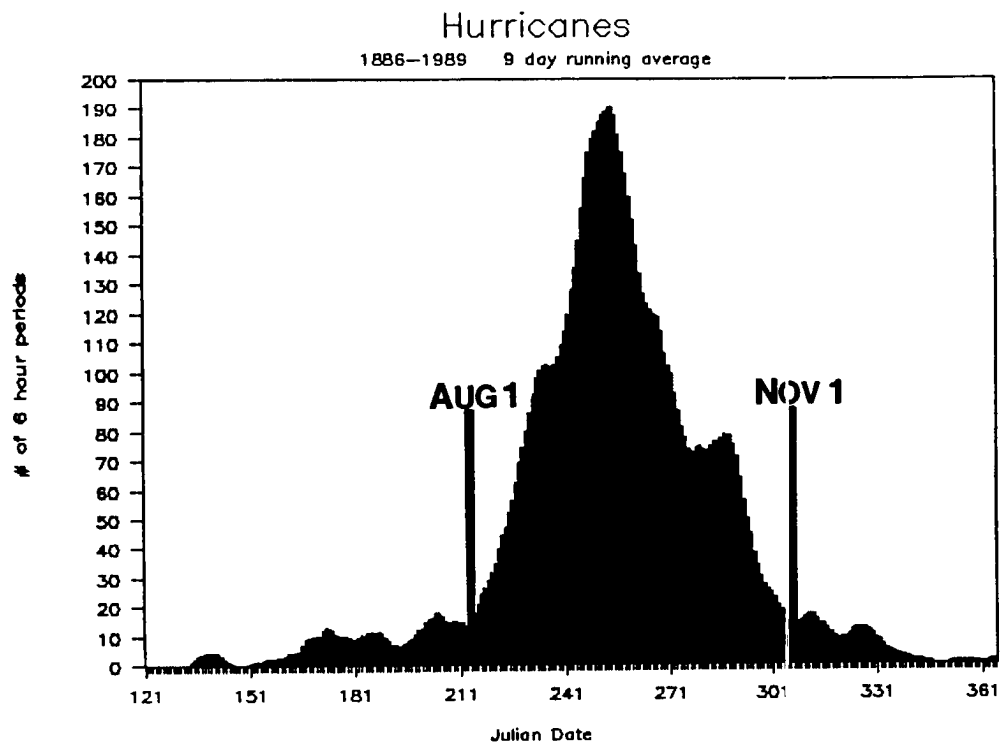
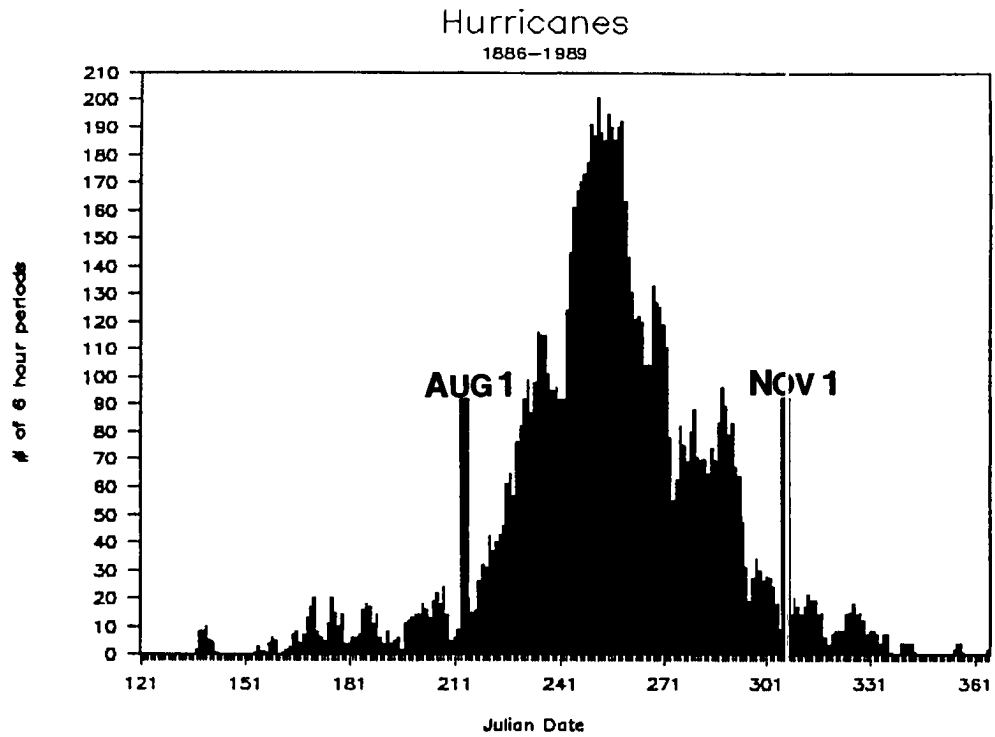


Figure 3.3: Intraseasonal variation of hurricanes only. Bottom panel uses nine day running average.

2 to 3 per year, that 104 years is not a long enough time series to give a detailed day-to-day interpretation of intraseasonal variability. Thus the secondary maxima apparent in the smoothed data near day 230 (August 18) in Fig. 3.4 may or may not be real. We can be confident that the earliest intense hurricanes can normally be expected is August 1 (Julian day 213). Late October (Julian day 300) marks the normal end of the intense hurricane season. This three-month period is considerably shorter than the “official” six-month hurricane season of June to November (six months).

Figure 3.5 combines the data of the three previous figures. The top panel shows qualitatively that the annual cycles of the three categories peak at about the same time. After normalization for the total number of occurrences of each, these three curves in the bottom panel show that the stronger tropical cyclones have a somewhat sharper peak of occurrence. In mid September intense hurricanes are recording about 2.5% of their total annual activity per day; this is in contrast to the incidence all tropical storms and hurricanes which peak at about 1.7% of their total annual activity per day.

The method of this comparison conceals some differences between the various intensities of tropical cyclones in that the categories presented tend to overlap. To do a proper comparison, we need to obtain the annual cycle for weak hurricanes (Category 1 and 2) as well as for tropical storms only. Again, the term ‘tropical storm’ refers only to named storms which are not of hurricane strength. Likewise, a ‘Category 1 and 2’ hurricane is a tropical cyclone that is of hurricane strength, but which is not a major storm having sustained winds at least 50 ms^{-1} . Fig. 3.6 and 3.7 show the annual cycle for tropical storms and weaker hurricanes, respectively.

With this information, we can properly compare the differences in intraseasonal peaks. Figure 3.8 is the same as Fig. 3.5 except that the comparison is for intense hurricanes, weaker hurricanes, and tropical storms. Note in the top panel that the occurrence of weaker hurricanes is very similar to that of the tropical storms, especially near the time of peak frequency. The major feature of the bottom panel is the strong gradation of peak sharpness in mid September going from tropical storms (1.4% per day), to weaker hurricanes (1.9%

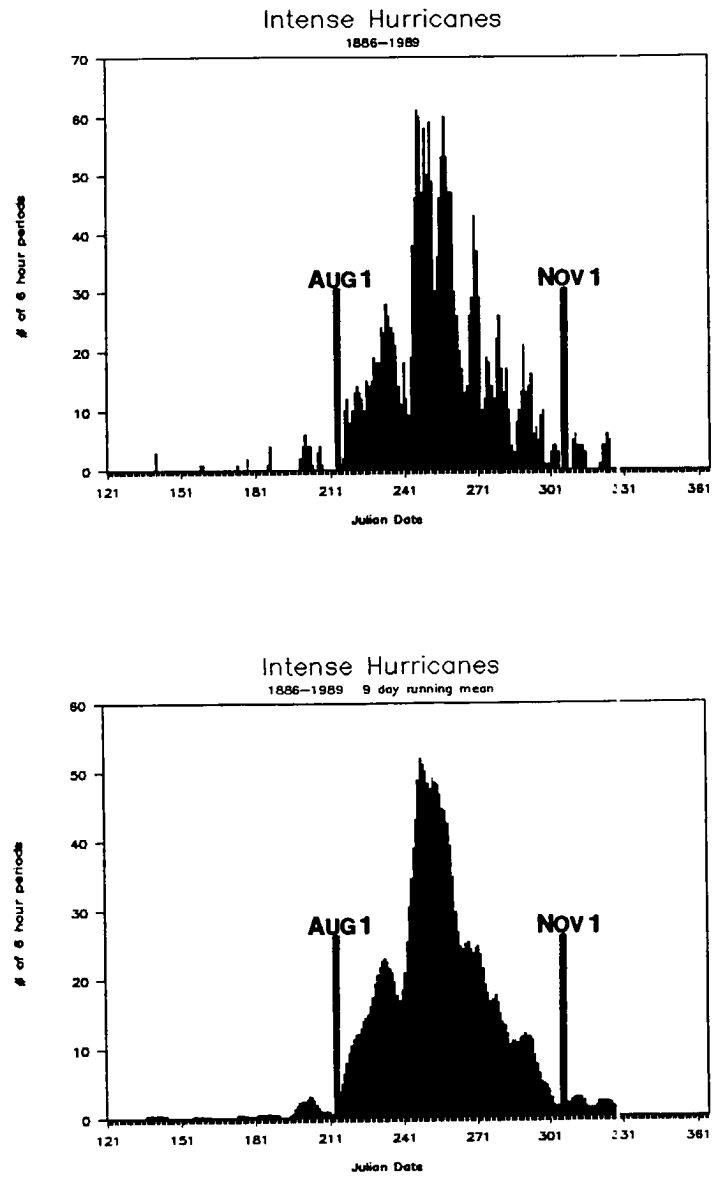


Figure 3.4: Intraseasonal variation of intense hurricanes. Bottom panel uses a nine day running average.

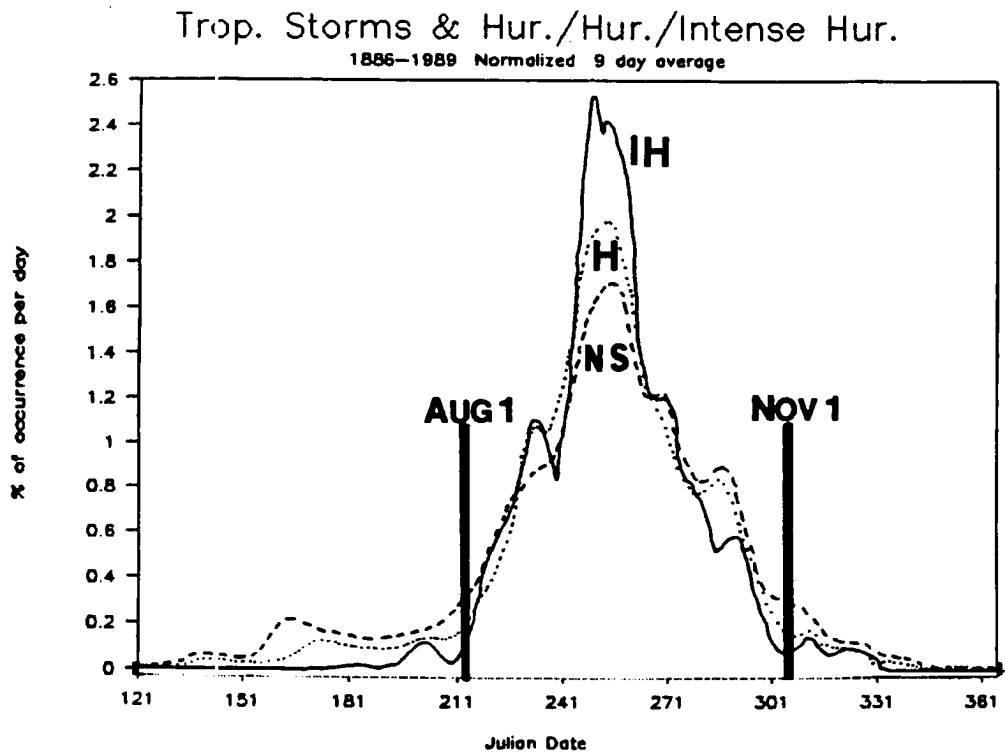
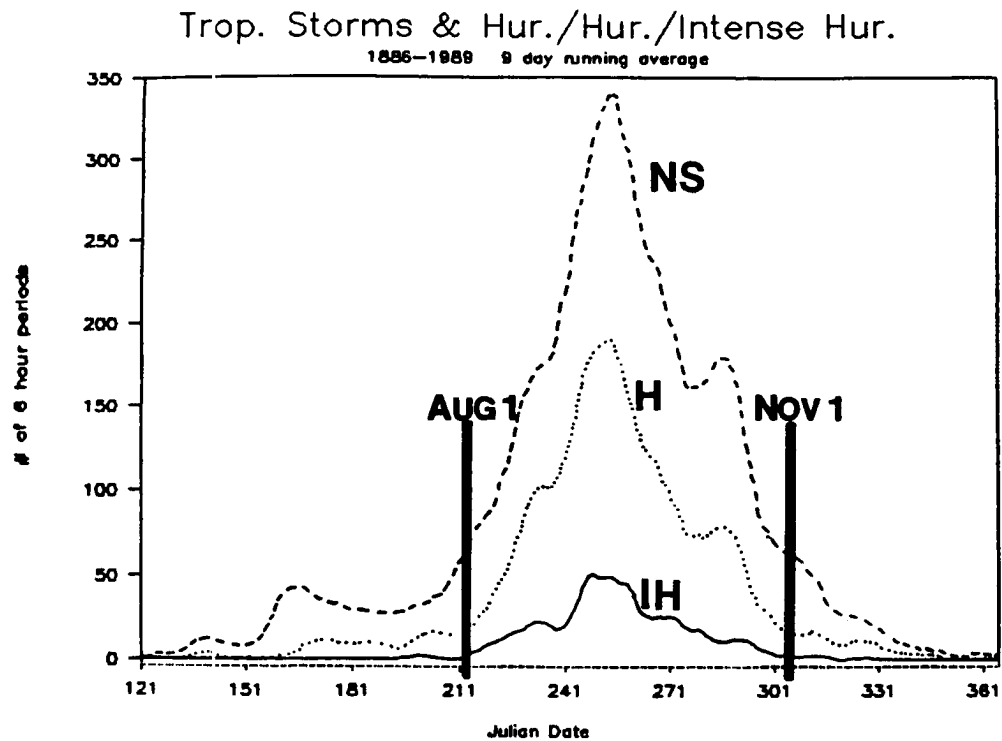


Figure 3.5: Intraseasonal variability (with a nine day running average) of intense hurricanes (IH, solid line), all hurricanes (H, dotted line), and all tropical storms and hurricanes (NS, dashed line). Top panel presents data in absolute number of occurrences. Bottom panel normalizes data by showing percent of activity per day.

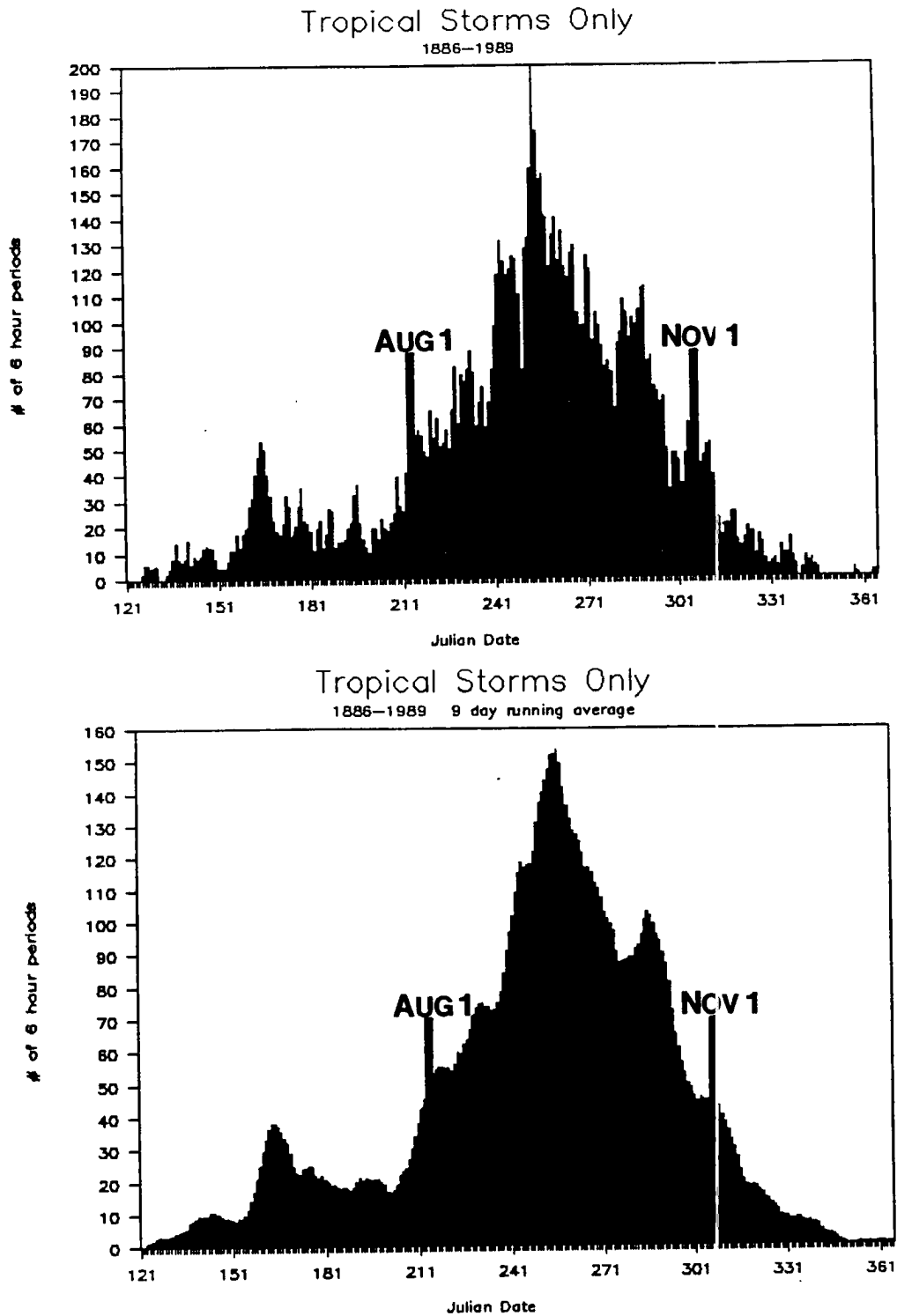


Figure 3.6: Intraseasonal variation of tropical storms. Bottom panel uses a nine day running average.

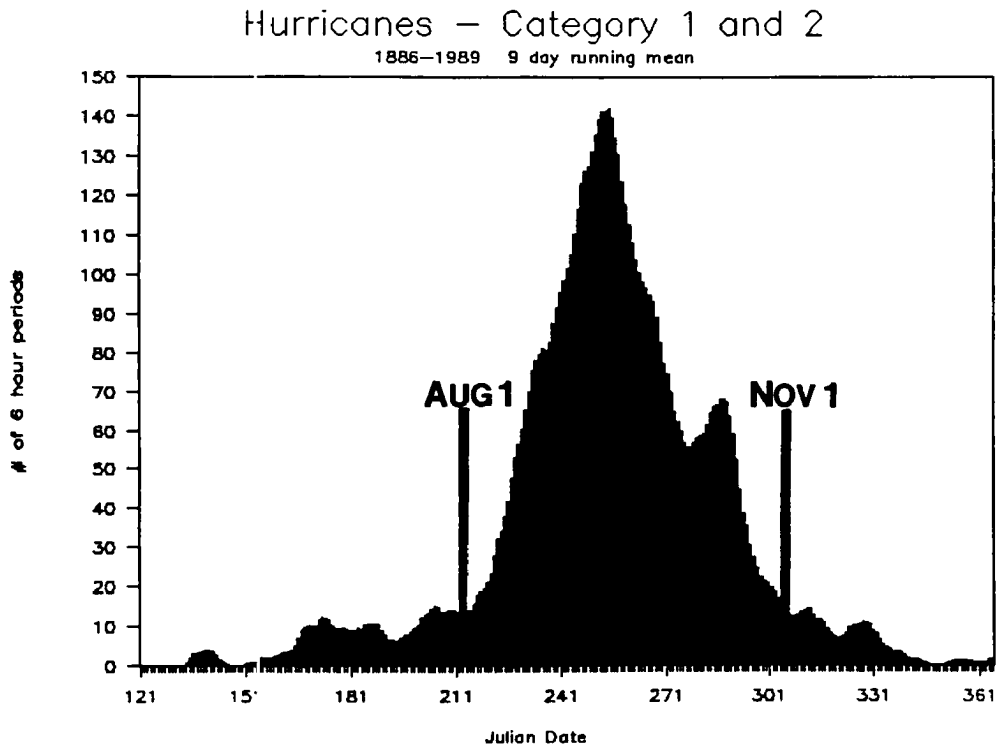
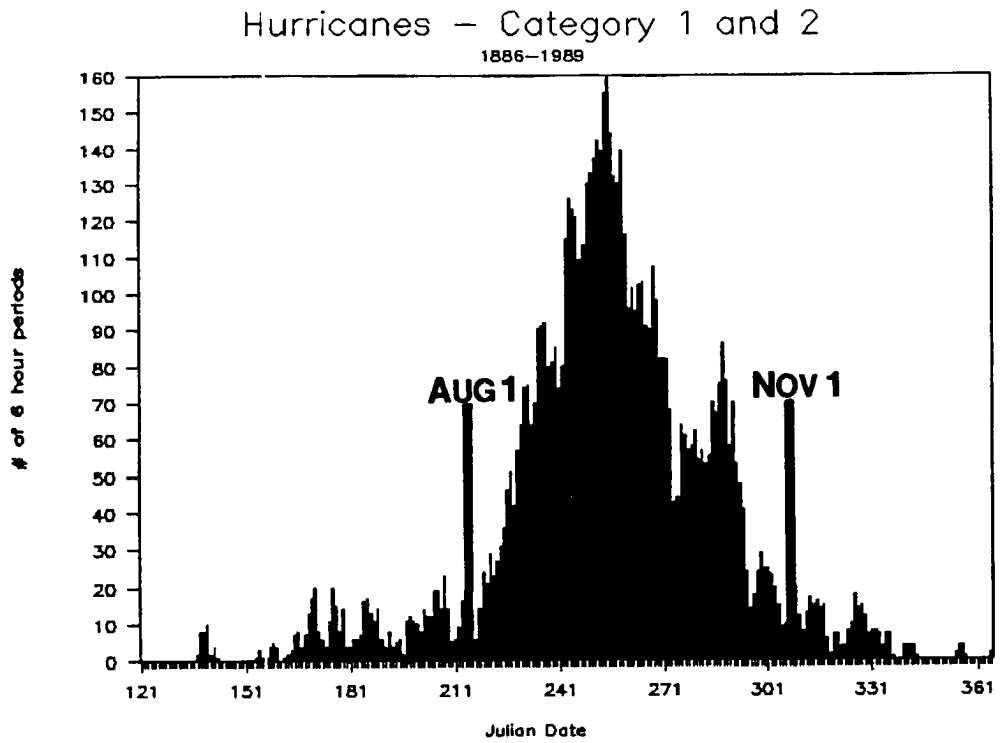


Figure 3.7: Intraseasonal variation of weaker hurricanes (Category 1 and 2). Bottom panel uses nine day running average.

per day), to intense hurricanes (2.5% per day). The period from September 1 to 20 (Julian days 244 to 263) comprises 43% of the total annual intense hurricane activity, 34% of the weaker hurricanes, but only 25% of the tropical storms. During the early season this activity relationship is reversed: by July 31, typically 13% of the tropical storm activity has occurred, as has 7% of the weaker hurricane activity, but only 2% of the intense hurricane activity.

The sharp intraseasonal peakedness of the intense hurricane activity is also mirrored in Fig. 3.9 for strong hurricanes which hit the U.S coast. Though the data presented show a noisy signal due to the infrequent occurrence (only 65 U.S. land-falling Category 3,4, and 5 hurricanes between 1899 and 1989), a strong peak in activity is centered near September 18. Very few intense hurricane strikes occur before August 1 and none after October 25. Figure 3.9 also stratifies the landfallings into Gulf Coast and East Coast/Florida categories (see section 3.2.2). Each of these geographic areas show distinct annual cycle differences, as summarized in Table 3.1.

Table 3.1: Variations of intense hurricane landfall by date for portions of the U.S. coast.

Region	Median Date of Occurrence	First Date of Occurrence	Last Date of Occurrence
Gulf Coast	Sep. 5	Jun. 16	Oct. 4
East Coast/Florida	Sep. 24	Aug. 12	Oct. 25
Differences (days)	19	57	21

These regional differences are related to the transience of seasonal favorable areas for tropical cyclone genesis as well as the general circulation variations. Before mid June, major hurricanes typically do not strike the U.S. From mid June to July, the very infrequent intense hurricanes that occur tend to form in the Gulf of Mexico or in the northwest Caribbean Sea and are typically steered toward the west or north, precluding any East Coast/Florida strikes. From August to early October, easterly waves are responsible for generating nearly all intense hurricanes and which can now occur nearly anywhere in the Atlantic basin. But by mid October, intense hurricanes form almost exclusively in

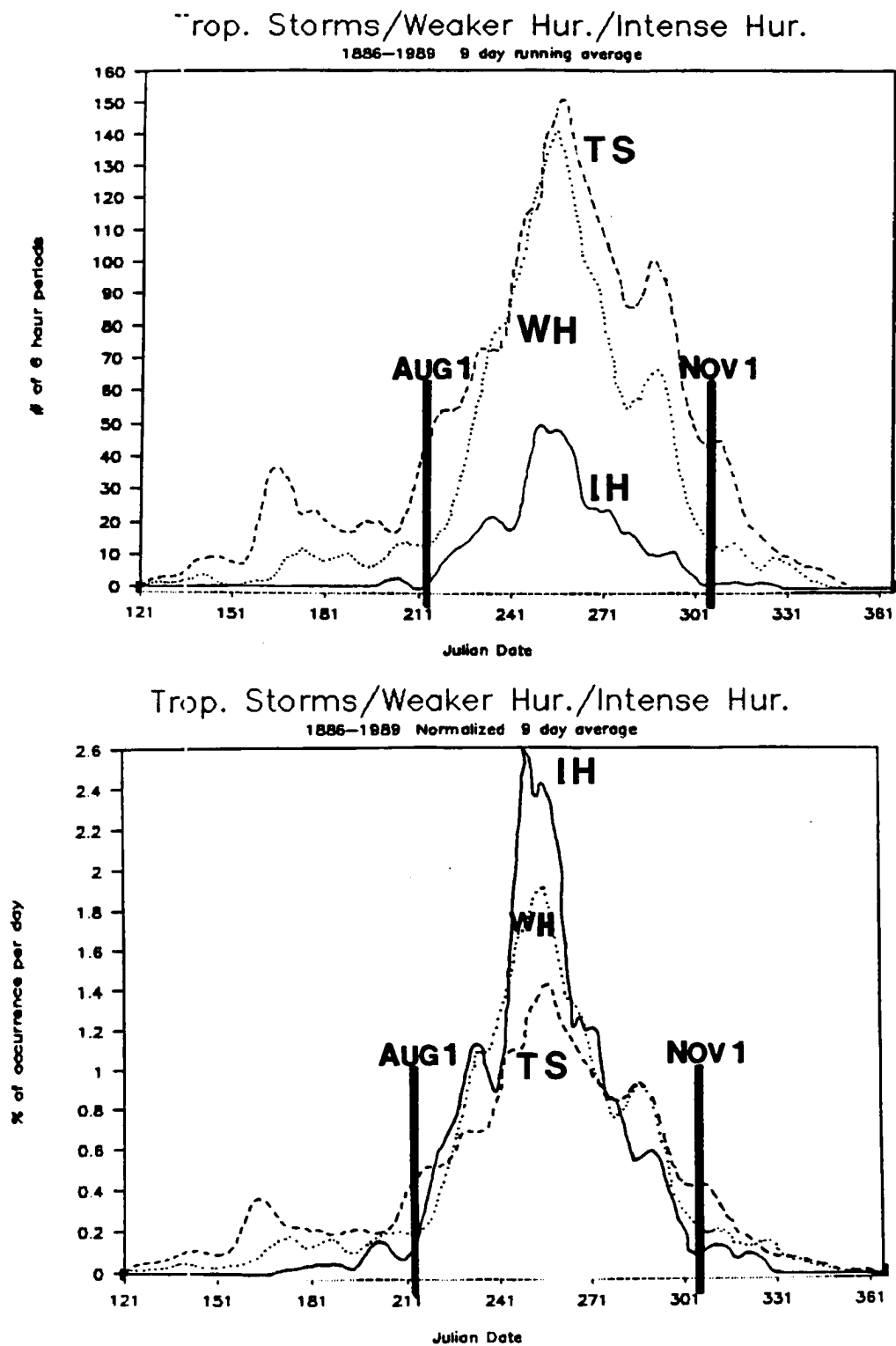


Figure 3.8: Intraseasonal variation (with a nine day running average) of intense hurricanes (IH, solid line), weaker hurricanes (WH, dotted line), and tropical storms (TS, dashed line). Top panel presents data in absolute number of occurrences. Bottom panel normalizes data by showing percent of activity per day.

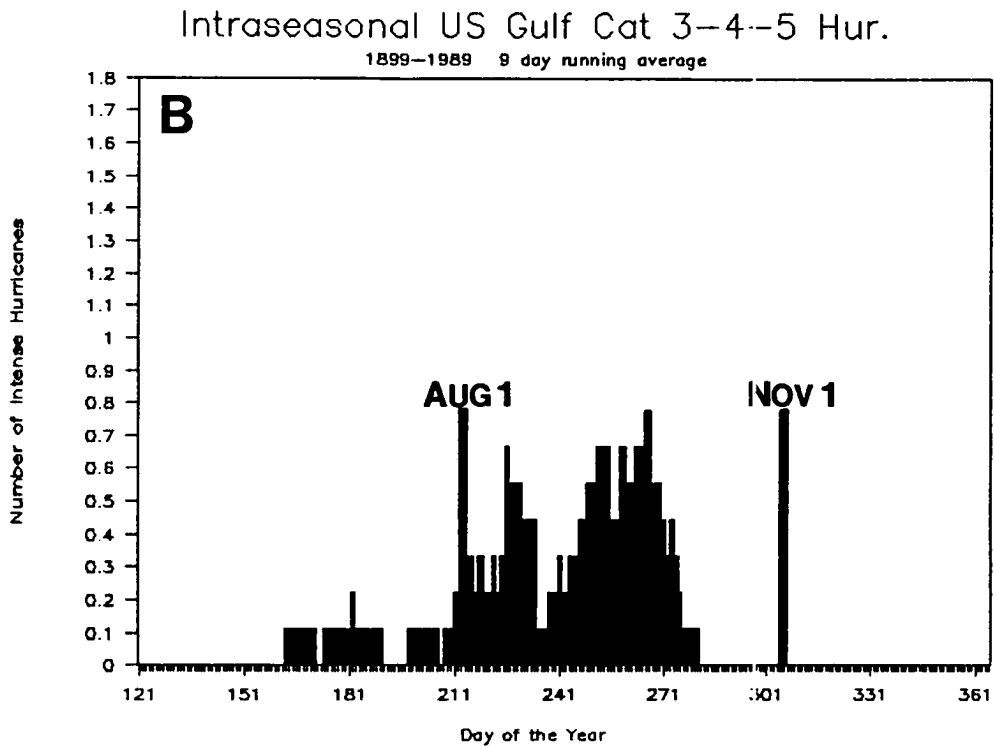
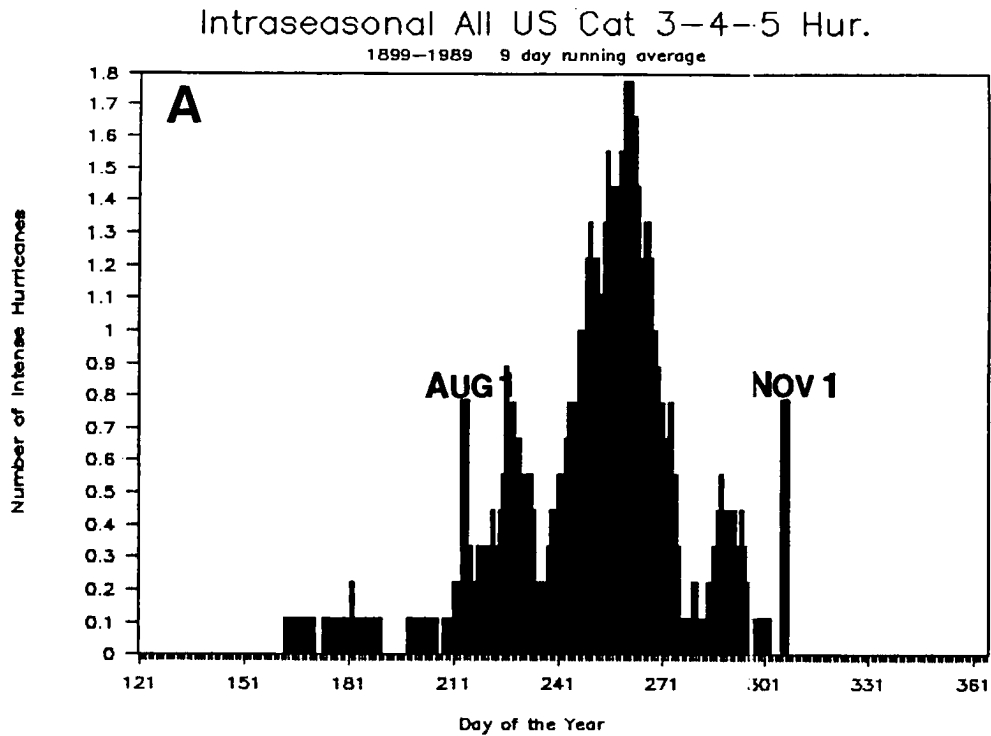


Figure 3.9: a-c: Intraseasonal variation with a nine day running mean of landfalling intense hurricanes for a) the entire U.S. coastline, b) the U.S. Gulf Coast, and c) the U.S. East Coast/Florida.

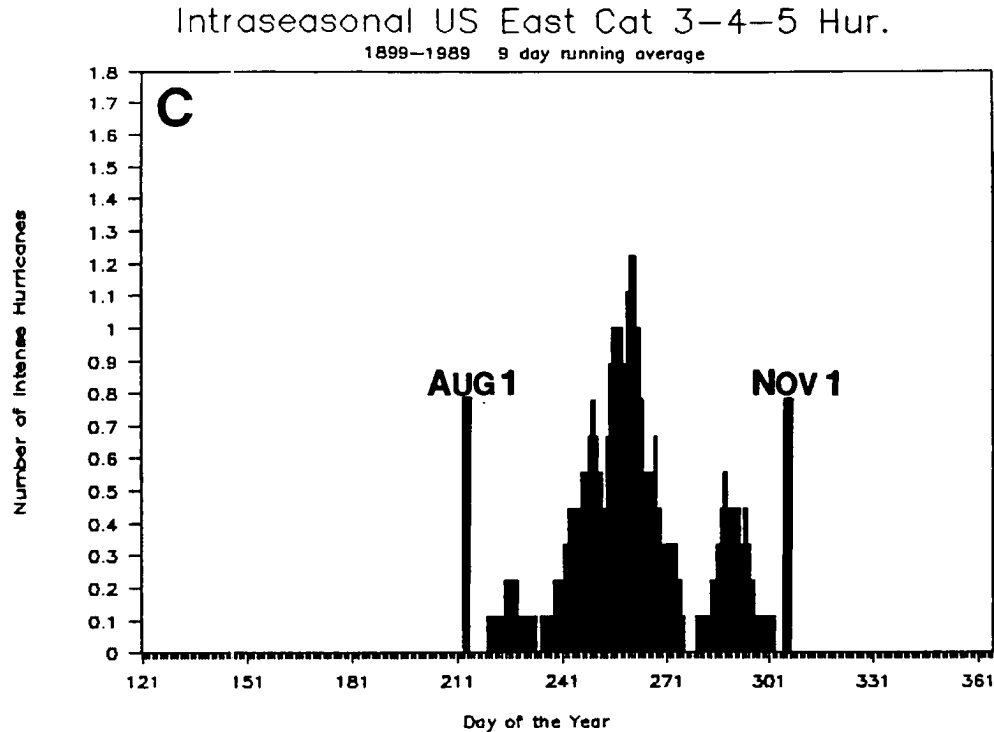


Figure 3.9: c: Continued.

the western Caribbean and typically take a north or northeasterly course, occasionally onto the Florida or the U.S. East Coast. The U.S. does not normally experience intense hurricanes after late October.

In summary, this information shows that besides being much less frequent, intense Atlantic basin hurricanes have a much narrower season of occurrence. Within the space of three weeks in September, we observe nearly half of all activity. In addition, major differences are seen in the regional annual cycle of U.S. landfalling intense hurricanes.

3.1.2 Monthly Variability

Table 3.2 summarizes the monthly frequency variation of Atlantic basin tropical cyclones. As was seen also in Figs. 3.1-3.9, the largest monthly differences between categories of storms are apparent in the early portion of the annual cycle (May to July), in the peak month (September), and in the late portion of the season (November and December). Note that, percentagewise, intense hurricane activity is equivalent to weaker

cyclones during August and October. Thus the sharp peak in September frequency corresponds to a reduction in the incidence of early and late season intense hurricanes relative to the incidence of tropical storms and weaker hurricanes.

Table 3.2: Monthly occurrence (in percent of total) of tropical cyclone days by various intensities and U.S. intense hurricane strikes.

Intensity	Ja-Apr	May	Jun	Jul	Aug	Sep	Oct	Nov	Dec
Trop. Storm & Hur.	0.2%	0.8	3.7	4.7	15.5	40.6	26.2	7.1	1.2
Hurricanes	0.2	0.4	1.3	3.6	15.1	47.7	25.5	5.2	1.1
Tropical Storms	0.1	1.1	5.9	5.7	15.8	34.4	26.9	8.9	1.2
Hur. - Cat 1,2	0.3	0.5	1.6	4.2	14.6	46.1	25.7	5.6	1.4
Hur. - Cat 3,4,5	0	0.1	0.1	1.4	16.8	53.3	24.7	3.6	0
U.S. landfall Cat 3/4/5	0	0	3.1	4.6	21.5	60.0	10.8	0	0
U.S. Gulf Cat 3/4/5	0	0	5.9	8.8	29.4	52.9	2.9	0	0
U.S. East/Florida Cat 3/4/5	0	0	0	0	12.9	67.7	19.4	0	0

3.2 Interseasonal Variability

In studies of the interannual variability of tropical cyclones, it is common practice to simply examine the yearly totals of named storms and/or hurricanes. This practice tends to oversimplify matters ignoring important features such as the duration and intensities of the individual storms. For example, the 1977 and 1988 Atlantic basin hurricane seasons had identical numbers of hurricanes (5—slightly below the long term mean). However, a visual inspection of the tracks in Fig. 3.10 suggests that 1988 was a much more ‘active’ season. This is also confirmed by noting other seasonal tropical cyclone statistics which better reflect cyclone duration and intensity:

Year	Hurricanes	Hurricane Days	Hurricanes Cat.3,4,5	Hurricanes Cat.3,4,5 Days	HDP
1977	5	7	1	1	18
1988	5	24	3	8	81
Ratio	1:1	1:3.4	1:3	1:8	1:4.5

As we will see in section 3.2.5, it is the intense hurricane activity that accounts for most U.S. hurricane linked damage. Since these intense cyclones have shown the largest yearly

and multidecadal variations of frequency (section 3.2.3), it is these cyclones that will be given special analysis.

3.2.1 Basinwide Tropical Cyclones

This section provides a summary of various tropical cyclone parameters of interest from 1886 to 1989 (the entire best track data set) and also for 1949 to 1989. The latter time period was chosen because of the greater reliability and data restrictions for extensive analysis.

Named Storms: The interseasonal variations of named storms (tropical storms and hurricanes) are presented in Fig. 3.11. The record shows a very large numerical range with only 1 event in 1890 and 1914 in contrast to 21 in 1933. However, only 4 seasons (9.8%) from 1949 to 1989 had 5 or fewer named storms compared to 20 (31.7%) from 1886 to 1948. Most of this recent decrease in relatively calm seasons is likely due to increased surveillance (section 2.1.1) rather than an actual physical difference affecting the incidence of tropical cyclones. The seasonal range in the modern era (1949 to 1989) is somewhat reduced: 4 in 1972 and 1983 versus 17 in 1969.

Hurricanes: Figure 3.12 shows the seasonal incidence of Atlantic basin hurricanes since 1886. Similar to the variation of named storms, hurricane frequency shows a large variation, from none recorded in 1907 and 1914 to 12 in 1969. The least number recorded in the last 41 years has been 2 in 1982.

Intense/Major Hurricanes: It is the intense hurricanes which show the largest variability with 8 recorded in 1950 and none recorded several times, most recently in 1968, 1972, and 1986. These are hurricanes reaching at least a Category 3 on the Saffir-Simpson Scale (Simpson, 1974). These intense or major hurricanes are portrayed in Fig. 3.13. It is apparent in this figure that large numbers of intense hurricanes occurred from the late 1940's to the 1960's. Again it is argued that data before the 1940's are deficient because of the lack of observational platforms. A small inconsistency in the wind-pressure relationship between the periods 1949-1969 versus 1970-1989 appears to have caused an

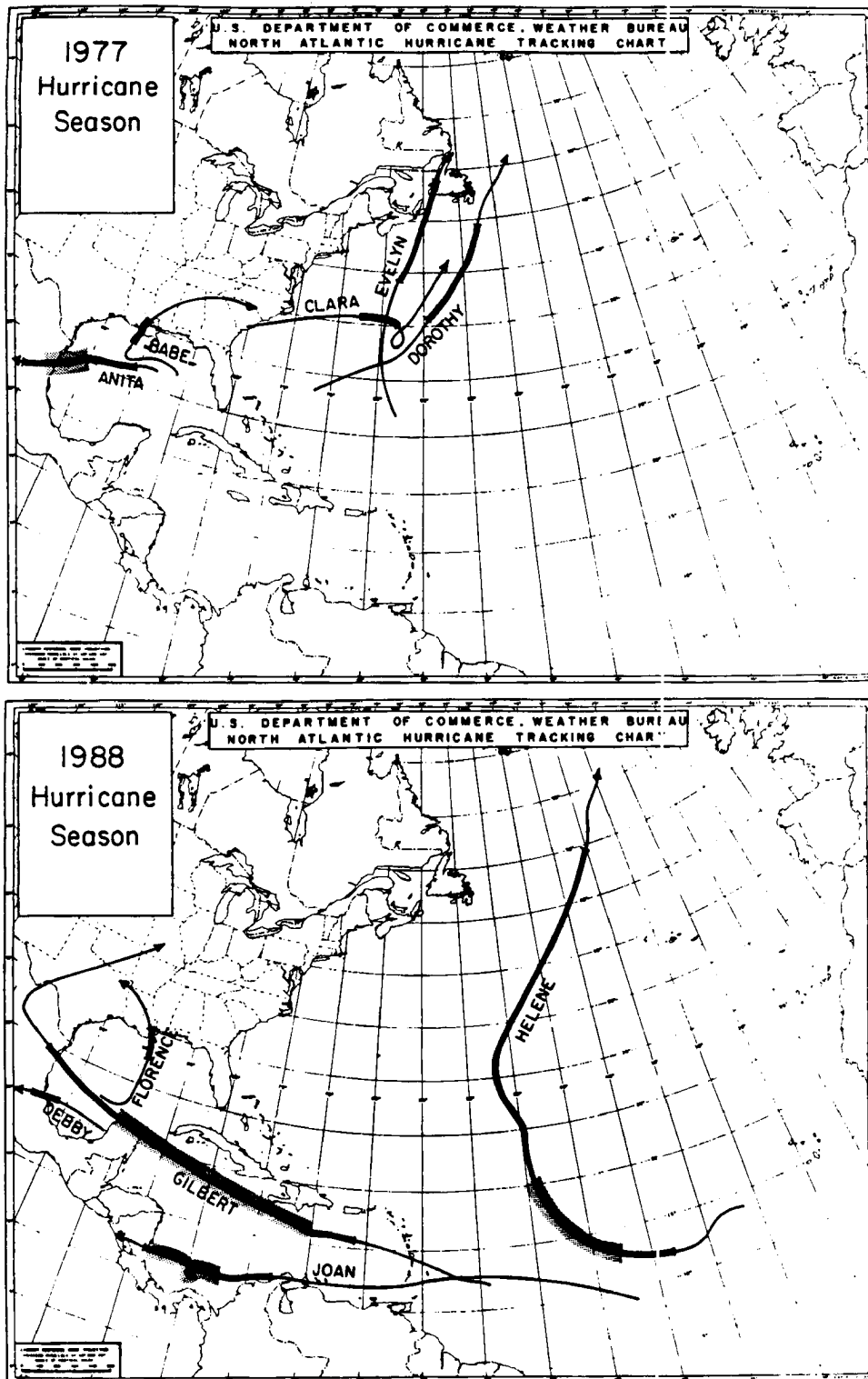


Figure 3.10: The 1977 (top) and 1988 (bottom) Atlantic basin hurricane activity. The thin solid line indicates tropical storm strength, the moderate solid line indicates weak hurricane (Category 1 or 2) strength, and the thick solid line indicates intense hurricane (Category 3, 4, or 5) strength.

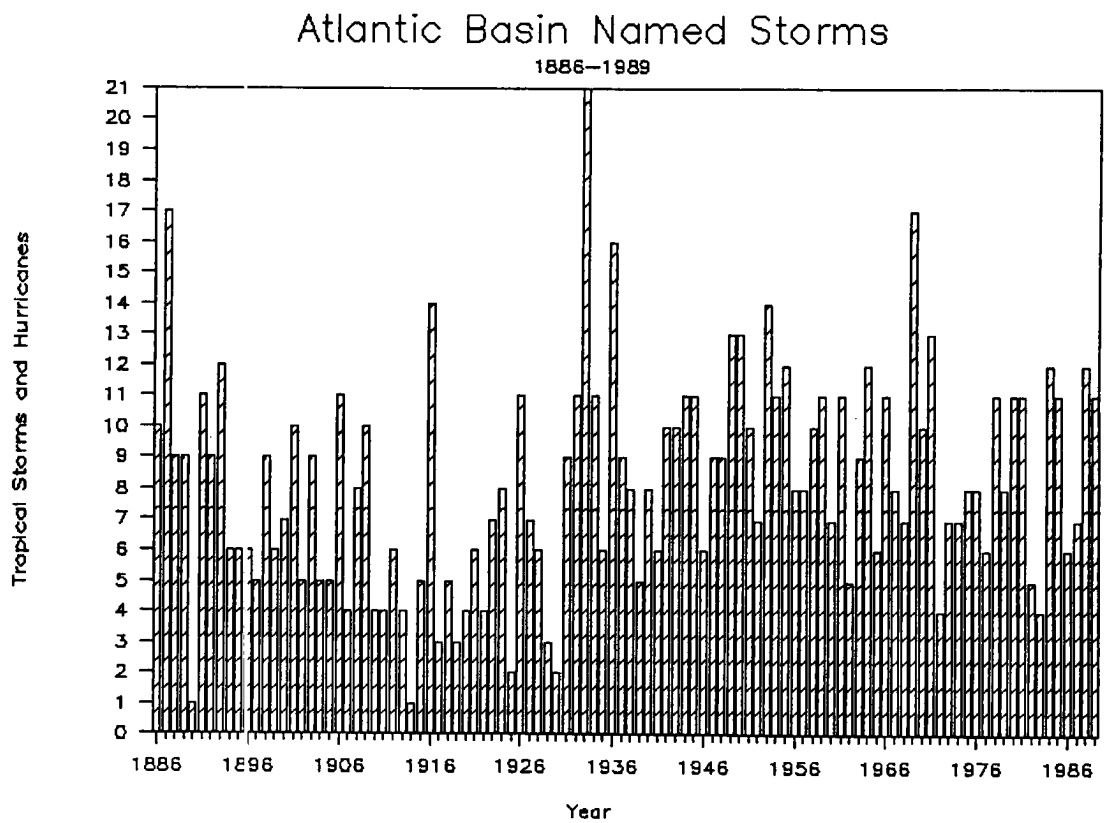


Figure 3.11: Atlantic basin named storms (tropical storms and hurricanes) for 1886-1989.

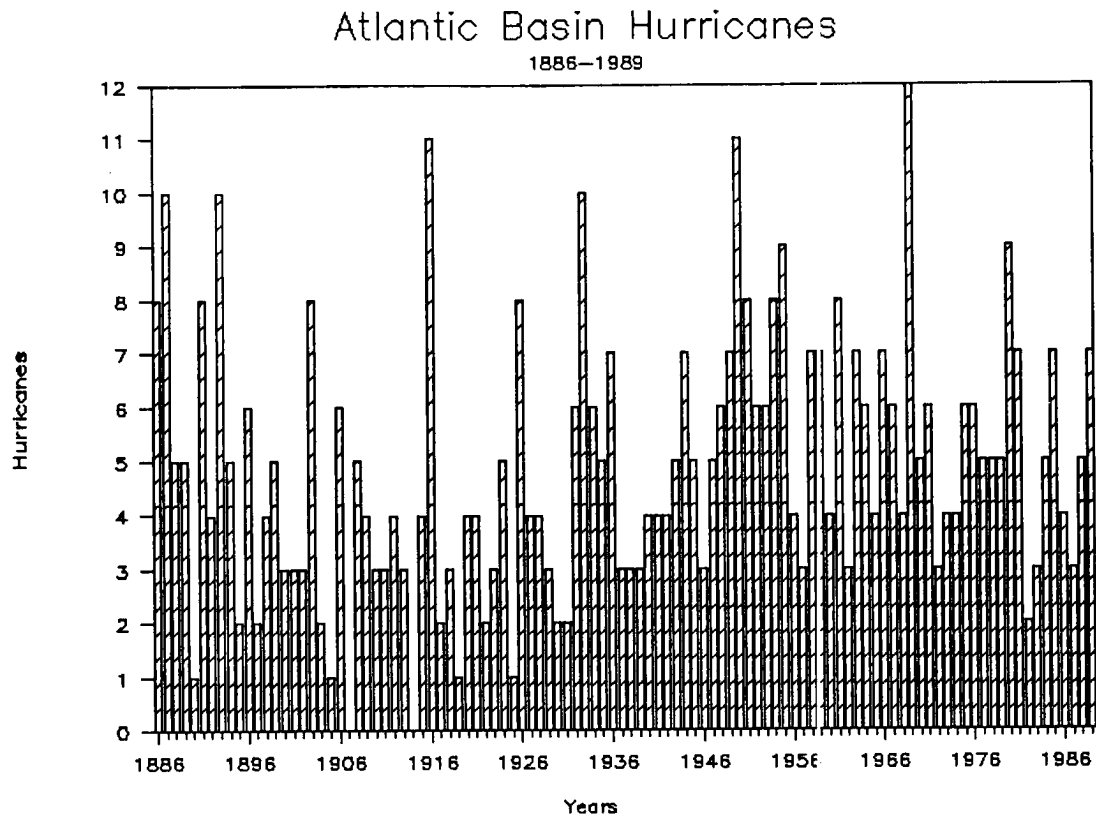


Figure 3.12: Atlantic basin hurricanes for 1886 to 1989.

overestimation of the intensity of some of the earlier period intense storms. This problem is investigated thoroughly in section 3.2.5.

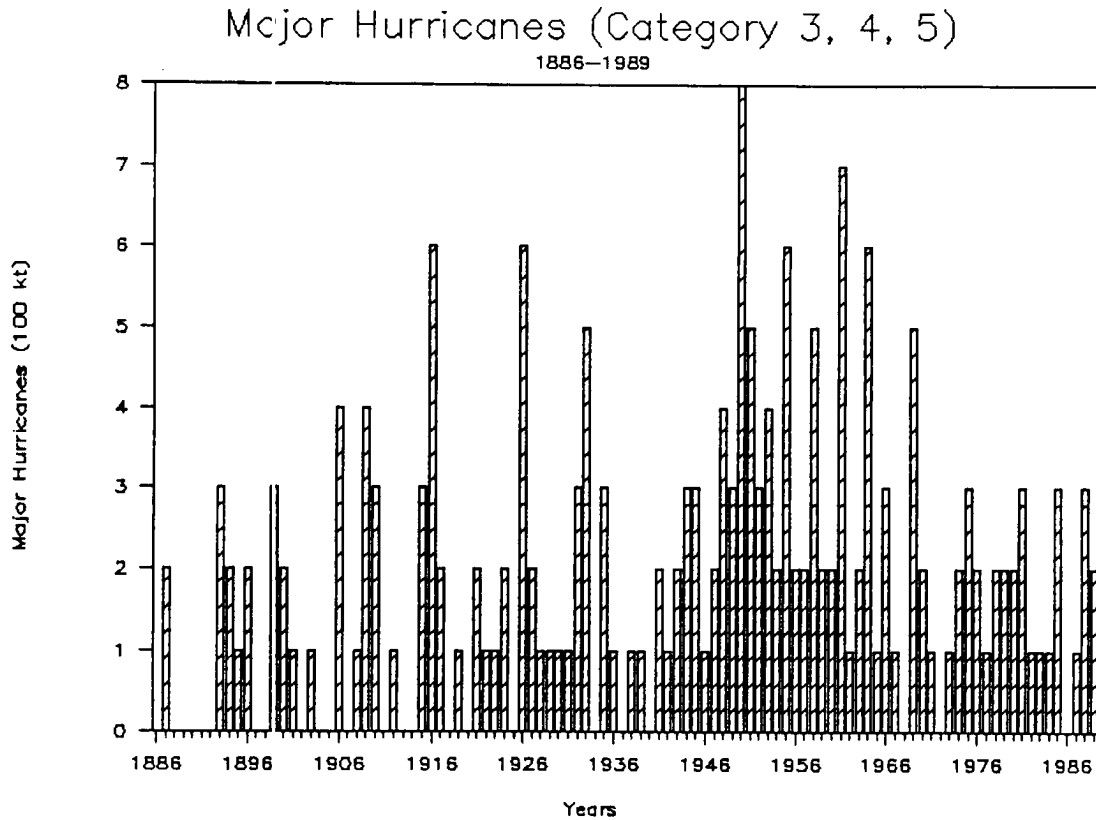


Figure 3.13: Atlantic basin intense hurricanes for 1886 to 1989.

Hurricane Destruction Potential: In an effort to incorporate a seasonal measure of the tropical cyclones' durations and intensities, Gray (1987) created a parameter termed the Hurricane Destruction Potential (HDP) (section 1.1.1). Figure 3.14 presents the interannual variability of HDP since 1886. Note that HDP shows the same strong year to year variability as that of the intense hurricanes.

Tropical Cyclone Days: Another method to incorporate storm duration into a seasonal measure index would be to use tropical cyclone days. Cyclones that persist for several days logically should be considered as contributing more to the activity of the tropical cyclone season than a similar number of storms that form and dissipate in a brief time. The long period variability of named storm days, hurricane days, and intense hurricane days are presented in Fig. 3.15.

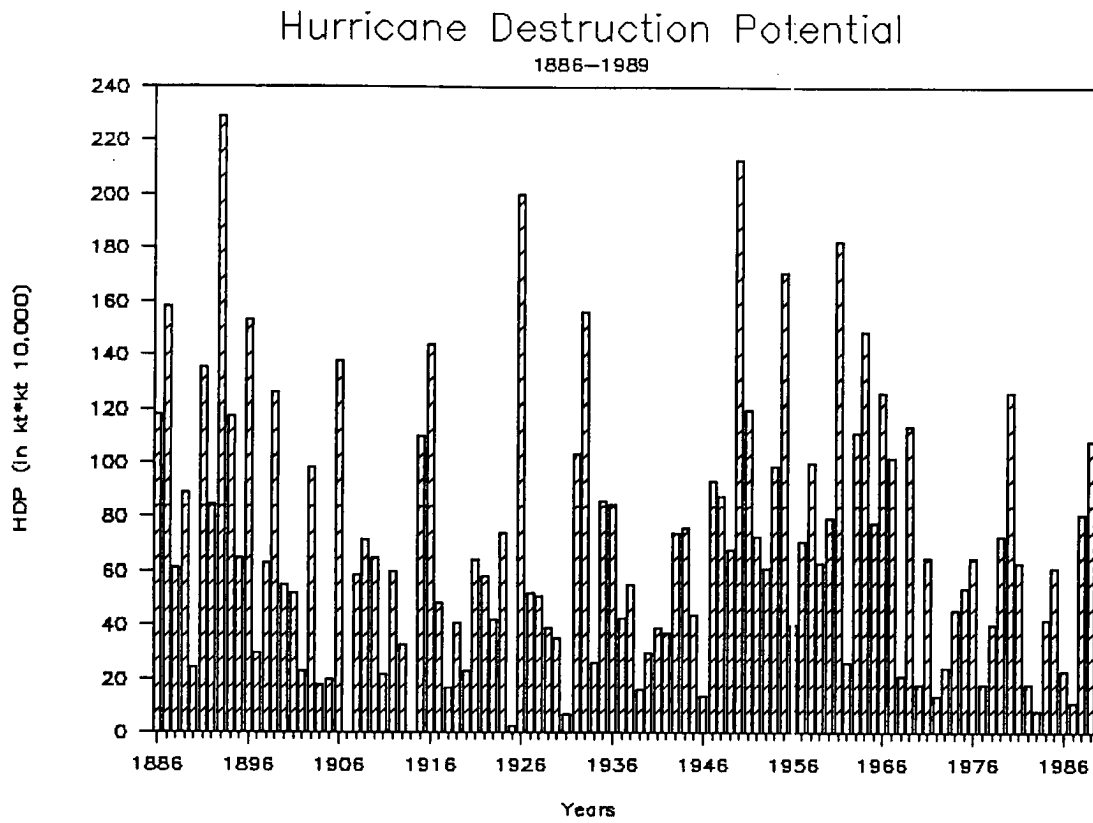


Figure 3.14: Atlantic basin Hurricane Destruction Potential (HDP) from 1886 to 1989.

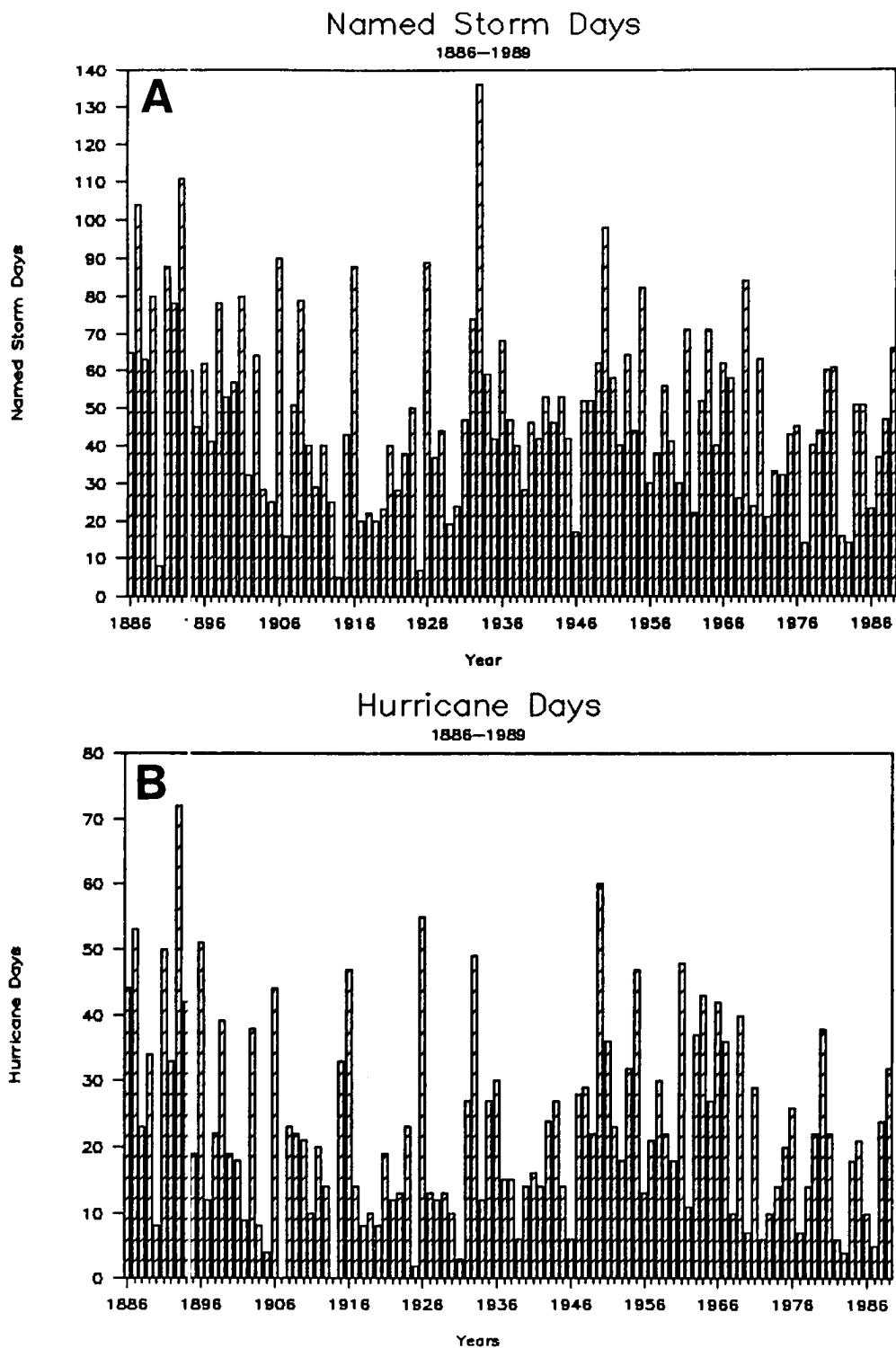


Figure 3.15: Atlantic basin tropical cyclone days: a) named storm days, b) hurricane days, c) intense hurricane days.

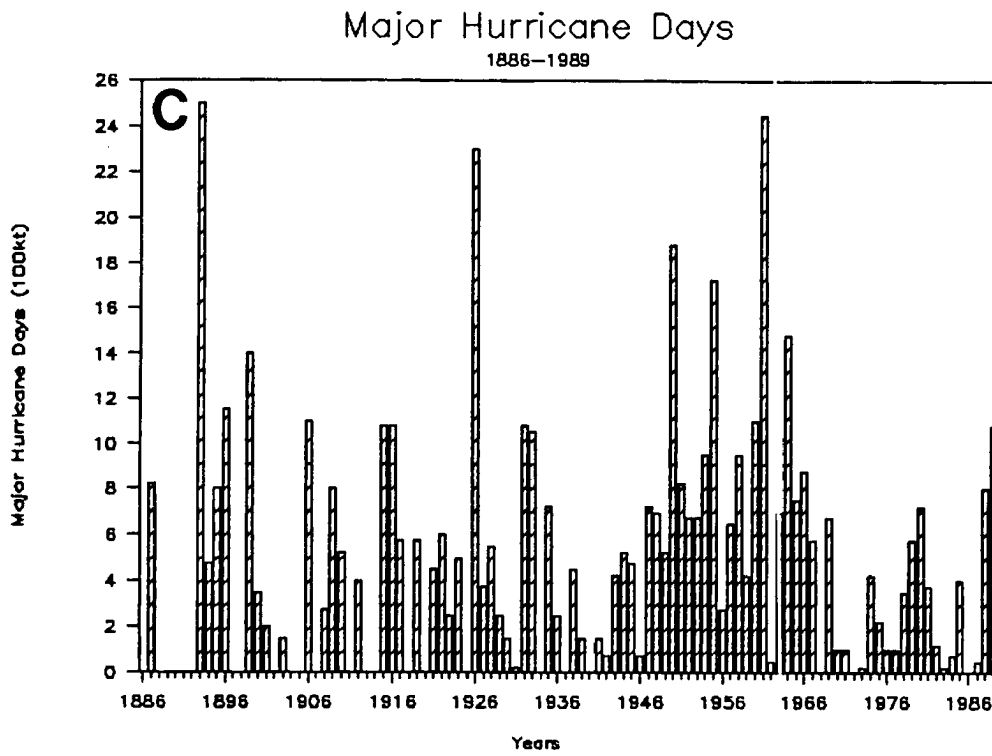


Figure 3.15: c: Continued

Linear Trends: An instructive way to analyze the interannual variability in these data is to superimpose the linear fit line on the data since 1949. The seven graphs in Fig. 3.16 show the linear trend for each parameter. All seven figures show a significant downward trend. The least reduction occurs in the number of named storms and hurricanes, the variables typically are given as measures of seasonal activity. Note the large decadal drops in activity as seen in the number of intense hurricanes and intense hurricane days.

Of course, the linear trend is not necessarily the best way to examine long term variations of these parameters. However, the trend data do seem to verify that the Atlantic basin tropical cyclone activity, especially of extremely intense hurricanes, has shown a strong decreasing tendency during the past few decades.

Additional Consideration—Subtropical Storms: As mentioned in section 1.1.1, the subtropical cyclone category of storm was created in 1968. Before 1968, subtropical storms would likely be counted as tropical storms. Hence, inclusion of subtropical cyclones in the named storm climatology appears appropriate. Figure 3.17 shows the seasonal number of cyclones that remained subtropical throughout their lifetime (top panel) along with the combined incidence of named and subtropical storm long term variability is shown with a linear fit line (bottom panel). There has been a deemphasis in the use of the subtropical storm designation during the last few years. The last storm officially bearing a subtropical designation was Tropical Storm Andrew in 1986 and the last purely subtropical storm was recognized in 1984, the 18-21 August, 1984, cyclone northeast of Bermuda. Nevertheless, addition of the subtropical cyclones to the current analysis only reinforces the conclusion that the total seasonal incidence of named storms has shown relatively little decline since 1949.

Basinwide Tropical Cyclone Variability Conclusions: Total Atlantic basin tropical cyclone activity expressed in named storms and hurricanes has not experienced a large multi-decadal decline. The total duration of cyclone activity expressed as named storm days and hurricane days has shown a more substantial decrease. The most obvious downward trend

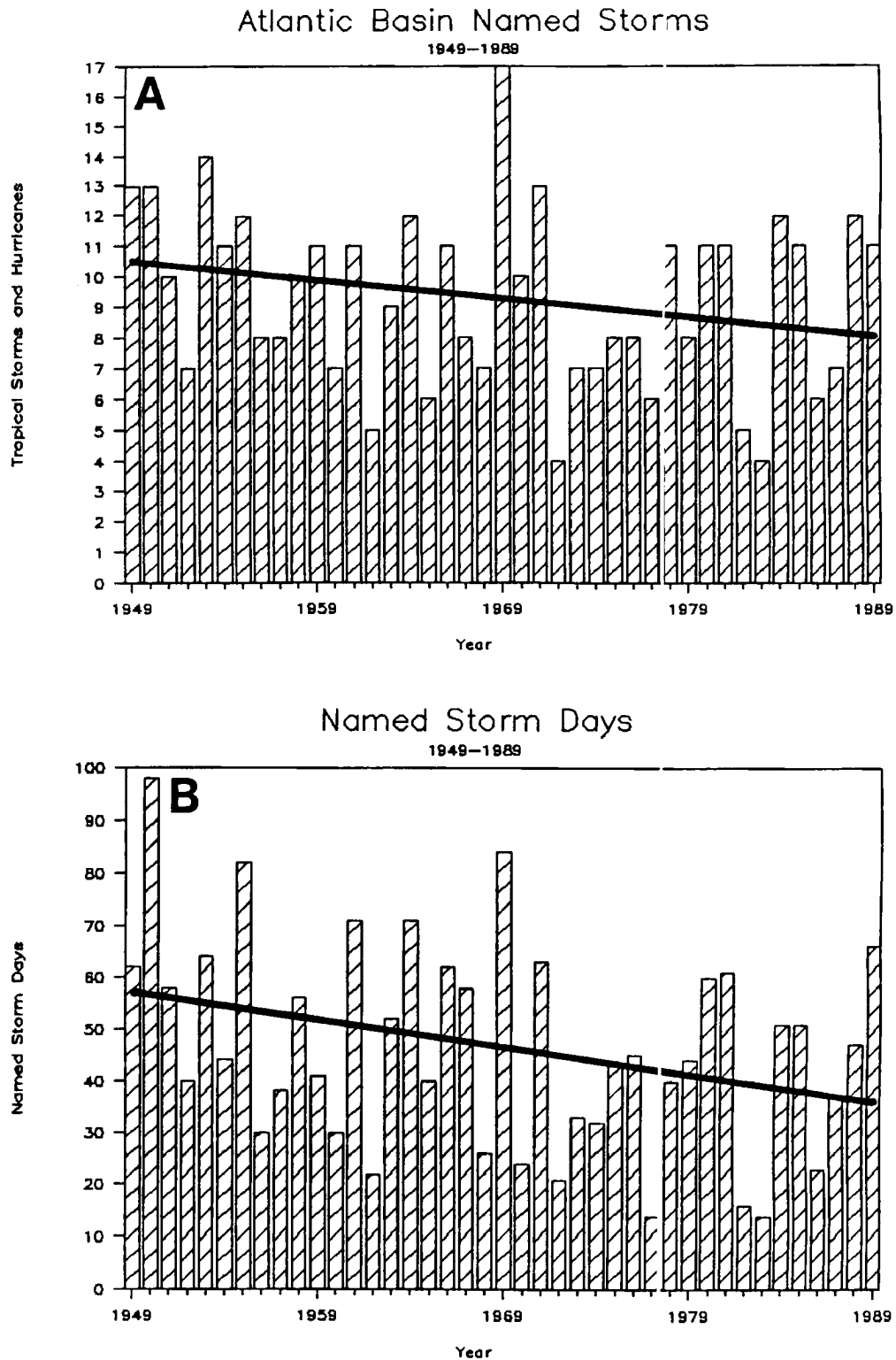


Figure 3.16: Atlantic basin tropical cyclone data from 1949 to 1989 with linear trends superimposed for a) named storms, b) named storm days, c) hurricanes, d) hurricane days, e) intense hurricanes, f) intense hurricane days, and g) HDP.

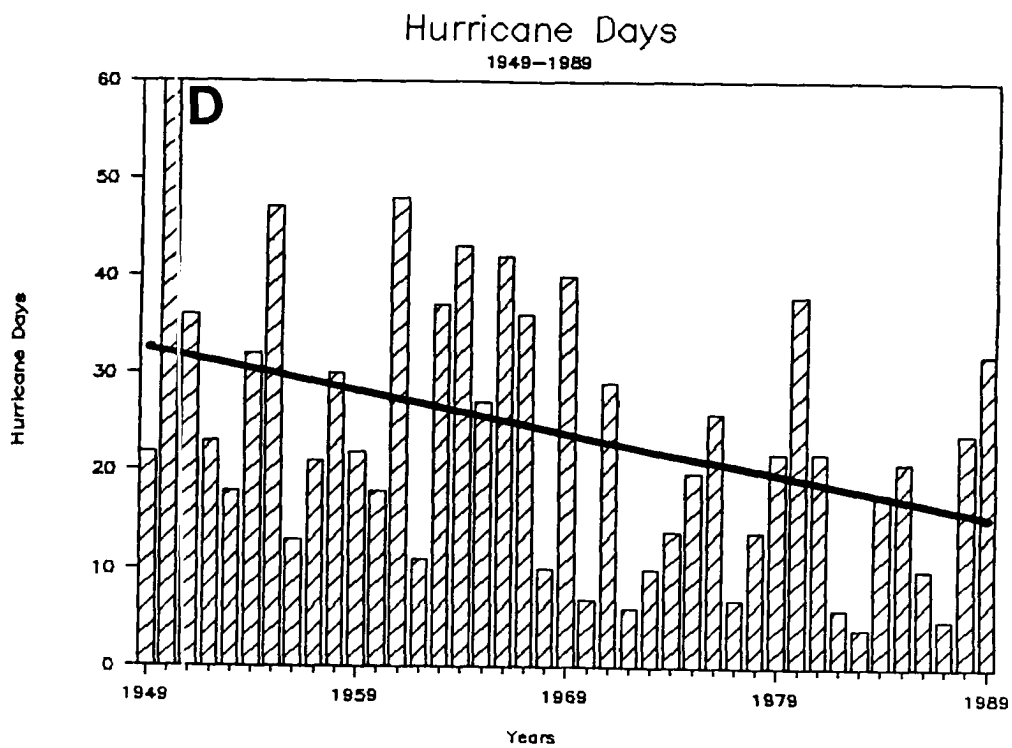
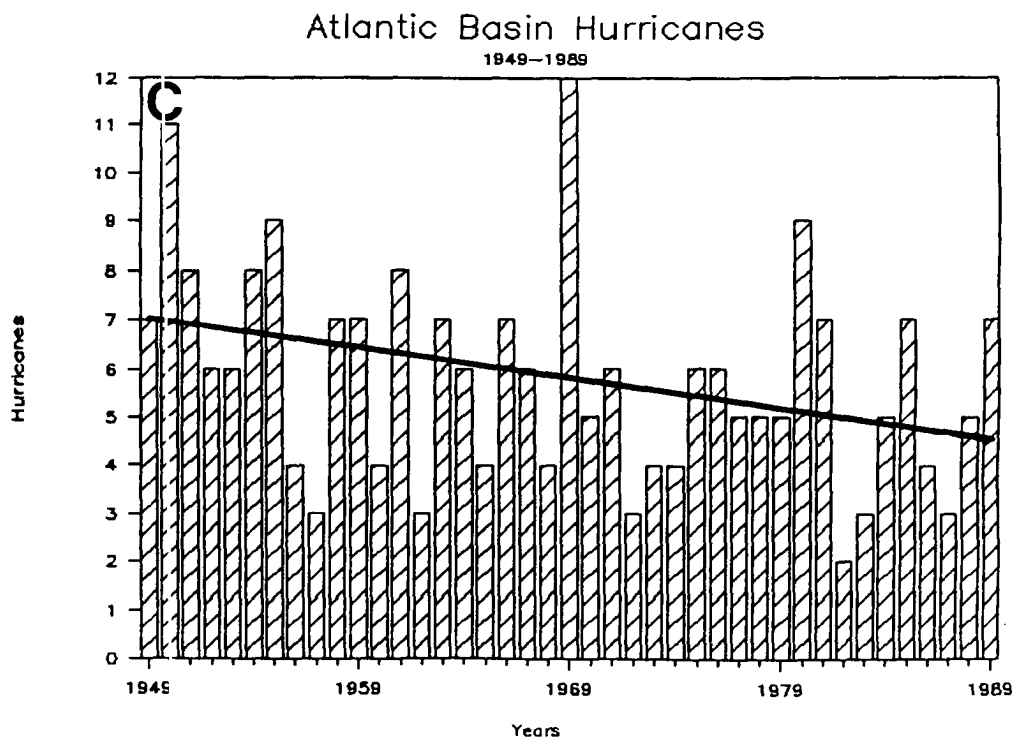


Figure 3.16: c-d: Continued.

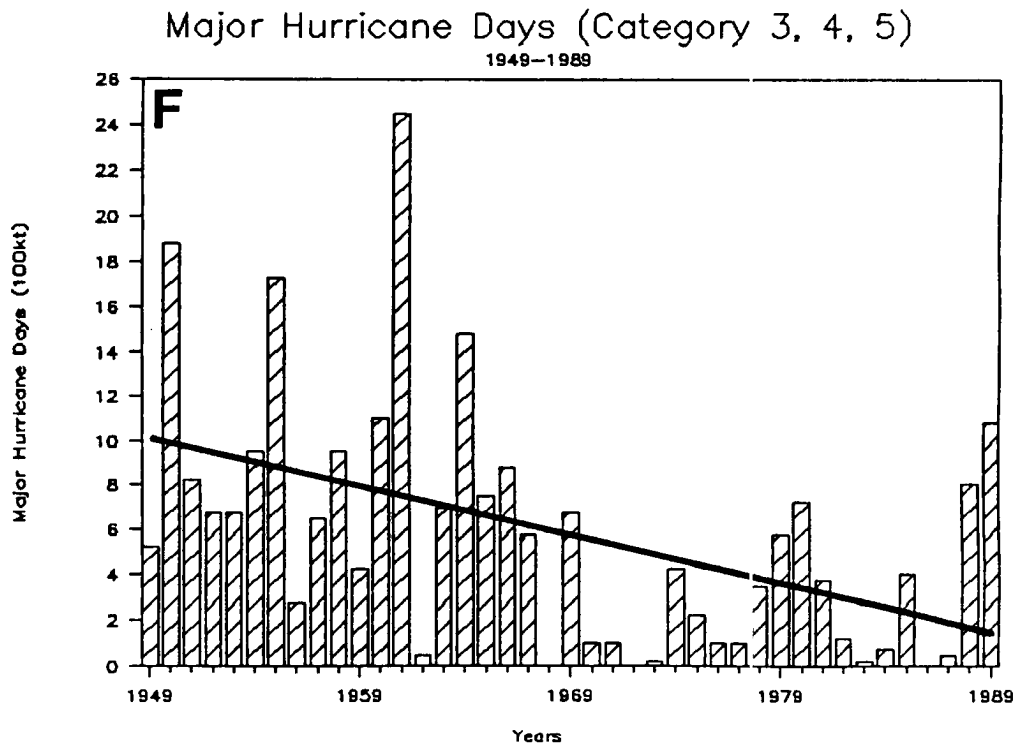
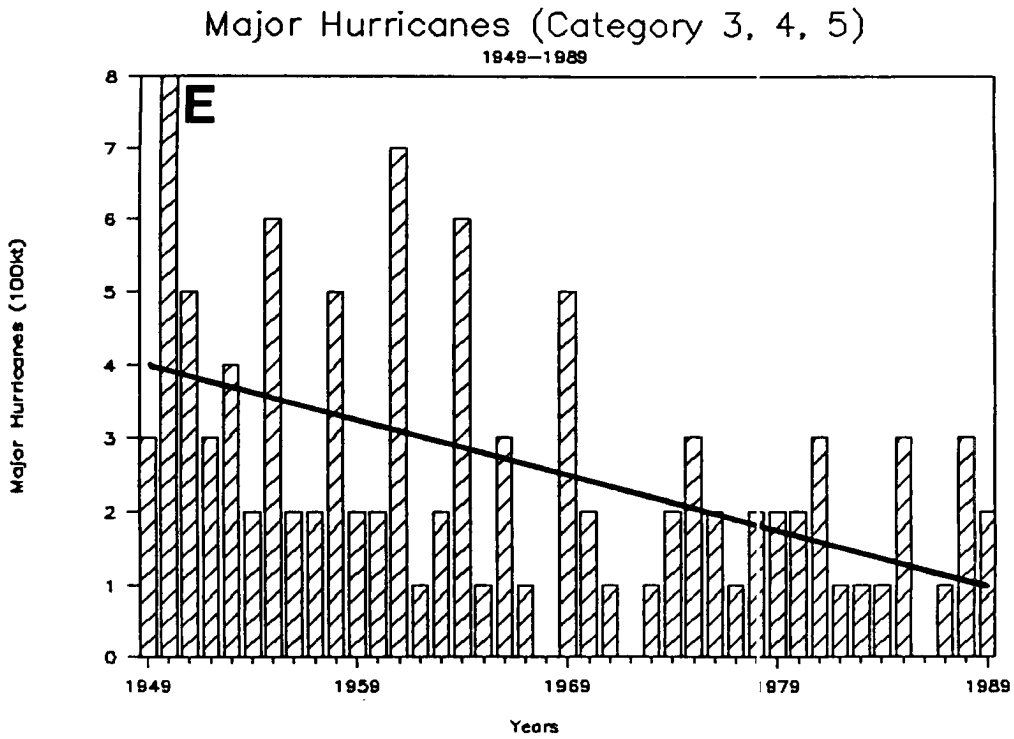


Figure 3.16: e-f: Continued

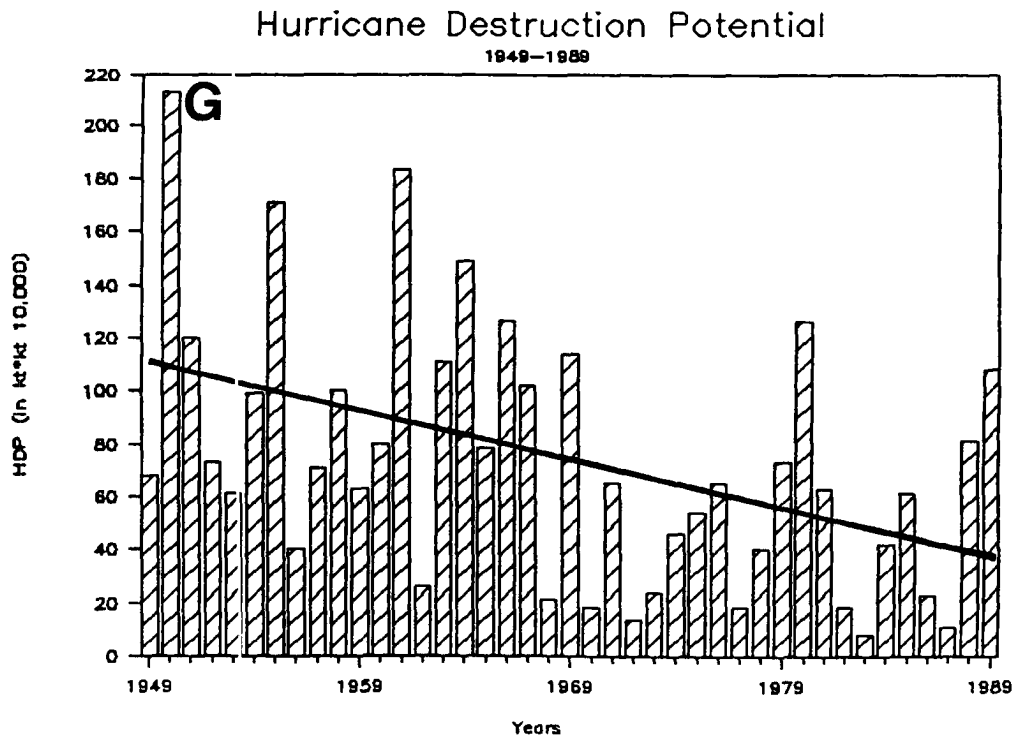


Figure 3.16: g: Continued

has occurred in the number and duration of intense cyclones; notably, the Saffir-Simpson Category 3, 4, and 5 hurricanes and in HDP.

Table 3.3 lists the values for the six basic tropical cyclone parameters, their means, standard deviations, coefficients of variability, and the linear trend expressed as a percentage decrease of each value. It is interesting to note that intense hurricanes experience both the largest coefficient of variation (i.e. largest interannual fluctuations) and the greatest downward linear trend.

3.2.2 U.S. Landfalling Tropical Cyclones

An advantage in utilizing landfalling tropical cyclone data is that the populated and closely monitored coastal region provides a more accurate record of episodic events. A negative feature of this parameter is that the relatively infrequent landfalling tropical cyclones require a longer data period to thoroughly document multidecadal patterns.

U.S. Landfalling Named and Subtropical Storms: Figure 3.18 illustrates the interannual variability of named storms (tropical storms and hurricanes) and subtropical storms

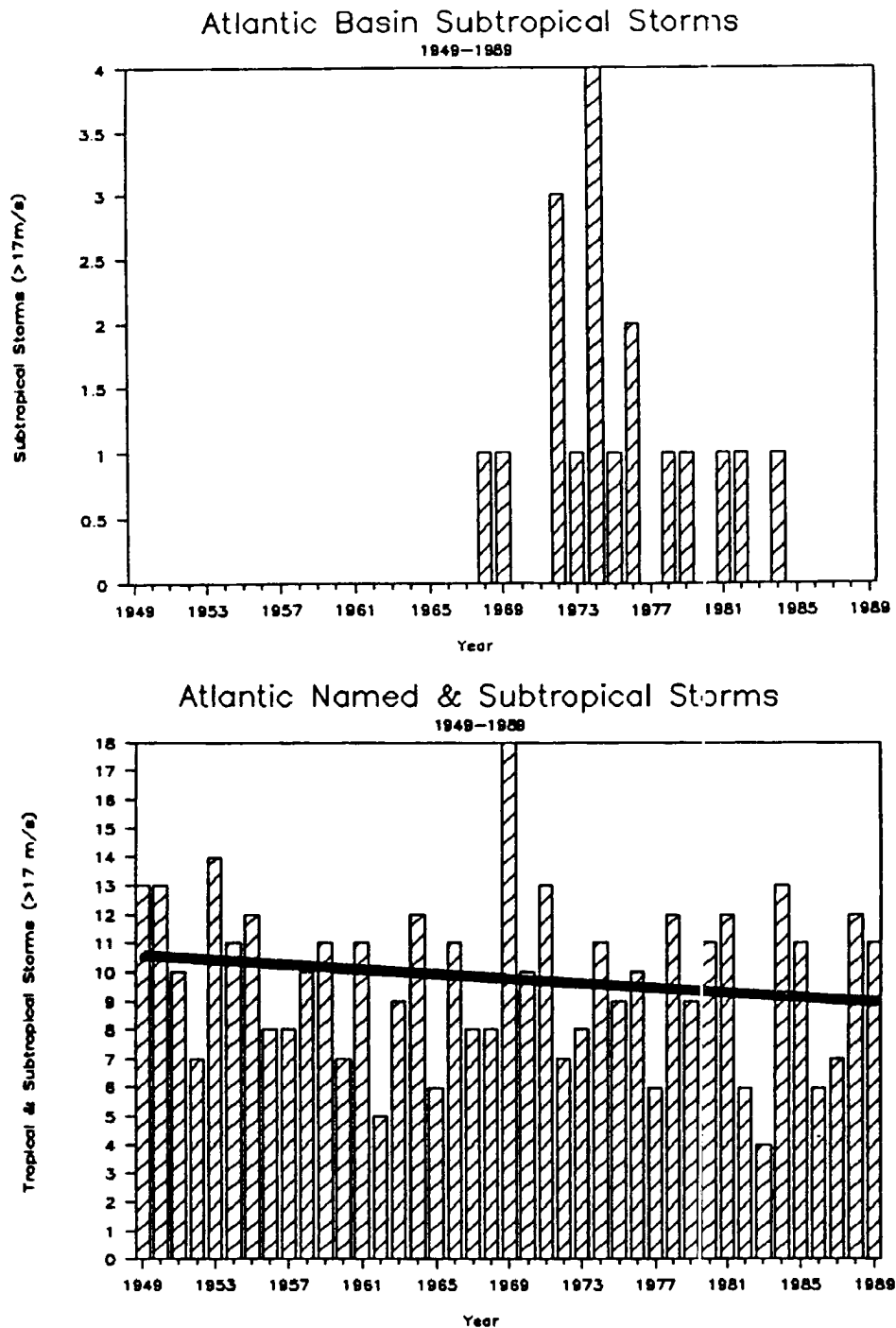


Figure 3.17: Atlantic basin subtropical storms 1949 to 1989 (top panel). Atlantic basin subtropical and named storms 1949 to 1989 with a linear trend superimposed are shown in the bottom panel.

Table 3.3 Atlantic basin tropical cyclone statistics for 1949 to 1989.

Year	Named Storms	Named Storm Days	Named and Subtropical Storms	Hurs. Hurs.	Hur. Days	Intense Hurs.	Intense Hur. Days	HDP
1949	13	62	13	7	22	3	5.25	68
1950	13	98	13	11	60	8	18.75	213
1951	10	58	10	8	36	5	8.25	120
1952	7	40	7	6	23	3	6.75	73
1953	14	64	14	6	18	4	6.75	61
1954	11	44	11	8	32	2	9.50	99
1955	12	82	12	9	47	6	17.25	171
1956	8	30	8	4	13	2	2.75	40
1957	8	38	8	3	21	2	6.50	71
1958	10	56	10	7	30	5	9.50	100
1959	11	41	11	7	22	2	4.25	63
1960	7	30	7	4	18	2	11.00	80
1961	11	71	11	8	48	7	24.50	183
1962	5	22	5	3	11	1	0.50	26
1963	9	52	9	7	37	2	7.00	111
1964	12	71	12	6	43	6	14.75	149
1965	6	40	6	4	27	1	7.50	78
1966	11	62	11	7	42	3	8.75	126
1967	8	58	8	6	36	1	5.75	102
1968	7	26	8	4	10	0	0.00	21
1969	17	84	18	12	40	5	6.75	114
1970	10	24	10	5	7	2	1.00	18
1971	13	63	13	6	29	1	1.00	65
1972	4	21	7	3	6	0	0.00	14
1973	7	33	8	4	10	1	0.25	24
1974	7	32	11	4	14	2	4.25	46
1975	8	43	9	6	20	3	2.25	54
1976	8	45	10	6	26	2	1.00	65
1977	6	14	6	5	7	1	1.00	18
1978	11	40	12	5	14	2	3.50	40
1979	8	44	9	5	22	2	5.75	73
1980	11	60	11	9	38	2	7.25	126
1981	11	61	12	7	22	3	3.75	63
1982	5	16	6	2	6	1	1.25	18
1983	4	14	4	3	4	1	0.25	8
1984	12	51	13	5	18	1	0.75	42
1985	11	51	11	7	21	3	4.00	61
1986	6	23	6	4	10	0	0.00	23
1987	7	37	7	3	5	1	0.50	11
1988	12	47	12	5	24	3	8.00	81
1989	11	66	11	7	32	2	10.75	108
Mean	9.3	46.7	9.8	5.8	23.7	2.5	5.8	73.8
Stan. Dev.	2.9	19.6	2.8	2.2	13.4	1.9	5.5	48.6
Coefficient Variation (%)	31.2	42.0	28.6	37.9	56.5	76.0	94.9	65.9
Downward Trend (%)	24	35	14	36	53	75	80	68

that made landfall along the US mainland. The initial study by Hebert and Taylor (1975) considered only storms since 1899 as it becomes more difficult to accurately differentiate the strength of the landfalling cyclones before that year. Note the considerable year to year difference in named storm frequency with only one storm occurring several times, most recently in 1977, and a maximum of eight occurring three times - 1909, 1916, and 1985.

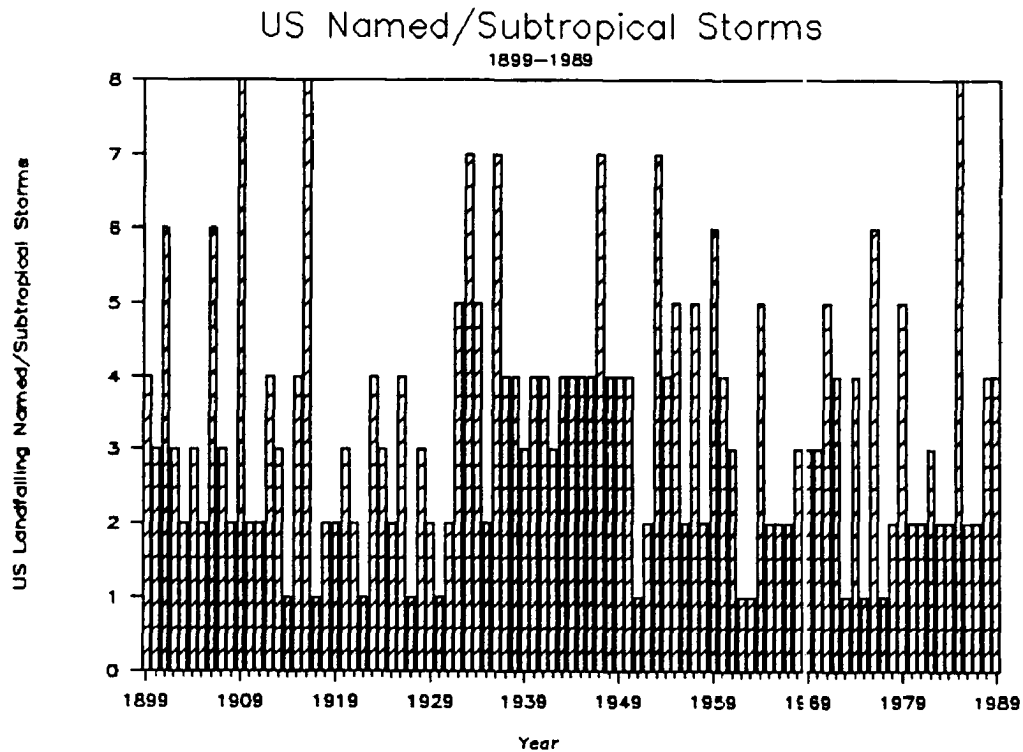


Figure 3.18: U.S. landfalling named storms (tropical storms and hurricanes) and subtropical storms for 1899 to 1989.

U.S. Landfalling Hurricanes: Yearly total hurricane strikes along the U.S. coastline are shown in Fig. 3.19. While there appears to be periods of increased activity (the 1940's) and decreased activity (the 1920's and 1970's), there seems to be no general increase in the frequency as occurs in basinwide hurricanes in Fig. 3.12. Again, the results in Fig. 3.12 are assumed to be due to improved surveillance throughout the basin, as opposed to a relatively constant level of recording along the U.S. coastline. Interannual variability in

Fig. 3.14 is very large with several years having no hurricane strikes recorded while others have as many as six hurricanes (1916 and 1985).

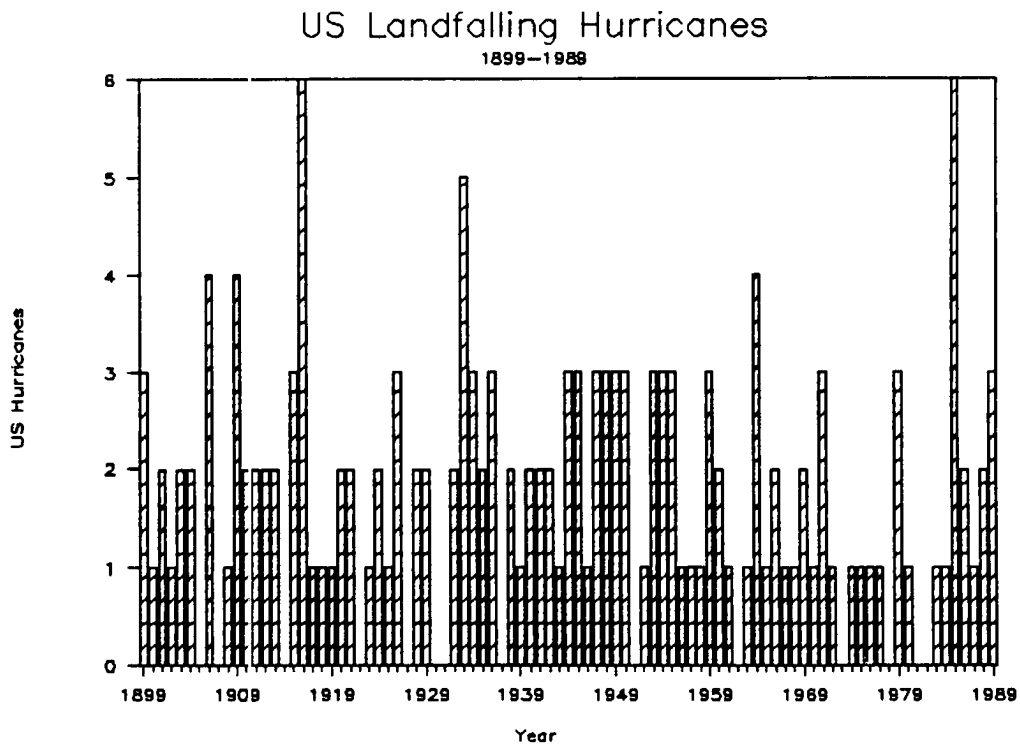


Figure 3.19: U.S. landfalling hurricanes in 1899 to 1989.

U.S. Landfalling Intense Hurricanes: As shown in Fig. 3.20, intense hurricanes make landfall along the U.S. coast much less frequently, averaging approximately two strikes every three years. The most intense hurricane strikes recorded in recent times is three, occurring in 1909, 1933, and 1954. Note that the values in Fig. 3.20 were not maximum sustained wind data in the Best Track data set (as were the intense hurricane days presented in Fig. 3.15) but are from Hebert and Taylor's (1975) determination of Saffir-Simpson category at landfall. Their analysis was based primarily on minimum sea level pressure at time of landfall, but also considered maximum sustained wind and storm surge. Thus, there are a few inconsistencies between the landfalling and Best Track data sets.

U.S. landfalling intense hurricanes - Gulf Coast versus East Coast: Inspection of the tracks of landfalling intense hurricanes along the U.S. East Coast, from the Florida peninsula to Maine, quickly reveals a strong decrease in the frequency of these storms during

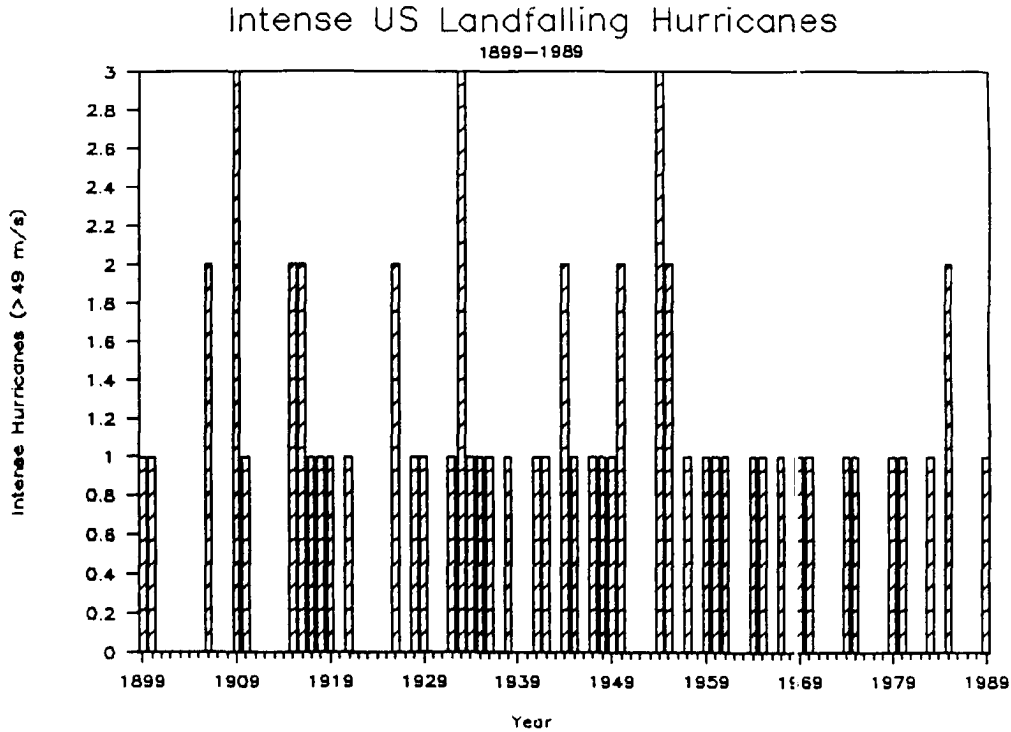


Figure 3.20: U.S. landfalling intense hurricanes from 1899 to 1989.

the 1970's and 1980's. Diagrams of landfalling intense hurricanes by decades [compiled by Sheets (1990)] also highlights this trend. Figure 3.21 shows the geographical regions under discussion.

Multidecadal variations are also evident in the two panels of Fig. 3.22, wherein clustering of activity on the Gulf Coast occurs in the late 1910's, the mid 1930's, and the 1960's and 1970's. Likewise, the East Coast has periods of higher activity during the late 1920's/early 1930's and the late 1940's/1950's. The most striking aspect is the calm period along the East Coast during the mid 1960's to 1980's. The only possible analog to this recent calm period would be the 1900's and 1910's when a total of just four intense hurricanes made landfall.

Even though the two coastal regions have distinct time periods of preferred activity, their long term mean frequencies are nearly the same; the Gulf Coast and East Coast/Florida both averaging about one intense hurricane strike every three years.

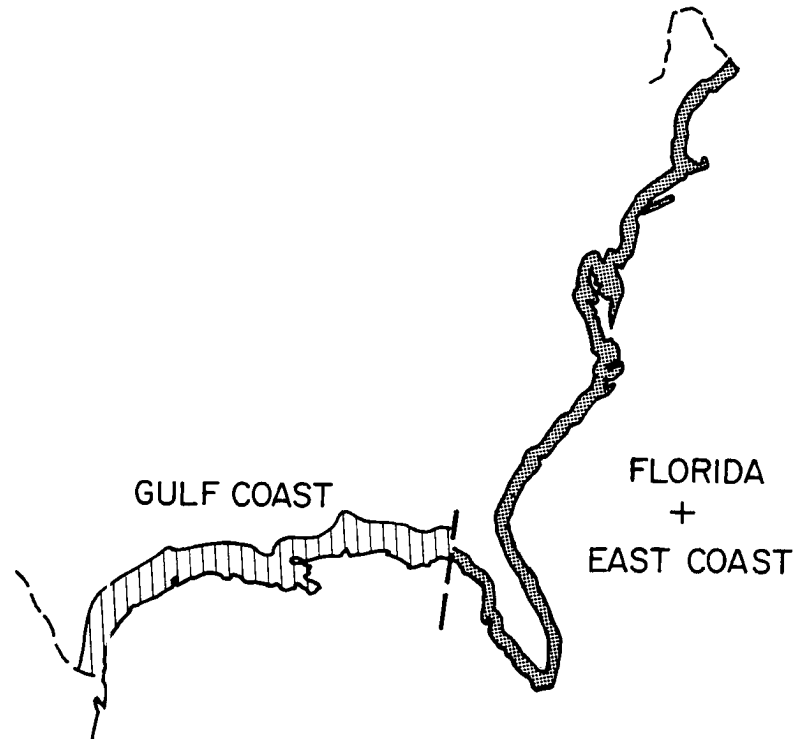


Figure 3.21: Specification of U.S. coastal regions which show considerable decadal differences in intense hurricane activity. The approximate separation line (dashed) is at the Apalachee Bay of Florida.

Linear trends: Figure 3.23 presents the same information as Figs. 3.18-3.22 with linear trend lines added to the data for the years 1949 to 1989. The trend line helps emphasize that the main long term changes in landfalling cyclone frequency (as well as for all storms) have not occurred with the weaker systems but in the major hurricanes. The number of landfalling named/subtropical storms have shown almost no decrease during the last 42 years.

The strong downward trend in the frequency of landfalling intense hurricanes has occurred entirely on the East Coast/Florida area. In fact, the Gulf Coast data in Fig. 3.23d show a slight rise by the linear trend since 1949. A question arises as to why there has been a decline in the frequency in the East Coast/Florida cyclones in recent years. The following chapters show that an associated meteorological phenomena, Sahel rainfall, has also experienced a large decadal decline and that the year to year hurricane activity, particularly that of intense hurricanes strongly relates to variations of Sahel rainfall.

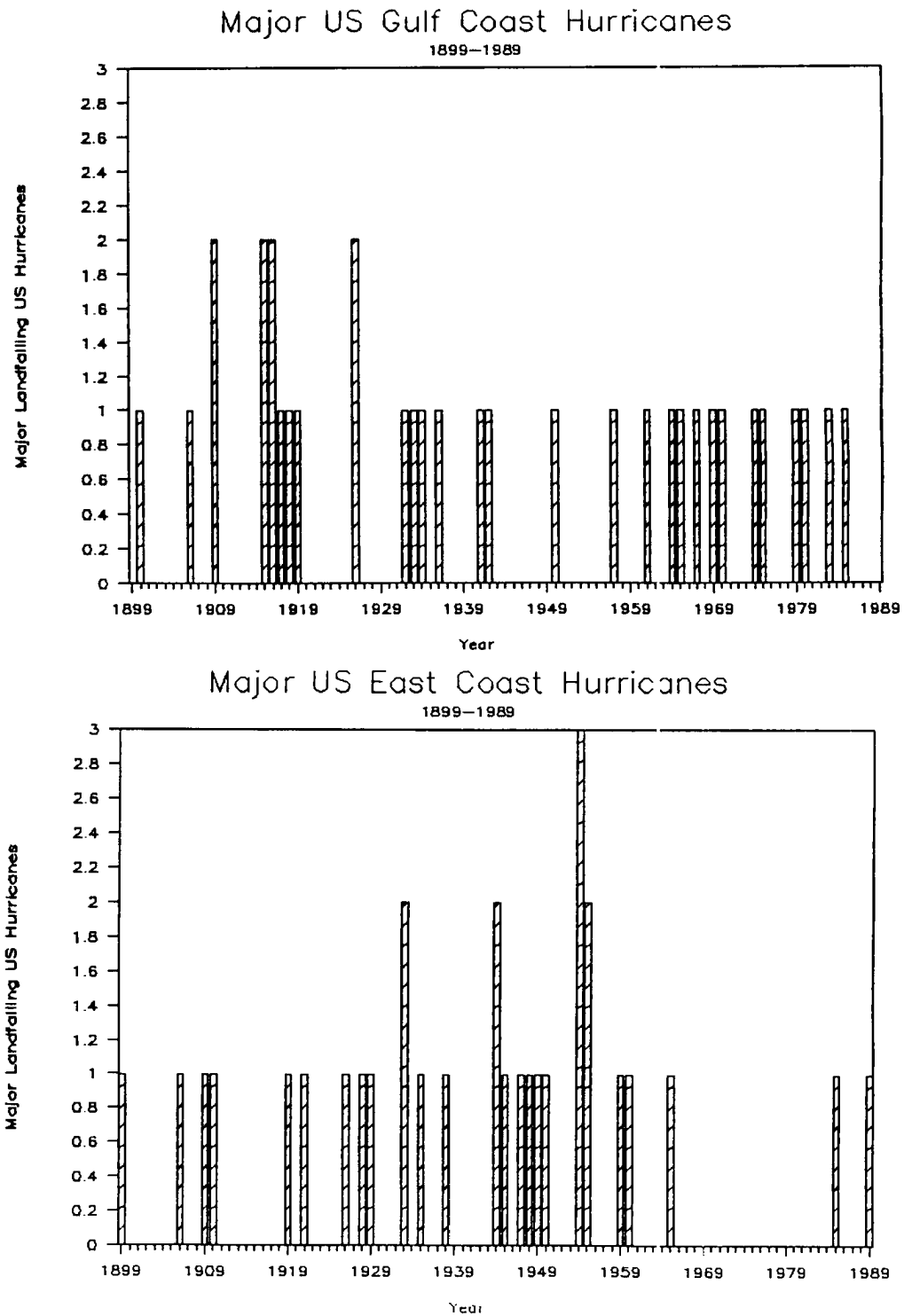


Figure 3.22: U.S. landfalling intense hurricane separated into two geographical regions: Gulf Coast (upper panel) and East Coast/Florida (bottom panel). The entire length of data (1899 to 1989) are presented.

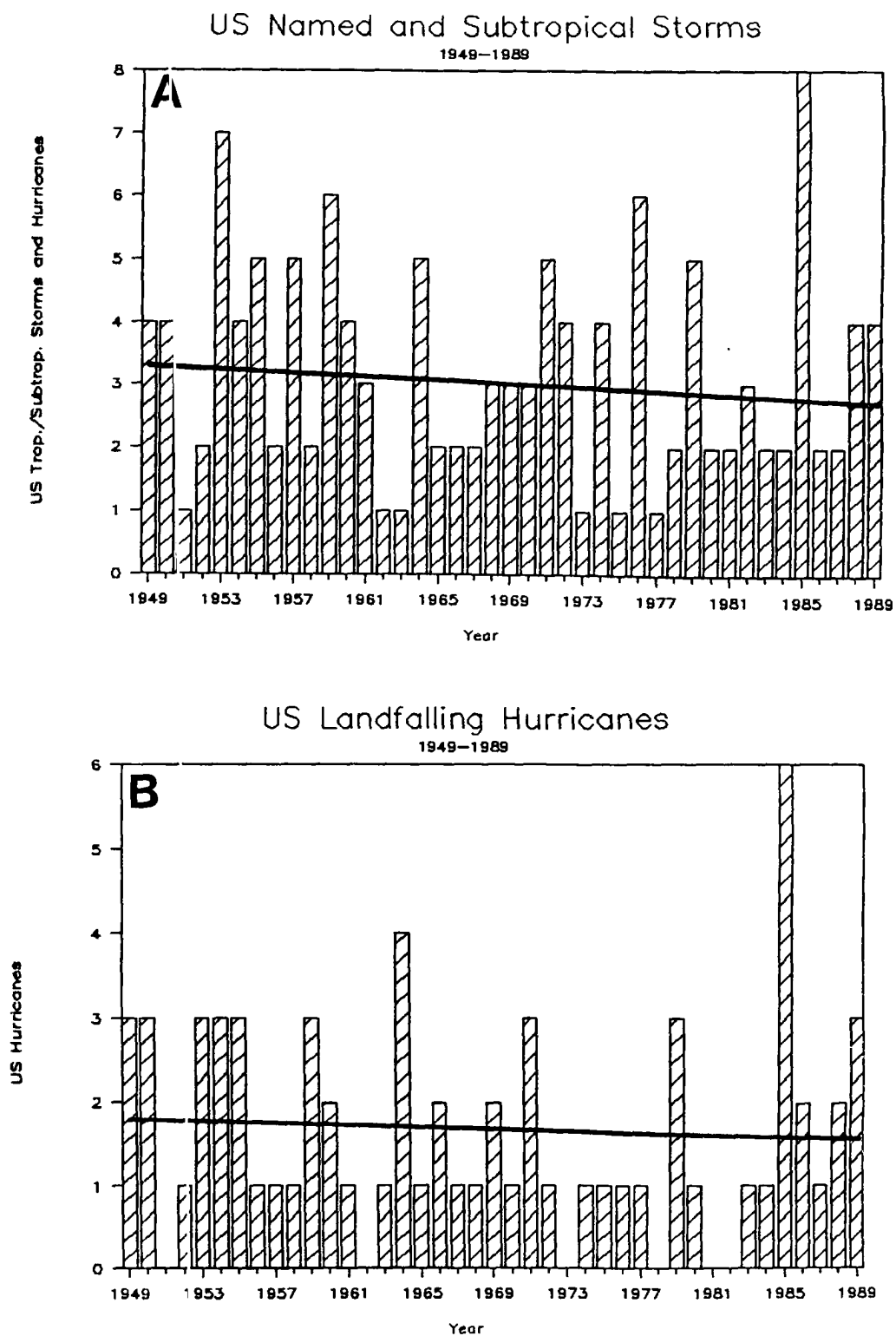


Figure 3.23: U.S. landfalling tropical cyclones from 1949 to 1989 with a linear trend line superimposed. Panels: a) named and subtropical storms, b) hurricanes, c) intense hurricanes, d) Gulf Coast intense hurricanes, e) East Coast/Florida intense hurricanes.

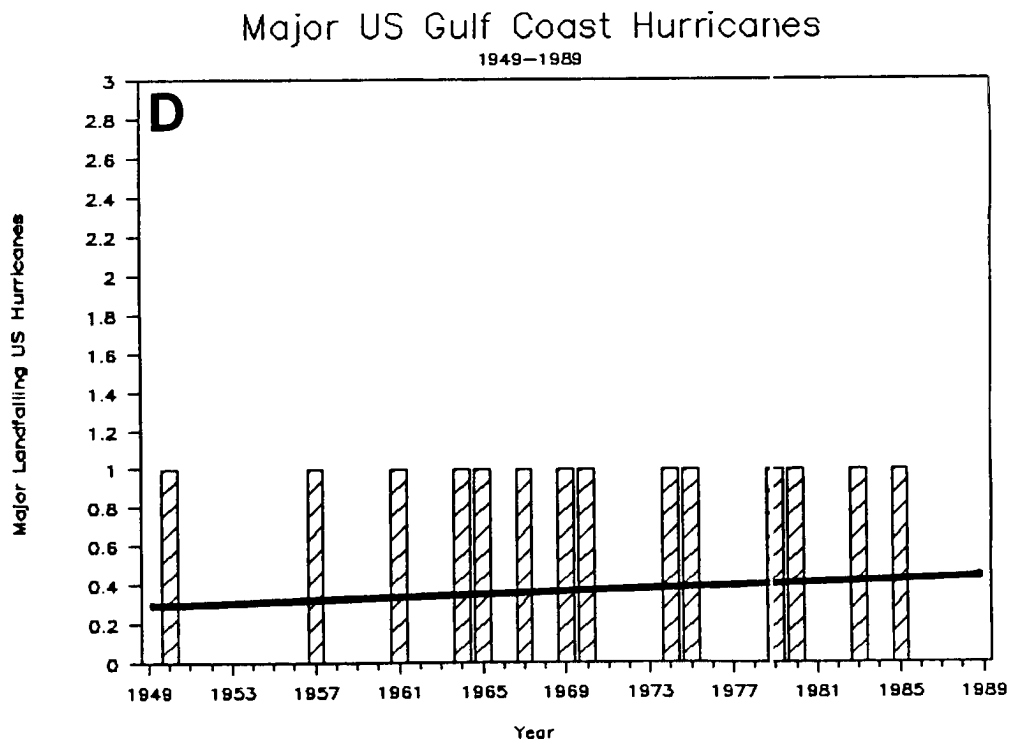
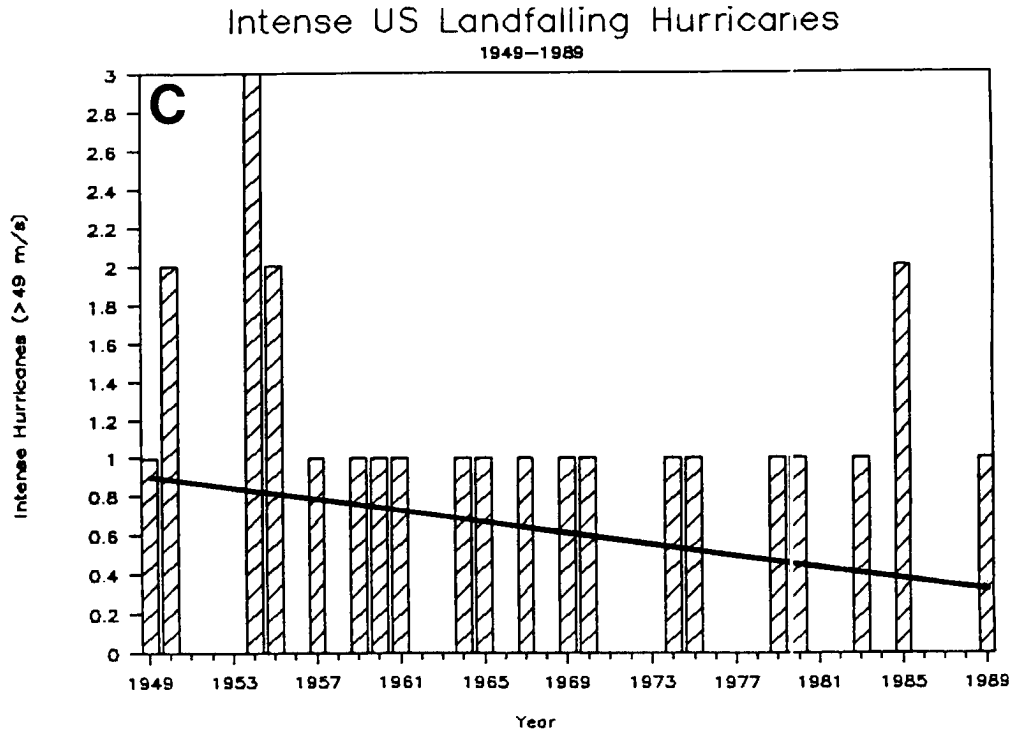


Figure 3.23: c-d: Continued.

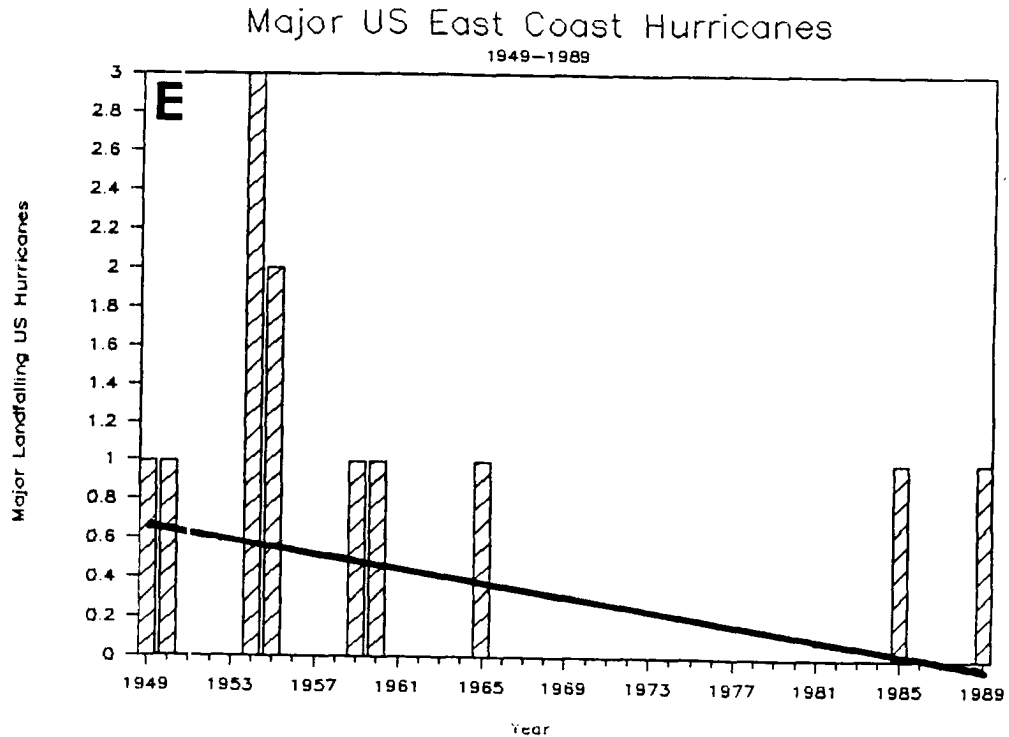


Figure 3.23: e: Continued.

Table 3.4 gives a year to year listing of the incidence of U.S. landfalling named/subtropical storms, hurricanes, intense hurricanes, Gulf Coast intense hurricanes, and East Coast/Florida intense hurricanes. Also provided are means, standard deviations, and coefficients of variation for 1899-1989, 1899-1948, and 1949-1989.

3.2.3 Tropical Cyclone Spawned U.S. Damage

As described in section 2.1.3, statistics on tropical storm and hurricane caused destruction in the U.S. were obtained from yearly summaries of the Monthly Weather Review. Storm by storm breakdowns of damage are contained in Table 3.5. To normalize dollar amounts for long term inflation, we chose to use a compounded 7% per year factor to modify the damage values, as well as compensate for coastal population and property growth. Other studies (such as Sheets (1990) and Hebert and Case (1990)) have only attempted to account for inflationary growth. A meaningful comparative assessment between years also must account for the large increase in U.S. coastal population and property development

Table 3.4: U.S. landfalling tropical cyclone activity 1899 to 1989.

Year	Named/ Subtrop. Storms	Hurs.	Intense Hurs.	Gulf Intense Hurs.	East Intense Hurs.
1899	4	3	1	0	1
1900	3	1	1	1	0
1901	6	2	0	0	0
1902	3	1	0	0	0
1903	2	2	0	0	0
1904	3	2	0	0	0
1905	2	0	0	0	0
1906	6	4	2	1	1
1907	3	0	0	0	0
1908	2	1	0	0	0
1909	8	4	3	2	1
1910	2	2	1	0	1
1911	2	2	0	0	0
1912	4	2	0	0	0
1913	3	2	0	0	0
1914	1	0	0	0	0
1915	4	3	2	2	0
1916	8	6	2	2	0
1917	1	1	1	1	0
1918	2	1	1	1	0
1919	2	1	1	1	0
1920	3	2	0	0	0
1921	2	2	1	0	0
1922	1	0	0	0	0
1923	4	1	0	0	0
1924	3	2	0	0	0
1925	2	1	0	0	0
1926	4	3	2	2	1
1927	1	0	0	0	0
1928	3	2	1	0	1
1929	2	2	1	0	1
1930	1	0	0	0	0
1931	2	0	0	0	0
1932	5	2	1	1	0
1933	7	5	3	1	2
1934	5	3	1	1	0
1935	2	2	1	0	1
1936	7	3	1	1	0
1937	4	0	0	0	0
1938	4	2	1	0	1
1939	3	1	0	0	0
1940	4	2	0	0	0
1941	4	2	1	1	0
1942	3	2	1	1	0
1943	4	1	0	0	0
1944	4	3	2	0	2

Table 3.4: Continued.

Year	Named/ Subtrop. Storms	Hurs.	Intense Hurs.	Gulf Intense Hurs.	East Intense Hurs.
1945	4	3	1	0	1
1946	4	1	0	0	0
1947	7	3	1	0	1
1948	4	3	1	0	1
1949	4	3	1	0	1
1950	4	3	2	1	1
1951	1	0	0	0	0
1952	2	1	0	0	0
1953	7	3	0	0	0
1954	4	3	3	0	3
1955	5	3	2	0	2
1956	2	1	0	0	0
1957	5	1	1	1	0
1958	2	1	0	0	0
1959	6	3	1	0	1
1960	4	2	1	0	1
1961	3	1	1	1	0
1962	1	0	0	0	0
1963	1	1	0	0	0
1964	5	4	1	1	0
1965	2	1	1	1	1
1966	2	2	0	0	0
1967	2	1	1	1	0
1968	3	1	0	0	0
1969	3	2	1	1	0
1970	3	1	1	1	0
1971	5	3	0	0	0
1972	4	1	0	0	0
1973	1	0	0	0	0
1974	4	1	1	1	0
1975	1	1	1	1	0
1976	6	1	0	0	0
1977	1	1	0	0	0
1978	2	0	0	0	0
1979	5	3	1	1	0
1980	2	1	1	1	0
1981	2	0	0	0	0
1982	3	0	0	0	0
1983	2	1	1	1	0
1984	2	1	0	0	0
1985	8	6	2	1	1
1986	2	2	0	0	0
1987	2	1	0	0	0
1988	4	2	0	0	0
1989	4	3	1	0	1

Table 3.4: Continued.

Year	Named/ Subtrop. Storms	Hurs.	Intense Hurs.	Gulf Intense Hurs.	East Intense Hurs.
Years: 1899 to 1989					
Mean	3.35	1.75	0.66	0.36	0.33
Stan.Dev.	1.76	1.29	0.77	0.56	0.59
Coeff. Var. (%)	52.5	73.7	116.7	115.6	178.8
Years: 1899 to 1948					
Mean	3.48	1.86	0.70	0.38	0.36
Stan.Dev.	1.78	1.30	0.81	0.63	0.56
Coeff. Var. (%)	51.1	70.0	115.7	165.3	155.6
Years: 1949 to 1989					
Mean	3.20	1.61	0.61	0.34	0.29
Stan.Dev.	1.73	1.27	0.73	0.47	0.63
Coeff. Var. (%)	54.1	78.9	119.7	138.2	217.2
Downward Trend (%)	15	11	55	-42	100

that has occurred in recent decades. Sheets (1990) documented a 60% rise in Atlantic coastal inhabitants, a 250% increase in Texas, and a 400% increase in Florida's coastal population from 1950 to 1985. Hence, 7% yearly adjustment, though fairly simplistic, is nevertheless a more realistic look at the interannual changes in tropical cyclone spawned damage than simply using inflation to normalize estimated dollar amounts.

Some discussion of Table 3.5 is appropriate. The years under consideration are 1949 to 1989. All cyclone strengths, from subtropical storms to category 5 hurricanes are indicated. The dollar amounts indicated from the Monthly Weather Review articles are listed, as well as the adjusted 1990 equivalent amount using the 7% per year normalization factor. Landfalling cyclones are also separated into Gulf Coast and East Coast/Florida categories. Some storms affected both regions through two distinct landfalls: notably, Tropical Storm Florence in 1960, Hurricane Betsy in 1965 and Hurricane Agnes in 1972. A separation was made of the damage caused by those storms into the Gulf and East coastal areas was made.

Another potentially useful set of tropical cyclone parameters are the yearly totals of damage, stratified both by intensity and by region. Table 3.6 presents Gulf Coast

Table 3.5: U.S. landfalling tropical cyclones and their associated damage in both current year and normalized 1990 dollars (in millions of dollars). Region designates U.S. Gulf Coast (G) and U.S. East Coast/Florida (E).

<u>Year</u>	<u>Factor</u>	<u>TC</u>	<u>Region</u>	<u>Landfall Intensity</u>	<u>Damage</u>	<u>Normalized 1990 Damage</u>		
1989	1.07	Allison	G	TS	500	535		
		Chantal	G	1	100	107		
		Hugo	E	4	7,000	7,490		
		Jerry	G	1	70	75		
1988	1.14	Beryl	G	TS	3	3		
		Chris	E	TS	1	1		
		Florence	G	1	2	2		
		Gilbert	G	1	50	57		
		Keith	E	TS	3	3		
1987	1.23	Unnamed	G	TS	7	9		
		Floyd	E	1	1	1		
1986	1.31	Bonnie	G	1	2	3		
		Charley	E	1	1	1		
1985	1.40	Bob	E	1	0	0		
		Danny	G	1	50	70		
		Elena	G	3	1,250	1,750		
		Gloria	E	3	900	1,260		
		Henri	E	TS	0	0		
		Isabel	E	TS	0	0		
		Juan	G	1	1,500	2,100		
		Kate	G	2	300	420		
		1984	1.50	Diana	E	2	65	98
				Isadore	E	TS	1	1
1983	1.61	Alicia	G	3	2,000	3,220		
		Barry	E	TS	0	0		
		Dean	E	TS	0	0		
1982	1.72	Chris	G	TS	2	3		
		Subtropical	E	Sub	10	17		
1981	1.84	Bret	E	TS	0	0		
		Dennis	E	TS	25	46		
1980	1.97	Allen	G	3	300	591		
		Danielle	G	TS	0	0		
1979	2.10	Bob	G	1	20	42		
		Claudette	G	TS	400	840		
		David	E	2	320	672		
		Elena	G	TS	10	21		
		Frederic	G	3	2,300	4,830		
1978	2.25	Amelia	G	TS	20	45		
		Debra	G	TS	0	0		
1977	2.41	Babe	G	1	10	24		
1976	2.58	Belle	E	1	100	258		
		Dottie	E	TS	0	0		
1975	2.76	Eloise	G	3	490	1,352		

Table 3.5: Continued.

<u>Year</u>	<u>Factor</u>	<u>TC</u>	<u>Region</u>	<u>Landfall Intensity</u>	<u>Damage</u>	<u>Normalized 1990 Damage</u>
1974	2.95	Carmen	G	3	150	442
		Subtropical	E	Sub	10	30
1973	3.16	Delia	G	TS	18	57
1972	3.38	Agnes	G	1	31	105
		Carrie	E	TS	2	7
		Dawn	E	TS	0	0
1971	3.62	Doria	E	TS	147	532
		Edith	G	2	25	90
		Fern	G	1	30	109
		Ginger	E	1	10	36
		Heidi	E	TS	0	0
1970	3.87	Alma	E	TS	0	0
		Becky	G	TS	0	0
		Celia	G	3	454	1,757
		Felice	G	TS	0	0
1969	4.14	Camille	G	5	1,421	5,883
		Gerda	E	1	0	0
		Jenny	E	TS	0	0
1968	4.43	Abby	E	TS	1	4
		Candy	G	TS	3	13
		Gladys	E	2	7	31
1967	4.74	Beulah	G	3	230	948
		Doria	E	TS	0	0
1966	5.07	Alma	G	2	10	51
		Inez	E	1	5	25
1965	5.42	Unnamed	G	TS	0	0
		Betsy	E	3	142	770
		Betsy	G	3	1,278	6,926
		Debbie	G	TS	25	136
1964	5.81	Unnamed	E	TS	1	6
		Abby	G	TS	1	6
		Cleo	E	2	128	744
		Dora	E	2	250	1,452
		Hilda	G	3	125	726
		Isabel	E	2	10	58
		Cindy	G	1	13	81
1963	6.21	Cindy	G	1	13	81
		Alma	E	TS	1	7
1962	6.65	Daisy	E	TS	1	7
		Carla	G	4	400	2,844
1961	7.11	Esther	E	TS	6	43

Table 3.5: Continued.

<u>Year</u>	<u>Factor</u>	<u>TC</u>	<u>Region</u>	<u>Landfall Intensity</u>	<u>Damage</u>	<u>Normalized 1990 Damage</u>
1960	7.61	Unnamed	G	TS	4	30
		Brenda	E	TS	5	38
		Donna	E	4	387	2,945
		Ethel	G	1	1	8
		Florence	E/G	TS	0	0
1959	8.15	Arlene	G	TS	1	8
		Cindy	E	1	0	0
		Debra	G	1	7	57
		Unnamed	E	TS	2	16
		Gracie	E	3	14	114
		Judith	E	TS	0	0
1958	8.72	Alma	G	TS	0	0
		Ella	G	TS	0	0
1957	9.33	Unnamed	G	TS	0	0
		Audrey	G	4	150	1,400
		Bertha	G	TS	0	0
		Debbie	G	TS	0	0
		Esther	G	TS	2	19
1956	9.98	Unnamed	G	TS	0	0
		Flossy	G	2	25	250
1955	10.68	Brenda	G	TS	0	0
		Unnamed	G	TS	0	0
		Connie	E	3	40	427
		Diane	E	1	800	8,544
		Ione	E	3	88	940
1954	11.43	Alice	G	TS	0	0
		Barbara	G	TS	0	0
		Carol	E	3	460	5,258
		Edna	E	3	40	457
		Hazel	E	4	252	2,880
		1953	12.23	Alice	G	TS
Barbara	E			1	1	12
Unnamed	E			TS	0	0
Carol	E			1	0	0
Florence	G			1	0.2	2
1952	13.09	Able	E	1	2.8	37
1951	14.00	How	E	TS	2	28
1950	14.98	Baker	G	1	0	0
		Easy	E	3	3.3	49
		King	E	3	28	419
		Love	E	TS	0	0
1949	16.03	I	E	1	0	0
		II	E	3	52	834
		V	G	TS	0	0
		X	G	2	6.7	107

and East Coast/Florida interseasonal destruction amounts and Table 3.7 shows the U.S. total damage amounts, listed by hurricane spawned damage only and by all tropical and subtropical cyclone damage.

Qualitatively, Table 3.6 is in agreement with Fig. 3.23 in that until recently East Coast hurricane damage amounts have been fairly low, while the Gulf Coast damage has been relatively constant throughout the period. This is true even though the mean East Coast (\$873 million) damage is almost identical to the Gulf Coast (\$888 million).

With the available data normalized to account for inflation and coastal growth, we can assess a relative U.S. damage potential based upon the various Saffir-Simpson categories. Table 3.8 shows tropical cyclone damage by various strength storms, both mean and median values. Median values are preferred for some analyses as the mean values are skewed by extreme outliers. Though admittedly a small data set for making an empirical formula for comparing damage amounts, the data illustrates the idea that the stronger hurricanes—especially the Category 3, 4, and 5 cyclones—cause exponentially increased hurricane damage. Note that the tropical storms are given a ‘J’ for potential damage. Cyclones striking the U.S. coast with tropical storm (or minimal hurricane, Category 1) intensify often produced enough beneficial rainfall to more than offset any minor storm surge or wind caused damage. There is also the possibility (or probability) that Table 3.8 may underestimate the damage that the extremely strong cyclones can do. For example, the extremely devastating 1989 Hurricane Hugo made landfall as a Category 4 but caused over \$7 billion in damage, well beyond the \$3 billion median for Category 4 hurricanes. Of the \$74 billion in U.S. damage during the past 41 years, 75% was caused by the intense category 3, 4, and 5 hurricane strikes, even though they comprise only 20% of all landfalling cyclones.

3.2.4 Ranking of Tropical Cyclone Activity

To facilitate discussion of ‘active’ and ‘calm’ hurricane seasons, a ranking was created which is based on the parameters for intense hurricanes as these have shown the largest interseasonal and interdecadal variability. Hurricane seasons are shown ranked by number

Table 3.6: U.S. landfalling tropical cyclone damage (in millions of 1990 dollars) stratified by region (Gulf Coast and East Coast/Florida) and by intensity (tropical storm and Saffir/Simpson categories—any subtropical strikes are indicated in parenthesis).

Year	Gulf Coast Storms					Total(all)
	T/S	Cat 1	Cat 2	Cat 3,4,5	Total(H)	
1949	0		107		107	107
1950		0			0	0
1951					0	0
1952					0	0
1953	0	2			2	2
1954	0,0				0	0
1955	0,0				0	0
1956	0		250		250	250
1957	0,0,0,19			1400	1400	1419
1958	0,0				0	0
1959	8	57			57	65
1960	0,0	8			8	38
1961				2844	2844	2844
1962					0	0
1963		81			81	81
1964	6			726	726	732
1965	0,136			6926	6926	7062
1966			51		51	51
1967				948	948	948
1968	13				0	13
1969				5883	5883	5883
1970	0,0			1757	1757	1757
1971		109	90		199	199
1972		105			105	105
1973	57				0	57
1974				442	442	442
1975				1352	1352	1352
1976					0	0
1977		24			24	24
1978	45,0				0	45
1979	840,21	42		4830	4872	5733
1980	0			591	591	591
1981					0	0
1982	3				0	3
1983				3220	3220	3220
1984					0	0
1985		70,2100	420	1750	4340	4340
1986		3			3	3
1987	9				0	9
1988	3	2,57			59	62
1989	535	107,75			182	717
Mean					888	930

Table 3.6: Continued.

Year	East Coast/Florida Storms					Total(H)	Total(all)
	TS	Cat 1	Cat 2	Cat 3,4,5			
1949		0		834		834	834
1950	0			49,419		468	468
1951	28					0	28
1952		37				37	37
1953	0	12,0				12	12
1954				5258,457,2880		8595	8595
1955		8544		427,940		9911	9911
1956						0	0
1957						0	0
1958						0	0
1959	16,0	0		114		114	130
1960	38,0			2945		2945	2983
1961	43					0	43
1962	7,7					0	7
1963						0	0
1964	6		744,1452,58			2254	2260
1965				770		770	770
1966		25				25	25
1967	0					0	0
1968	4		31			31	35
1969	0	0				0	0
1970	0					0	0
1971	532,0	36				36	568
1972 ¹	7,0					0	7
1973						0	0
1974	(30)					0	30
1975						0	0
1976	0	258				258	258
1977						0	0
1978						0	0
1979			672			672	672
1980						0	0
1981	0,46					0	46
1982	(17)					0	17
1983	0,0					0	0
1984	1		98			98	99
1985	0,0	0		1260		1260	1260
1986		1				1	1
1987		1				1	1
1988	1,3					0	4
1989				7490		7490	7490
Mean						873	892

Table 3.7: U.S. landfalling tropical cyclone damage (in millions of 1990 dollars) by hurricanes (H) and all storms (all).

Year	Total (H)	Total (all)	Year	Total H	Total(all)
1949	941	941	1970	1757	1757
1950	468	468	1971	235	767
1951	0	28	1972	7	112
1952	37	37	1973	0	57
1953	14	14	1974	442	472
1954	8595	8595	1975	1352	1352
1955	9911	9911	1976	258	258
1956	250	250	1977	24	24
1957	1400	1419	1978	0	45
1958	0	0	1979	5544	6405
1959	171	195	1980	591	591
1960	2953	3021	1981	0	46
1961	2844	2887	1982	0	20
1962	0	7	1983	3220	3220
1963	81	81	1984	98	99
1964	2980	2992	1985	5600	5600
1965	7696	7832	1986	4	4
1966	76	76	1987	1	10
1967	948	948	1988	59	66
1968	31	48	1989	7672	8207
1969	5883	5883			
			Mean	1735	1823
			S. D.	2719	2841

Table 3.8: Summary of U.S. tropical cyclone spawned damage (in 1990 dollars) by category of cyclone.

Intensity (cases)	Mean Damage	Median Damage	"Potential Damage"	Percent of Total Damage
Tropical Storm (60)	\$40,000,000	< \$1,000,000	0	3
Hur.—Cat 1 (28)	423,000,000	24,000,000	1	16
Hur.—Cat 2 (11)	361,000,000	107,000,000	4	6
Hur.—Cat 3 (19)	1,741,000,000	940,000,000	40	44
Hur.—Cat 4 (5)	3,512,000,000	2,880,000,000	120	23
Hur.—Cat 5 (1)	5,883,000,000	5,883,000,000	240	8

of intense hurricane days and, in the case of equivalent hurricane day values, by HDP in Table 3.9. The predominance of the 1950's and 1960's as more active years (nine out of the top ten) is in stark contrast to the 1970's and 1980's (eight of the ten calmest years).

Table 3.9: Atlantic basin tropical cyclone activity ranked by seasonal total of intense hurricane days (and HDP) from 1949 to 1989.

Intense Hurricane				Intense Hurricane			
Rank	Year	Days	HDP	Rank	Year	Days	HDP
1.	1961	24.50	183	22.	1959	4.25	63
2.	1950	18.75	213	23.	1974	4.25	46
3.	1955	17.25	171	24.	1985	4.00	61
4.	1964	14.75	149	25.	1981	3.75	63
5.	1960	11.00	80	26.	1978	3.50	40
6.	1989	10.75	108	27.	1956	2.75	40
7.	1958	9.50	100	28.	1975	2.25	54
8.	1954	9.50	99	29.	1982	1.25	18
9.	1966	8.75	126	30.	1971	1.00	65
10.	1951	8.25	120	30.	1976	1.00	65
11.	1988	8.00	81	32.	1970	1.00	18
12.	1965	7.50	78	32.	1977	1.00	18
13.	1980	7.25	126	34.	1984	0.75	42
14.	1963	7.00	111	35.	1962	0.50	26
15.	1969	6.75	114	36.	1987	0.50	11
16.	1952	6.75	73	37.	1973	0.25	24
17.	1953	6.75	61	38.	1983	0.25	8
18.	1957	6.50	71	39.	1986	0.00	23
19.	1967	5.75	102	40.	1968	0.00	21
20.	1979	5.75	73	41.	1972	0.00	14
21.	1949	5.25	68				

3.2.5 Overestimation of Intense Hurricanes and Removal of Bias

One can question the accuracy of 1950's and 1960's intense hurricane day values, especially during the early days of hurricane reconnaissance. The extreme decadal differences in intense hurricane activity between the 1950's/1960's and the 1970's/1980's suggest that the procedure for tropical cyclone intensity analysis may have changed and inadvertently led to an artificial decline in strong cyclones.

To test this hypothesis, we examined the wind-pressure relationships between the two periods. A simplified empirical relationship between maximum sustained wind speeds

and concurrent surface central pressures for Atlantic tropical cyclones was given by Kraft (1961):

$$V_{max} = 14 * (1013 - P_c)^{.5}$$

where

V_{max} is the maximum sustained wind speed (in kt)

and

P_c is the minimum sea level pressure (in mb).

One advantageous feature of the Best Track (i.e., HURDAT) data set is that whereas wind speeds are reported for every six hours of the tropical cyclone's existence even if an estimation was required, "all [central] pressures on HURDAT are observed and that no pressures were determined from the winds" (Jarvinen *et al.*, 1984). Since there have been no appreciable changes in the measurement procedures for surface pressure (barometric readings aboard ships and during landfall, and aircraft dropwindsondes), one can deduce that changes in the wind pressure relationship were due to changes in the technique for measuring (estimating) sustained wind speeds.

The Best Track data set reports the maximum sustained wind speeds in five knot intervals. To attempt a more precise estimate of the strength of the cyclones is not possible with the uncertainties of the various observational platforms. Table 3.10 presents the means and standard deviations of the pressure readings, stratified for the decades under consideration. Note the general trend to lower pressure values for a given wind speed category; supporting the proposition that during the 1950's and 1960's wind speeds were somewhat overestimated. It is also interesting that standard deviations of the pressure values were much larger during the first two decades, suggesting that there was more uncertainty as to what wind speed to assign to strong hurricanes.

Table 3.11 was constructed to ascertain period bias. This table shows a combined decadal classification containing at least ten cases per wind division. The corresponding wind speed suggested by Kraft's relationship is also included, next to the observed min-

Table 3.10: Means and standard deviations of observed minimum pressures from Atlantic basin tropical cyclones by five knot intervals for the last four decades. Number of observations are in parenthesis.

Wind Speed (kt)	1949–1959			1960–1969			1970–1979			1980–1989		
	#	Mean (mb)	SD (mb)	#	Mean (mb)	SD (mb)	#	Mean (mb)	SD (mb)	#	Mean (mb)	SD (mb)
100	(11)	969	20	(51)	968	10	(13)	967	8	(30)	961	9
105	(12)	964	13	(29)	962	13	(8)	960	3	(18)	958	6
110	(21)	958	15	(52)	961	12	(12)	954	9	(22)	953	6
115	(5)	963	23	(22)	956	14	(8)	949	5	(17)	949	7
120	(3)	961	8	(33)	950	11	(8)	947	8	(26)	940	5
125	(13)	958	13	(17)	943	9	(5)	937	4	(12)	938	9
130	(5)	944	12	(14)	939	12	(5)	937	9	(6)	934	7
135	(3)	947	25	(5)	942	10				(2)	934	11
140	(2)	943	5	(6)	928	15	(3)	933	7	(5)	919	14
145				(1)	935	—	(4)	926	2	(4)	914	15
150				(1)	935	—	(3)	925	1	(1)	940	—
155										(5)	912	14
160										(1)	888	—
165				(1)	909	—				(1)	899	—

imum pressure. As the criterion used to define intense hurricanes and intense hurricane days is a threshold of 50 ms^{-1} (96 kt, see section 1.1.1), the decadal bias should be centered around that intensity value. Strong hurricanes which have recently been described as 100 kt cyclones have been observed to carry a mean minimum sea level pressure of 963 mb, almost precisely the pressure specified for a 100 kt hurricane by Kraft's equation. However, the 100 kt hurricanes in the 1950's and 1960's were observed to have mean pressures of 968 mb, giving an equivalent Kraft wind speed of only 94 kt. Actually, the 105 kt hurricanes of the earlier period have the minimum required pressure (and Kraft derived wind speed) for an intense Category 3 hurricane. There is even a larger 10 to 15 kt bias for stronger storms but, since the threshold for intense hurricane categorization is at 100 kt, that bias will not affect intense hurricane and intense hurricane day calculations (though it would affect HDP).

Therefore, to remove the 5 kt bias at the intense hurricane threshold for the seasons of 1949 to 1989, we simply revised the threshold of intense hurricane status upward to 105 kt for the years prior to 1970. This adjustment effectively reduced the numbers of intense hurricanes and intense hurricane days during the earlier period by 15-25%. The resulting

Table 3.11: Means of observed minimum pressures from Atlantic basin tropical cyclones by five knot intervals for two decadal groupings. Number of cases are shown in parenthesis. The Kraft suggested wind speed corresponding to the mean minimum pressures are also provided.

Wind Speed (kt)	1949-1969			1970-1989		
	#	Mean (mb)	Kraft's Wind (kt)	#	Mean (mb)	Kraft's Wind (kt)
100	(62)	968	94	(43)	963	99
105	(41)	963	99	(26)	959	103
110	(73)	960	102	(34)	953	108
115	(27)	957	105	(25)	949	112
120	(36)	951	110	(34)	942	118
125	(30)	950	111	(17)	937	122
130	(19)	940	120	(11)	935	124

values are depicted in Fig. 3.24 with a linear trend line superimposed. Table 3.12 provides the original data in both tabular form with and without the bias removed. However, as the new trend lines show, bias in the 1950's and 1960's storm strength only accounts for a small portion of the long term trend in the number and duration of intense Atlantic basin hurricanes. The bias is not a factor in the counts of U.S. landfalling intense hurricanes as those were based upon actual measured minimum pressures. The reduction in both overall strong hurricane activity and in U.S. landfalling intense cyclones is thus believed to be a manifestation of a real physical change in the ocean-earth-atmosphere system.

3.2.6 African Easterly Wave Genesis Variability Versus Tropical Cyclone Intensity

An important consideration in understanding the intra- and interseasonal variability of the Atlantic basin tropical cyclones lies in understanding their origins. A change in the availability or intensity of African spawned easterly waves, for example, could lead to substantial tropical cyclone variability. Information on the origins for all Atlantic basin named storms from 1967 to 1989 were made available for this study. The recent beginning date, 1967, is due to the lack of continuous satellite surveillance to trace tropical storm and hurricane "seedlings" (first described as such in Simpson *et al.*, 1968).

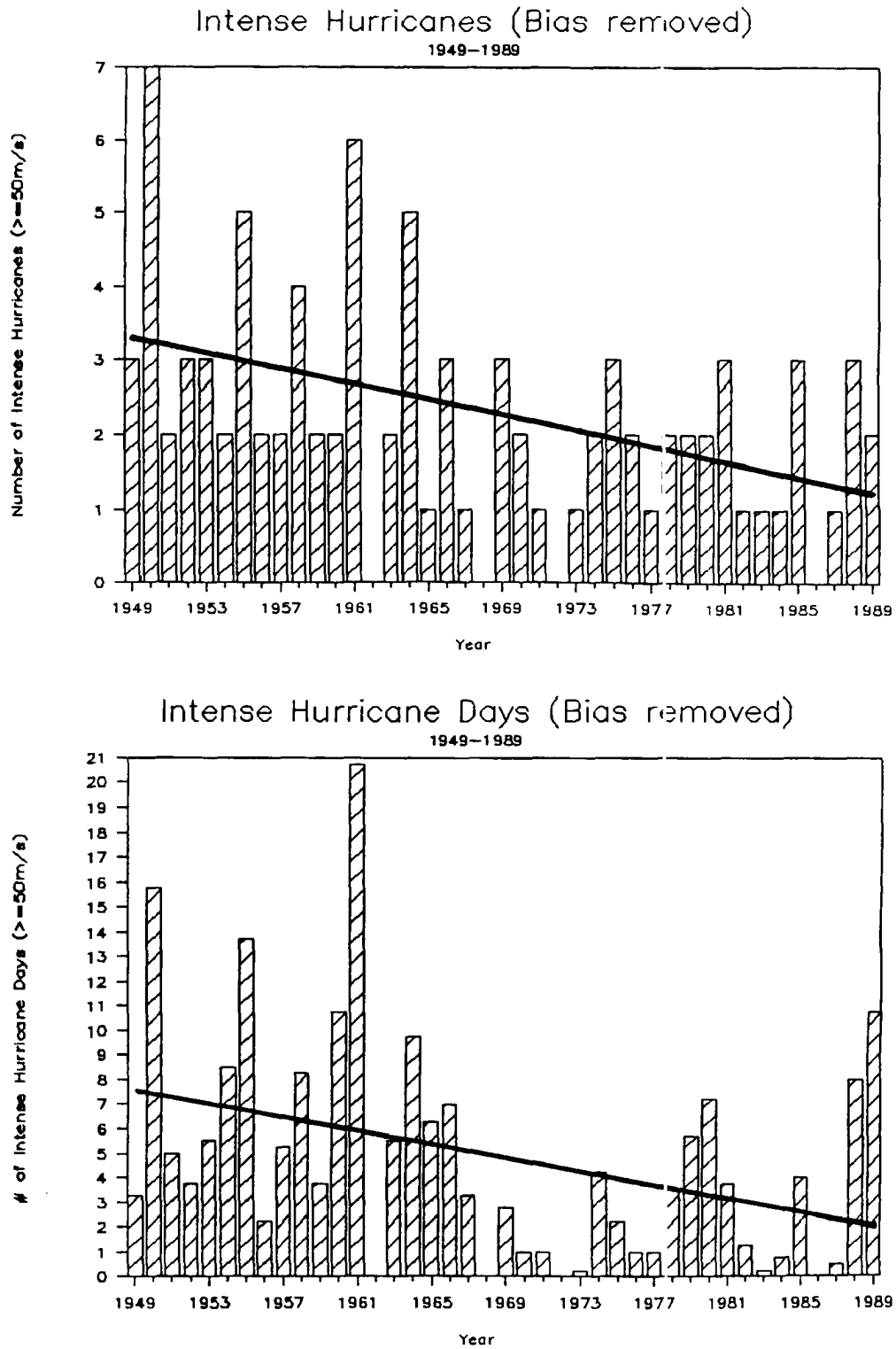


Figure 3.24: Atlantic basin intense hurricane (upper panel) and intense hurricane days (bottom panel) with a 5 kt bias removed from the data with a linear trend line superimposed.

Table 3.12: Atlantic basin intense hurricanes and intense hurricane days from original data set and with a 5 kt bias removed.

Year	Intense Hur.	Intense Hur. [bias out]	Intense Hur. Days	Intense Hur. Days [bias out]	Year	Intense Hur.	Intense Hur. [bias out]	Intense Hur. Days	Intense Hur. Days [bias out]
1949	3	3	5.25	3.25	1970	2	2	1.00	1.00
1950	8	7	18.75	15.75	1971	1	1	1.00	1.00
1951	5	2	8.25	5.00	1972	0	0	0.00	0.00
1952	3	3	6.75	3.75	1973	1	1	0.25	0.25
1953	4	3	6.75	5.50	1974	2	2	4.25	4.25
1954	2	2	9.50	8.50	1975	3	3	2.25	2.25
1955	6	5	17.25	13.75	1976	2	2	1.00	1.00
1956	2	2	2.75	2.25	1977	1	1	1.00	1.00
1957	2	2	6.50	5.25	1978	2	2	3.50	3.50
1958	5	4	9.50	8.25	1979	2	2	5.75	5.75
1959	2	2	4.25	3.75	1980	2	2	7.25	7.25
1960	2	2	11.00	10.75	1981	3	3	3.75	3.75
1961	7	6	24.50	20.75	1982	1	1	1.25	1.25
1962	1	0	0.50	0.00	1983	1	1	0.25	0.25
1963	2	2	7.00	5.50	1984	1	1	0.75	0.75
1964	6	5	14.75	9.75	1985	3	3	4.00	4.00
1965	1	1	7.50	6.25	1986	0	0	0.00	0.00
1966	3	3	8.75	7.00	1987	1	1	0.50	0.50
1967	1	1	5.75	3.25	1988	3	3	8.00	8.00
1968	0	0	0.00	0.00	1989	2	2	10.75	10.75
1969	5	3	6.75	2.75					
					Mean	2.5	2.2	5.8	4.8
					S.D.	1.9	1.5	5.5	4.6

Avila (1990) has shown that the incidence of tropical waves has been relatively constant from year to year, ranging from 49 to 69 with no obvious relationship to the concurrent incidence of tropical storms and hurricanes. Avila has reported a drop in the number of tropical depressions, especially since 1982, but this trend may be artificially induced through changes in classification procedure for satellite pictures. Another piece of evidence suggesting little change in number of easterly wave spawned depressions is the lack of a significant downward trend in the number of named storms (section 3.2.1).

What can be analyzed with some degree of confidence are the differences in the relative contributions easterly waves make toward the frequency of tropical cyclones of various strengths (Table 3.13). Note in Table 3.13 that intense hurricanes is the only category that has more than a two thirds easterly wave origin. When we analyze Western Sahel rainfall in comparison to the easterly wave contributions in section 5.9.4, we see a substantial modulation of the easterly wave contribution.

Table 3.14 lists all intense hurricanes since 1967, along with their origins as designated by Avila (personal communication). Note that nearly all intense hurricanes are generated

Table 3.13: Absolute and relative contribution of easterly waves toward the genesis of various tropical cyclone categories using data from 1967 to 1989. Mean annual values are shown in parenthesis.

Category	Total Number	Easterly Waves	Others	Percent from Easterly Waves
Named Storms	205 (8.9)	128 (5.6)	77 (3.3)	62 %
Hurricanes	122 (5.3)	80 (3.5)	42 (1.8)	66 %
Intense Hurricanes	39 (1.7)	34 (1.5)	5 (0.2)	87 %

from African-spawned easterly waves, with the remainder due to upper tropospheric cold lows and quasi-stationary frontal regions.

Table 3.14: A tabular breakdown of origins attributed to intense (Category 3, 4, or 5) hurricanes since 1967 (from Avila, personal communication).

Year	Cyclone Name	Easterly Wave	Cold Low	Frontal Zone
1967	Beulah	X		
1969	Camille	X		
	Debbie	X		
	Francelia	X		
	Gerda		X	
	Inga	X		
1970	Celia	X		
	Ella	X		
1971	Edith	X		
1973	Ellen	X		
1974	Becky		X	
	Carmen	X		
1975	Caroline	X		
	Eloise	X		
	Gladys	X		
1976	Belle	X		
	Frances	X		
1977	Arita	X		
1978	Ella			X
	Greta	X		
1979	David	X		
	Frederic	X		
1980	Allen	X		
	Frances	X		
1981	Floyd	X		
	Harvey	X		
	Irene	X		
1982	Debby	X		
1983	Alicia			X
1984	Diana			X
1985	Elena	X		
	Gloria	X		
	Kate	X		
1987	Eraily	X		
1988	Gilbert	X		
	Helene	X		
	Joan	X		
1989	Gabrielle	X		
	Hugo	X		

Chapter 4

AFRICAN RAINFALL VARIABILITY

As discussed in section 1.2, Gray (1987) linked the general downtrend in Atlantic basin tropical cyclone activity to the Sahel drought. While the incidence of named storms and hurricanes showed little multidecadal (i.e., 1947–1969 versus 1970–1986) variation, the frequency and duration of intense hurricanes showed a two to one decrease between the earlier versus the later period. The analysis of Sahelian rainfall by Lamb (1985) also showed a large precipitation decrease starting around 1970. It was from there that detailed research began into the association between these two meteorological phenomena.

4.1 Lamb Index

Lamb (1978b) created a standardized index of April to October Subsaharan rainfall using 20 stations, ranging from 11 to 18° North and from 8° East to the western coast of Africa (Fig. 4.1). This index, herein referred to as the 'Lamb Index', represents the monsoonal rainfall for the western and central Sahel regions. In his original study, Lamb utilized data for 1941 to 1974. Here, the Lamb Index is updated through 1989 (Fig. 4.1). It is obvious that the 1950's and 1960's were substantially rainier than the 1970's and 1980's, with the exceptions of 1988 and 1989.

Lamb also uses the methodologies of Kraus (1977) (see Chapter 1) for combining rainfall station data. In general, the 20 station locations chosen are relatively well dispersed and have a fairly complete record. Table 4.1 describes the individual station locations, April to October rainfall means and standard deviations, the number of years available (out of a possible 41), and how strongly each station individually correlate to the Lamb Index itself. (Latitudes, longitudes, years of record and other station information can be

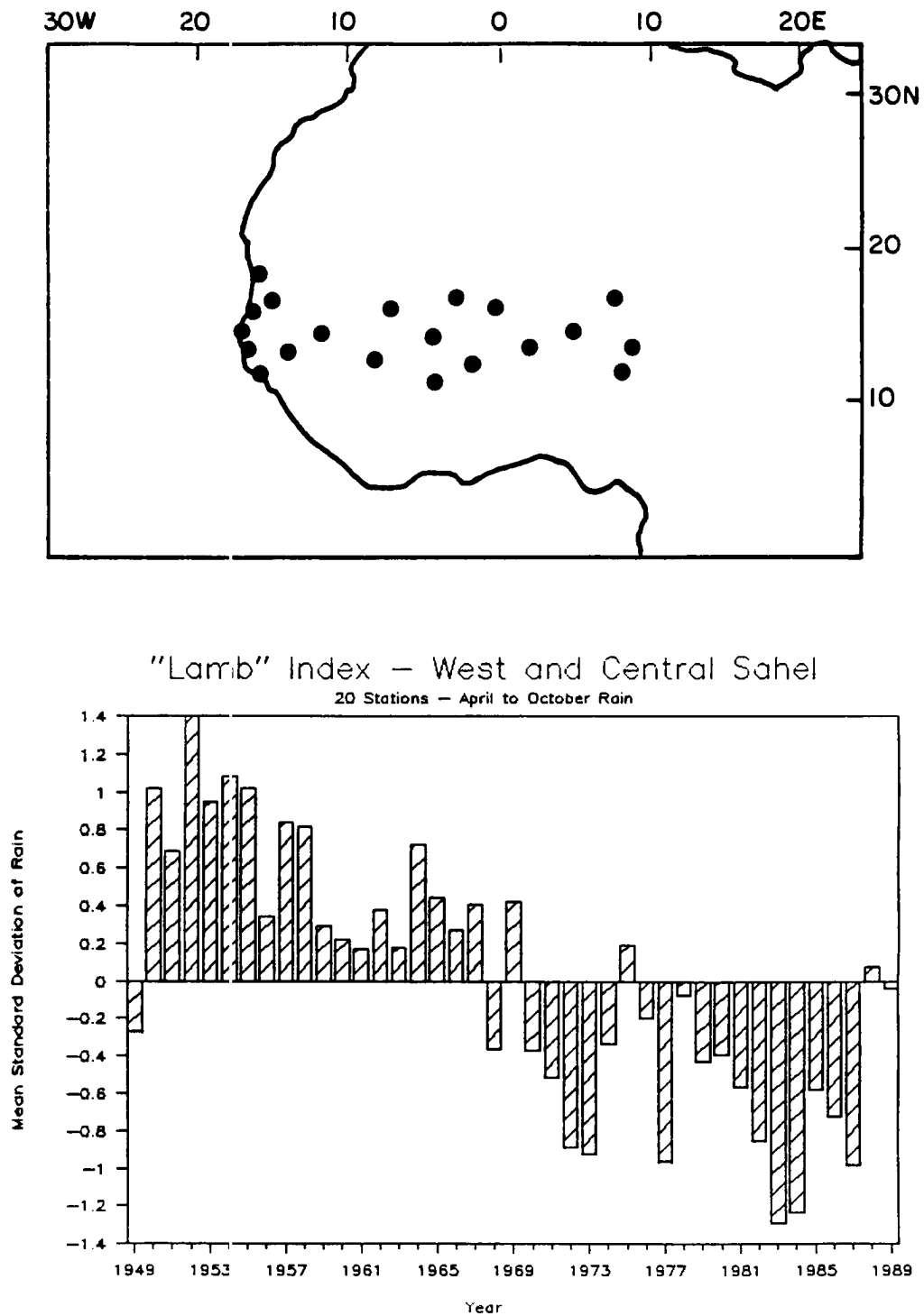


Figure 4.1: Location of the 20 rainfall stations utilized in the Lamb Index (top panel). Mean standard deviations of rainfall for the 20 station April to October Lamb Index of the western and central Sahel (bottom panel). (Updated and modified from Lamb (1978b).)

accessed in Appendix 1.) The stations used in the index show a huge range of rainfall means—from 95 mm in Nouakchott, Mauritania to 1733 mm at Bissau Airport, Guinea-Bissau. These values cover the whole range of climates characterized by Nicholson (1979) as Sahelo-Sahara (50–100 mm), Sahel (100–400 mm), Soudan (400–1200 mm), and rain-forest (>1200 mm). Even so, almost all the stations correlate with the Lamb Index at values greater than $r = 0.60$; the exceptions (Saint Louis, Senegal; Ouagadougou and Bobo Dioulasso, Burkina Faso) are either coastal location or are on the southern fringe of the data network.

Table 4.1: The 20 stations used in the Lamb Index: CSU Rainfall Data Base identification number, station name and country, April to October mean and standard deviation (in mm), years of data in analysis, correlation coefficients versus the Lamb Index, and correlation coefficient versus intense hurricane days. (Asterisks refer to significance levels: 0.100 for ‘*’, 0.025 for ‘**’, and 0.005 for ‘***’.)

Station	Rainfall Data			Correlation	vs. Intense	
	Mean	SD	Yrs	vs. Index	Hurr. Days	
				r	r	
0102 Agadez, Niger	136.3	64.09	41	0.714	0.540	***
0107 Niamey-Aero, Niger	558.1	150.40	41	0.679	0.338	**
0108 Birni N’Konni, Niger	528.2	145.65	41	0.798	0.366	**
0111 Zinder-Aero, Niger	453.5	127.53	41	0.771	0.547	***
0117 Tombouctou, Mali	178.7	58.47	41	0.605	0.426	***
0118 Gao, Mali	222.5	80.00	40	0.707	0.369	**
0123 Kayes, Mali	669.7	129.76	41	0.705	0.436	***
0124 Mopti, Mali	510.7	130.03	41	0.751	0.277	*
0140 Noukchott, Mauritania	94.9	60.03	41	0.802	0.559	***
0145 Nema, Mauritania	258.3	97.93	41	0.795	0.428	***
0148 Saint Louis, Senegal	292.8	137.30	41	0.535	0.470	***
0149 Podor, Senegal	257.6	126.33	41	0.673	0.634	***
0152 Dakar/Yoff, Senegal	470.9	209.20	41	0.740	0.595	***
0157 Tambacounda, Senegal	809.3	198.73	41	0.696	0.463	***
0162 Bathurst/Yundum, Gambia	1090.9	321.32	41	0.874	0.531	***
0163 Bissau Airport, Guinea-Bissau	1732.7	387.81	40	0.716	0.572	***
0453 Kano, Nigeria	772.9	188.76	40	0.697	0.391	**
0485 Ouagadougou, Burkina	815.5	156.24	41	0.446	0.051	
0487 Bobo Dioulasso, Burkina	1055.6	228.42	41	0.545	0.307	**
0619 Bamako Ville, Mali	1002.8	184.71	41	0.654	0.399	***

Also shown in Table 4.1 are the individual station correlations versus intense hurricane days. Very strong correlations (greater than $r = 0.50$) are found for the western Sahel region (Mauritania, Senegal, The Gambia, and Guinea-Bissau stations) as well as in central Niger. The entire Lamb Index correlates from the intense hurricane days as strongly as

with the largest individual station correlation, at $r = 0.63$. Removing the long term bias (described in section 3.2.5), reveals a slightly smaller correlation of $r = 0.55$. Both relationships are depicted in the scatter plots of Fig. 4.2. Note that rainfall conditions that are drier than a Lamb Index of -0.80 are associated with negligible intense hurricane activity. This implies that there may be a certain threshold value of rain in this region, below which essentially no intense hurricane activity occurs. (Also see section 5.7.).

Other tropical cyclone parameters also show high correlations with the Lamb Index, though not as high as for intense hurricane activity (Table 4.2). Note that all tropical cyclone parameters are significantly correlated at a level of 0.005, except named storms which are significant at a 0.025 level.

Table 4.2: Correlation coefficients for April to October Lamb Index rainfall values versus Atlantic basin tropical cyclone parameters. (Asterisks refer to significance levels: 0.100 for ‘*’, 0.025 for ‘**’, and 0.005 for ‘***’.)

Tropical Cyclone Parameter	Correlation Coefficient	Tropical Cyclone Parameter	Correlation Coefficient
Named Storms	0.36 **	Named Storm Days	0.50 ***
Hurricanes	0.47 ***	Hurricane Days	0.61 ***
Intense Hurricanes	0.60 ***	Intense Hurricane Days	0.63 ***
Int. Hur. (Bias Out)	0.55 ***	Int. Hur. Days (Bias Out)	0.55 ***
HDP	0.64 ***		

This analysis of Lamb’s Index reveals that a strong concurrent rainfall—tropical cyclone association is present, especially for the westernmost Sahel. This association is strongest for the intense hurricanes, the ones that we documented as causing three quarters of all tropical cyclone spawned damage in the United States. Also, if specifying the strength of the monsoon by 1 August is possible, an additional strong predictive parameter can be added to the seasonal hurricane forecast scheme.

The remainder of this chapter examines the annual march of African monsoon rainfall and for the strongest spatial and temporal rainfall patterns for both the concurrent and predictive correlations with intense hurricane activity.

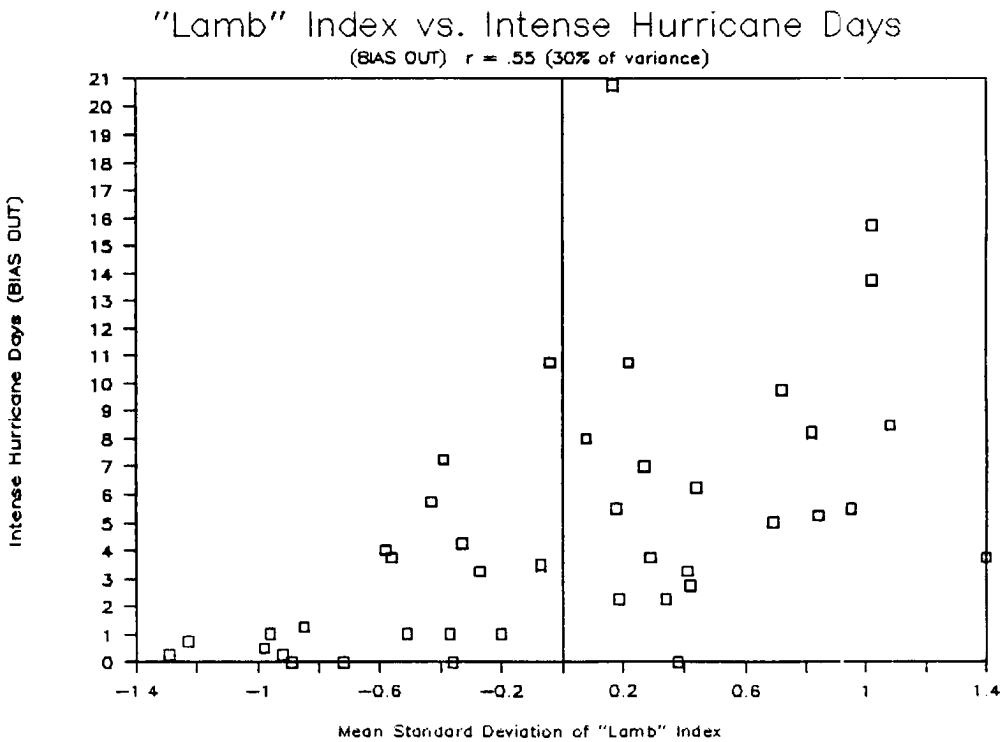
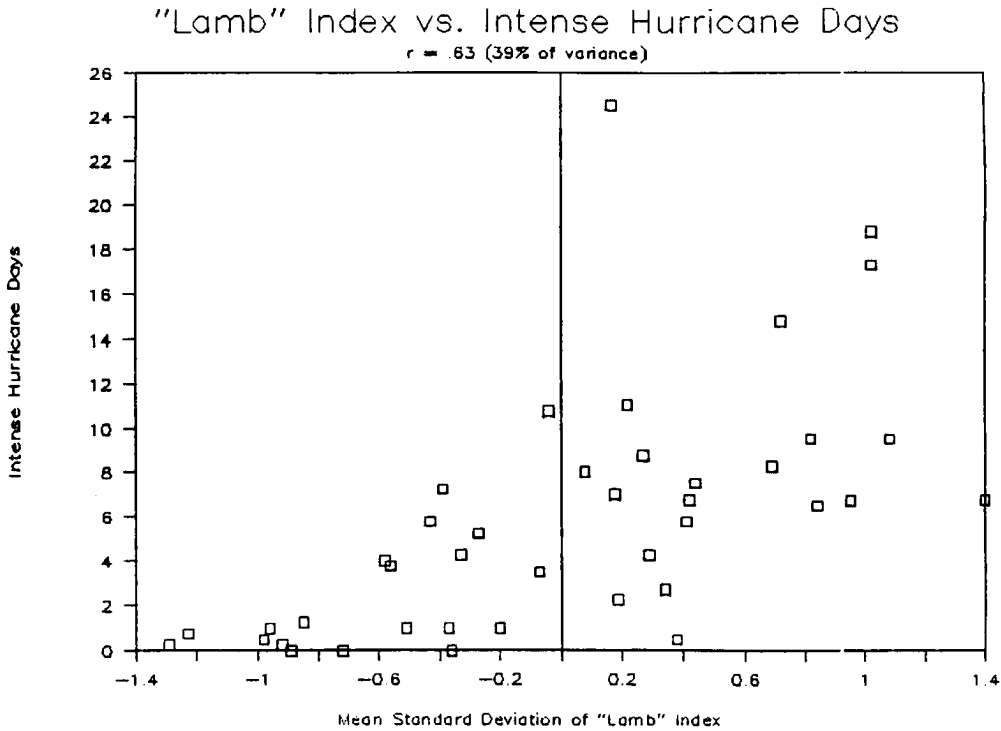


Figure 4.2: Scatter plot of 1949 to 1989 values of April to October Lamb Index rainfall versus intense hurricane activity. The top panel presents the original data correlations that relate at $r = 0.63$. The bottom panel utilizes intense hurricane day data with the overestimation bias removed. With this bias out, the rain and intense hurricane activity correlate at $r = 0.55$.

4.2 The Annual Cycle

African rainfall is related primarily to the annual movement of the ITCZ or African monsoonal trough (Fig. 4.3). The latitude of the rainfall maximum migrates over 2000 km, from 8° North to 11° South. The ITCZ is also impressive in its latitudinal extent as measured by the 100 mm isohyet, extending meridionally for almost 2000 km. Direct midlatitude baroclinic influences are relatively minor, with wintertime rainfall observed only at the most poleward ($> 30^\circ$ latitude) portions of the continent.

Note in the annual mean map (Fig. 4.4), that significant precipitation does not fall over about half of northern Africa. The 100 mm isohyet reaches only to about 18° North, in association with the most northward extent of the ITCZ. Small areas near 30° North are associated with the southward extent of the midlatitude baroclinic systems. This can be taken to define the range of the Saharan desert. Table 4.3 summarizes the monthly extent of both monsoon and midlatitudinal rainfall. For this study the “monsoon rainfall maximum” is defined as the centroid of the monthly 100 mm rainfall area.

Table 4.3: Monthly latitudinal extent of the monsoonal rainfall maximum, the northernmost position of the Northern Hemisphere’s monsoonal 10 mm isohyet and the southernmost position of the Northern Hemisphere’s midlatitude 10 mm isohyet.

Month	Monsoonal Rainfall Maximum	Monsoonal 10 mm Isohyet	Midlatitude 10 mm Isohyet
January	11°S	7°N	30°N
February	10°S	8°N	31°N
March	6°S	10°N	32°N
April	1°S	12°N	32°N
May	3°N	14°N	33°N
June	6°N	17°N	34°N
July	8°N	19°N	—
August	8°N	22°N	—
September	5°N	20°N	34°N
October	1°N	15°N	31°N
November	5°S	10°N	31°N
December	10°S	8°N	30°N

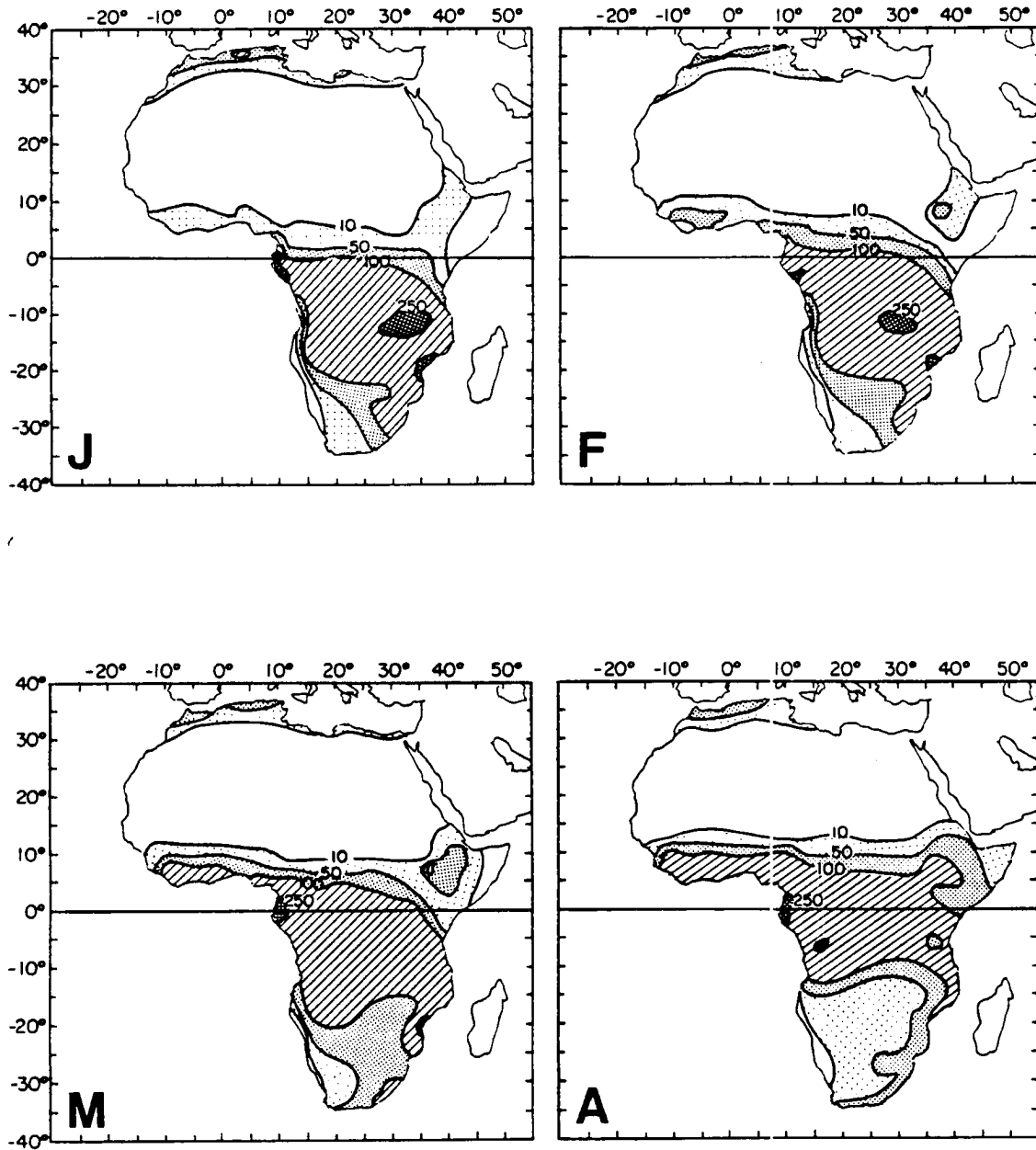


Figure 4.3: Monthly mean precipitation maps of Africa using data from 1949 to 1989. Contours are at 10, 50, 100, 250, 500, and 1000 mm. Month is indicated in lower left corner.

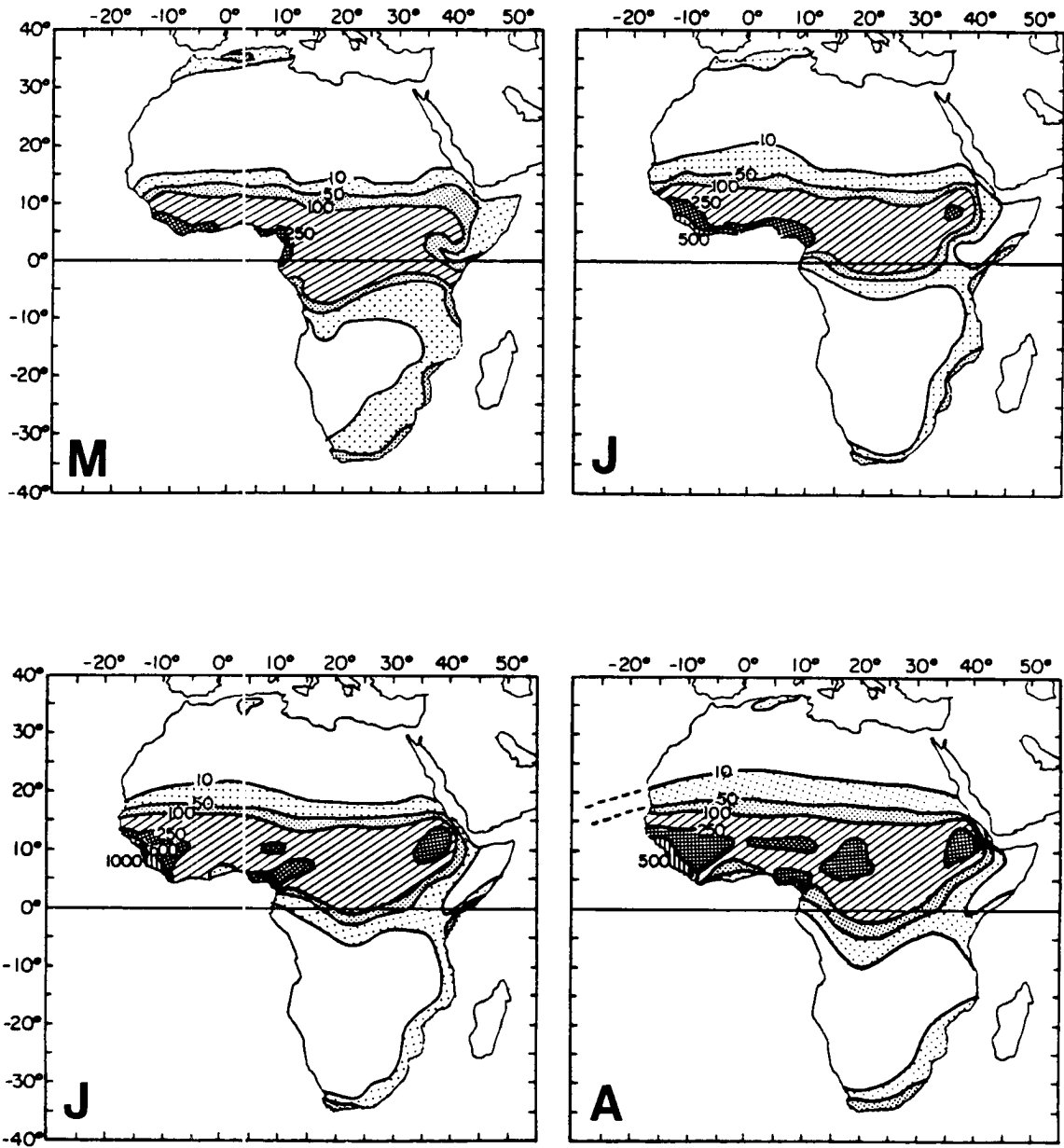


Figure 4.3: Continued.

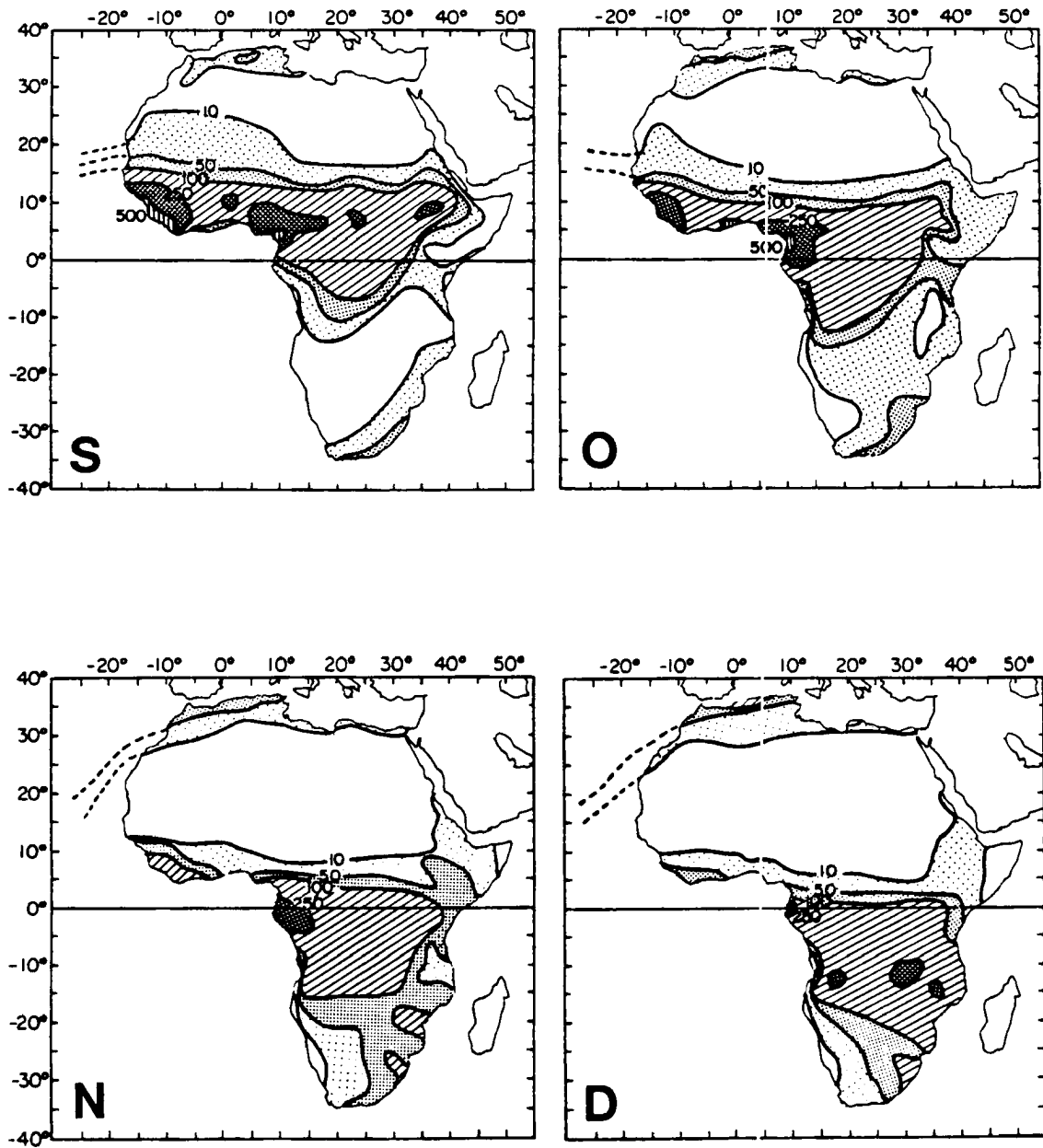


Figure 4.3: Continued.

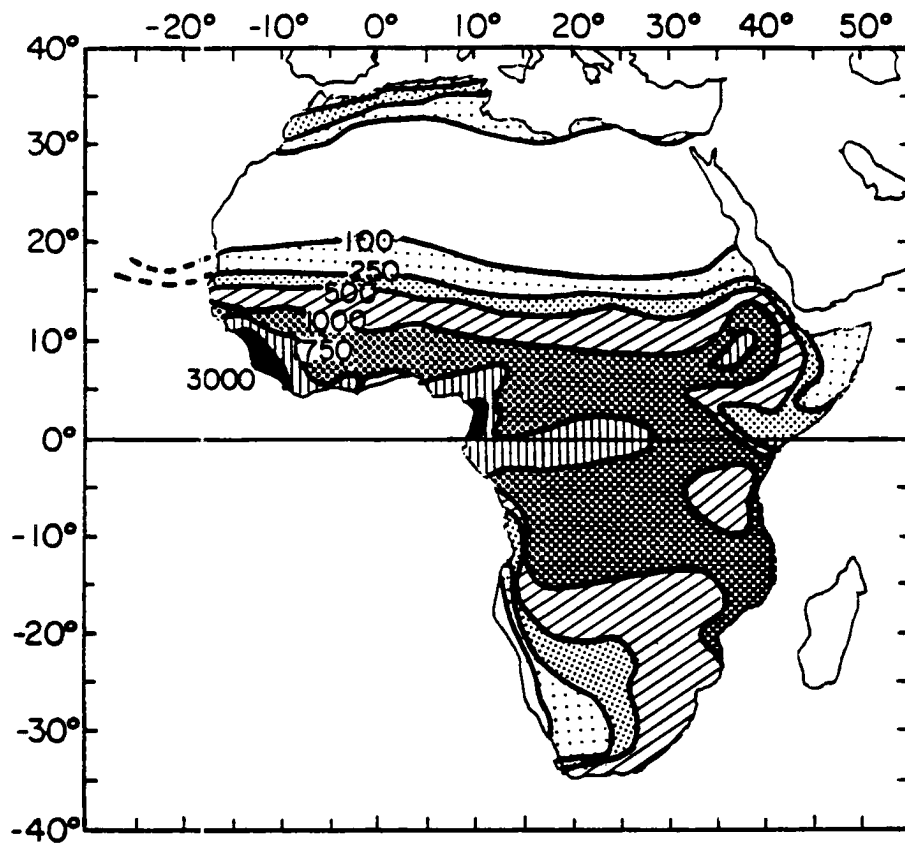


Figure 4.4: Annual mean precipitation over Africa using 1949 to 1989 data. Contours are at 100, 250, 500, 1000, 1750, and 3000 mm.

It is during the northern hemisphere summer monsoon season when substantial rainfall occurs north of 12°N that the Sahel gets almost all of its precipitation. Figure 4.5 depicts the percentage of annual total precipitation which falls during June to September. Note that the Sahel region could be broadly defined as stations that receive over 87.5% of their annual precipitation in this four month period. The area specified by such a definition would stretch almost in straight lines across northern Africa from 12° to 20°N .

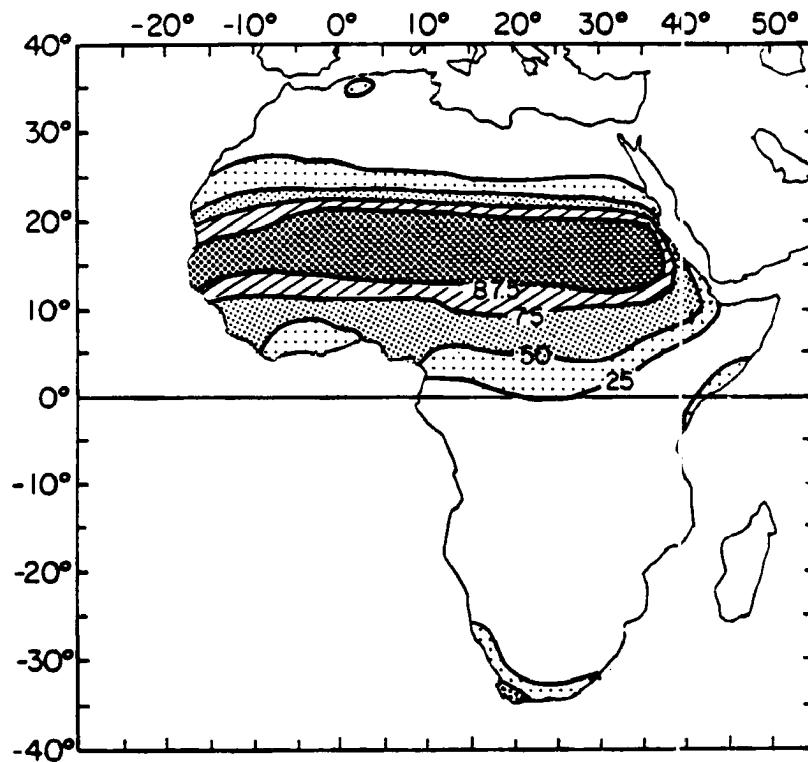


Figure 4.5: Percentage of June through September precipitation to the annual mean using data from 1949 to 1989. Contours are at 25, 50, 75, and 87.5%.

From approximately 10°N to 10°S , Africa has two distinct rainfall maxima, one each during spring and fall. It is this second (fall) rainfall maximum along the Gulf of Guinea coast that appears to play an essential part in the following year's northern hemisphere's monsoon strength (section 4.4).

4.3 Correlation with Current Year Tropical Cyclones

Given that the Lamb Index for 1949 to 1989 has a very strong relationship with tropical cyclones and that over 98% of the associated rainfall in the April to October period falls after 1 June, it becomes likely that an even stronger concurrent correlation can be developed between tropical cyclones and the Sahel monsoon rainfall. Certain regions within Lamb's station network, especially in the westernmost Sahel, showed the highest correlations. Also it is possible that some portions of the rainy season contribute little or nothing to the signal between cyclones and rainfall.

The next step was an analysis of monthly data using linear correlation coefficients between monthly rainfall of individual stations versus seasonal intense hurricane days. Intense hurricane days are used for the criterion to be correlated against because, as previously discussed, they show the largest year to year variability (by coefficient of variation), experience the greatest interdecadal trend (by linear best fit), and cause the vast majority of hurricane related damage in the U.S. Four hundred and three stations throughout Africa which had a minimum of 12 years (between 1949 and 1989) of rainfall data and were utilized for this analysis. The locations of individual stations are listed in Appendix 1.

Figure 4.6 presents smoothed fields of linear correlation coefficients obtained on a month by month basis for stations that had monthly mean rainfall of at least 10 mm. For example, the first diagram shows correlations for January rainfall versus intense hurricane activity that occurred later, during the hurricane season (i.e., in August through October). These January to July maps show any predictive (for intense hurricane activity) correlations, the August to October diagrams show concurrent relationships, and the November and December figures depict antecedent associations.

Each map presents areas of positive and negative correlations. A significant association required that the rainfall-hurricane correlation show persistence for at least three months with a strength of at least $r = \pm 0.30$. For instance, the Gulf of Guinea region por-

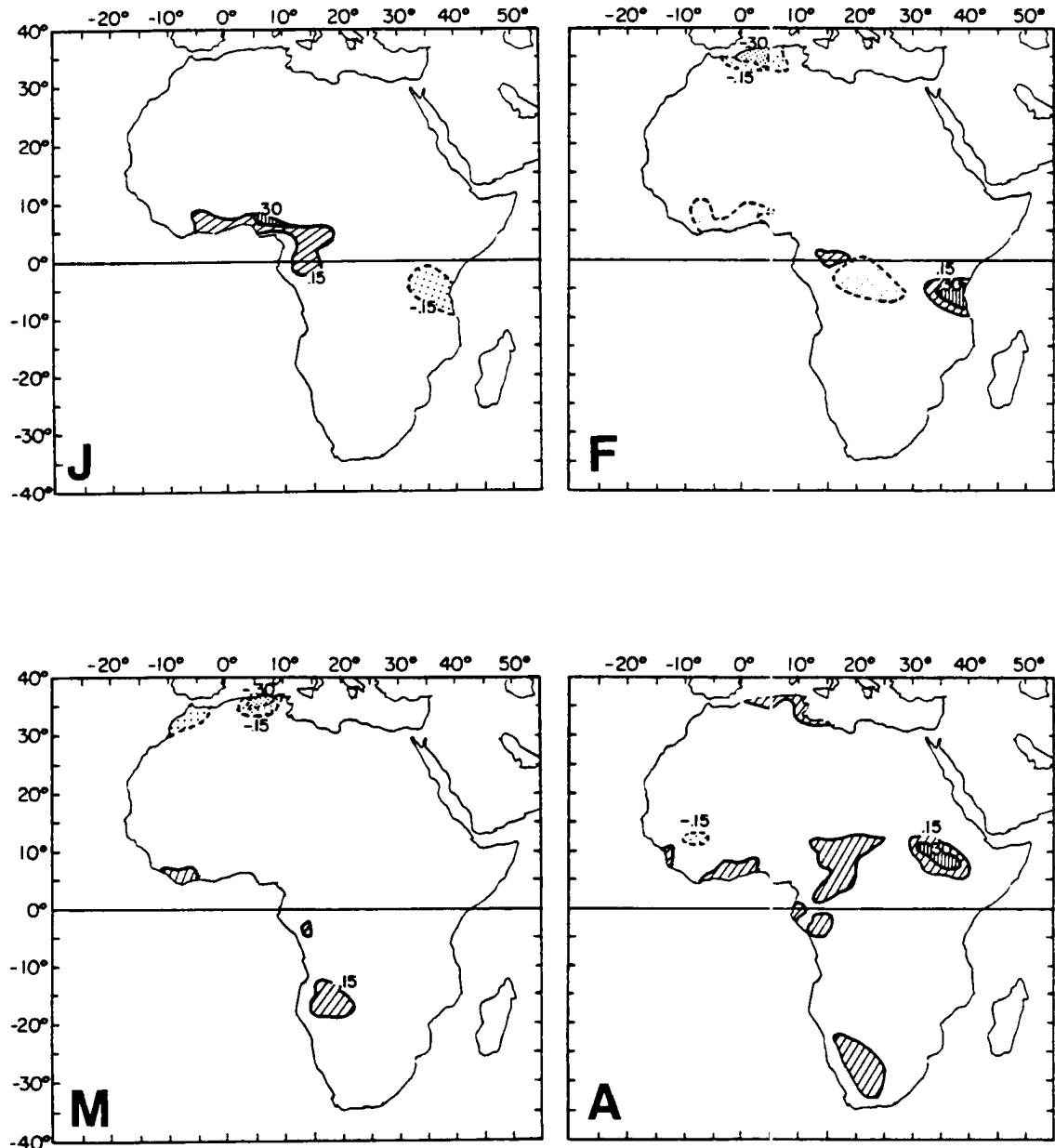


Figure 4.6: Smoothed values of linear correlation coefficients for individual station monthly rainfall versus seasonal intense hurricane days. Contours are at $r = \pm 0.15, 0.30, \text{ and } 0.45$. Month is indicated in lower left corner.

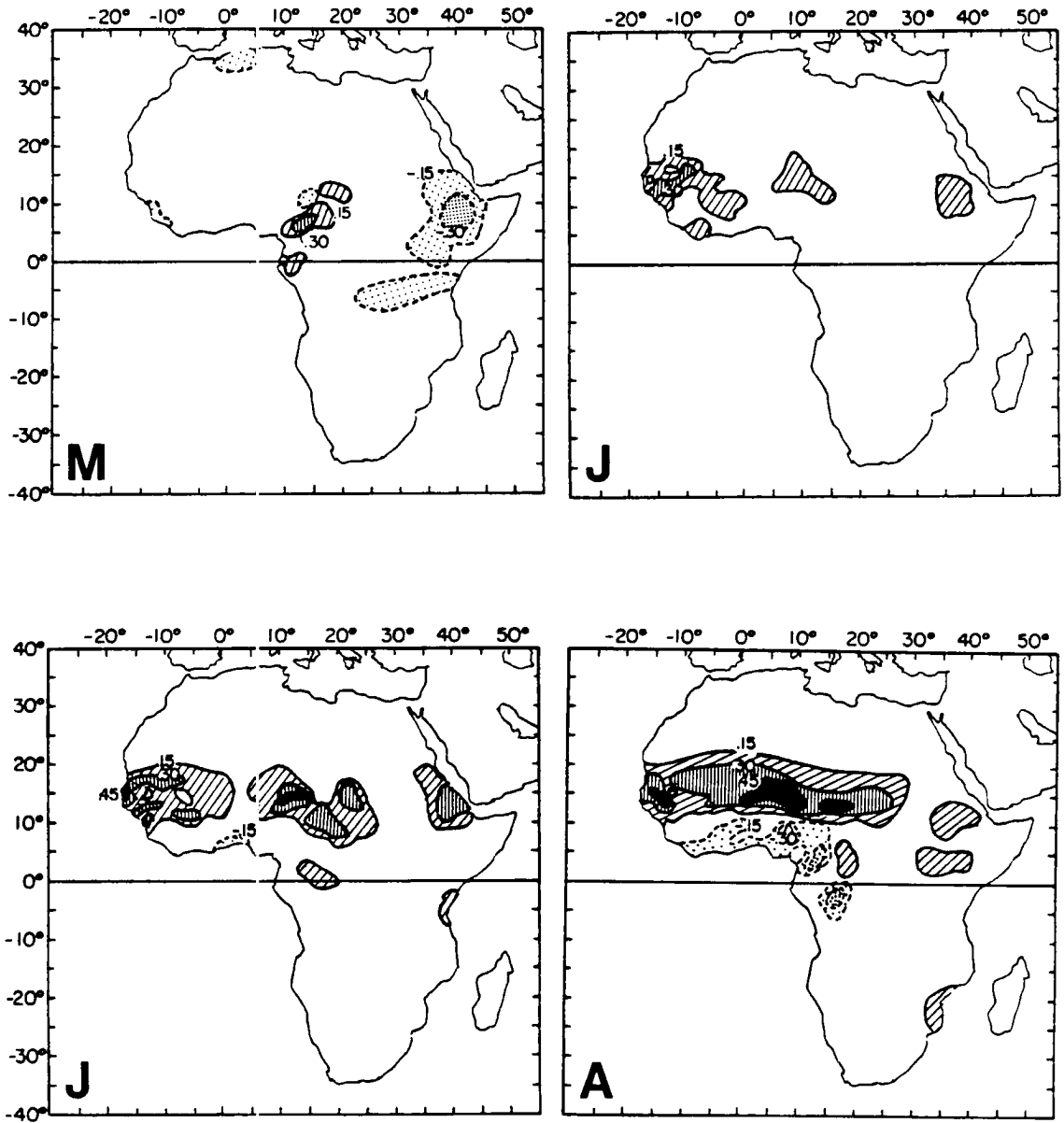


Figure 4.6: Continued.

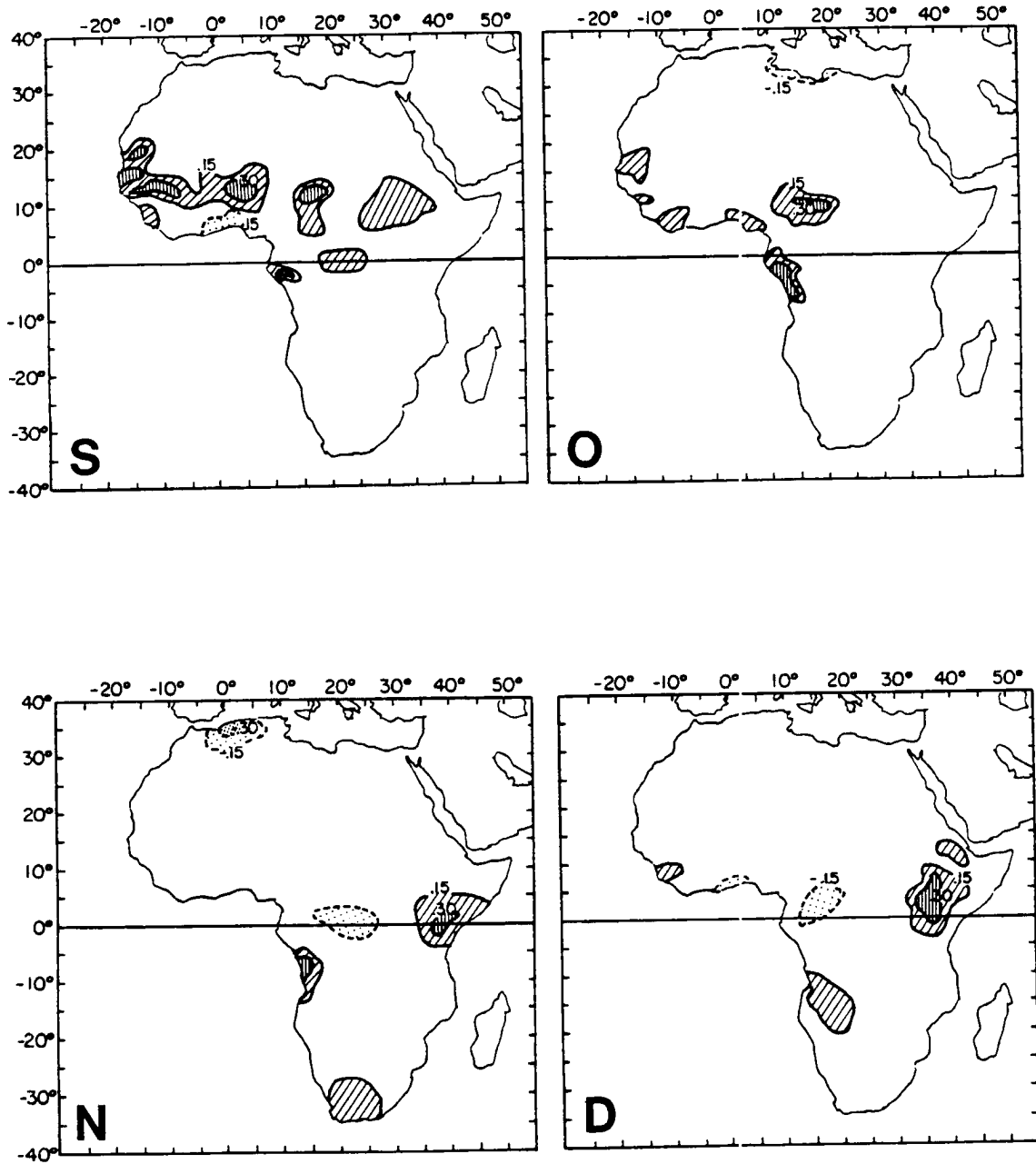


Figure 4.6: Continued.

trays positive correlations in January, negative in February, and then back to positive in March. Hence, these associations inferred are not to contain any real physical relationship.

Only one coupled region passes the month-to-month test of persistence with fairly high correlations. This involves a strong positive association throughout the Sahel with a associated weaker negative correlation along the Gulf of Guinea. The Sahel consistently shows this relationship from June to October, while the negative correlation along the Gulf is seen during July through September. As was suggested from the analysis of the Lamb Index, it is the western and central Sahel which show the highest correlations, wherein several monthly correlation values of $r = 0.50$ and greater occur. This differs from the earlier analysis of the seven month Lamb Index in that April and May rains play no part in the association with tropical cyclones.

The presence of a negative relationship of Sahelian rainfall with the Gulf of Guinea region to its south is consistent with the findings of Nicholson (1986). Nicholson showed that the Sahel and the Gulf of Guinea often, but not always, show opposite anomalies during the same year. When the Sahel is comparatively rainy, the area along the Gulf of Guinea is usually dry. Conversely, when the Gulf of Guinea receives above normal rainfall, the Sahel is often drier than normal.

Correlations of intense hurricane days versus the annual individual station rainfall are shown in Fig. 4.7. This analysis again emphasizes the strong association between the two parameters, especially in the westernmost Sahel. Linear correlation coefficients show substantial areas where correlation values of at least $r = 0.60$ are found. The Gulf of Guinea area displays only a very weak negative correlation, likely because the months of July, August, and September account for only a small proportion of the annual rainfall. The remainder of the continent shows very weak, inconsequential correlations.

A rainfall index for the westernmost Sahel has been created to more accurately represent this rainfall-hurricane relationship in terms of concurrent spatial and temporal associations. While the documentation of a concurrent relationship is essential, it does not provide any predictive signals for hurricane activity. With the availability of strong

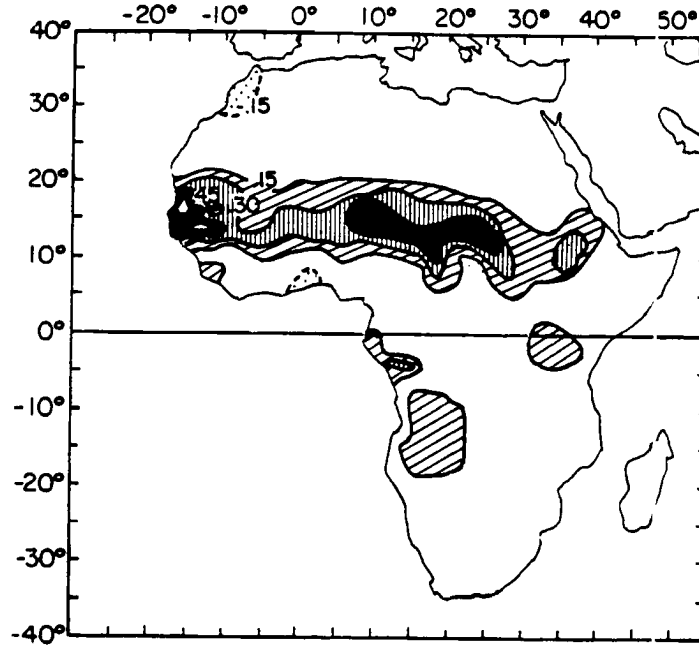


Figure 4.7: Smoothed values of linear correlation coefficients for individual station annual rainfall versus seasonal intense hurricane days. Contours are at $r = \pm 0.15, 0.30, 0.45,$ and 0.60 .

positive correlations in June and July, however, a rainfall index composed from those two months is found to be very useful for a 1 August seasonal forecast of hurricanes. This is discussed in Chapter 7.

4.4 Correlation with Following Year Tropical Cyclones

In order to determine the best rainfall-hurricane association, an analysis was carried out for the rainfall data in the previous year to subsequent seasonal tropical cyclone activity. No a priori assumptions were made in these cases: there were no known previous studies showing that any association existed between African rainfall and hurricane activity nearly a year later. This experiment was carried out with little expectations of success. Though, fortunately, our expectations proved incorrect as a number of meaningful associations was found.

As in the previous analysis, monthly rainfall at individual stations throughout all of Africa were correlated against intense hurricane days in the following season (Fig. 4.8). Only three regions appear to have persistent strong correlations of this sort: the Western

Sahel during June to August (with positive association), the Gulf of Guinea region in July to November (positive), and east central Africa from September to December (negative). The annual rainfall correlations in Fig. 4.9 also show the three regions quite distinctly.

For the first association, it is concluded that the weak ($r = 0.35$ or less) positive correlations in the west Sahel are merely a reflection of the monsoon's characteristic to persist in either a dry or wet regime for several years at a time. Note in Fig. 4.1 how the rainfall in the Lamb Index tends to persist with very high amounts of rain in the 1950's, slightly above normal rainfall in the 1960's, and generally below normal rainfall from the early 1970's onward. Any year being dry, for instance, the next year has a good likelihood of also being dry as well. And the associated intense hurricane activity would likely also be below average. This type of "persistence" forecast, while possibly showing a degree of skill, was nevertheless discarded for stronger appearing correlations elsewhere.

The second region under consideration is along the Gulf of Guinea for the months of July to November. There are positive correlations that are consistently above $r = 0.40$ for large portions of this area. This stronger relationship is also seen in the annual map. Because of the duration and magnitude of these anomalies, this region appears to offer a potential predictive signal. Chapter 6 explores this association.

The last area of interest is located just south of the equator in eastern Africa. The negative correlations appear in the same general vicinity between the months of September to December. However, the correlations are, in general, fairly weak (values up to $r = -0.40$ but usually substantially lower). Since the Gulf of Guinea association is stronger, there will be no further current work on the association seen in eastern Africa, but future research may center on this area.

While the first six months in this analysis showed no substantial predictive relationships, the Gulf of Guinea region during the months of July to November does appear to offer a reasonably strong positive association with following year intense tropical cyclone days. It is likely that this is due to a feedback from the receding monsoon in the Guinea area late year rainfall acts to enhance the next year's rainfall in the Sahel. It is this Gulf of

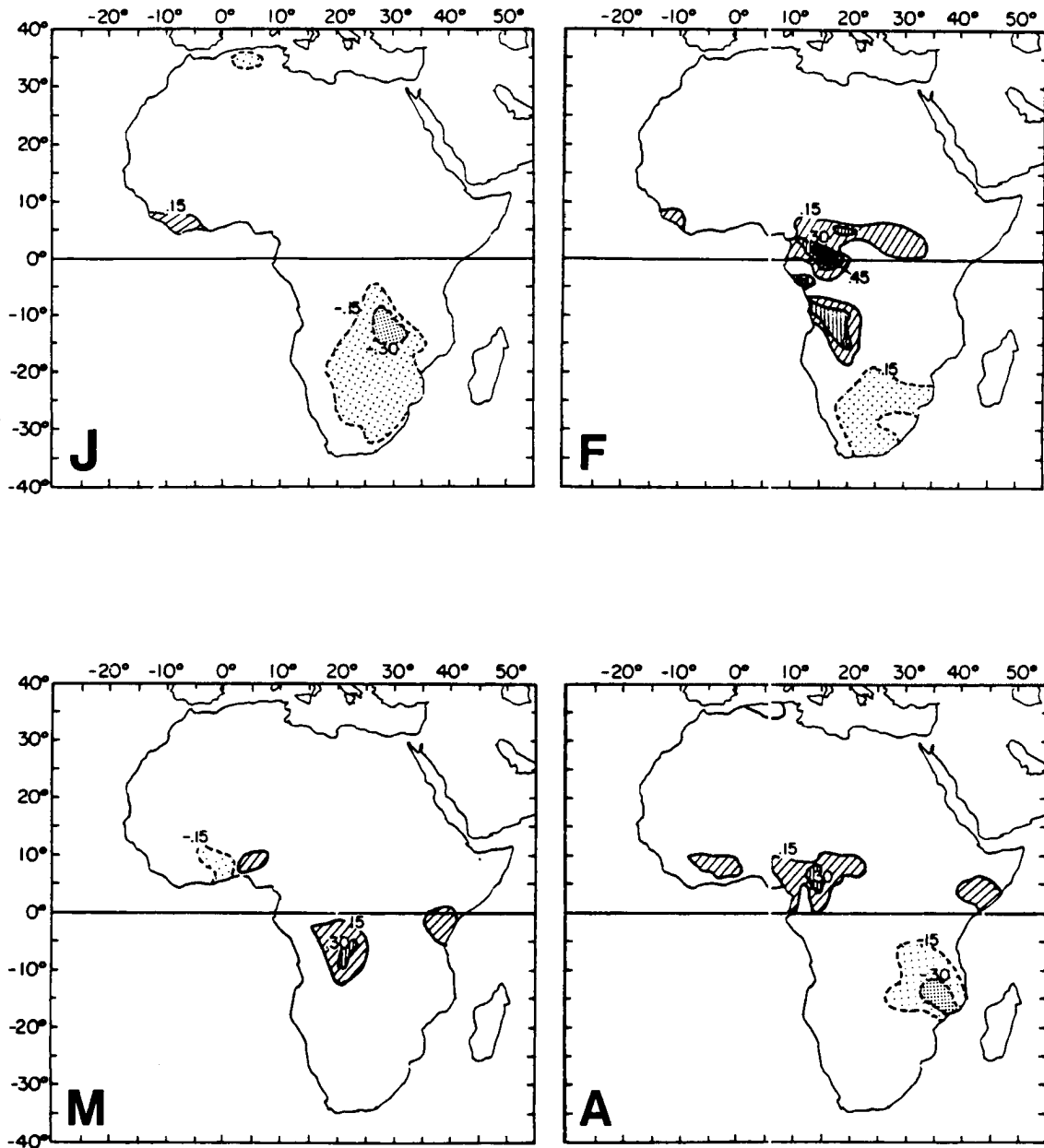


Figure 4.8: Smoothed values of linear correlation coefficients for individual monthly station rainfall versus seasonal intense hurricane days in the following year. Contours are at $r = \pm 0.15$, 0.30 , and 0.45 . Month is indicated in the lower left corner.

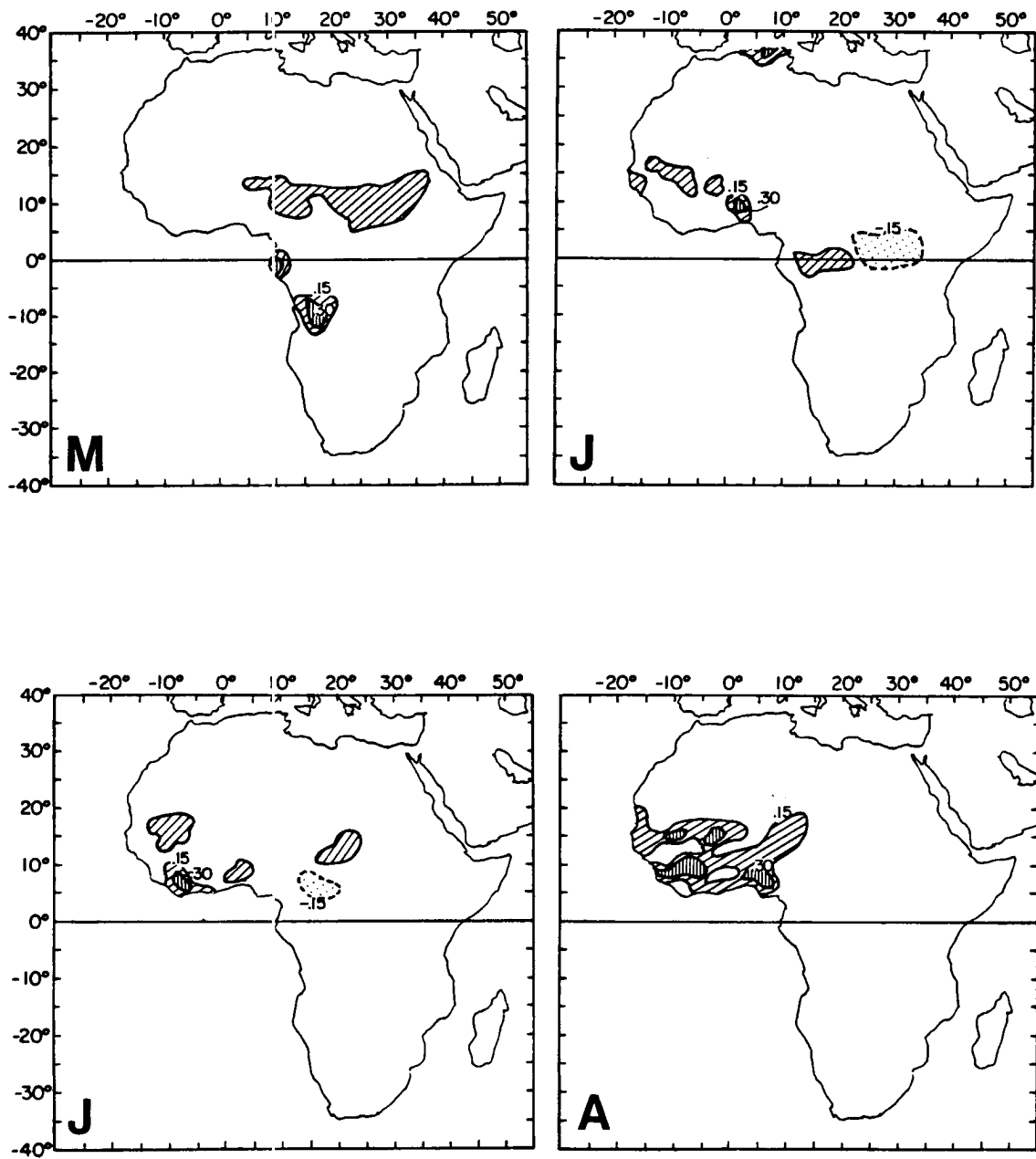


Figure 4.8: Continued.

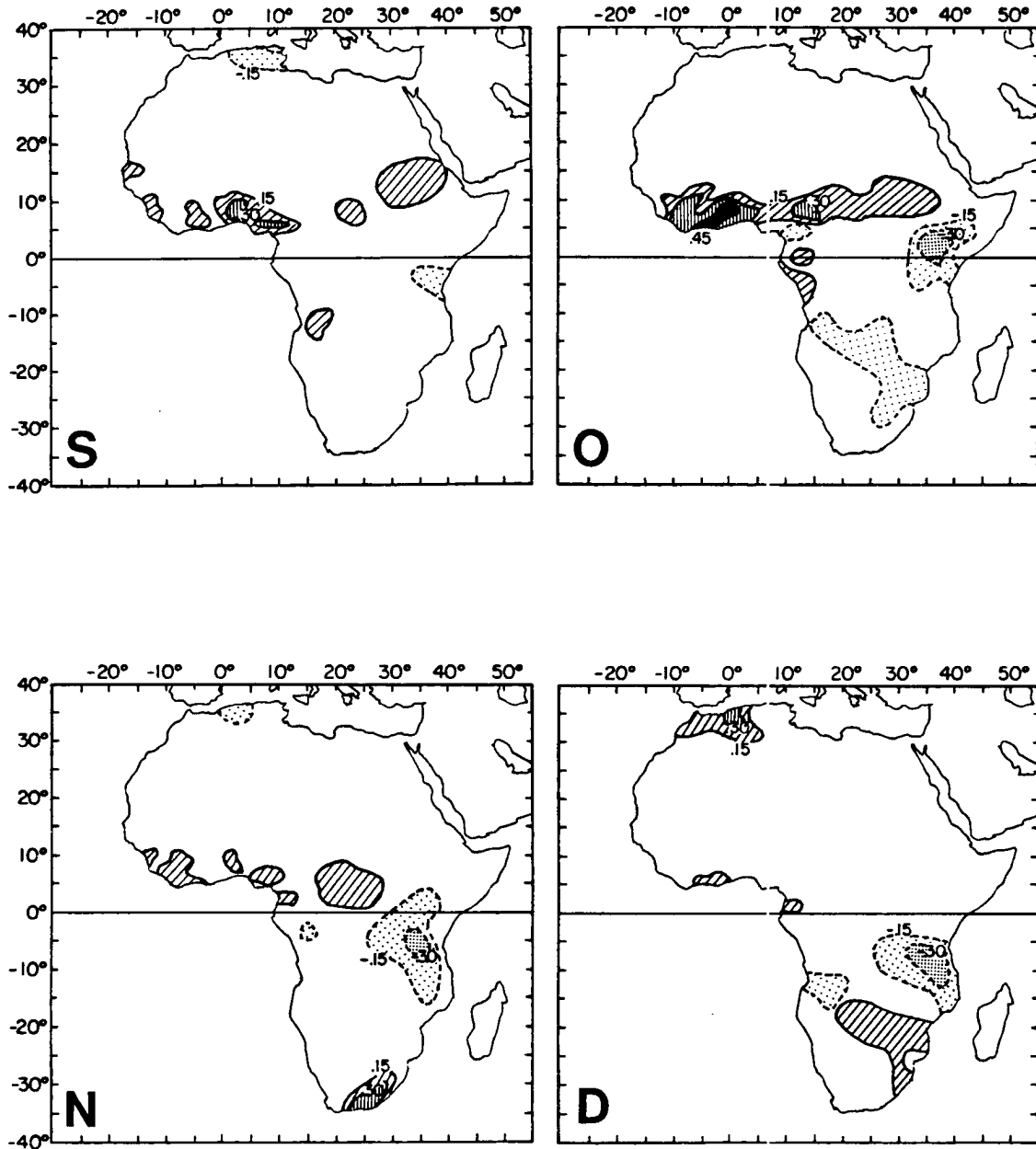


Figure 4.8: Continued.

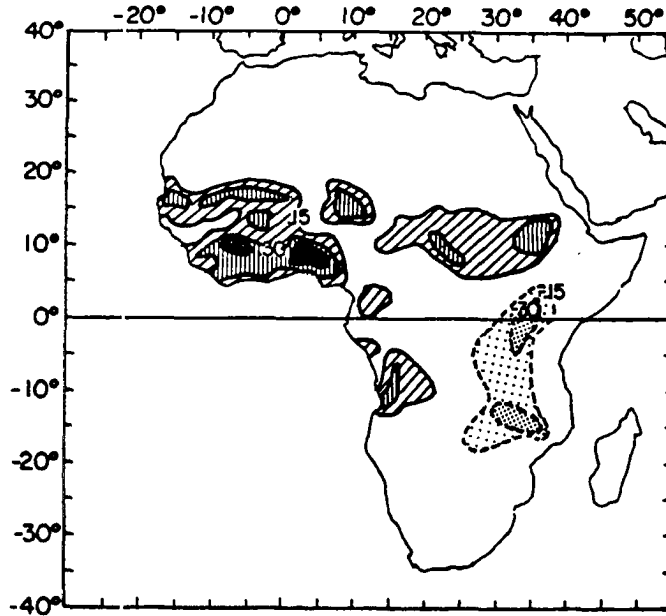


Figure 4.9: Smoothed values of linear correlation coefficients for individual station annual rainfall versus following year seasonal hurricane days. Contours are at $r = + 0.15$, 0.30 , and 0.45 .

Guinea-Sahel rainfall association that is hypothesized to cause the observed correlations with intense hurricane activity. (Mechanisms for causing this multimonth lag relationship will be discussed in Chapter 10). In using the late season Gulf of Guinea rainfall to forecast the Sahel's rainfall more than a half year into the future, we are also making an extended range prediction of the amount of Atlantic basin intense hurricane activity.

Chapter 5

“SEEDLING” RAINFALL INDEX

A new index of Western Sahel rainfall has been created. This index is similar to the previously mentioned Lamb Index in the method of construction and in the general location it represents. To differentiate the two, the term, “Seedling Index”, is used to designate the index created here. This is in deference to the name first used by Simpson *et al.* (1968) to describe tropical disturbances that formed the genesis point for tropical cyclones. They called the disturbances “seedlings” from which hurricanes could grow. That much of the West African rainfall is produced by these “seedlings” while still over Africa makes the Seedling Index an appropriate name for an index derived from the rainfall.

5.1 June to September African Rainfall

Combinations of the monthly rainfall were determined that June to September rainfall has the strongest concurrent relationship with intense hurricane days. Though October rainfall data also appears to contain additional positive correlations, its inclusion did not strengthen the multimonth association. Instead, the June to October correlation was found to be slightly degraded from the June to September value.

It is during this four month June to September period that most precipitation occurs over the Sahel (Fig. 4.5). Figure 5.1 shows mean precipitation throughout Africa for June to September. West Africa experiences a large meridional gradient of precipitation, going from over 2000 mm to less than 25 mm along a 1000 km portion of the west coast.

Consistent with what was observed with the Lamb Index, Sahel rainfall shows an increasingly positive correlation as the intensity category of the tropical cyclone increases. The three analyses in Fig. 5.2 show linear correlation coefficients for named storms,

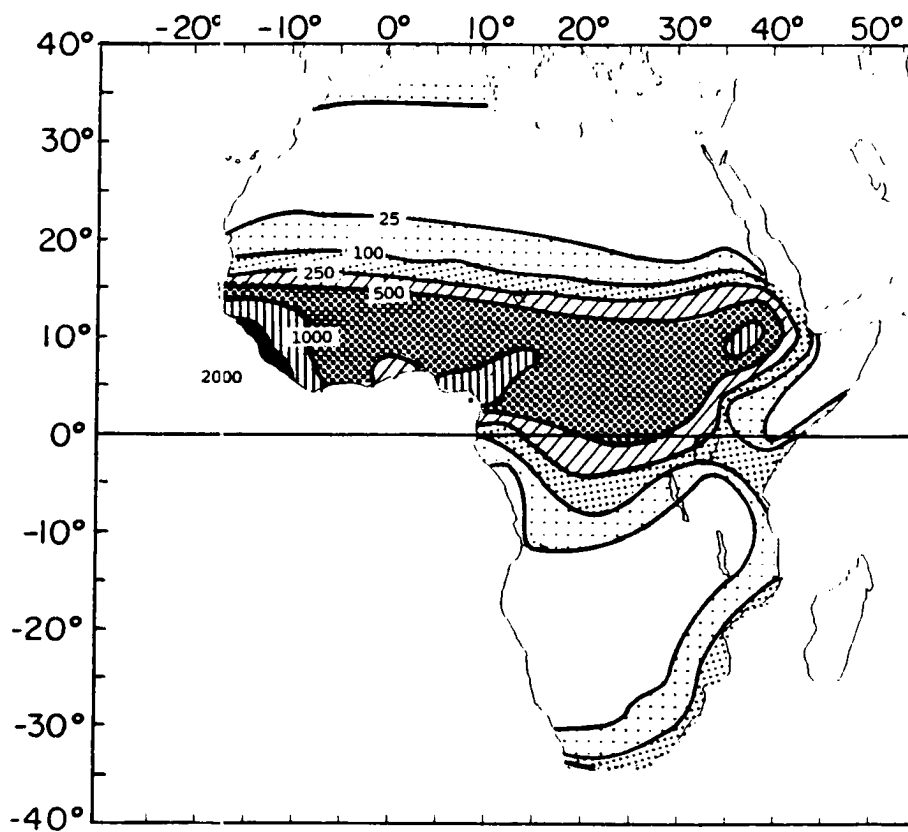


Figure 5.1: June to September precipitation over Africa using data from 1949 to 1989. Contours are at 25, 100, 250, 1000, and 2000 mm.

hurricanes, and intense hurricanes, versus June to September rainfall at individual stations. These correlations were computed using data from 1949 to 1989, but as mentioned in the previous chapter, many of the stations have spotty temporal coverage. Consequently, stations with as few as 12 years of good quality data are included in the analysis.

All three analyses show a basic structure of positive correlation throughout the Sahel. Strongest correlations occur at the westernmost portion of the Sahel and an area of weak negative correlations occurs along the Gulf of Guinea. For correlations with named storms, the strongest values are only $r = 0.35$ in the Sahel. For the intense hurricanes, values of $r = 0.65$ and higher occur in the Western Sahel. Figure 5.3 is an enlargement of the northern Africa region with the correlation coefficients for intense hurricane days versus rainfall. Note the very high associations which occur.

5.2 Active Versus Calm Tropical Cyclone Seasons

Ranking of tropical cyclone activity data, from the most active to the least active seasons (see section 3.2.4) provides a methodology for analyzing differences in African rainfall on a multi-year composite basis. The ten most active years (> 8.00 intense hurricane days) and the ten least active years (≤ 1.00 intense hurricane day and < 65 HDP) were shown in Table 3.9. Ten years of each characteristic type of season is an appropriate sample in that ten years represents about 25% of the total 41 years used in the analysis (1949 to 1989).

Figure 5.4 contrasts the rainfall anomalies over Africa during active versus calm tropical cyclone seasons. An analysis which used absolute rainfall (as in Fig. 5.1) does not lend itself to easy visual determination of differences. The anomalies in Fig. 5.4 are presented in terms of relative standard deviations from normal at each station. The largest anomalies in the westernmost Sahel show deviations of nearly $\sigma = 1.00$ in the active years and $\sigma = -1.00$ in the calm years. These ten year individual station averages reveal very large systematic differences occurring over a widespread area, suggesting a strong concurrent relationship between Sahel rainfall and intense hurricane activity. Also seen in Fig. 5.4 is

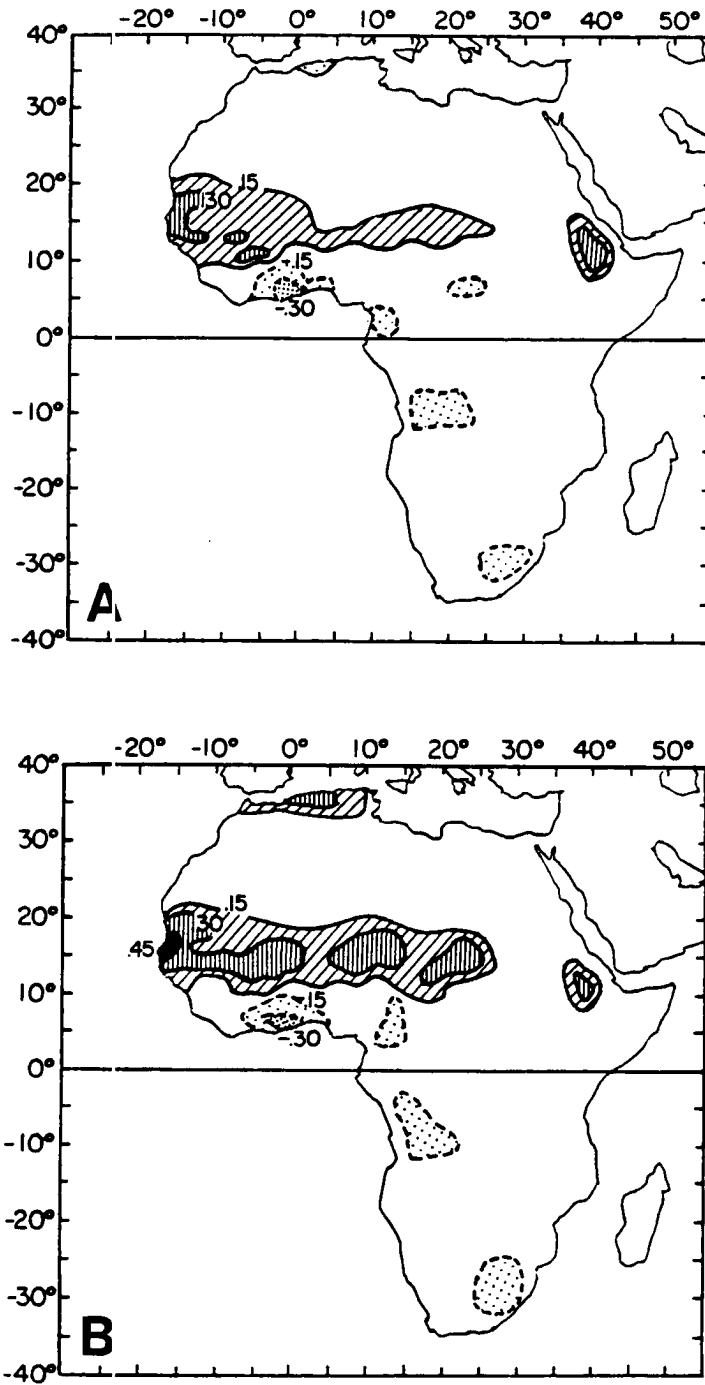


Figure 5.2: Correlation coefficients of individual station June to September rainfall versus a) named storms, b) hurricanes, and c) intense hurricanes. Stations were only included in the analysis if they had at least 12 years of data between 1949 and 1989. Contours indicate values of $r = \pm 0.15, 0.30, 0.45,$ and 0.60 . Positive correlations are within solid contours, while negative contours are indicated by dashed lines.

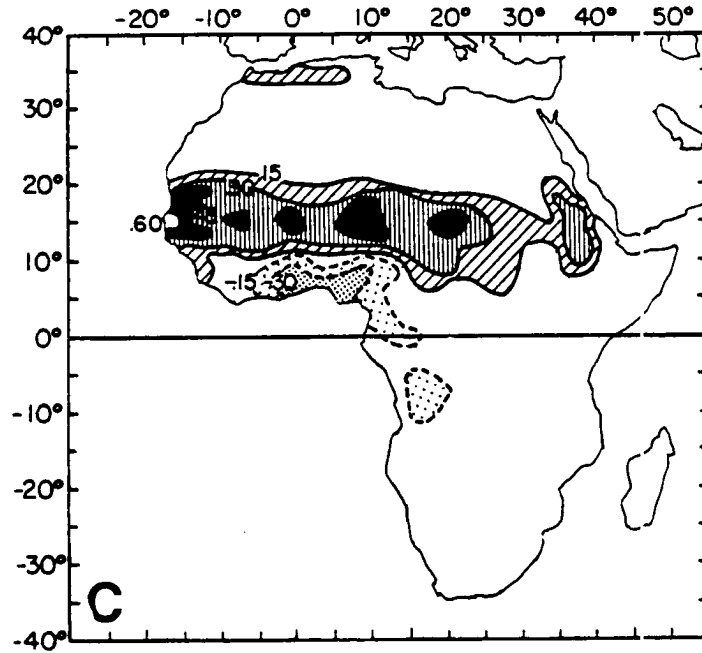


Figure 5.2: c: Continued.

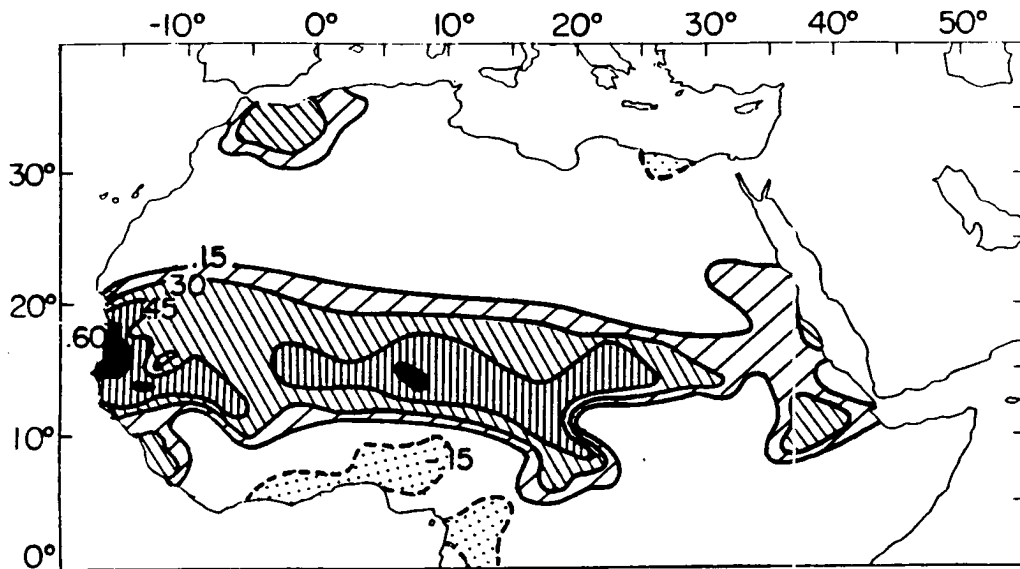


Figure 5.3: Same as Fig. 5.2 with June to September rainfall versus intense hurricane days.

a weaker opposite tendency for the Gulf of Guinea region to be drier in active years and wet during calm seasons.

5.3 Single Station Example: Dakar, Senegal

As the Western Sahel shows the largest concurrent relationships, a detailed look at a single reliable station, Dakar, Senegal, is instructive. Poised on the westernmost point in continental Africa, the weather station at Dakar (WMO #616410) has been continuously monitoring precipitation since 1898. Dakar measurements show quite clearly the very strong rainfall-tropical cyclone association.

So as to be consistent with the remainder of this report, only data from 1949 to 1989 are analyzed. During that time period, Dakar had a mean June to September rainfall of 428 mm with a rather large standard deviation of 174 mm. Similar to stations throughout the Sahel, Dakar has experienced a large downturn in rainfall during the last 20 years (Fig. 5.5). Rainfall in the 1950's and 1960's usually ranged between 400 to 700 mm while during the 1970's and 1980's, rainfall amounts varied from 200 to 500 mm, a substantial reduction.

The relationship to tropical cyclone activity is very high, with the strongest association with the more intense storms (Table 5.1). Even though this station was chosen because of the strength of its correlations, it is surprising that rainfall from a single station can display such a strong relationship with anything. This is especially notable when one considers that the rain received in Senegal is primarily convective and is therefore subject to wide variations that occur locally from individual thunderstorms. Figure 5.6 shows the scatter plot of June to September Dakar rainfall versus intense hurricane days as an example from Table 5.1.

5.4 Development of the June to September Seedling Index

An accepted way of creating rainfall indices for a particular region is to combine station data after normalizing by their mean standard deviations for the period of interest (see section 1.1.2). The 38 June to September Western Sahel rainfall stations used with

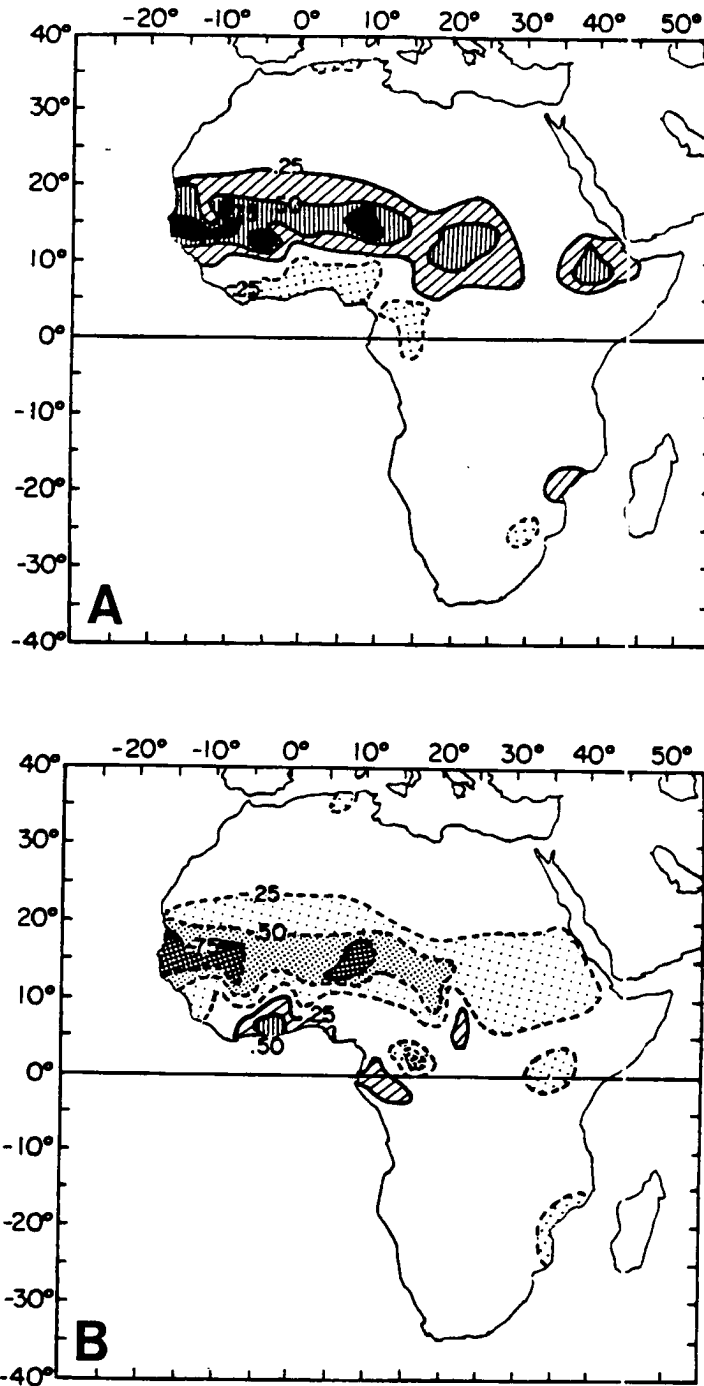


Figure 5.4: June to September African rainfall contrast of the ten most active tropical cyclone seasons (a) and the ten calmest seasons (b) between 1949 and 1989. Contours are in mean standard deviations. Solid contours indicate positive deviations (i.e. wetter than normal) and dashed contours indicate negative deviations (i.e. drier than normal). The ten active years are 1961, 1950, 1955, 1964, 1960, 1989, 1958, 1954, 1966, 1951; the ten calm years are 1972, 1968, 1986, 1983, 1973, 1987, 1962, 1984, 1977.

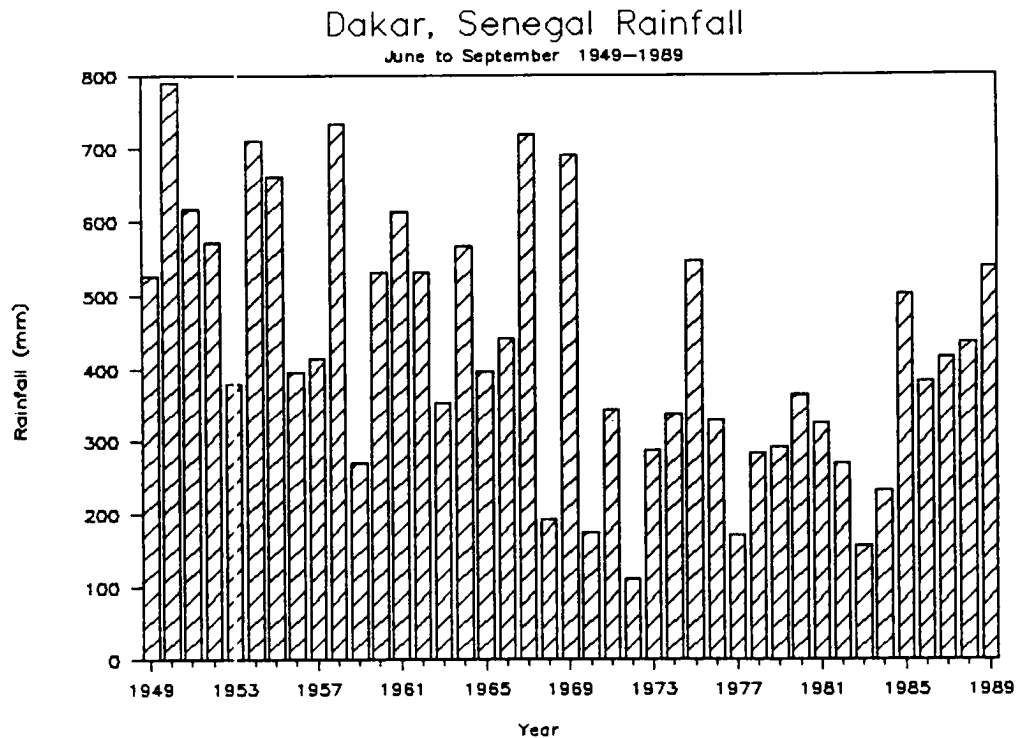


Figure 5.5: June to September rainfall for Dakar, Senegal (14.7°N, 17.5°W) from 1949 to 1989.

Table 5.1: Correlation coefficients for June to September Dakar, Senegal rainfall versus Atlantic basin tropical cyclone parameters for the years 1949 to 1989. (Asterisks refer to significance level: 0.100 for ‘*’, 0.025 for ‘**’ and 0.005 for ‘***’.)

Tropical Cyclone Parameter	Correlation Coefficient	Tropical Cyclone Parameter	Correlation Coefficient
Named Storms	0.43***	Named Storm Days	0.66***
Hurricanes	0.62***	Hurricane Days	0.72***
Intense Hurricanes	0.68***	Intense Hurricane Days	0.68***
Int. Hur. (Bias Out)	0.62***	Int. Hur. Days (Bias Out)	0.61***
HDP	0.73***		

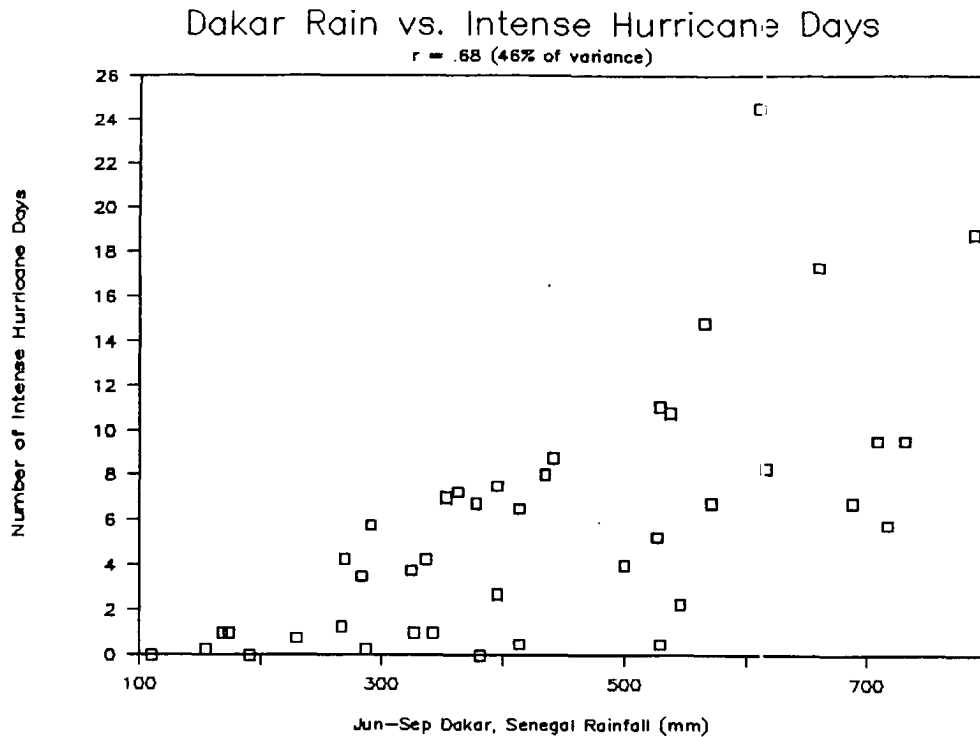


Figure 5.6: Scatter plot of 1949 to 1989 values of June to September Dakar, Senegal rainfall versus intense hurricane activity. The two parameters have a linear correlation coefficient of $r = 0.68$.

such a method are portrayed in Fig. 5.7. One can see that the selected region includes portions of the westernmost Sahel countries of Senegal, Gambia, Guinea-Bissau, Mauritania, and Mali. All available stations within this boundary were included if they provided at least 30 years of rainfall data during the period 1949 to 1989. Though this data threshold may appear low (only 73% of years needed), the quantity of data available over the Western Sahel is, in fact, actually much better than for much of the rest of Africa.

Figure 5.8 portrays the June to September rainfall anomalies for this index which will be referred to as the Seedling Index. Note the strong similarity of magnitude and phase in comparison with those presented in the Lamb Index (Fig. 4.1). The two indices are shown together as the scatter plot in Fig. 5.9. Even though the indices are very close for most years, there are eight years of rainfall that show substantial difference ($\Delta\sigma > 0.40$ or $\Delta\sigma < -0.40$) between the two indices. These are 1950 (0.46), 1952 (-0.41), 1953 (-0.41), 1955 (0.44), 1958 (0.45), 1961 (0.59), 1968 (-0.41), and 1989 (0.59). Positive values imply that the June to September Seedling Index is wetter than the Lamb Index. These

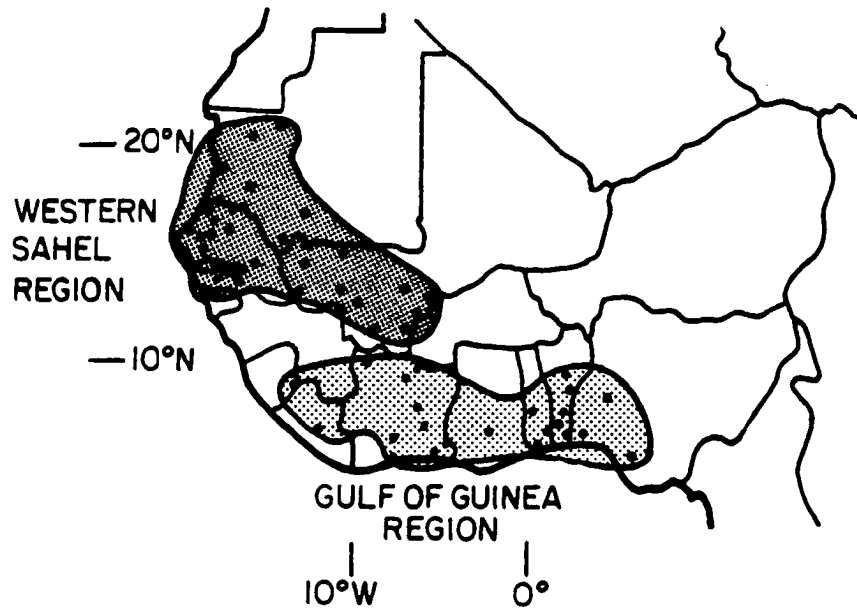


Figure 5.7: Location of rainfall stations which comprise the Seedling Index (the “Western Sahel Region”) and the Gulf of Guinea Index (Chapter 6).

large positive and negative values must be due to relative rainfall differences between the Western and Central Sahel, since the Seedling Index only includes stations in the Western Sahel. The second diagram in Fig. 5.8 is the June to September Seedling Index but wherein the strong downward linear trend has been removed from the data. It will be shown conclusively that the strong correlations between the Western Sahel rainfall and tropical cyclones are not dependent upon concurrent trends in both data sets.

Unlike the data for the Lamb Index which consistently had 18 to 20 out of the possible 20 stations available every year for the analysis, the June to September Seedling Index shows a larger range in the number of available stations. Table 5.2 shows the mean standard deviations for all stations (the same information as in Fig. 5.8) as well as the number of stations that were included in each year’s calculations. Data for the years 1949, 1950, 1987, 1988 and 1989 are comparatively incomplete as the AID data set from which several key stations were drawn were not available for those time periods.

Table 5.3 provides basic information on the stations utilized in the June to September Seedling Index. As with the stations used in the Lamb Index (section 4.1), this index region

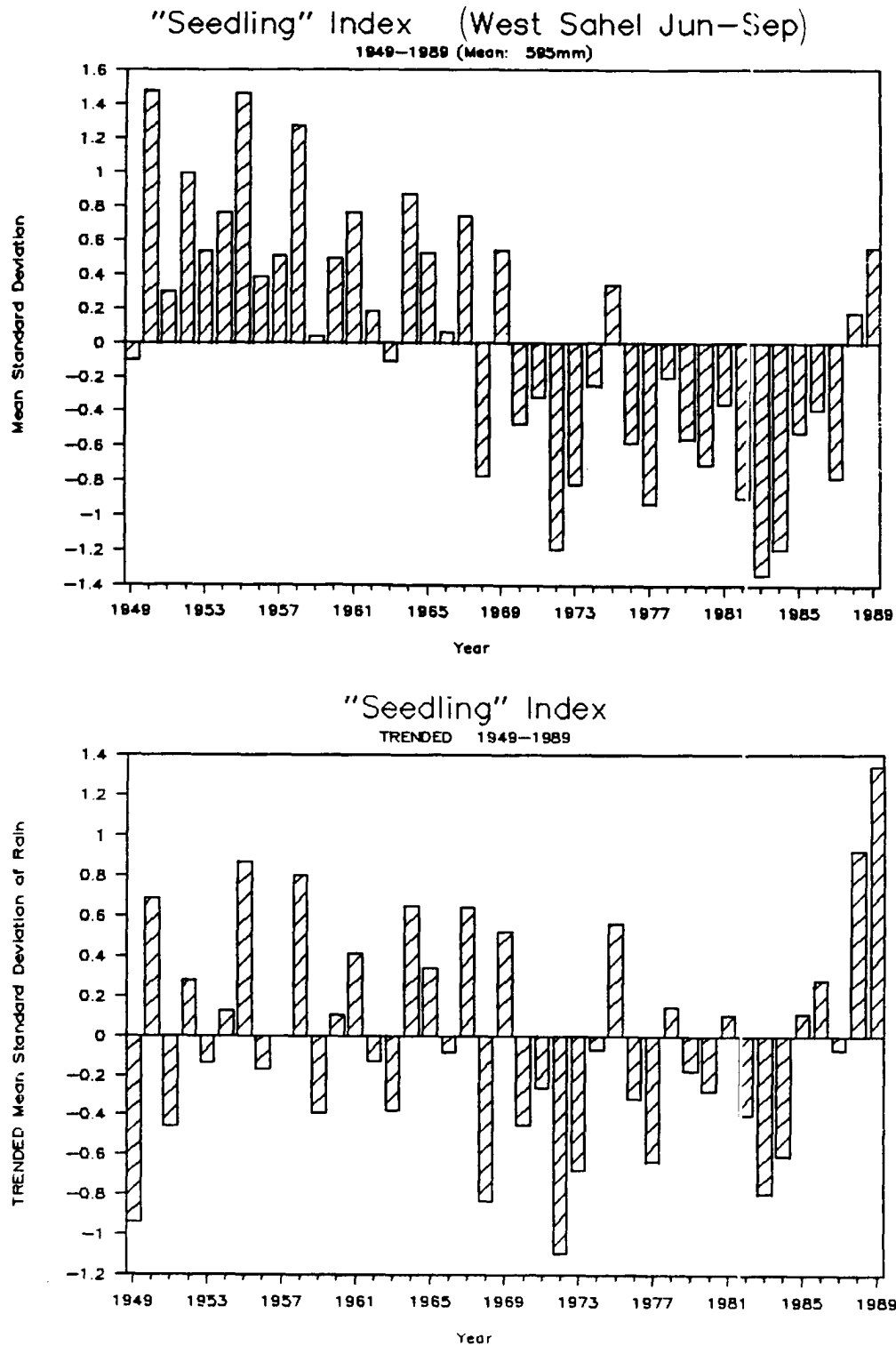


Figure 5.8: Mean standard deviations of rainfall for the 38 station June to September Seedling Index of the Western Sahel (top panel). The same Seedling Index with the downward linear trend removed from the data (bottom panel). Data presented are from 1949 to 1989.

Table 5.2: Mean standard deviations and data availability (out of a possible 38 stations per year) for the June to September Seedling Index.

Year	Standard Deviation	Number of Stations	Year	Standard Deviation	Number of Stations
1949	-0.10	24	1970	-0.47	37
1950	1.48	24	1971	-0.32	37
1951	0.30	37	1972	-1.19	38
1952	0.99	37	1973	-0.82	38
1953	0.54	38	1974	-0.25	38
1954	0.76	38	1975	0.34	38
1955	1.46	38	1976	-0.58	38
1956	0.38	38	1977	-0.93	37
1957	0.51	38	1978	-0.20	38
1958	1.27	37	1979	-0.56	38
1959	0.04	36	1980	-0.70	37
1960	0.49	35	1981	-0.36	37
1961	0.76	38	1982	-0.90	37
1962	0.18	37	1983	-1.34	37
1963	-0.11	38	1984	-1.19	37
1964	0.87	38	1985	-0.52	37
1965	0.52	37	1986	-0.39	37
1966	0.06	38	1987	-0.78	26
1967	0.74	37	1988	0.17	26
1968	-0.77	37	1989	0.55	25
1969	0.54	37			

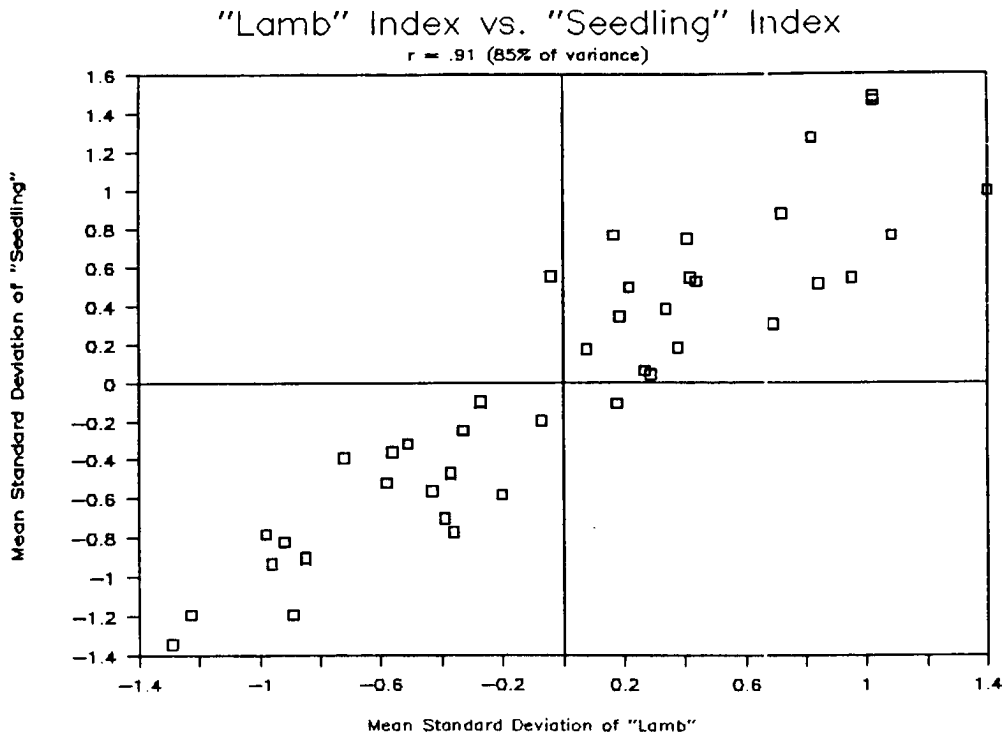


Figure 5.9: Scatter plot of April to October Lamb Index rainfall anomalies (x - axis) versus June to September Seedling Index rainfall anomalies (y - axis) for the years 1949 to 1989. The two indices correlate at $r = 0.91$.

covers a wide meridional band (11 to 20°N) and therefore a large range of rainfall means. The stations themselves show a high degree of individual internal correlation with the entire June to September Seedling Index, with only 3 of 38 stations showing correlations of less than $r = 0.62$. This level of internal consistency is better than in the Lamb Index wherein 4 of 20 stations do not show as strong a relationship with the mean Index.

Table 5.4 shows a month by month breakdown of the combined 38 station means and standard deviations including the percent contribution to the main June to September rainfall period and the entire rainy season of May to November. The remaining months of December to April (not shown) receive only about 1% of the annual mean rainfall. Note that the main rainfall month is August but with both July and September receiving considerable amounts as well. It is also seen that with the higher means in July through September we also have lower overall variability (i.e. a lower coefficient of variation) in these months. This difference is a result of the fringe months for the monsoon (i.e., May to June and October to November) having either no rainfall or else receive considerable

Table 5.3: The 38 stations used in the June to September Seedling Index: CSU Rainfall Data Base identification number, station name and country, June to September rainfall mean and standard deviation (in mm), years of data in the analysis, correlation coefficients versus the Seedling Index, and correlation coefficient versus intense hurricane days. (Asterisks refer to significance level: 0.100 for ‘*’, 0.025 for ‘**’ and 0.005 for ‘***’.)

Station	Rainfall Data			vs. Index	vs. Intense
	Mean	SD	Years	r	Hurr. Days r
0119 Niore Du Sahel, Mali	489.1	158.06	41	0.800	0.498***
0123 Kayes, Mali	615.3	119.91	41	0.624	0.461***
0125 Kita, Mali	869.7	185.74	41	0.696	0.449***
0126 Segou, Mali	593.7	127.86	41	0.773	0.542***
0127 San, Mali	638.5	106.99	41	0.583	0.560***
0128 Kenieba, Mali	1053.8	238.20	39	0.758	0.496***
0130 Bamako/Senou, Mali	823.3	166.28	41	0.666	0.480***
0131 Koutiala, Mali	789.0	173.56	41	0.692	0.636***
0132 Bougouni, Mali	924.8	176.56	41	0.702	0.592***
0133 Sikasso, Mali	930.4	141.17	40	0.532	0.437***
0138 Atar, Mauritania	66.0	43.81	41	0.506	0.347**
0139 Akjoujt, Mauritania	58.7	45.29	40	0.628	0.555***
0140 Nouakchott, Mauritania	86.8	55.66	41	0.833	0.584***
0142 Boutilimit, Mauritania	135.2	76.36	41	0.726	0.607***
0143 Rosso, Mauritania	225.8	103.19	39	0.683	0.551***
0146 Kiffa, Mauritania	283.9	117.81	41	0.771	0.452***
0148 Saint Louis, Senegal	256.8	103.34	41	0.661	0.486***
0149 Podor, Senegal	235.4	120.57	41	0.697	0.612***
0150 Linguere, Senegal	403.6	113.86	41	0.735	0.623***
0151 Matam, Senegal	409.4	177.42	41	0.661	0.503***
0152 Dakar/Yoff, Senegal	426.4	177.13	41	0.851	0.675***
0154 Thies, Senegal	527.1	202.63	37	0.863	0.643***
0155 Diourbel, Senegal	549.0	177.07	41	0.860	0.624***
0156 Kaolack, Senegal	619.9	182.84	39	0.745	0.530***
0157 Tambacounda, Senegal	727.0	170.07	41	0.696	0.462***
0162 Bathurst/Yundum, Gambia	1003.8	288.19	41	0.882	0.545***
0163 Bissau Airport, Guinea-Bissau	1542.1	337.73	40	0.773	0.574***
0611 Bansang, Gambia	823.7	290.44	34	0.781	0.562***
0615 Georgetown, Gambia	811.7	189.83	31	0.783	0.518***
0617 Basse Met, Gambia	858.5	202.31	33	0.774	0.711***
0627 Boghe, Gambia	250.4	89.88	36	0.750	0.610***
0630 Selibaby, Mauritania	493.5	145.51	36	0.781	0.495***
0632 Louga, Senegal	336.3	157.19	31	0.826	0.570***
0635 Mbour, Senegal	576.8	216.54	36	0.835	0.538***
0636 Niore Du R.p, Senegal	685.6	184.95	33	0.808	0.495***
0637 Velingara Casamance, Senegal	863.6	208.37	34	0.691	0.689***
0638 Sedhiou, Senegal	1094.6	303.71	36	0.764	0.553***
0639 Bambey Met, Senegal	538.5	151.72	36	0.871	0.586***

amounts of rain (25–100 mm). This variability explains why only the June to September period was chosen for inclusion in the Seedling Index; it encompasses the large majority of the annual rainfall for the region.

Table 5.4: Monthly means, standard deviations, ratios, and coefficients of variation for the 38 stations used in the Seedling Index.

	May	Jun	Jul	Aug	Sep	Oct	Nov	Jun–Sep	May–Nov
Mean	18mm	66	149	217	162	51	4	595	668
Sta. Dev.	15mm	38	65	94	74	48	9	164	177
Coeff. Var.	83%	57	44	43	46	94	225	28	26
% Jun–Sep Mean	—	11%	25	36	28	—	—	100	—
% May–Nov Mean	3%	10	22	32	24	8	1	89	100

5.5 Correlation with Tropical Cyclones

The next step was to determine the association of the Seedling Index with various tropical cyclone parameters. It should be kept in mind that the index was created to optimize the rainfall association with intense hurricane days with no special consideration for other tropical cyclone parameters. The reason for this being that intense hurricanes: 1) show the largest interannual and interdecadal variation (section 3.2.1); 2) cause over three-quarters of the US damage among landfalling tropical cyclones (section 3.2.3); and 3) relate strongest to Western Sahel rainfall (sections 4.1 and 5.1).

Table 5.5 shows concurrent associations between the June to September Seedling Index and various Atlantic basin tropical cyclone parameters. The aim of obtaining stronger correlations than were possible with the Lamb Index (section 4.1) is achieved. However, in comparison with Dakar, Senegal (section 5.3), the correlations are slightly degraded. Since Dakar has the strongest single station correlation in the region, a small decrease should be expected when moving to a wider 38 station index. Note, however, that correlations with intense hurricanes and intense hurricane days are stronger for the Index as a whole.

The relationship between this Western Sahel rainfall and the strongest cyclones is quite robust. Figure 5.10 depicts this relationship in a scatter plot of the June to September Seedling Index versus intense hurricane days. Again, as was seen for the Lamb Index,

Table 5.5: Correlation coefficients for June to September Seedling Index rainfall versus Atlantic basin tropical cyclone parameters for the years 1949 to 1989. (Asterisks refer to significance level: 0.100 for '*', 0.025 for '**' and 0.005 for '***'.)

Tropical Cyclone Parameter	Correlation Coefficient	Tropical Cyclone Parameter	Correlation Coefficient
Named Storms	0.41***	Named Storm Days	0.62***
Hurricanes	0.52***	Hurricane Days	0.69***
Intense Hurricanes	0.71***	Intense Hurricane Days	0.75***
Int. Hur. (Bias Out)	0.68***	Int. Hur. Days (Bias Out)	0.69***
HDP	0.72***		

values drier than about $\sigma = -0.80$ have negligible intense hurricane activity (≤ 1 intense hurricane day). The amount of variance explained between the two parameters in Fig. 5.7 is more than 57%. This value becomes only slightly lowered when the bias is removed from the intense hurricane data.

One test that can be done to determine whether the strong correlations are simply due to coexisting concurrent trends in the data sets is to break the record into two periods and then check the comparative correlations for each sub period. The obvious years for such a break should be between 1969 and 1970, as the relatively uninterrupted drought began at that time. The correlations with intense hurricane days then become:

$$1949 \text{ to } 1969 \text{ (21 years)} \dots r = 0.66$$

$$1970 \text{ to } 1989 \text{ (20 years)} \dots r = 0.65,$$

which are just slightly lower than the overall relationship of $r = 0.75$. Both subsets are significant to the 0.005 level. Since the trend is essentially removed by stratifying the data into two separate time periods, this is one confirmation that the relationship is not trend dependent.

A second method for checking for trend induced associations would be to remove any linear trend from both data sets. The bottom panel in Fig. 5.8 showed a detrended time series of the June to September Seedling Index. Though both the rainfall index and the intense hurricane activity show very substantial decreasing linear trends, adjusting the

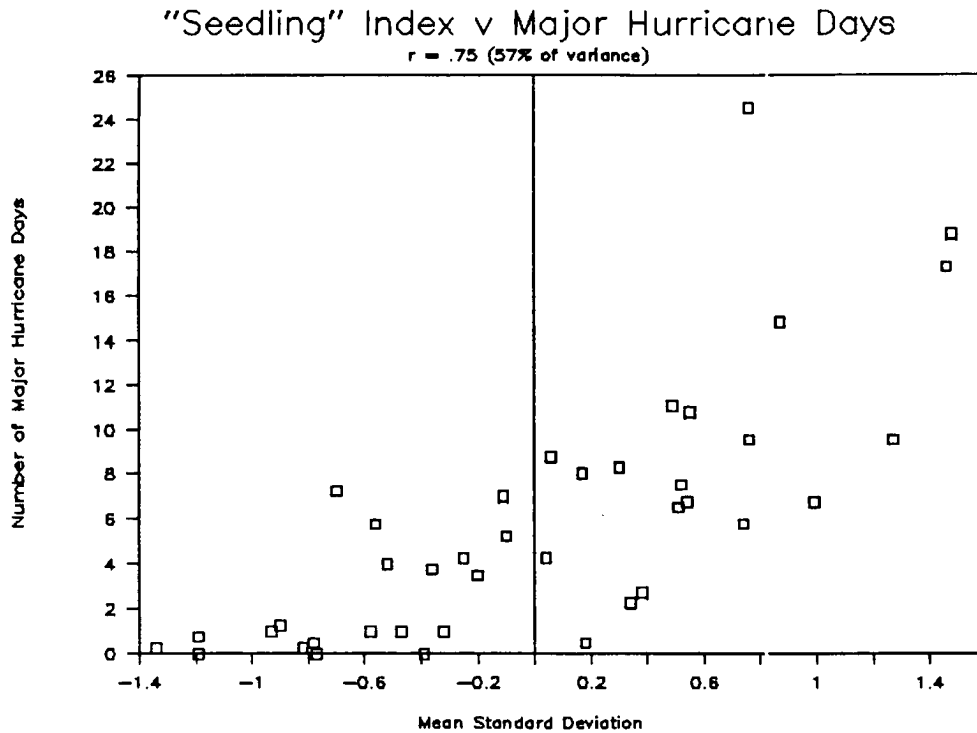


Figure 5.10: Scatter plot of 1949 to 1989 values of June to September Seedling Index rainfall versus intense hurricane days. The two parameters have a linear correlation coefficient of $r = 0.75$.

data to remove the trends has very little effect. Detrended intense hurricane days correlate to detrended June to September Seedling Index at $r = 0.68$, only slightly lower than the $r = 0.75$ value presented earlier for the original relationship. (For the bias removed intense hurricane days data set, the detrended relationship also shows only a slight decrease from $r = 0.69$ to $r = 0.65$.)

These two tests further substantiate that there is a strong concurrent interannual relationship between the strength of the Western Sahel monsoonal rains and Atlantic basin intense hurricane activity. This association is extremely resilient even when the large downward interdecadal trends have been removed from both parameters. Independent data tests for the periods of 1922 to 1948 and 1990 have also been analyzed and are discussed in Chapter 9.

5.6 Correlation with Other Tropical Cyclone Associated Factors

Though general circulation differences associated with tropical cyclone and Sahel rainfall variations have been studied separately, it was logical to test other features known to be associated with tropical cyclone variability [see Gray (1984c,d, 1989b,c)] for relationships with Sahel rainfall variability.

El Niño: Equatorial eastern and central Pacific SST anomalies (described in Chapter 2) for the months of August to October are a good measure of El Niño intensity at the height of the hurricane season. Figure 5.11 presents scatter plot of these SST anomalies versus the June to September Seedling Index. The linear correlation coefficient for these data is $r = -0.32$, significant to the 0.025 level.

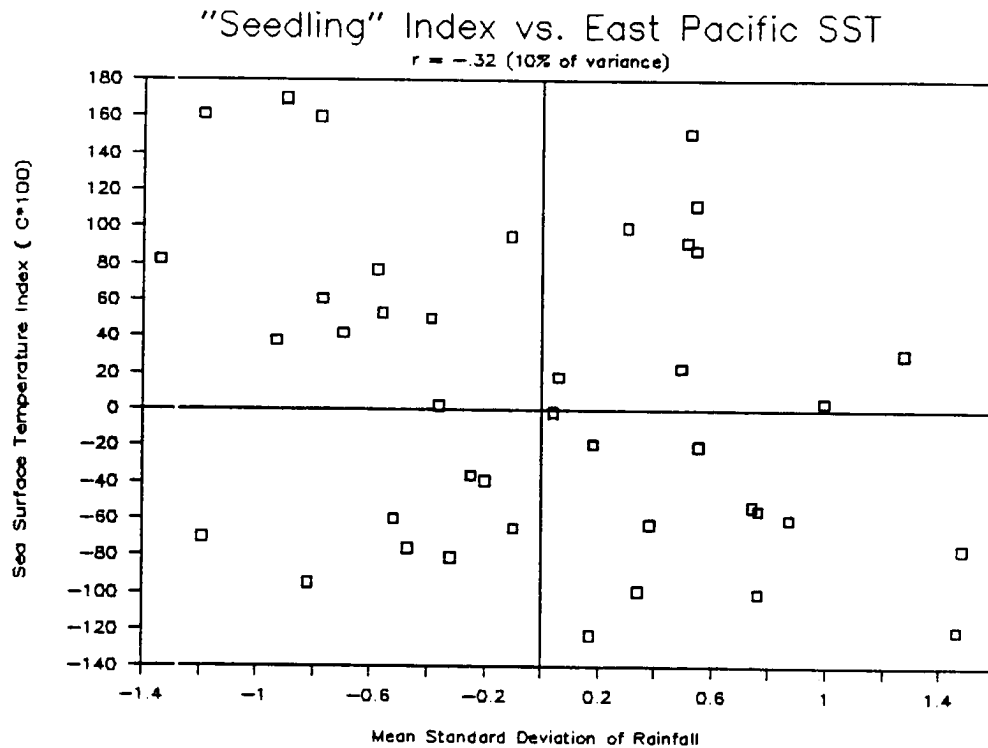


Figure 5.11: Scatter plot of June to September Seedling Index rainfall versus equatorial Pacific SST anomalies using data from 1949 to 1989. The two parameters correlate at $r = -0.32$.

To further test for associations between El Niño and Western Sahel rainfall, a breakdown was made for the SST data into warm events and non-warm events. Also included is the qualitative categorization of the El Niño which Gray (1989a) has used (after Quinn

et al., 1978) for seasonal hurricane forecasting. The results suggest that there may be a small reduction in Western Sahel rainfall during El Niño events. Both tests are significant to the 0.100 level. However, as an El Niño does not insure a dry year in the Sahel the relationship is weak. For example, 1953, 1957 and 1965 are substantial El Niño events by both methods. However, Western Sahel rainfall during each of these three years was about a half a standard deviation above normal. Thus, it is possible that where the El Niño phenomena may be a small negative factor for Sahel rainfall, it is masked by other more significant factors.

Table 5.6: Comparison of June to September Seedling Index rainfall (\bar{x}) stratified for two measures of El Niño phenomena: Equatorial east and central Pacific Ocean August to October sea surface temperature anomalies $> 0.75^\circ\text{C}$ and qualitative El Niño designation. The number of cases between 1949 and 1989 is shown in parenthesis.

	Warming Event			No Warming			Rainfall Reduction
	#	\bar{x}	σ_x	#	\bar{x}	σ_x	Warm/Non-Warm ($\Delta\sigma$)
Equatorial Pacific SSTs $> 0.75^\circ\text{C}$	(11)	-0.23	0.71	(30)	0.10	0.71	0.33
“Moderate” or “Strong” El Niños	(8)	-0.40	0.75	(33)	0.11	0.69	0.55

QBO: The large modulation of tropical cyclone variability associated with the stratospheric QBO as observed previously by Gray (1984c) and Shapiro (1989) is hard to see in the June to September Seedling Index. The scatter plot in Fig. 5.12 shows the large amounts of noise in the values of June to September Western Sahel rainfall versus September stratospheric zonal winds at 50 mb. The correlation is only $r = 0.22$, explaining a mere 5% of the variance between the two parameters (significant at the 0.100 level).

A secondary check of the QBO’s possible association with Sahel rainfall is to stratify the stratospheric zonal winds into separate west and east phases. Table 5.7 presents a summary of 41 years of data in this format in relation to the amount of rainfall in the Western Sahel. This analysis would suggest that there is a small QBO modulation of

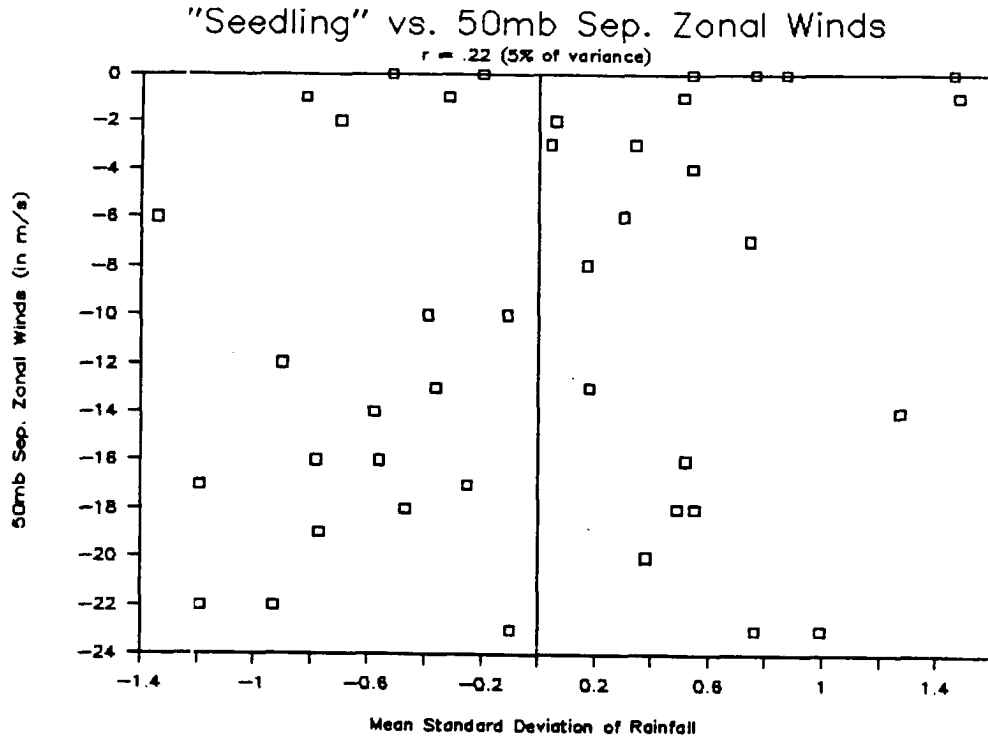


Figure 5.12: Scatter plot of June to September Seedling Index rainfall versus stratospheric zonal winds using data from 1949 to 1989. The two parameters correlate at $r = 0.22$.

rainfall. Rainfall is somewhat enhanced in west phase years and somewhat reduced in east phase years.

Table 5.7: June to September Seedling Index (\bar{x} rainfall stratified by the QBO phase using data available from 1949 to 1989. Number of cases in each phase are in parenthesis. The east years reported mean zonal winds $< -10ms^{-1}$; the west years were those with winds $\geq -10ms^{-1}$.

	#	\bar{x}	σ_x	Rainfall Difference in West versus East (σ)
West Phase Years	(21)	0.16	0.70	0.31
East Phase Years	(20)	-0.15	0.71	

200 mb Zonal Wind Anomalies (ZWA) and Sea Level Pressure Anomalies (SLPA): These lower Caribbean basin parameters show strong negative correlations with tropical cyclones (Gray, 1984d, 1989c d) (see Chapter 1 for definition, Chapter 2 for data sources). The associations are largely independent of the strength of the tropical cyclones under consideration (i.e., named storms are as well correlated as is intense hurricane activity). ZWA

and SLPA also show negative associations of the same order of magnitude with the June to September Seedling Index. Figures 5.13 and 5.14 show scatter plots for the relationships of June to September Western Sahel rainfall with ZWA and SLPA, respectively. These relationships are much stronger ($\sim r = -0.60$) than what was observed in the El Niño and QBO analysis; both are significant at the 0.005 level. It is strongly implied that the same general circulation features affecting the West Indies are also the primary physical mechanisms behind the teleconnection between the Western Sahel rainfall and Atlantic basin tropical cyclone activity.

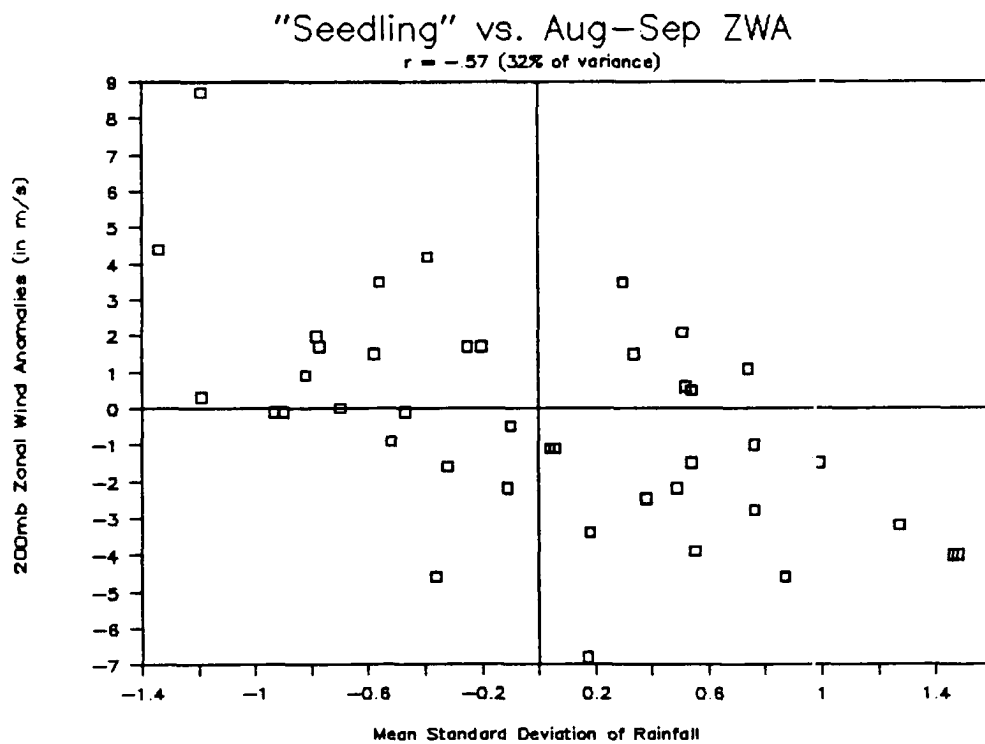


Figure 5.13: Scatter plot of June to September Seedling Index rainfall versus 200 mb zonal wind anomalies using data from 1949 to 1989. The two parameters correlate at $r = -0.57$.

5.7 Threshold Values of Rainfall

There appears to be a "threshold" value of Western Sahel rainfall occurring in years with a "substantial" number (> 1.00) of intense hurricane days. The magnitude of rainfall fluctuations of the Western Sahel is such that during the wettest years (1950, 1955 and 1958) about 135% of normal rainfall occurs, while in the driest years (1972, 1983 and

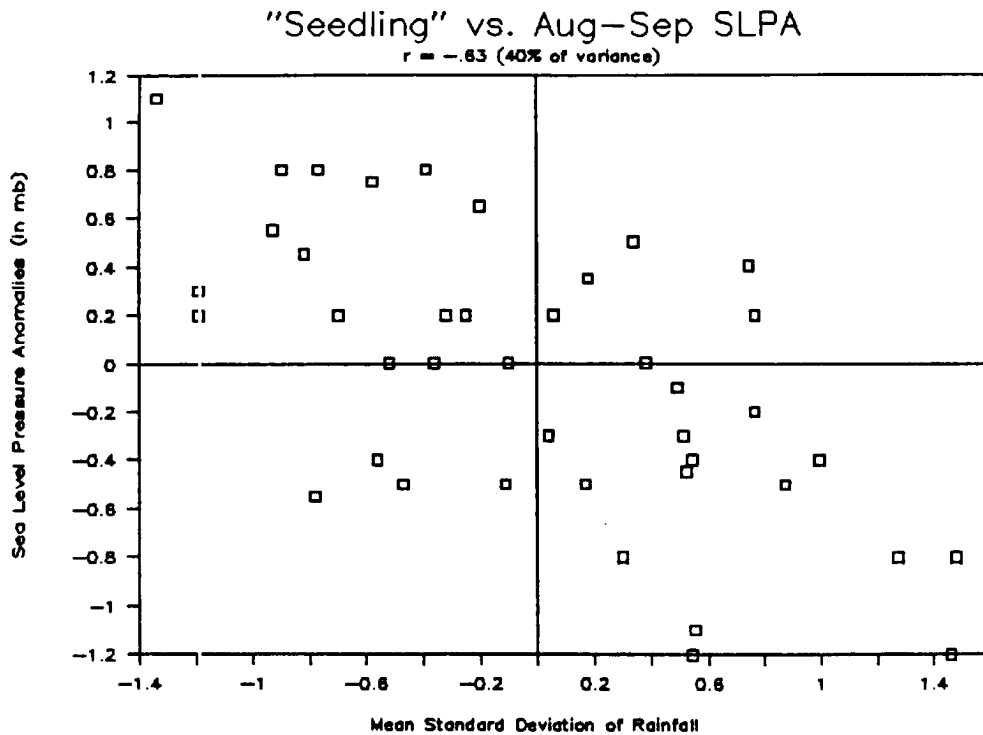


Figure 5.14: Scatter plot of June to September Seedling Index rainfall versus Caribbean basin sea level pressure anomalies using data from 1949 to 1989. The two parameters correlate at $r = -0.63$.

1984) rainfall is about 65% of normal. These values only reflect the mean conditions of the 38 stations in the June to September Seedling Index. Drier, more northerly stations show larger fluctuations percentagewise and conversely, the southerly wetter stations show smaller year to year changes.

Figure 5.15 shows the variation of the association between Seedling Index rainfall and intense hurricane activity for increasingly longer rain periods. The June-only rainfall period shows the lowest correlation (at $r = 0.52$) and also shows no minimum rainfall threshold needed for intense hurricane activity to occur. In other words, based on June rainfall only, there is no apparent minimum threshold for strong hurricanes to occur.

June plus July rainfall totals show a stronger relationship, but again there is no apparent cutoff point and accumulated rainfall from June to August is required before a threshold value can be determined. This value is shown to be $\sigma = -0.80$ in Fig. 5.15c, corresponding to about 75% of average. This value well agrees with the entire June to September Seedling Index in Fig. 5.10.

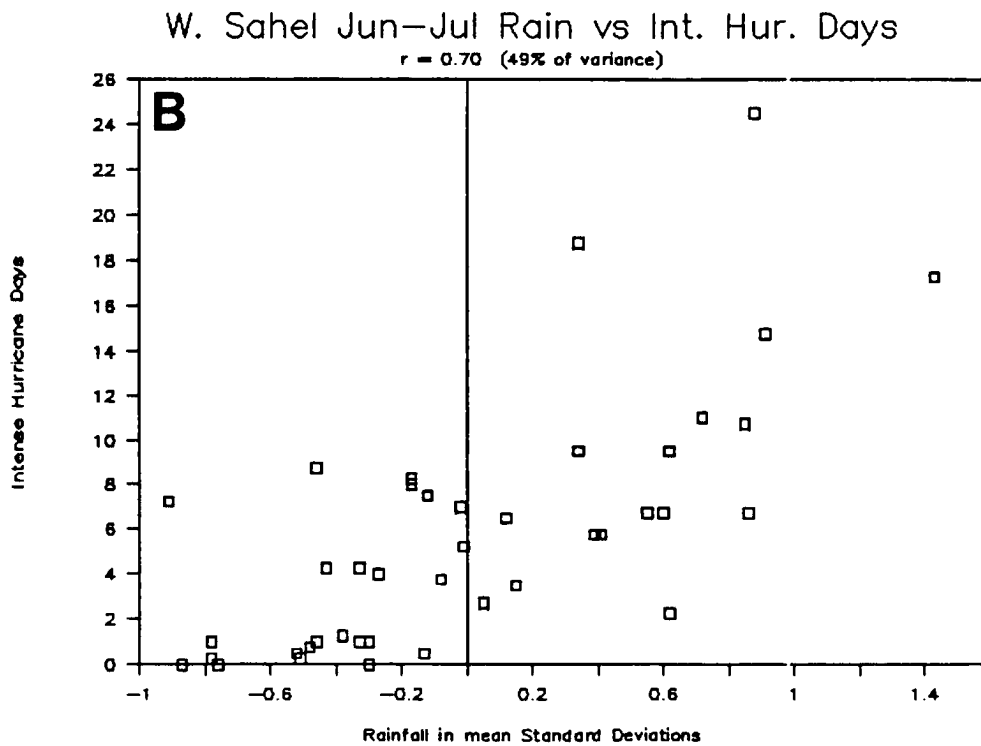
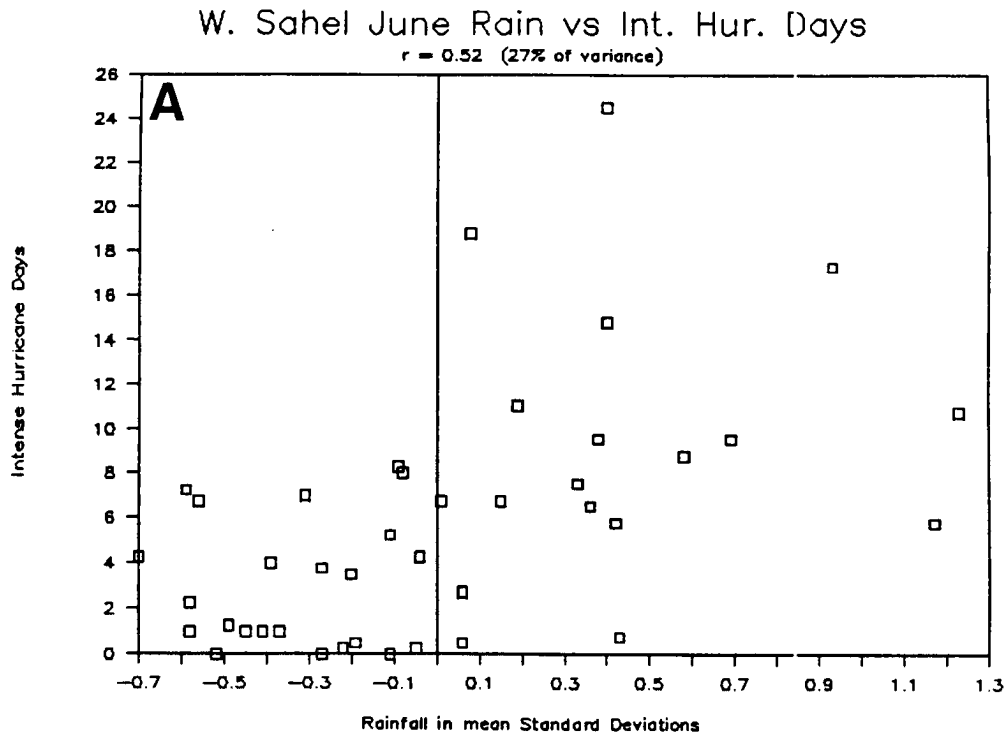


Figure 5.15: Scatter plots of various Seedling Index time periods versus intense hurricane activity. A) June rainfall (correlates at $r = 0.52$), B) June to July rainfall (correlates at $r = 0.70$), and C) June to August rainfall (correlates at $r = 0.72$). Data analyzed is for 1949 to 1989.

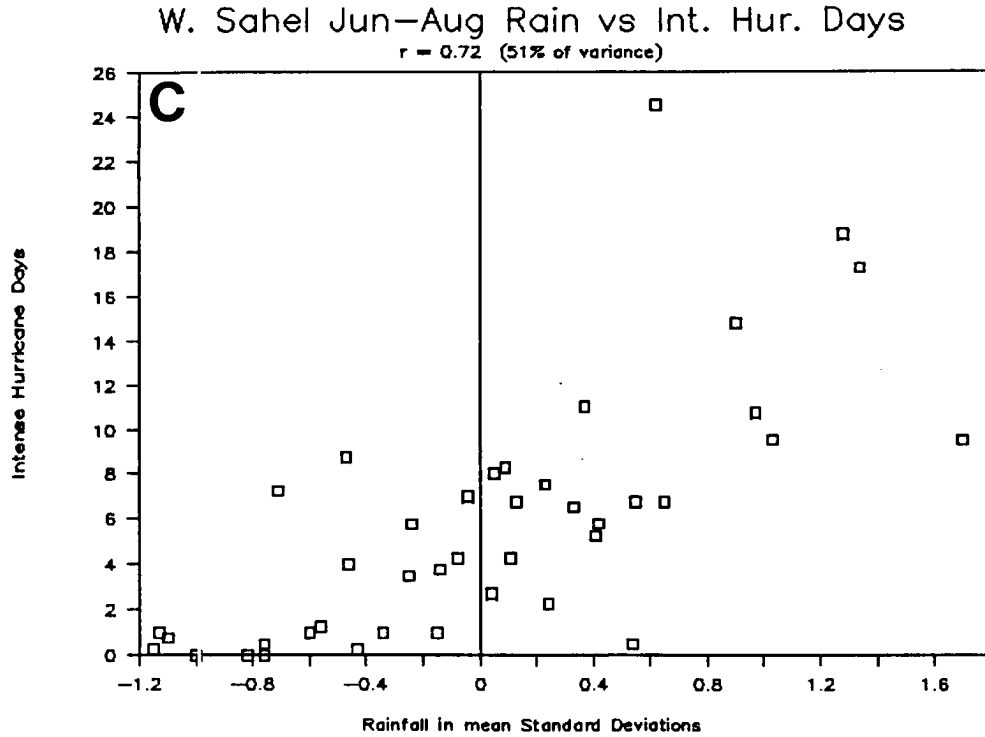


Figure 5.15: c: Continued.

This is important information but it cannot be used in a predictive sense since the threshold value is not apparent until 1 September. Still the identification of such a feature may be useful for understanding the physical mechanisms that connect African monsoon rainfall and Atlantic basin tropical cyclones.

5.8 Ranking of “Seedling” Index Rainfall Values

To facilitate discussions of ‘wet’ and ‘dry’ Western Sahel rainfall years, rankings based upon the June to September Seedling Index rainfall values from 1949 to 1989 were also created (Table 5.8). This allows composite analyses to be performed for groupings of wet versus dry seasons. Another use of the ranked data is with rank correlation tests versus tropical cyclone activity. Figure 5.16 shows a scatter plot of ranked rainfall versus ranked tropical cyclone data from section 3.2.4. The correlation coefficient between the two ranked data sets is $r = 0.80$, or 64% of the variance explained. This value is notably higher than the linear correlation between the June to September Seedling Index and

intense hurricane days ($r = 0.76$), suggesting that a linear relationship between the two may not be the best description of the association.

Table 5.8: June to September Seedling Index, ranked by rainfall amounts expressed as mean standard deviations, for 1949 to 1989.

Rank	Year	Index Value	Rank	Year	Index Value
1.	1950	1.48	22.	1949	-0.10
2.	1955	1.46	23.	1963	-0.11
3.	1958	1.27	24.	1978	-0.20
4.	1952	0.99	25.	1974	-0.25
5.	1964	0.87	26.	1971	-0.32
6.	1954	0.76	27.	1981	-0.36
7.	1961	0.76	28.	1986	-0.39
8.	1967	0.74	29.	1970	-0.47
9.	1989	0.55	30.	1985	-0.52
10.	1969	0.54	31.	1979	-0.56
11.	1953	0.54	32.	1976	-0.58
12.	1965	0.52	33.	1980	-0.70
13.	1957	0.51	34.	1968	-0.77
14.	1960	0.49	35.	1987	-0.78
15.	1956	0.38	36.	1973	-0.82
16.	1975	0.34	37.	1982	-0.90
17.	1951	0.30	38.	1977	-0.93
18.	1962	0.18	39.	1984	-1.19
19.	1988	0.17	40.	1972	-1.19
20.	1966	0.06	41.	1983	-1.34
21.	1959	0.04			

5.9 Wet Versus Dry Seasons

Compositing parameters for the wettest and the driest Western Sahel rainfall seasons accentuates physical differences between the two regimes. In any single season, other factors which occasionally exert strong control on the variability of tropical cyclones may obscure the tropical cyclone—African rainfall signal. This problem is reduced in a composite analysis approach. For the following analyses, data for the ten wettest years (mean June to September Seedling Index value of $\sigma = 0.94$) are contrasted with the ten driest years (mean index value of $\sigma = -0.92$). The listing of these years is shown in Table 5.8.

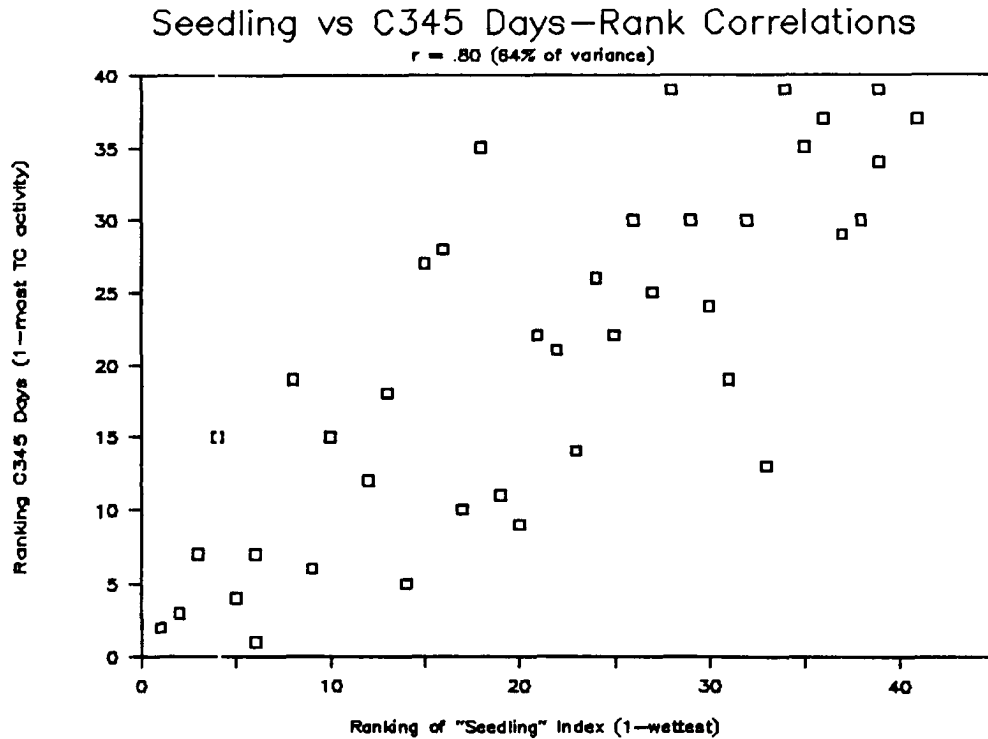


Figure 5.16: Scatter plot of ranked June to September Seedling Index rainfall versus ranked intense hurricane activity from 1949 to 1989. Correlation is $r = 0.80$.

5.9.1 Geographic Rainfall Variations

The June to September Seedling Index includes only stations in the westernmost Sahel. It is instructive to observe how rainfall variation occurs throughout the remainder of Africa. Figure 5.17 contrasts African rainfall in the ten wettest versus the ten driest June to September Seedling Index years. Observe that while the strongest deviations are in the Seedling region as expected, the entire Sahel shows the same variability. Also the earlier noted tendency for the Gulf of Guinea to show inverse anomalies is true here as well.

The realization that the entire Sahel shows strong consistency of rainfall variations, as well as correlation with tropical cyclone activity (sections 4.3 and 5.1) should allow virtually any measure of Sahel rainfall (i.e., Lake Chad levels, Niger and Senegal river runoff, agricultural production) to be used to extrapolate backward through past few centuries to obtain an estimate of Atlantic basin tropical cyclone activity. Attempts like this should now be explored.

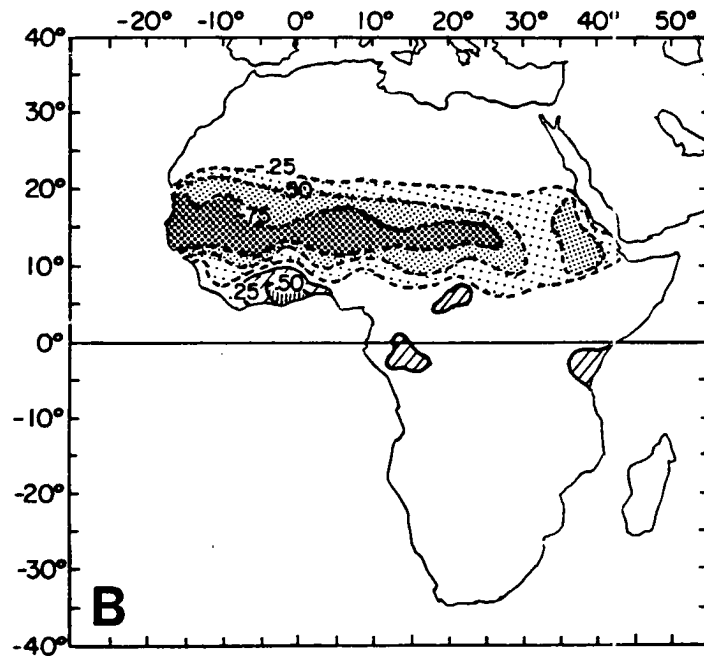
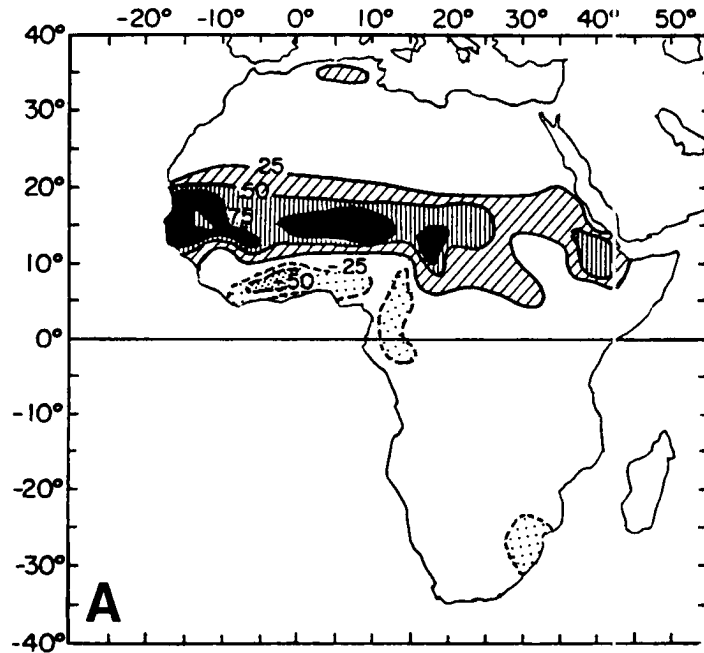


Figure 5.17: June to September African rainfall anomalies during the ten wettest (A) and the ten driest (B) June to September Seedling Index rainfall years. Contours are in $\sigma = \pm 0.25, 0.50, \text{ and } 0.75$. Solid contours indicate positive deviations (i.e. wetter than normal) and dashed contours indicate negative deviations (i.e. drier than normal).

5.9.2 Tropical Cyclone Variability

There is much benefit in observing the climatological variability of individual cyclone tracks. Spatial differences quickly come to light and we can discern whether a reduction in the number of tropical cyclone days is due more to a reduction in the total number of systems or to a decrease in the mean lifetime of the cyclones. With this perspective in mind we examine both weak and strong cyclones.

Tropical and Subtropical Storms: We have noted previously that Western Sahel rainfall correlates moderately well with named tropical storm statistics, hurricane statistics correlate strongly; and the most intense hurricanes correlate the strongest. It is logical to assume with these overlapping categories that the weakest tropical cyclones would have a negligible relationship with Western Sahel rain. This is the case as the linear correlation coefficient for this association is $r = -0.13$, actually showing a slight negative tendency. Figure 5.18 graphically shows that in general, the weaker systems number about the same and have similar lifetimes during both wet and dry stratifications. It is noticeable that in the driest years, a larger number of systems dissipated in the central Atlantic Ocean, east of the Lesser Antilles and also that a larger number of systems occurred north of 30°N and east of the U.S.

Hurricanes: Figure 5.19 contrasts hurricane tracks in the ten wettest versus the ten driest Western Sahel years. The most identifiable feature in this analysis is the large reduction in total number of hurricanes during the dry regime. Secondly, only three or four dry year systems would likely be considered as "Cape Verde" hurricanes; the ones which begin to form in the eastern Atlantic and then track westward from near the Cape Verde Island across the Atlantic as hurricanes. Conversely, as many as 20 or more systems could be so designated during the wet years. Thirdly, the latitude at which the hurricanes definitely develop appears to be farther north during the dry years.

Intense Hurricanes: Figure 5.20 presents a striking contrast between the large number of intense hurricanes in the ten wettest years versus little activity in the ten driest years. This is a surprisingly strong wet versus dry modulation.

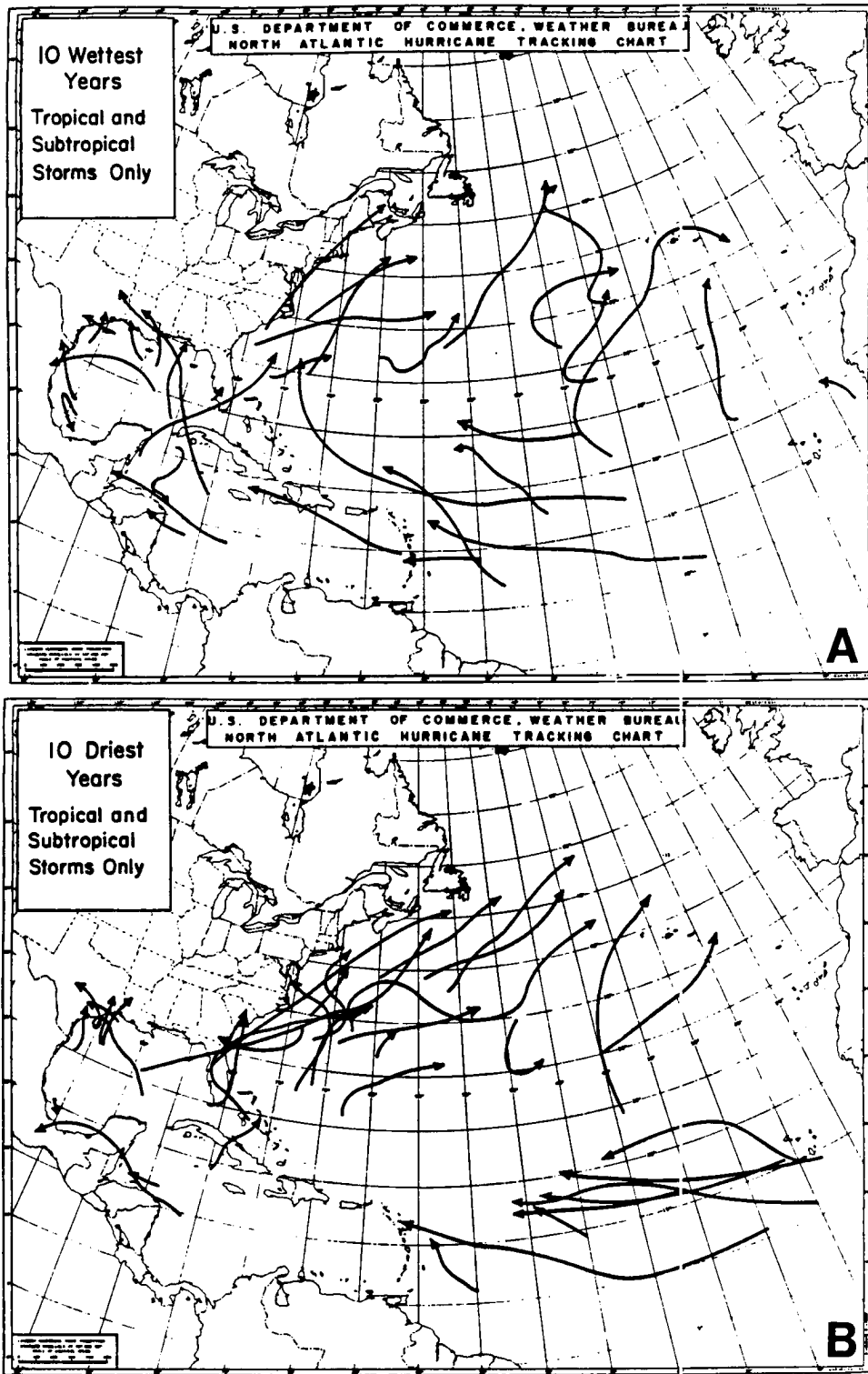


Figure 5.18: Tropical and subtropical storm tracks in the ten wettest (A) versus the ten driest (B) Western Sahel years from 1949 to 1989.

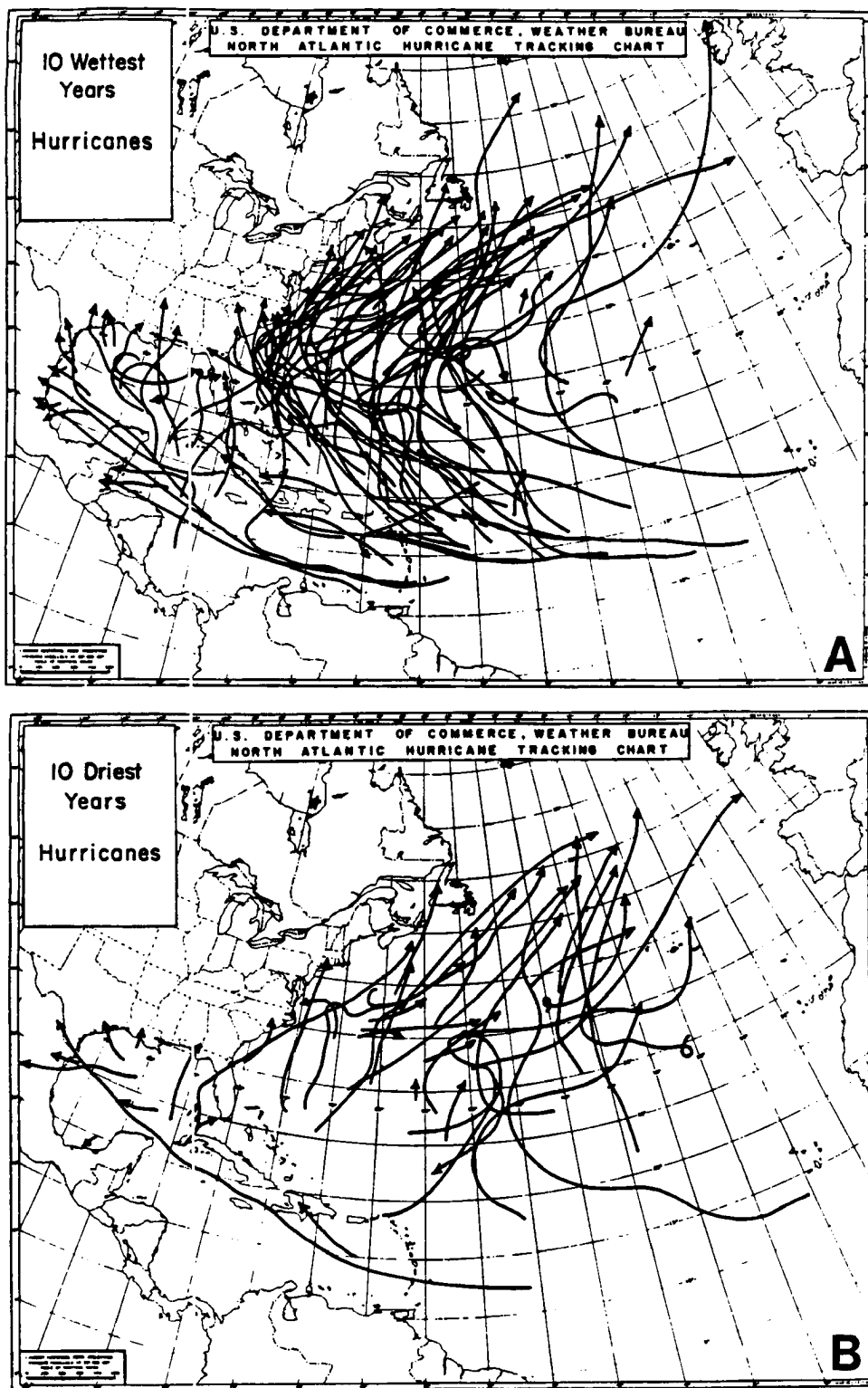


Figure 5.19: Hurricane tracks in the ten wettest (A) versus the ten driest (B) Western Sahel years between 1949 and 1989.

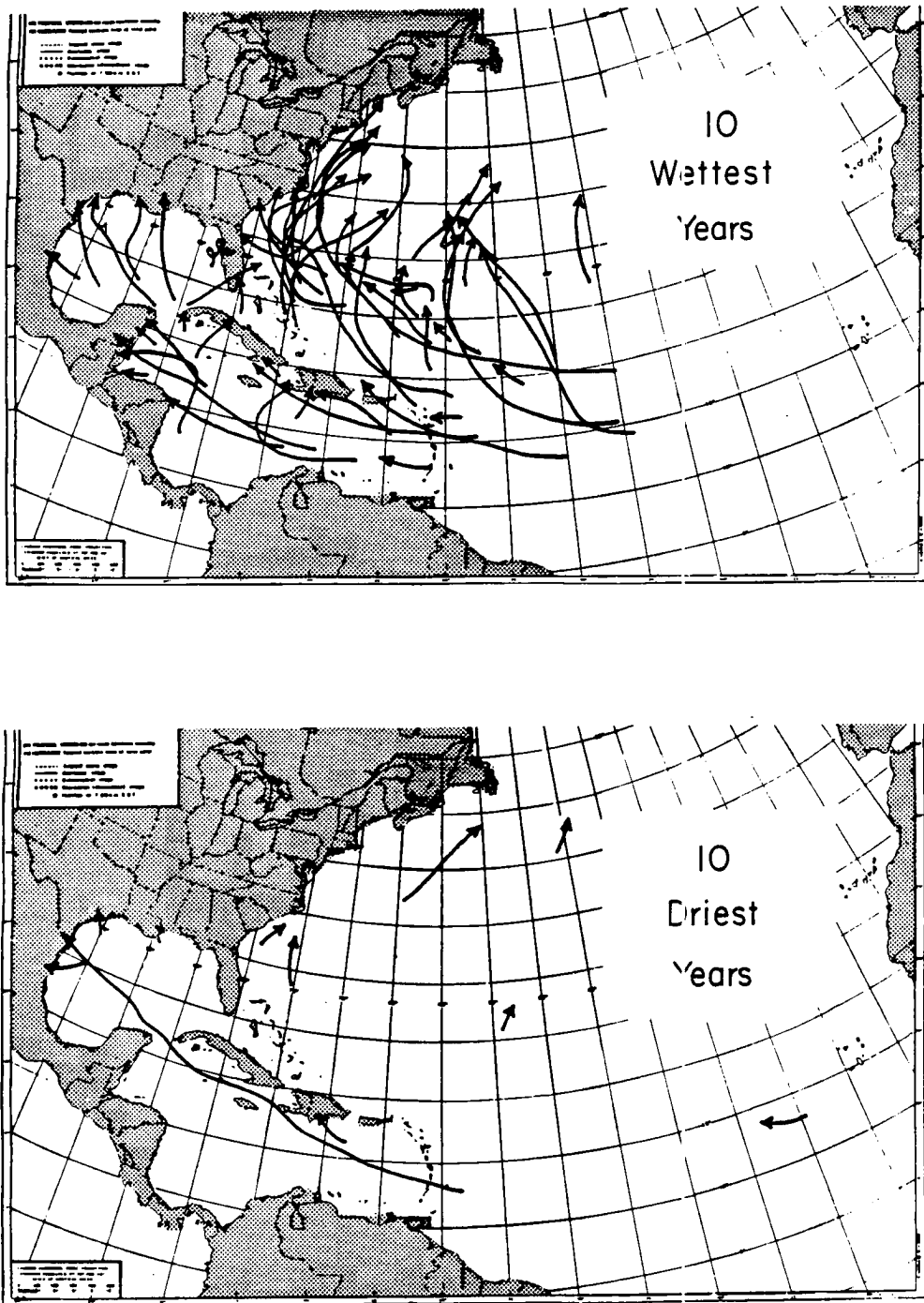


Figure 5.20: Intense hurricane tracks in the ten wettest (A) versus the ten driest (B) Western Sahel years from 1949 to 1989.

Major U.S. Landfalling Hurricanes: Figure 5.21 presents a partially independent verification of Fig. 5.20. This contrast of wet versus dry year intense hurricanes which made landfall on the continental US stands out clearly when the entire hurricane strength track for the cyclones are shown. Both figures indicate that intense hurricane activity, whether measured by U.S. landfalling systems or by overall activity in the basin, is much higher in wet versus dry years.

Summary: The graphical data in the preceding figures, as well as additional tropical cyclone parameters (including U.S. damage) are summarized in Table 5.9. This table confirms that Atlantic basin tropical cyclones are concurrently related to Western Sahel rainfall, that the relationship is strongest for the most intense hurricanes, and that this association is also manifest as the landfalling storms striking the U.S. The effect upon the U.S. is most pronounced for intense hurricanes striking the East Coast and for damage from hurricanes along that coastline.

We can also test the hypothesis that the duration of the tropical cyclones show wet versus dry year differences. Table 5.10 presents data on variations of the tropical cyclone duration, calculated simply by dividing the mean number of cyclones into the cyclone days. It is observed that there is a slight trend for shorter lived named storms during dry versus wet years, the largest differences (more than 2 to 1) are observed for the duration of the strongest hurricanes.

5.9.3 Easterly Wave Genesis Variations

One possible mechanism which can account for the covariation of tropical cyclones and the Western Sahel rainfall concerns differences in the genesis point of the cyclones. Although more than half of all tropical storms and hurricanes in the Atlantic basin can be attributed to easterly waves, most intense hurricanes have their origin from these waves.

As noted in section 2.1.4, reliable estimates of the genesis point of Atlantic basin cyclones have only been available since 1967. Consequently, utilizing the ten wettest versus the ten driest Western Sahel years is not possible as the majority of the wet years occurred before that date. From Table 5.2, we can designate all years since 1967 with

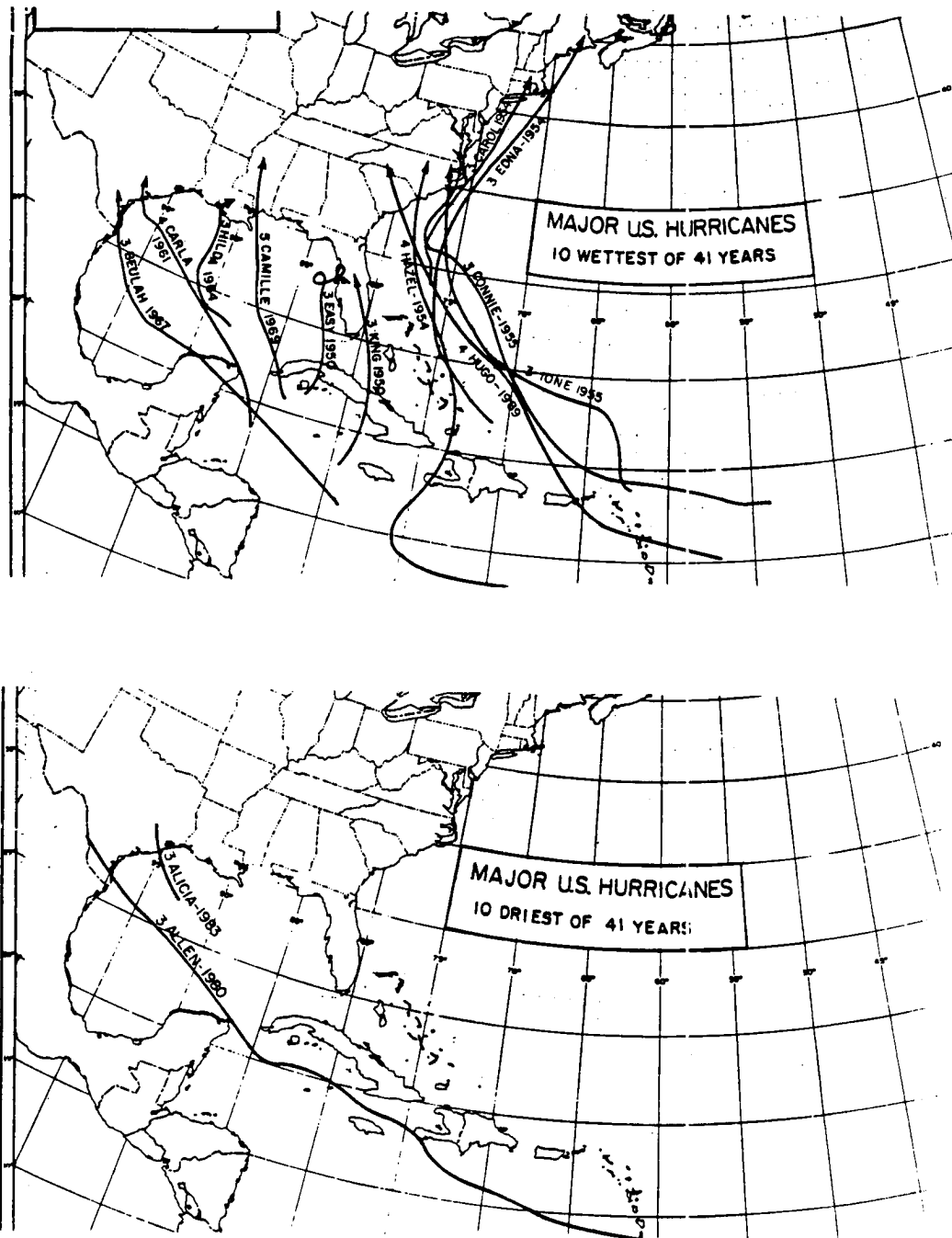


Figure 5.21: US landfalling intense hurricanes in the ten wettest (A) versus the ten driest (B) Western Sahel years from 1949 to 1989. The entire hurricane force portion of the track is presented along with the hurricane name and Saffir-Simpson category at landfall.

Table 5.9: Summary of the variability of tropical cyclone parameters during the ten wettest Western Sahel years (as measured by the June to September Seeding Index) and the ten driest years from 1949 to 1989. Damage is expressed in millions of 1990 dollars. (Asterisks refer to significance level: 0.100 for '*', 0.025 for '**' and 0.005 for '***'.)

Tropical Cyclone Parameter	Wettest Years' Mean	Percent of Normal	Driest Years' Mean	Percent of Normal	Ratio Wet/Dry	
Trop./Subtropical	3.4	86	3.6	91	0.94	
Named Storms	11.2	120	7.1	76	1.58	***
Named Storm Days	67.0	143	31.7	68	2.11	***
Hurricanes	8.0	138	4.4	76	1.82	***
Hurricane Days	39.1	165	13.0	55	3.01	***
Intense Hurricanes	4.5	180	1.0	40	4.50	***
Intense Hurricane Days	12.6	217	1.2	21	10.31	***
HDP	131.2	175	34.7	46	3.78	***
US Landfalling:						
Named/Subtropical	3.4	106	2.6	81	1.30	
Hurricanes	2.1	130	0.8	50	2.62	**
Intense Hurricanes	1.2	197	0.2	33	6.00	***
Intense Gulf Coast	0.5	147	0.2	59	2.50	*
Intense East Coast	0.7	241	0.0	0	∞	**
Hurricane Damage	\$3934	223	\$433	25	9.09	***
' ' Gulf Coast	1058	119	394	44	2.69	
' ' East Coast	2876	329	39	4	73.74	***

Table 5.10: Variation in the duration of named storms, hurricanes, and intense hurricanes in the ten wettest and ten driest Western Sahel years as measured by the June to September Seeding Index from 1949 to 1989. (Asterisks refer to significance level: 0.100 for '*', 0.025 for '**' and 0.005 for '***'.)

Tropical Parameter	41-Year Mean Days	41-Year S. D. Days	Wettest Years' Mean Days	Percent of Normal %	Driest Years' Mean Days	Percent of Normal %	Ratio Wet/Dry
Named Storms	4.9	1.1	6.0	122	4.5	92	1.33***
Hurricanes	3.9	1.49	4.9	126	3.0	77	1.63***
Intense Hurricanes	2.3	1.68	2.8	122	1.2	52	2.33***

positive rainfall anomalies as “wet” years and those seasons with negative anomalies as “dry” years. This stratification separated the 23 years available into 5 wet years (with a mean value of $\sigma = 0.47$) and 18 dry years ($\sigma = -0.68$). Table 5.11 shows the results of this analysis along with the means from all available years (from Section 3.3). It is observed that a much higher incidence of easterly wave contribution occurs when the Western Sahel is wet. We can see that the increased incidence of cyclones in these wet years is due to more storms forming from easterly waves. In addition, the non wave cyclones, though not explicitly described above, show a slightly higher incidence in the dry years. We may speculate that in the wet years, general circulation conditions favor more easterly waves becoming tropical cyclones and especially developing into intense hurricanes. During the dry years, the general circulation is unfavorable for the development of easterly wave spawned storms, while the midlatitude spawned systems are slightly enhanced.

Table 5.11: Mean annual easterly wave contributions toward various tropical cyclone intensity categories for the Seedling Index wet (5) and dry years (18), as well as the entire 23 year data set.

Tropical Cyclone Intensity	Wet Years (5)			Dry Years (18)			All Years (23)		
	Total #	East. #	Waves %	Total #	East #	Waves %	Total #	East #	Waves %
Named Storms	11.4	8.0	70	8.2	4.9	59	8.9	5.6	62
Hurricanes	7.2	5.8	81	4.8	2.8	59	5.3	3.5	66
Int. Hurricanes	2.8	2.6	93	1.4	1.1	80	1.7	1.5	87

5.10 Persistence of Rainfall

As was seen in the analysis of the Lamb Index in section 4.1, rainfall in the Sahel has strong year to year persistence. If the current year is dry, it is likely that next year will also be drier than normal. Conversely, wet years in the Sahel often follow a wet year. This type of forecasting, the use of persistence only, is often described as a “no skill” forecast.

As shown in Fig. 5.22, the use of persistence from one year to the next to forecast Sahel rainfall shows a moderate degree of success with the June to September Seedling Index. One quarter of the variance for the following year’s rainfall is explained by persistence of

conditions (significant to the 0.005 level). However, in the years where there is an abrupt switch from dry to wet or vice versa, large errors occur. For instance, 1967 was a very wet year with rainfall averaging $\sigma = 0.74$ throughout the Western Sahel region. In the following year, 1968 averaged a very dry $\sigma = -0.77$ for the Seedling Index and the Sahel plunged into the drought wherein it has remained, more or less, since that time. It is hoped that with further study, the Sahel can be shown to be a region where a degree of predictability beyond the simple use of persistence can be developed.

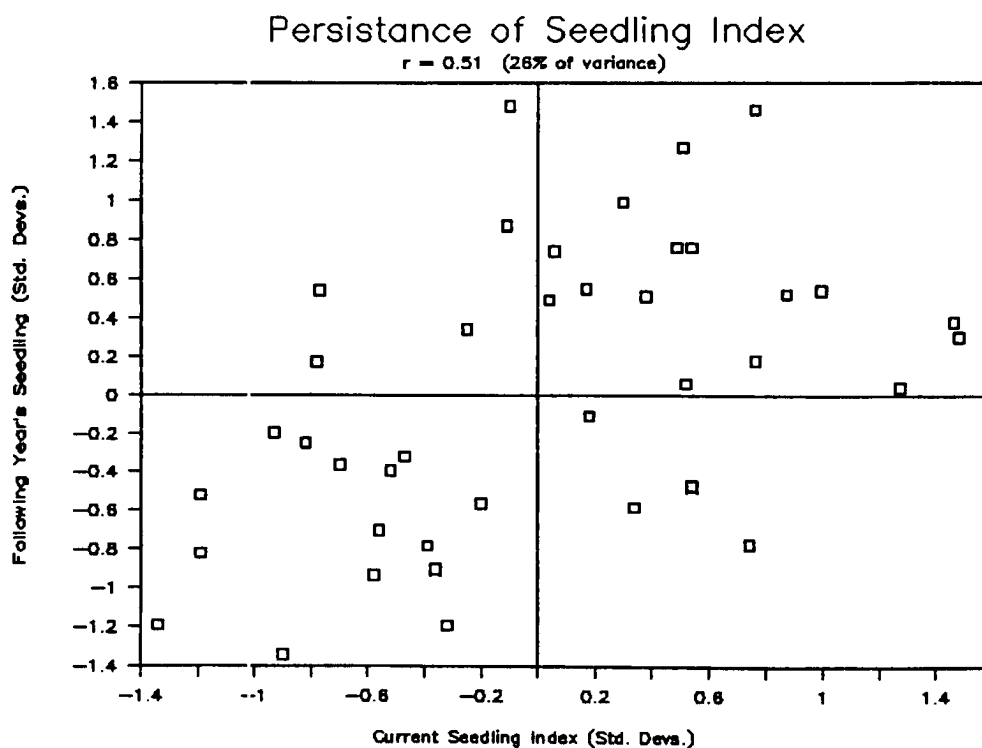


Figure 5.22: The scatter plot of the current year's June to September Seedling Index (using data from 1949 to 1988) versus the following year's Seedling Index (1950 to 1989). The two parameters correlate at $r = 0.51$.

5.11 August to September "Seedling" Index Subset

The issuing of a seasonal tropical cyclone forecast in early August (Gray, 1990b), and knowledge that over 98% of intense hurricane activity occurs after this date (section 3.1.1) leads to the use of a June to July Western Sahel rainfall index. This greatly assists with the forecast. It will be shown how the earlier June to July rainfall relates to the rainfall occurring in the following months of August to September.

Figure 5.23 shows values of an August to September the Seedling Index from 1949 to 1989. This bar graph is very similar to that presented in Fig. 5.8 for the entire June to September time period. The correlation coefficient between the two dependent rainfall data sets is $r = 0.96$. The anomaly values are similar since the means for August to September comprise almost two thirds of the June to September total rainfall.

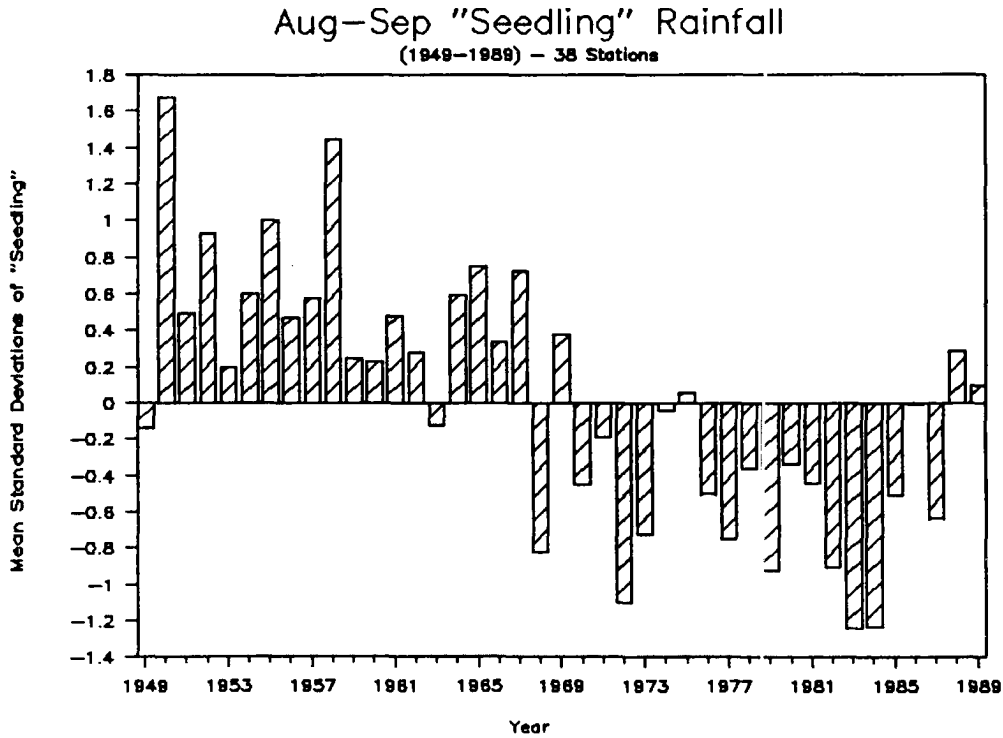


Figure 5.23: Mean standard deviations of rainfall for the 38 station August to September subset of the Seedling Index of the Western Sahel. Data is analyzed for the years 1949 to 1989.

In general, the various tropical cyclone parameters correlate with August to September rainfall similarly to the entire June to September period, but are weaker overall (Fig. 5.24 and Table 5.12). This was expected since the original analysis which created the Seedling Index also looked over all possible monthly combinations to find the optimal period of correlation.

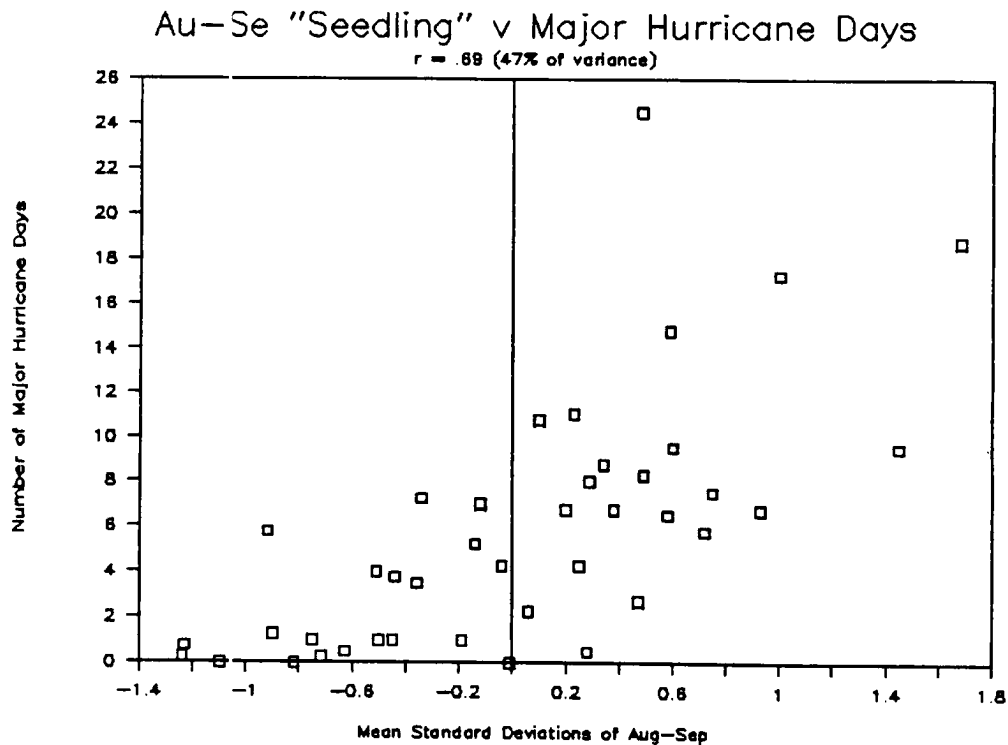


Figure 5.24: Scatter plot of 1949 to 1989 values of the August to September Seedling Index rainfall subset versus intense hurricane days. The two parameters have a linear correlation coefficient of $r = 0.69$.

Table 5.12: Correlation coefficients for August to September Seedling Index rainfall subset versus Atlantic basin tropical cyclone parameters for the years 1949 to 1989. (Asterisks refer to significance level: 0.100 for '*', 0.025 for '**' and 0.005 for '***'.)

Tropical Cyclone Parameter	Correlation Coefficient	Tropical Cyclone Parameter	Correlation Coefficient
Named Storms	0.35**	Named Storm Days	0.55***
Hurricanes	0.50***	Hurricane Days	0.68***
Intense Hurricanes	0.65***	Intense Hurricane Days	0.69***
Int. Hur. (Bias Out)	0.62***	Int. Hur. Days (Bias Out)	0.62***
HDP	0.70***		

Chapter 6

GULF OF GUINEA RAINFALL INDEX

6.1 August to November Gulf of Guinea Rainfall

As discussed in Chapter 4, rainfall along the Gulf of Guinea region during the late summer and fall appears to be related to Atlantic basin tropical cyclone activity in the following year. Using methodology similar to that presented in the previous chapter, correlations are enhanced by using rainfall data for the August to November time period. During that time, the ITCZ begins its southward retreat over the African continent, from the Northern to the Southern hemisphere. However, the greatest mean rainfall is north of the equator during the four months of August to November (see Fig. 6.1). Light amounts of precipitation occur between 10 and 30°S in conjunction with the ITCZs southward push.

The area of interest extends from the Gulf of Guinea to 10° North and from 10°E to 15° W longitude, encompassing the countries of Sierra Leone, southern Guinea, Liberia, Cote D'Ivoire, Ghana, Togo, Benin, and southern Nigeria (see Fig. 5.7). The movement of the ITCZ through this area, as noted in section 4.2, causes two rainy seasons: one as the axis of the ITCZ is moving northward in May to early July and the other as the ITCZ slides south again in late August to early November. It is the second rainfall maxima that has a strong association with Atlantic hurricane activity during the following year.

The original analysis described in section 4.4 indicated that there is a substantial lag correlation of nearly a year. Therefore, the following analysis was obliged to use rainfall data for 1948 as well.

Correlation maps for Africa (Figs. 6.2 and 6.3) suggest that very strong correlations exist between August to November rainfall along the Gulf of Guinea and all tropical

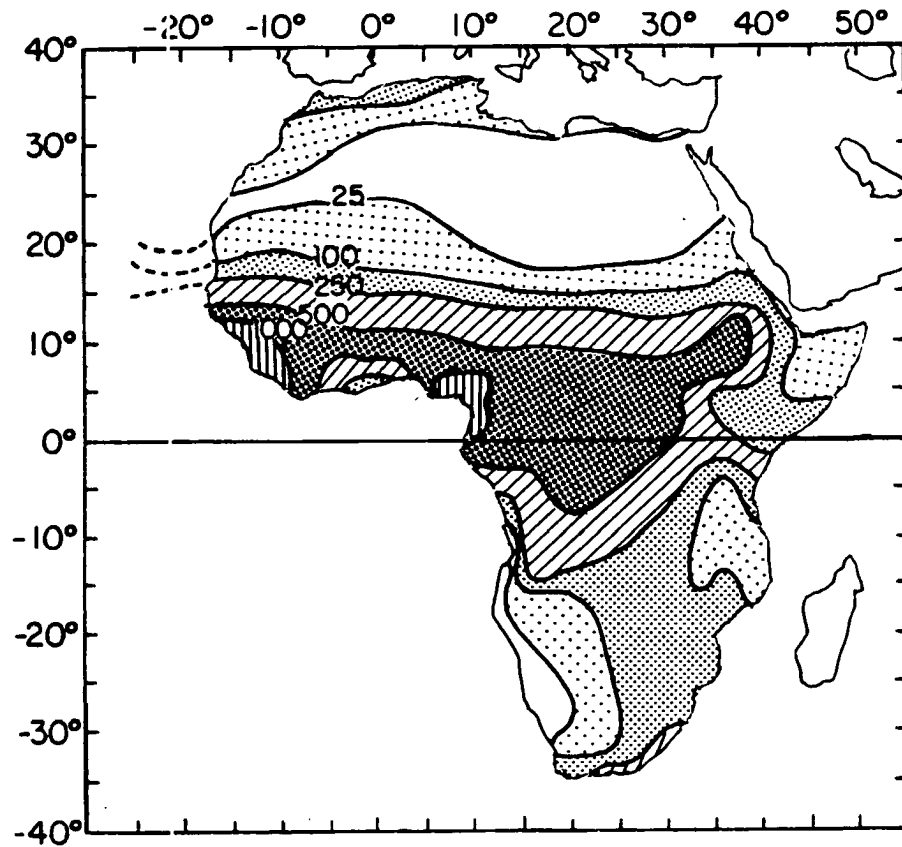


Figure 6.1: August to November precipitation over Africa using data from 1948 to 1989. Contours are at 25, 100, 250, 500, and 1000 mm.

cyclone intensities. A weaker positive association in the Sahel region is more apparent for increasing intense cyclone activity. This association is a result of the strong persistence of rainfall in this area (section 5.10). Observe that the persistence signal is spatially separated from and shows much weaker correlations than does the Gulf of Guinea region.

To confirm that this Gulf of Guinea association is due to a feedback into the next year's monsoon, Fig. 6.4 presents a map of correlations between individual station rainfall and the following year's June to September Seedling Index. As expected, positive correlations mark the persistence of rainfall in the Sahel. However, the Gulf of Guinea region again has stronger, more widespread positive correlations. This analysis makes a convincing suggestion that larger amounts of monsoonal rainfall in the second rainy season along the Gulf of Guinea somehow provide the potential for above normal rainfall in the Western Sahel.

6.2 Development of the Gulf of Guinea Rainfall Index

To facilitate a more quantitative discussion of the relationship of rainfall to tropical cyclones, an index of the Gulf of Guinea rainfall is created. Figure 6.5 shows year by year values of the August to November Gulf of Guinea rainfall index. The locations of the twenty four stations that comprise the index are displayed in Fig. 5.7. All rainfall stations within the region's boundaries that have a minimum of 17 years of data between 1948 and 1989 are included in the Index. One obvious aspect of Fig. 6.5 is that this rainfall time series shows much less downward trend than is seen in the Sahel June to September Seedling Index.

Table 6.1 details the data availability for the Gulf of Guinea rainfall index for each year from 1948 to 1989. Yearly values with less than ten stations are suspect, especially the years 1981 (with just 2 stations) and 1984 (with 4). The country of Guinea has had a poor record for rainfall data in the past few decades. None of its stations could meet the 17 year minimum. Fortunately, with the recent addition of more Nigerian and CAC historical data (see section 2.2), the reliability of the Gulf of Guinea Index has been much improved. Appendix 2 updates the Index to include this additional data.

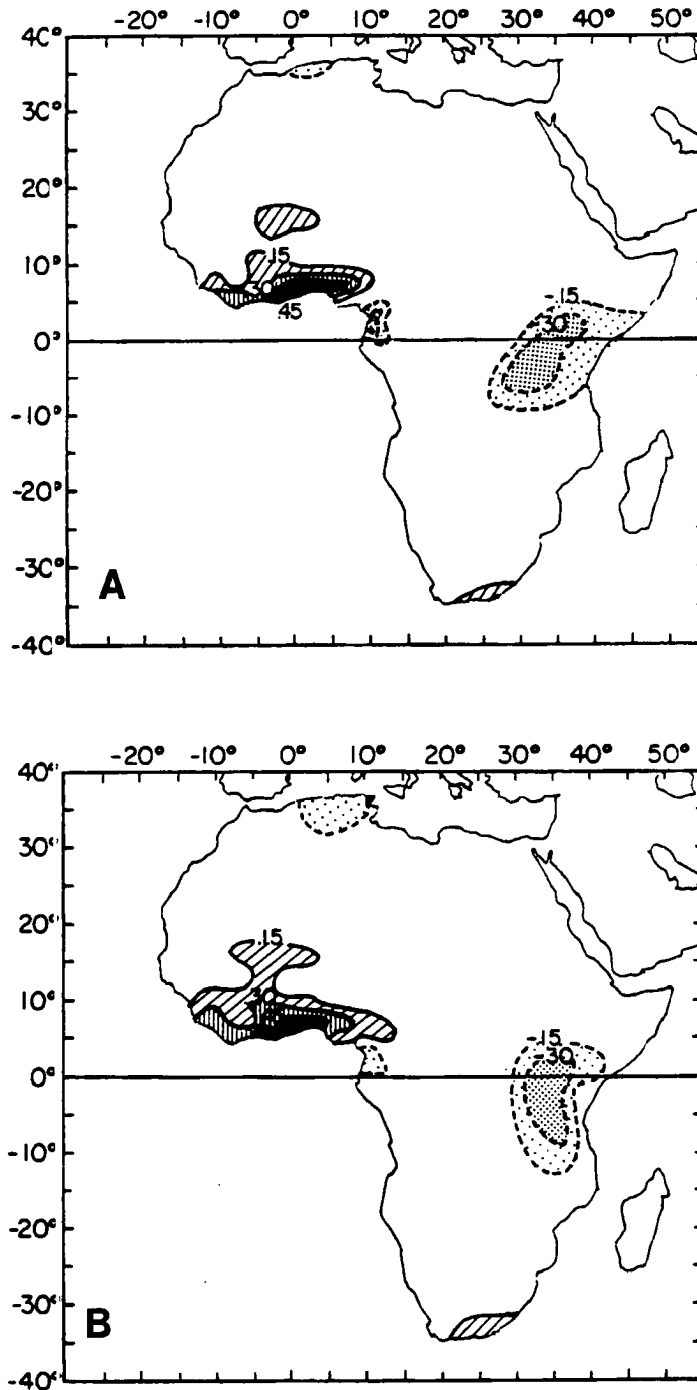


Figure 6.2: Correlation coefficients of individual station August to November rainfall versus the following year A) named storms, B) hurricanes, and C) intense hurricanes. Stations were only included in the analysis if they had at least 12 years of data between 1948 and 1989. Contours indicate values of $r = \pm 0.15$, 0.30 , and 0.45 . Positive correlations are within solid contours, while negative contours are indicated by dashed lines.

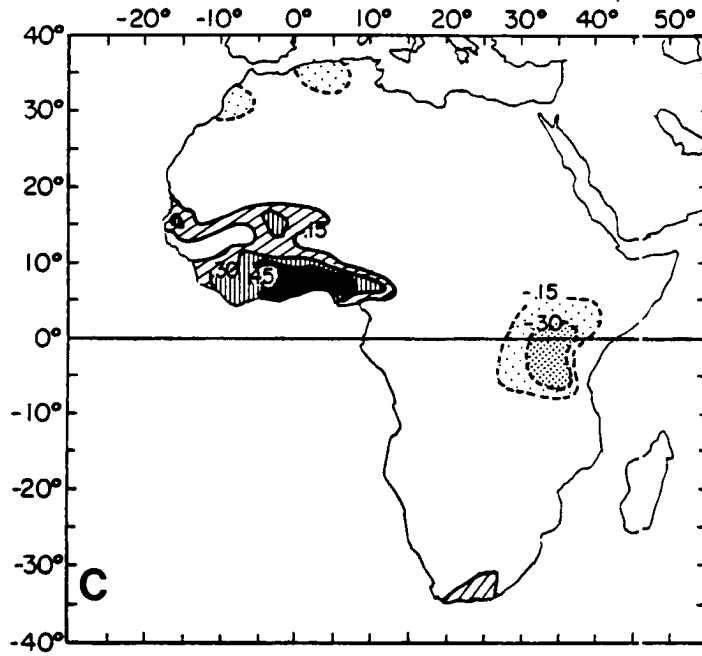


Figure 6.2: c: Continued.

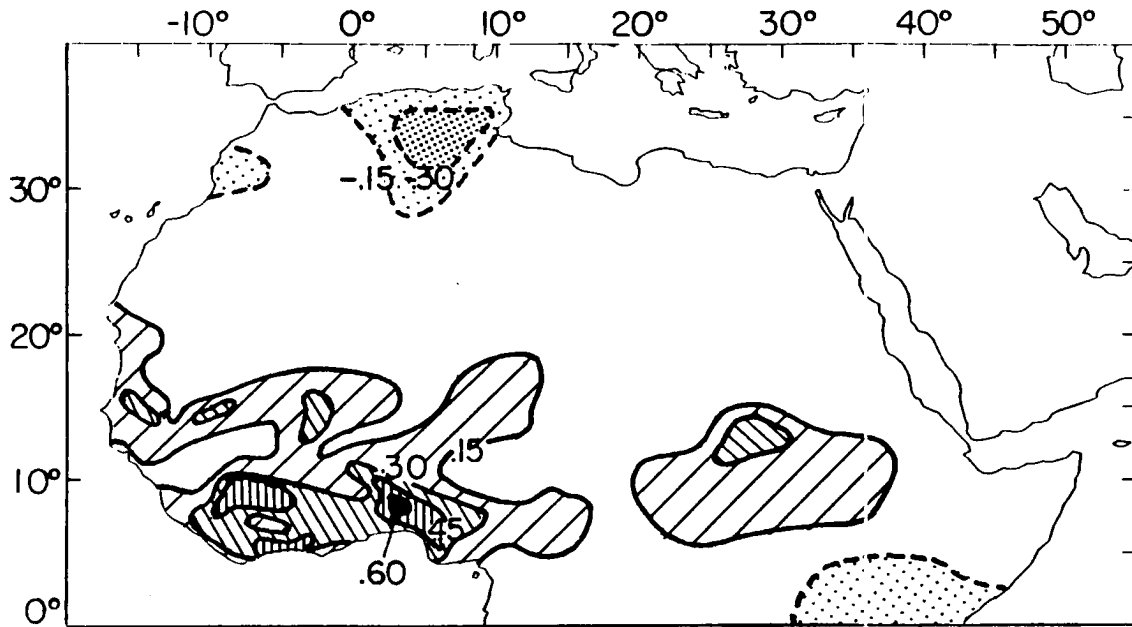


Figure 6.3: Same as Fig. 6.2 with August to November rainfall versus following year intense hurricane days.

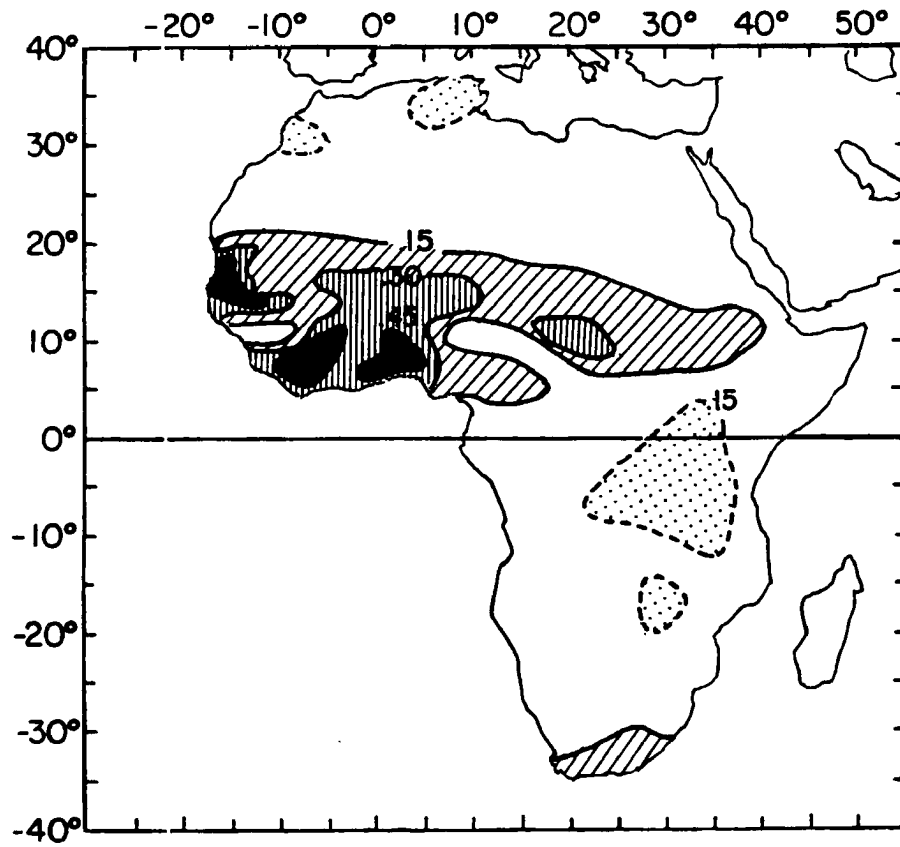


Figure 6.4: Same as Fig. 6.2 with August to November rainfall versus following year Western Sahel June to September Seedling Index.

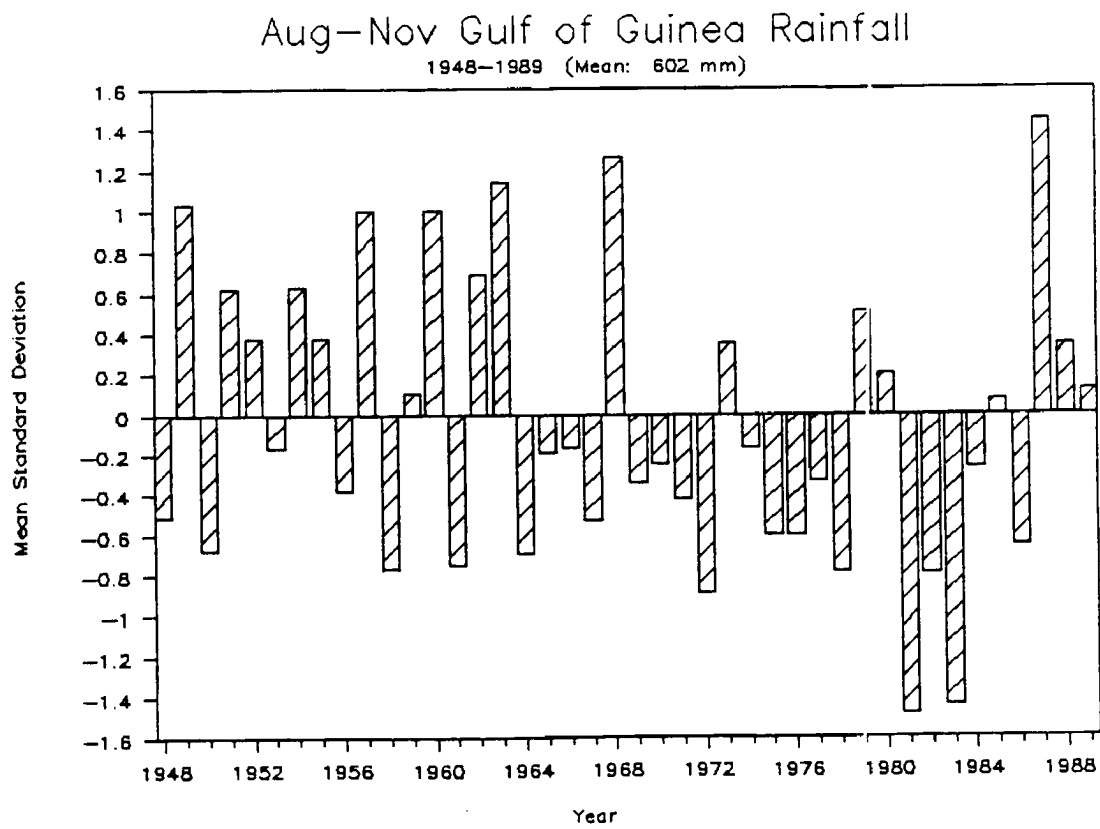


Figure 6.5: Yearly values of the 24 station August to November Gulf of Guinea Index of rainfall expressed in terms of relative standard deviations. Data presented are from 1948 to 1989.

Table 6.1: Mean standard deviations and data availability (out of a possible 24 stations per year) for the August to November Gulf of Guinea Index.

Year	Standard Deviations	Number of Stations	Year	Standard Deviations	Number of Stations
1948	-0.51	19	1970	-0.25	22
1949	1.03	19	1971	-0.42	22
1950	-0.68	19	1972	-0.89	20
1951	0.62	23	1973	0.35	19
1952	0.38	23	1974	-0.17	19
1953	-0.17	23	1975	-0.60	11
1954	0.63	23	1976	-0.60	14
1955	0.38	23	1977	-0.33	16
1956	-0.38	23	1978	-0.78	15
1957	1.00	23	1979	0.51	14
1958	-0.77	23	1980	0.20	15
1959	0.10	15	1981	-1.48	2
1960	1.00	15	1982	-0.79	9
1961	-0.75	21	1983	-1.44	11
1962	0.69	22	1984	-0.27	4
1963	1.14	24	1985	0.07	9
1964	-0.69	23	1986	-0.65	9
1965	-0.19	14	1987	1.44	8
1966	-0.17	19	1988	0.34	9
1967	-0.53	21	1989	0.12	17
1968	1.26	21			
1969	-0.34	18			

Table 6.2 presents information on individual station for the Gulf of Guinea rainfall index. The stations show a good deal of internal consistency with the index itself. Most of the stations show correlations of at least $r = 0.65$ (42.5% of variance). The stations lower than $r = 0.57$ are all on the borders of the region (e.g. Daru, Sierra Leone; Odi-
enne, Ferkessedougou, Dimbokro and Sassandra, Cote D'Ivoire; Roberts Field; Liberia). Individual station correlations with intense hurricane days in the following year vary from a low of $r = 0.13$ (at Ilorin, Nigeria) to $r = 0.70$ (at Dimbokro, Cote D'Ivoire) with the majority of stations being in the range of $r = 0.4$ to 0.6 . Section 6.3 will document the association of the entire Index with tropical cyclone activity.

Table 6.2: The 24 stations used in the Gulf of Guinea Index: CSU Rainfall Data Base identification number, station name and country, August to November rainfall mean and standard deviation (in mm), years of data in analysis, correlation coefficients versus the Gulf of Guinea Index, and correlation coefficient versus intense hurricane days. (Asterisks refer to significance level: 0.100 for '*', 0.025 for '**' and 0.005 for '***'.)

Station	Rainfall Data			vs. Index	vs. Intense	
	Mean	SD	Years	r	Hurr. Days	
0182 Daru, Sierra Leone	1217.2	186.10	27	0.542	0.541	***
0455 Ilorin, Nigeria	573.2	145.57	23	0.756	0.703	***
0459 Lagos/Ikeja, Nigeria	508.7	199.72	25	0.790	0.274	*
0460 Warri, Nigeria	1250.9	237.23	26	0.685	0.473	**
0467 Parakou, Benin	530.8	125.27	40	0.602	0.614	***
0468 Tchaourou, Benin	585.6	189.84	17	0.883	0.453	*
0469 Save, Benin	442.2	154.11	40	0.844	0.578	***
0470 Bohicon, Benin	410.9	156.95	37	0.784	0.418	***
0471 Cotonou, Benin	337.0	204.54	40	0.789	0.310	**
0475 Atakpame, Togo	559.3	159.40	34	0.719	0.388	**
0476 Tabligbo, Togo	338.7	131.64	21	0.906	0.613	***
0477 Lome, Togo	213.2	133.01	35	0.803	0.419	**
0480 Kumasi, Ghana	521.6	147.17	28	0.677	0.420	**
0490 Odienne, Ivory Coast	850.5	165.40	30	0.412	0.568	***
0491 Korhogo, Ivory Coast	678.3	189.03	29	0.701	0.552	***
0492 Ferkessedougou, Ivory Coast	650.9	163.62	22	0.515	0.561	***
0493 Bondoukou, Ivory Coast	454.7	128.08	32	0.775	0.360	**
0495 Bouake, Ivory Coast	445.0	167.13	32	0.574	0.298	*
0496 Gagnoa, Ivory Coast	527.6	146.26	30	0.634	0.447	***
0498 Dimbokro, Ivory Coast	379.4	155.77	31	0.511	0.134	
0500 Abidjan, Ivory Coast	431.4	198.93	31	0.718	0.523	***
0501 Adiake, Ivory Coast	542.3	210.06	26	0.790	0.517	***
0504 Sassandra, Ivory Coast	371.1	211.87	31	0.533	0.369	**
0506 Roberts Field, Liberia	1656.3	407.48	32	0.550	0.336	**

Unlike the Sahel, the Gulf of Guinea region experiences significant rainfall all year round (Table 6.3). The only month which normally has less than 25 mm of precipitation is January, the time of the southernmost retreat of the ITCZ. The two rainy seasons are not separated by complete dryness. Moderate drying is experienced in July and August. Similar to the Sahel, the months with lower rainfall means have relatively higher standard deviations, indicating that these drier months show more variability. There is also a tendency for the timing of the onset of the rainy season in March to May to be more variable than the timing of the retreat of the rainy season in October and November.

Table 6.3: Monthly, multi-monthly and annual means, standard deviations, ratios and coefficients of variation for the 24 stations used in the Gulf of Guinea Index.

	Jan	Feb	Mar	Apr	May	Jun	Jul
Mean	16 mm	50	95	151	186	274	206
Std. Dev.	21 mm	36	48	65	77	102	122
Co. Variation	131%	72	51	43	41	37	59
% Annual	1%	3	6	9	12	17	13
	Aug	Sep	Oct	Nov	Dec	Aug–Nov	Annual
Mean	163 mm	207	163	68	29	602	1609
Std. Dev.	87 mm	90	80	47	31	180	366
Co. Variation	53%	43	49	69	107	30	23
% Annual	10%	13	10	4	2	37	100
% Aug–Nov	27%	35	27	11	—	100	—

While the time period of interest, August to November, has mean precipitation of over 600 mm, it comprises just slightly over a third of the annual total precipitation along the Gulf of Guinea. One can also obtain a good approximation of August to November rainfall totals by the end of October; just 11% of the four month rainfall occurs in November.

6.3 Correlation with Tropical Cyclones

Table 6.4 gives linear correlation coefficients between the August to November Gulf of Guinea rainfall index and a variety of tropical cyclone parameters. The same tendency exists here as in the June to September Seedling Index region. That is, the rainfall–hurricane association becomes stronger as the intensity of the cyclones increases. A scatter plot of intense hurricane activity versus the Gulf of Guinea Index is seen in Fig. 6.6.

Removing the bias from the intense hurricane data does not substantially reduce the strong positive correlations. In fact, intense hurricane numbers actually show a slightly higher association after the bias has been taken out.

Table 6.4: Correlation coefficients between August to November Gulf of Guinea Index rainfall and following year Atlantic basin tropical cyclone parameters for the years 1948 to 1988 (1949 to 1989 for the tropical cyclone data). (Asterisks refer to significance level: 0.100 for ‘*’, 0.025 for ‘**’ and 0.005 for ‘***’.)

Tropical Cyclone Parameter	Correlation Coefficient	Tropical Cyclone Parameter	Correlation Coefficient
Named Storms	0.50***	Named Storm Days	0.58***
Hurricanes	0.56***	Hurricane Days	0.60***
Intense Hurricanes	0.66***	Intense Hurricane Days	0.65***
Int. Hur. (Bias Out)	0.68***	Int. Hur. Days (Bias Out)	0.61***
HDP	0.64***		

Though not necessarily representative of any real physical process, the correlations with named storms and hurricanes are stronger here than for the June to September Seedling Index (section 5.5). This association is a surprise in that there is no obvious reason for more information concerning named storms and hurricanes to be tied to the Gulf of Guinea Index on a predictive basis than there is in the June to September Seedling Index on a concurrent basis.

Even though there is only a small downward long term trend in the Gulf of Guinea rainfall, a check was made to take into account the possibility of trend induced associations. By making a least squares fit to the data in Fig. 6.5 and then removing that trend from the data, a check can be made with detrended information. Linear correlation coefficients between the detrended Gulf of Guinea Index and detrended intense hurricane days shows that the relationship actually gets stronger, $r = 0.71$, explaining a full 50% of the variance in the major hurricane activity. Also, taking into account the bias in the intense hurricanes before detrending gives a correlation of $r = 0.67$, again higher than the relationship in the original analysis.

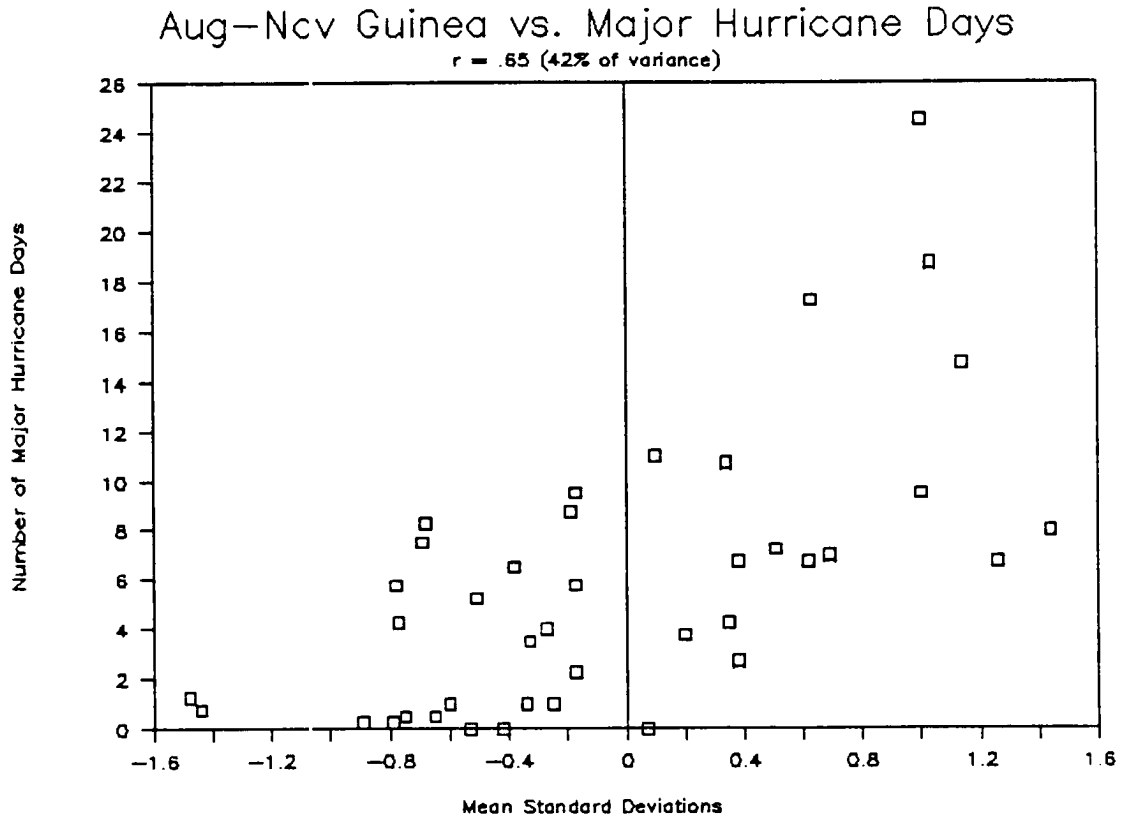


Figure 6.6: Scatter plot of 1948 to 1988 values of August to November Gulf of Guinea Index rainfall versus 1949 to 1989 intense hurricane days. The two parameters have a linear correlation coefficient of $r = 0.65$.

Ranked values of the Gulf of Guinea Index are shown in Table 6.5. A rank correlation was performed with the tropical cyclone activity, thus providing a check for nonlinear associations. This procedure gives a value of $r = 0.64$ with the intense hurricane days, virtually unchanged from the linear correlation. The ranking utilizes the 42 years of data from 1948 to 1989, whereas the linear correlations shown so far do not include the relationship between 1989 Gulf of Guinea rainfall versus 1990 tropical cyclone activity. This last year of information will be discussed in Chapter 9 when an independent verification of the analysis is developed.

Table 6.5: August to November Gulf of Guinea Index ranked by rainfall amounts in mean standard deviations from 1948 to 1989. The 1989 value (asterisked) will not be used here for rank correlations.

Rank	Year	Index Value	Rank	Year	Index Value
1.	1987	1.44	22.	1965	-0.19
2.	1968	1.26	23.	1970	-0.25
3.	1963	1.14	24.	1984	-0.27
4.	1949	1.03	25.	1977	-0.33
5.	1957	1.00	26.	1969	-0.34
6.	1960	1.00	27.	1956	-0.38
7.	1962	0.69	28.	1971	-0.42
8.	1954	0.63	29.	1948	-0.51
9.	1951	0.62	30.	1967	-0.53
10.	1979	0.51	31.	1975	-0.60
11.	1952	0.38	32.	1976	-0.60
12.	1955	0.38	33.	1986	-0.65
13.	1973	0.35	34.	1950	-0.68
14.	1988	0.34	35.	1964	-0.69
15.	1980	0.20	36.	1961	-0.75
16.	*1989*	0.12	37.	1958	-0.77
17.	1959	0.10	38.	1978	-0.78
18.	1985	0.07	39.	1982	-0.79
19.	1953	-0.17	40.	1972	-0.89
20.	1966	-0.17	41.	1983	-1.44
21.	1974	-0.17	42.	1981	-1.48

Rankings of data also allow a comparison of the ten wettest versus the ten driest Gulf of Guinea years (Table 6.6). This comparison further confirms the differences suggested by the correlations, that there is a substantial 6–11 month lead time predictability of

the Atlantic basin tropical cyclone activity from August to November Gulf of Guinea rainfall and that this long lead time association is strongest for the more intense cyclones. This large increase in storm frequency with greater rainfall manifests itself in more US landfalling tropical cyclones and hurricane spawned damage, especially intense hurricanes and associated damage along the East Coast. Wet year versus dry year track differences for intense hurricanes are depicted in Fig. 6.7. Note that there is a large decrease in overall intense hurricane activity in the Caribbean and the Atlantic but not so much in the Gulf of Mexico. Speculation on physical mechanisms responsible for these differences will be presented in Chapter 10.

Table 6.6: Summary of the variability of following year tropical cyclone parameters in the ten wettest August to November Gulf of Guinea years and the ten driest years from 1948 to 1988. Damage is expressed in millions of 1990 dollars. (Asterisks refer to significance level: 0.100 for ‘*’, 0.025 for ‘**’ and 0.005 for ‘***’.)

Tropical Cyclone Parameter	Wettest Years' Mean	Percent of Normal	Driest Years' Mean	Percent of Normal	Ratio Wet/Dry
Named Storms	11.6	125	7.5	81	1.55***
Named Storm Days	66.1	142	35.4	76	1.86***
Hurricanes	8.0	138	4.4	76	1.82***
Hurricane Days	39.0	165	16.1	68	2.42***
Intense Hurricanes	4.7	188	1.6	64	2.94***
Intense Hurricane Days	12.0	207	2.9	50	4.14***
HDP	132.1	176	46.3	62	2.85***
US Landfalling:					
Named/Subtrop.	3.1	97	2.5	78	1.24
Hurricanes	1.9	118	1.0	62	1.90
Intense Hurricanes	0.8	131	0.4	66	2.00
Intense Gulf Coast	0.3	88	0.3	88	1.00
Intense East Coast	0.5	172	0.2	69	2.50
Hurricane Damage	\$2277	129	\$1673	95	1.36
'—Gulf Coast	1010	114	1508	170	0.67
'—East Coast	1267	145	165	19	7.68

6.4 Correlation with Seedling Index

The physical link behind the association of the late summer and fall Gulf of Guinea rainfall with Atlantic tropical cyclone activity in the following year is not well understood.

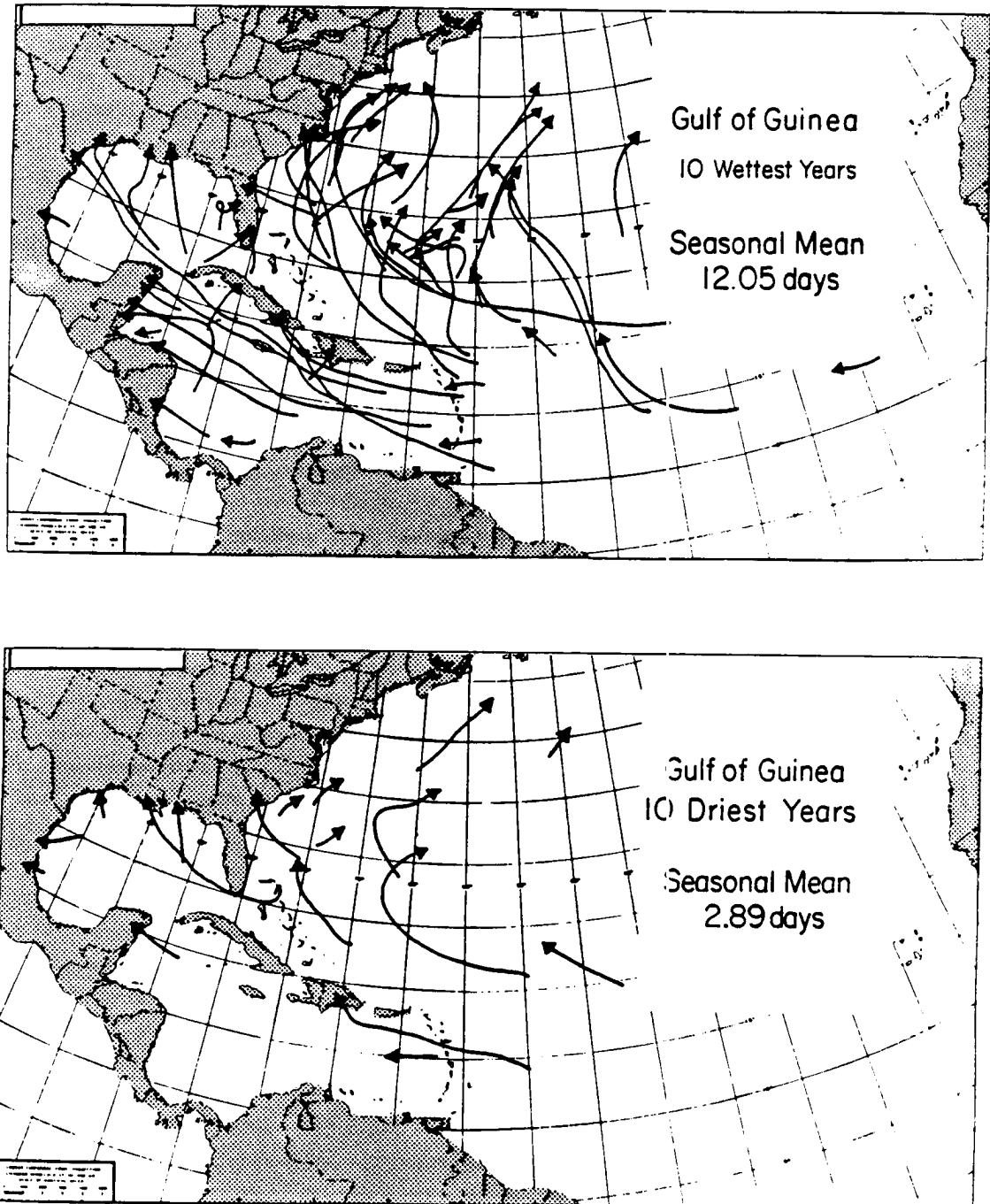


Figure 6.7: Intense hurricane tracks in the years following the ten wettest (upper panel) versus the ten driest (bottom panel) August to November Gulf of Guinea years from 1948 to 1988.

However, it is apparent that a wet August to November along the Gulf of Guinea seems to make it more likely that there will be an above normal rainy season in the Sahel during the following summer and conversely, drier conditions along the Gulf of Guinea appear to contribute to a weaker monsoon (manifested as lower amounts of rainfall) in the Sahel several months later.

In corroboration of this statement, Fig. 6.8 shows a scatter plot of August to November Gulf of Guinea rainfall versus the following year's June to September Seedling Index. Over 40% of the variance in the Western Sahel's rainfall is explained by rain in the Gulf of Guinea the year previous. Thus, this association should be used as an aid in forecasting Sahel rainfall.

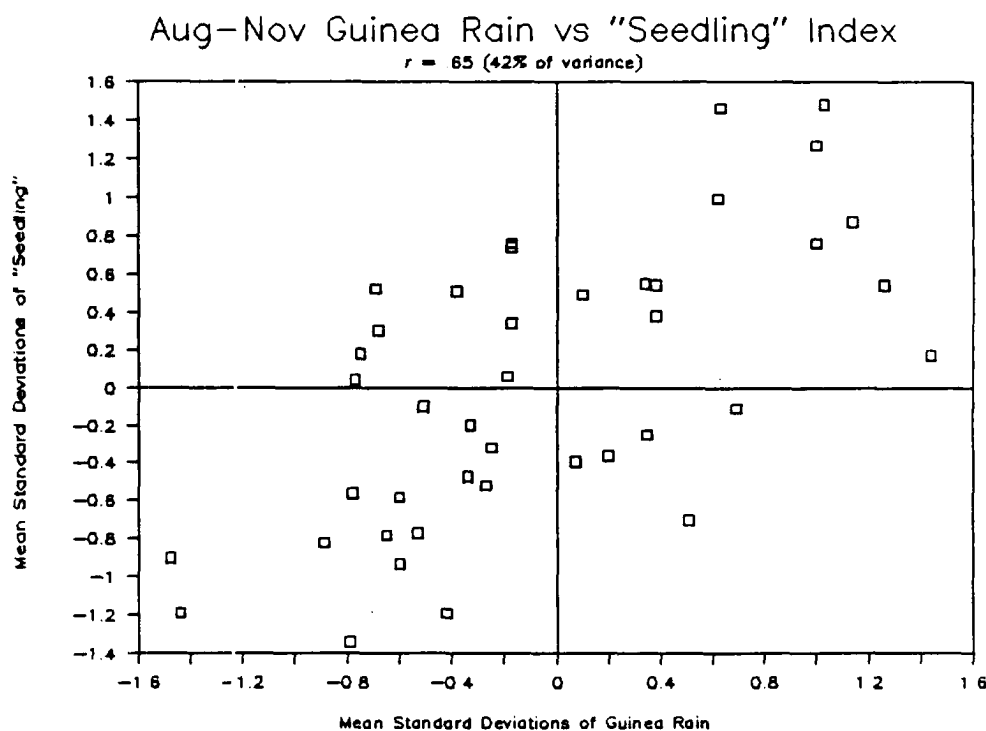


Figure 6.8: Scatter plot for August to November Gulf of Guinea Index rainfall anomalies (1948 to 1988) versus following year June to September Seedling Index rainfall anomalies (1949 to 1989). The two indices correlate at $r = 0.65$.

To test this relationship we detrended data for both indices and then recomputed the correlations. This procedure actually improved the relationship, to values of $r = 0.83$, or 68% of the variance explained. This improved Gulf of Guinea–Sahel rainfall association

is depicted in Fig. 6.9. Note that the detrended relationship between the Gulf of Guinea rainfall and intense hurricane activity is also stronger than the original data set.

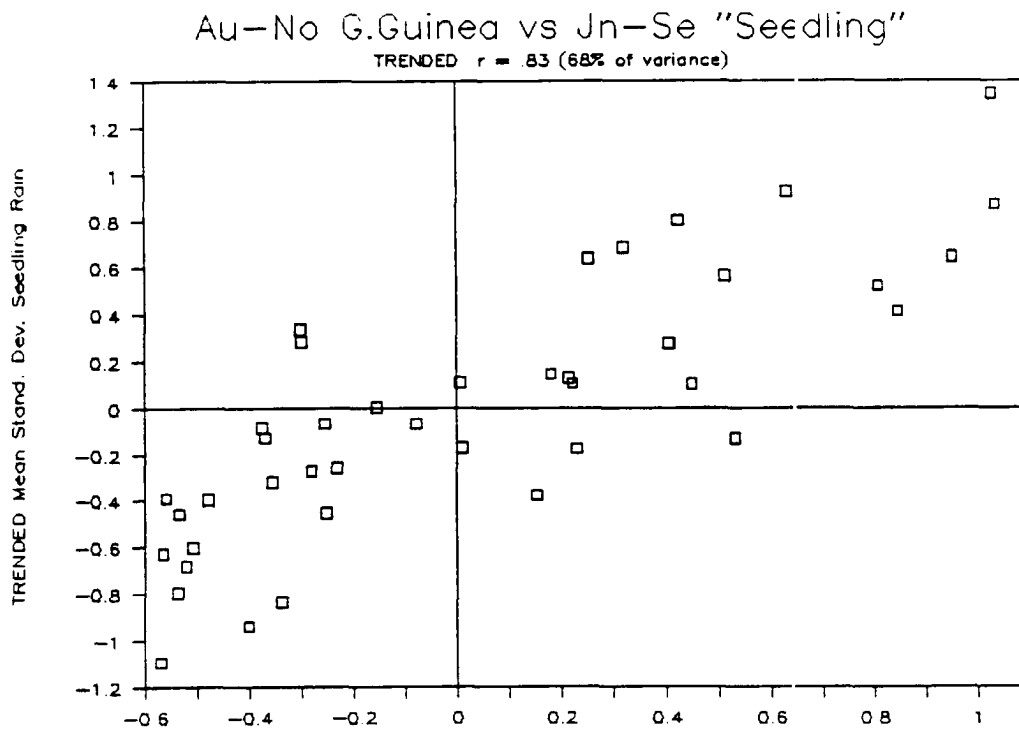


Figure 6.9: As in Fig. 6.8 but with the use of detrended data. The two indices correlate at $r = 0.83$.

Thus the hypothesis of a multi-month feedback from the Gulf of Guinea region to the Western Sahel appears to be well supported by the observations. The connection to tropical cyclone variability can then be understood as a byproduct of monsoon dynamics. The use of detrended analysis does not degrade the relationship but instead indicates that it operates independently of forces that may have caused the multidecadal downward trend in the Sahel rainfall.

Chapter 7

JUNE TO JULY WESTERN SAHEL RAINFALL INDEX

It was shown in section 4.3 that a strong relationship exists between Western Sahel rainfall and Atlantic basin hurricane activity during the months of June to September. The question arises as to how valid is this relationship during the first two summer months? The months of June and July are very important for two reasons: 1) The early season monsoonal rainfall can be useful for forecasting the remainder of the rainy season as was previously shown by Bunting *et al.* (1975); 2) June to July rainfall data can be used to forecast seasonal hurricane activity after 1 August. While the "official" hurricane season begins on 1 June, it is not until 1 August that the more active portion of the season starts. As was shown in section 3.1.2, more than 98% of the intense hurricane activity occurs in the months of August to November. Gray (1984d, 1990b) has utilized this secondary starting date for issuing an updated seasonal tropical cyclone forecast at the beginning of August.

This chapter quantitatively defines this early season Western Sahel rainfall through an indexing procedure and explores it in relation to the other African rainfall indices and to Atlantic basin tropical cyclone activity.

7.1 June to July Western Sahel Rainfall

Average June plus July rainfall throughout Africa during the years 1949 to 1989 is shown in Fig. 7.1. The spatial distribution of this rainfall is very similar to that for the entire June to September rainy period (Fig. 5.1). The main rainband extends west-to-east, from about 2 to 13°N, throughout North Africa except for the Somalian peninsula.

Small amounts of precipitation from extratropical systems occur at both extreme poleward portions of the continent.

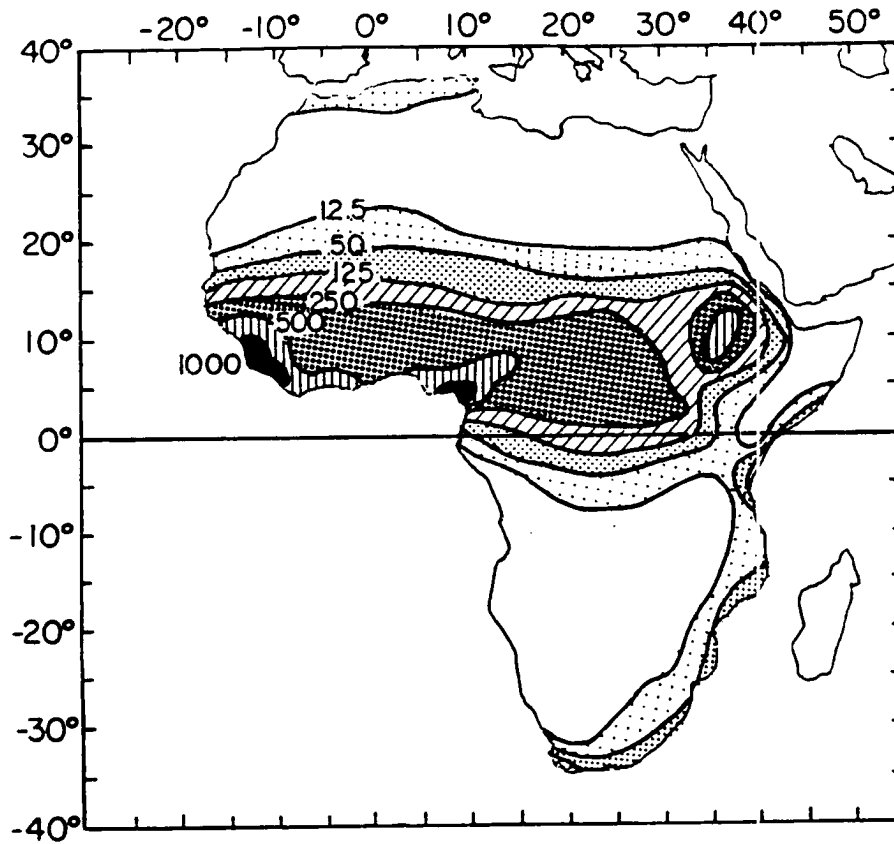


Figure 7.1: June to July precipitation over Africa using data from 1949 to 1989. Contours are at 12.5, 50, 125, 250, 500, and 1000 mm.

Figures 7.2 and 7.3 show how the two month rainfall totals at each station correlate against various tropical cyclone parameters. Stations are only included in the analysis if a minimum of 12 out of 41 years of data are available. The relationship to tropical cyclones becomes increasingly stronger as more intense cyclones are considered but not to the extent observed for the entire June to September rainfall period. Although rainfall in the entire Sahel during June and July appears to relate well to seasonal tropical cyclone activity, it is the westernmost portion of the region that has the highest correlations. There are also indications of a negative, but much weaker association along the Gulf of Guinea.

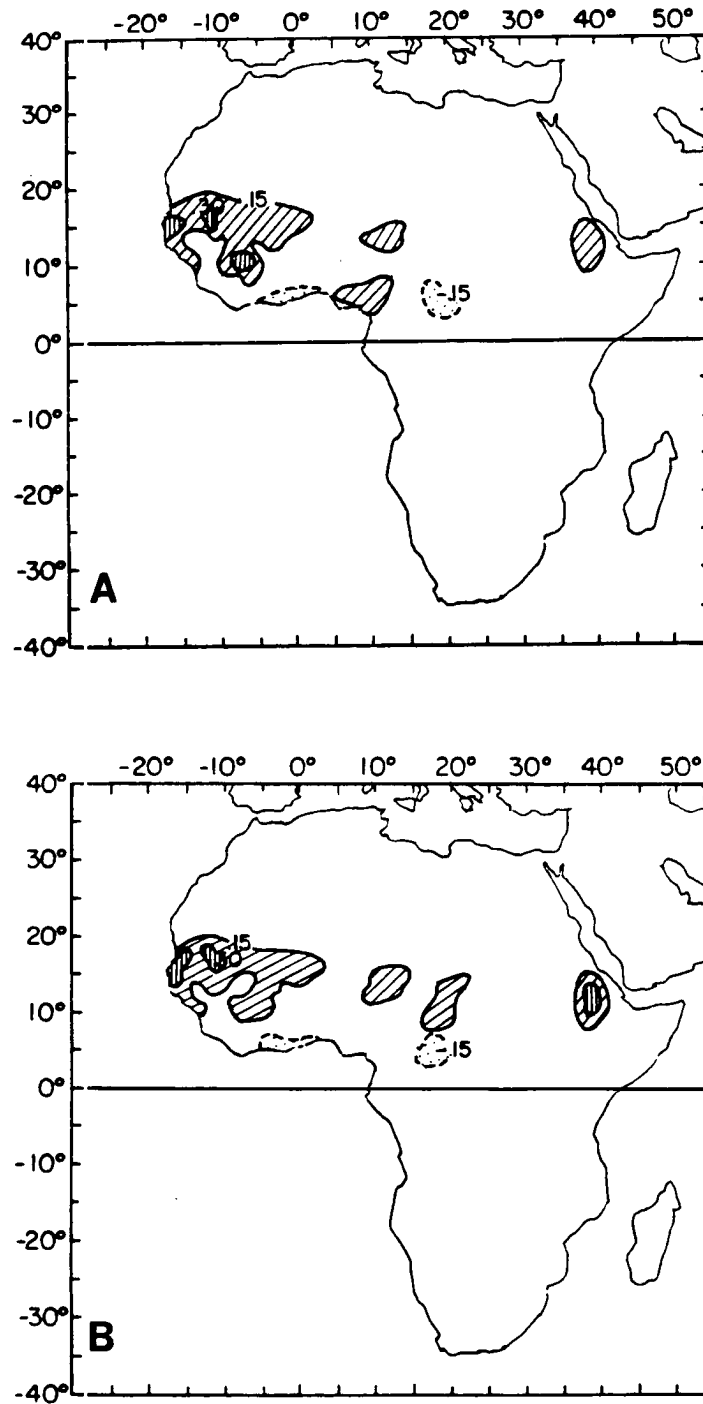


Figure 7.2: Correlation coefficients of individual station June to July rainfall versus a) named storms, b) hurricanes, and c) intense hurricanes. Stations were only included in the analysis if they has at least 12 years of data between 1949 and 1989. Contours indicate values of $r = \pm 0.15$, 0.30 , 0.45 , and 0.60 . Positive correlations are within solid contours, while negative contours are indicated by dashed lines.

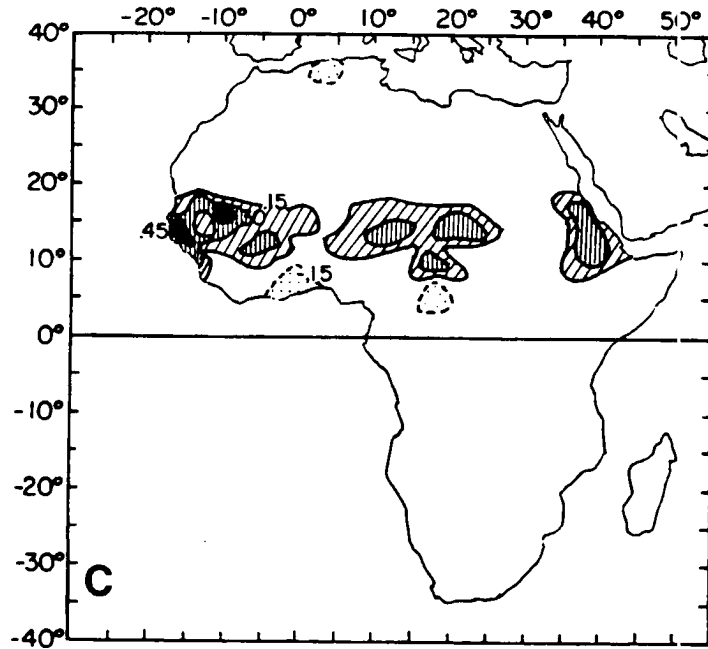


Figure 7.2: c: Continued.

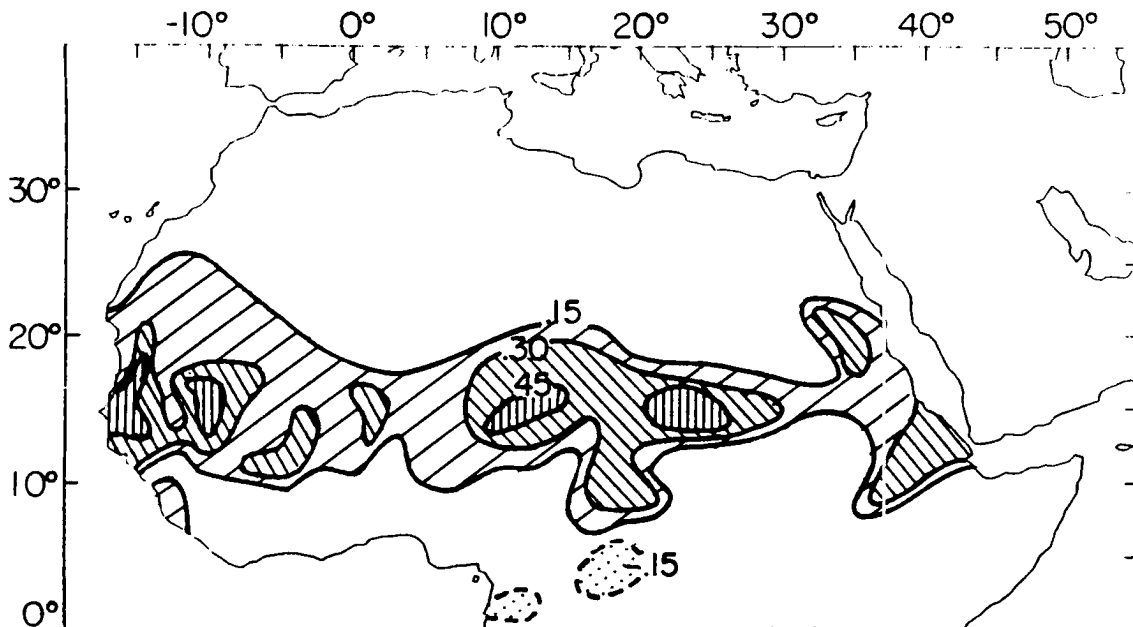


Figure 7.3: Same as Fig. 7.2 with June to July rainfall versus intense hurricane days.

It is assumed that the June to July rainfall reflects how the monsoon is establishing itself in terms of latitude and strength for the remaining summer months. Bunting *et al.* (1975) explained this association as a “persistence” of monsoon conditions. Figure 7.4 shows the correlations of individual station June to July rainfall versus August to September rainfall in the Western Sahel. The strong correlations between early season (June to July) rainfall versus the main rainy season (August to September) confirms Bunting’s assessment. It is possible that the association seen here is due entirely to similar concurrent downward trends in the rainfall data creating an artificial positive correlation. In section 7.4, it is shown that, for the most part, we may discount this idea.

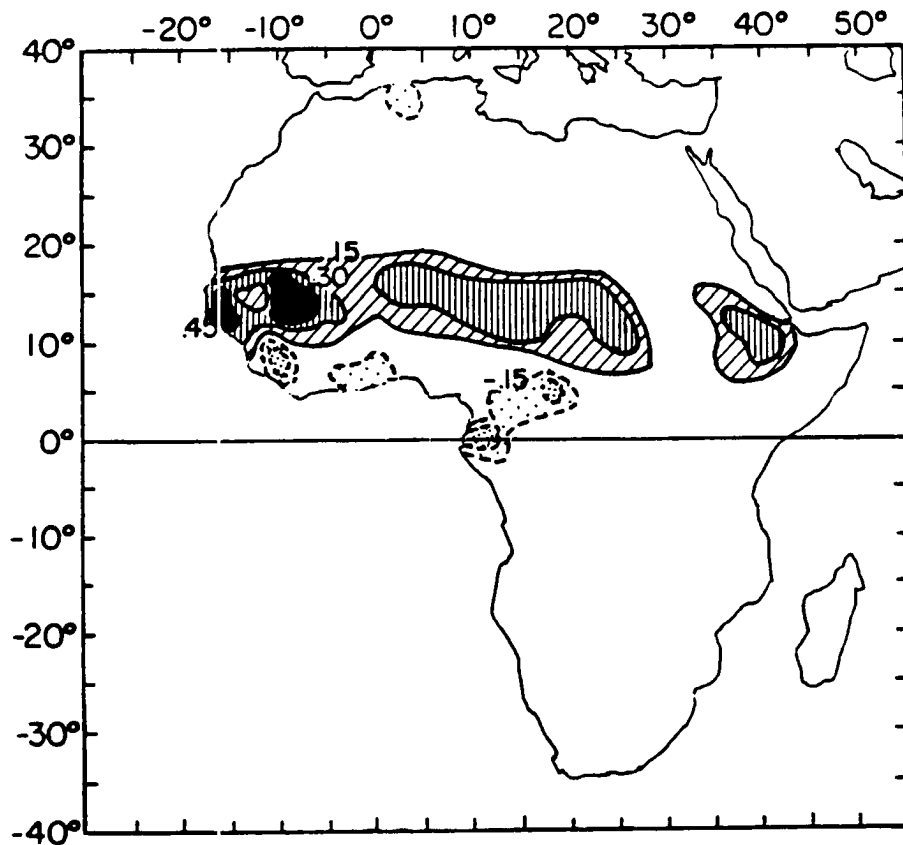


Figure 7.4: Same as Fig. 7.2 with June to July rainfall versus same year Western Sahel August to September Rainfall Index.

7.2 Development of the June to July Rainfall Index

Using the same methodology as in section 5.4, a June to July Western Sahel Rainfall Index was created. Though extensive tests were performed to find the optimal spatial domain for the rainfall-tropical cyclone association, no significant improvement over the 38 stations chosen for the June to September Seedling Index was observed. Therefore, the same stations utilized for the June to September Seedling Index are also the ones chosen for the June to July Western Sahel Rainfall Index.

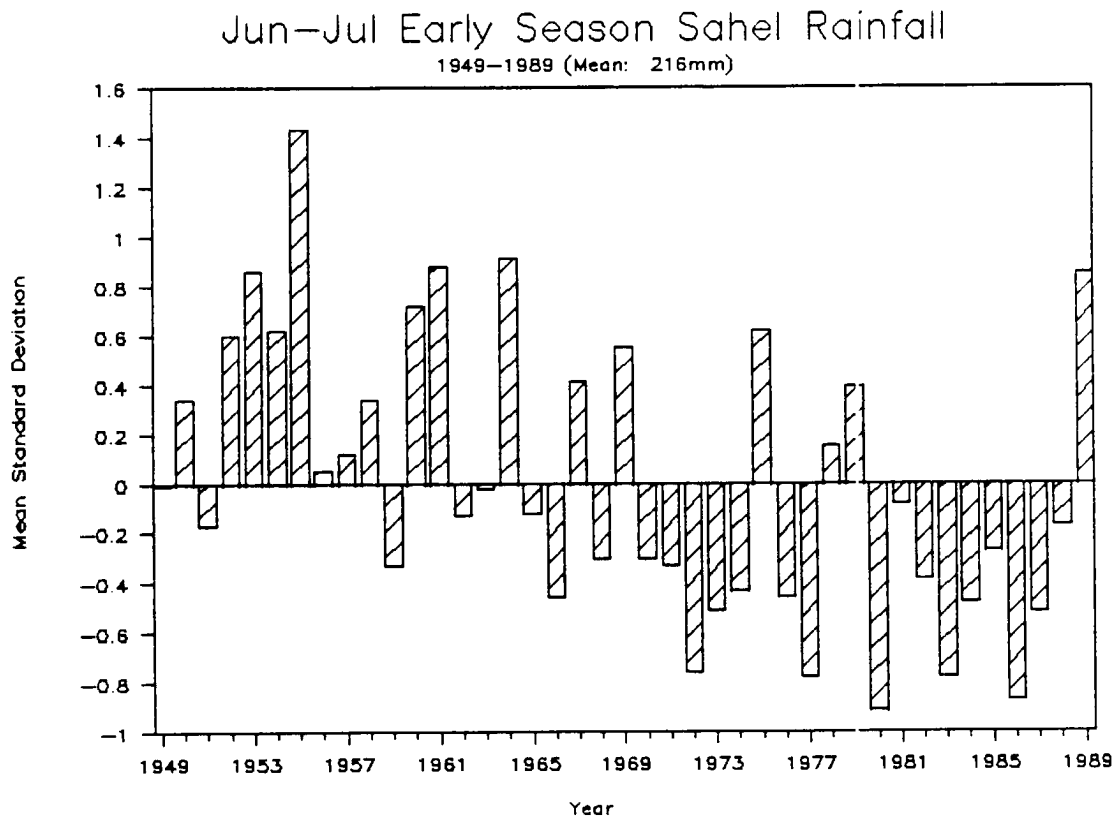


Figure 7.5: Yearly values of the 38 station June to July Western Sahel Index of rainfall expressed in terms of relative standard deviation. Data presented are from 1949 to 1989.

Figure 7.5 shows the interannual variations of this early season Western Sahel rainfall index. While the time series does have a significant multidecadal downtrend in the data, this decline of the rainfall is not as large or as persistent as in the entire June to September Seedling Index. The overall quality of the June to July data is, in general, excellent. Only stations with 30 years of the possible 41 were included. Many of the stations in the index had the full complement of 41 years. Table 7.1 details the year by year values of the

index represented by the bar graph of Fig. 7.5. The years 1949–1950 and 1988–1989 have approximately ten dozen less stations. This occurs because the AID data was not uniformly recorded prior to 1951 and is not yet available for the last two years.

Table 7.1: Mean standard deviations and data availability (out of a possible 38 stations per year) for the June to July Western Sahel Index.

Year	Standard Deviation	Number of Stations	Year	Standard Deviation	Number of Stations
1949	-0.01	24	1970	-0.30	37
1950	0.34	24	1971	-0.33	37
1951	-0.17	38	1972	-0.76	38
1952	0.60	37	1973	-0.51	38
1953	0.86	38	1974	-0.43	38
1954	0.62	38	1975	0.62	38
1955	1.43	38	1976	-0.46	38
1956	0.05	38	1977	-0.78	37
1957	0.12	38	1978	0.15	38
1958	0.34	36	1979	0.39	38
1959	-0.33	37	1980	-0.91	38
1960	0.72	35	1981	-0.08	37
1961	0.88	38	1982	-0.38	37
1962	-0.13	37	1983	-0.78	37
1963	-0.02	38	1984	-0.48	37
1964	0.91	38	1985	-0.27	37
1965	-0.12	37	1986	-0.87	37
1966	-0.46	38	1987	-0.52	34
1967	0.41	37	1988	-0.17	26
1968	-0.30	37	1989	0.85	25
1969	0.55	37			

Table 7.2 presents detailed information regarding June to July rainfall data for the 38 stations including individual station correlations to the June to July Rainfall Index itself and with intense hurricane days. Locations of the individual stations were shown in Fig. 5.7. Observe that while there is a wide range of average rainfall amounts, from less than 10 mm to over 500 mm during these two months, individual stations show a high degree of internal spatial consistency, most stations having a correlation of at least 0.6 with the June to July Index. Stations which correlate at values less than $r = 0.40$ (Segou, San and Bamako in Mali; and Atar in Mauritania), are all at the boundaries of the Index region. The correlations with intense hurricane activity range from a minimum of $r = 0.15$ to a

maximum of $r = 0.67$; but most of the values range from $r = 0.35$ to $r = 0.55$. We will now describe the combined association between the 38 station index and various tropical cyclone and African rainfall parameters.

7.3 Correlation with Tropical Cyclones

The statistical relationship between the June to July rainfall in the Western Sahel and seasonal tropical cyclone activity can now be determined. Table 7.3 displays the linear correlation coefficients for various parameter associations. These associations, similar to those for the entire June to September period, are strongest for the highest intensity of cyclones and for those parameters which include a component of storm track duration. A scatter plot of the rainfall versus intense hurricane days is shown in Fig. 7.6.

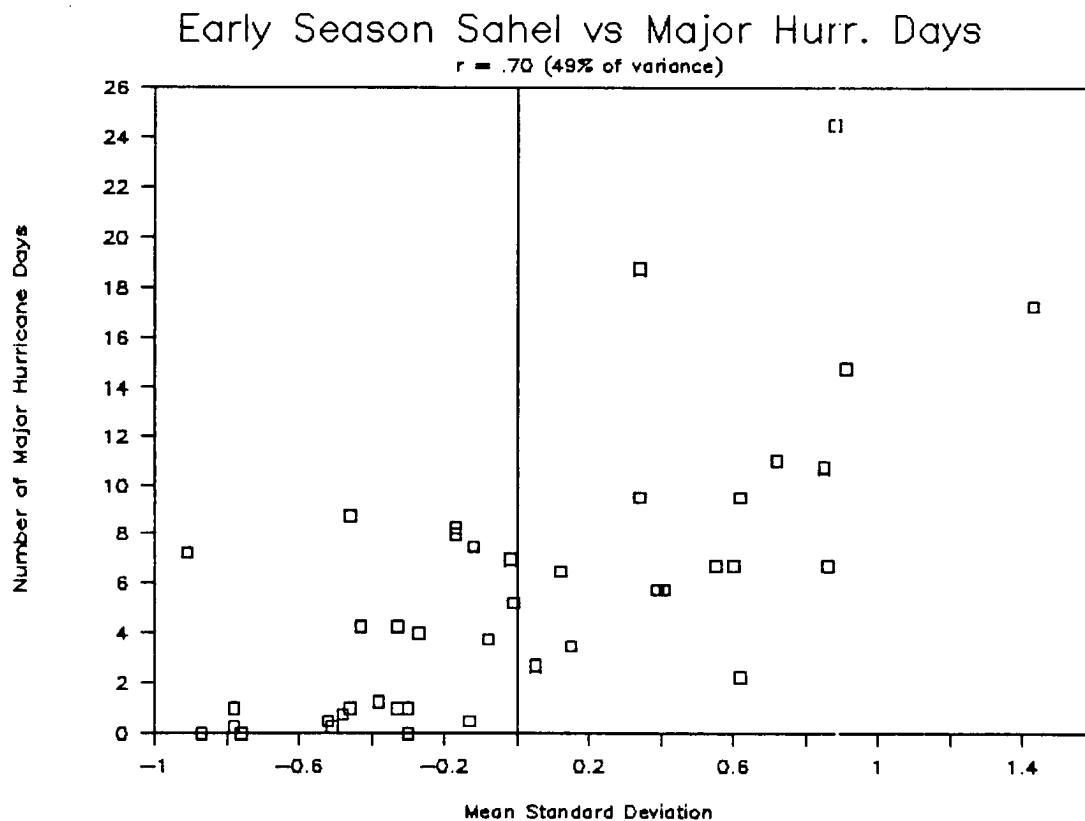


Figure 7.6: Scatter plot of 1949 to 1989 values of June to July Western Sahel Index rainfall versus intense hurricane days. The two parameters have a linear correlation coefficient of $r = 0.70$.

Table 7.2: The 38 stations used in the June to July Western Sahel Rainfall Index. Data include: CSU Rainfall Data Base identification number, station name and country, June to July mean and standard deviation (in mm), years of data in analysis, correlation coefficients versus the June to July Rainfall Index, and correlation coefficient versus intense hurricane days. (Asterisks refer to significance level: 0.100 for ‘*’, 0.025 for ‘**’ and 0.005 for ‘***’.)

Station	Rainfall Data			vs. Jun-Jul	vs. Intense
	Mean	SD	Years	Rainfall Index r	Hurr. Days r
0119 Niore Du Sahel, Mali	197.2	71.71	41	0.541	0.331 **
0123 Kayes, Mali	252.1	74.53	41	0.434	0.274 *
0125 Kita, Mali	371.7	97.65	41	0.428	0.325 **
0126 Segou, Mali	257.2	70.18	41	0.355	0.179
0127 San, Mali	274.2	64.52	41	0.194	0.225 *
0128 Kenieba, Mali	427.8	93.86	39	0.575	0.492 ***
0130 Bamako/Senou, Mali	365.8	98.17	41	0.399	0.328 **
0131 Koutiala, Mali	342.7	86.32	41	0.458	0.452 ***
0132 Bougouni, Mali	400.7	98.38	41	0.549	0.470 ***
0133 Sikasso, Mali	400.2	89.58	41	0.407	0.393 **
0138 Atar, Mauritania	9.9	12.59	41	0.303	0.244 *
0139 Akjoujt, Mauritania	9.6	13.16	41	0.577	0.363 **
0140 Nouakchott, Mauritania	13.1	18.41	41	0.478	0.207 *
0142 Boutilimit, Mauritania	31.8	37.58	41	0.723	0.528 ***
0143 Rosso, Mauritania	57.4	53.40	39	0.678	0.453 ***
0146 Kiffa, Mauritania	93.9	51.18	41	0.651	0.581 ***
0148 Saint Louis, Senegal	55.7	68.50	41	0.500	0.254 *
0149 Podor, Senegal	62.8	53.83	41	0.770	0.484 ***
0150 Linguere, Senegal	130.5	61.73	41	0.607	0.340 **
0151 Matam, Senegal	150.3	131.23	41	0.486	0.311 **
0152 Dakar/Yoff, Senegal	88.9	70.97	41	0.765	0.548 ***
0154 Thies, Senegal	128.8	68.15	38	0.857	0.582 ***
0155 Diourbel, Senegal	152.0	73.07	41	0.747	0.400 ***
0156 Kaolack, Senegal	192.5	83.83	39	0.681	0.442 ***
0157 Tambacounda, Senegal	291.3	74.61	41	0.406	0.150
0162 Bathurst/Yundum, Gambia	327.1	112.42	41	0.677	0.443 ***
0163 Bissau Airport, Guinea-Bissau	573.4	189.35	40	0.635	0.575 ***
0611 Bansang, Gambia	313.4	120.75	34	0.441	0.407 **
0615 Georgetown, Gambia	313.3	92.83	31	0.492	0.473 ***
0617 Basse Met, Gambia	327.3	102.18	33	0.604	0.428 **
0627 Boghe, Gambia	77.6	48.74	36	0.688	0.491 ***
0630 Selibaby, Mauritania	176.4	69.28	37	0.619	0.497 ***
0632 Louga, Senegal	78.1	58.37	33	0.787	0.479 ***
0635 Mbour, Senegal	142.4	83.35	36	0.858	0.671 ***
0636 Niore Du Rip, Senegal	240.1	78.44	35	0.728	0.510 ***
0637 Velingara Casamance, Senegal	334.6	102.00	35	0.534	0.427 **
0638 Sedhiou, Senegal	416.5	138.06	36	0.680	0.423 **
0639 Bambey Met, Senegal	135.8	66.92	37	0.740	0.456 ***

Table 7.3: Correlation coefficients of June to July Western Sahel rainfall Index versus Atlantic basin tropical cyclone parameters for the years 1949 to 1989. (Asterisks refer to significance level: 0.100 for ‘*’, 0.025 for ‘**’ and 0.005 for ‘***’.)

Tropical Cyclone Parameter	Correlation Coefficient	Tropical Cyclone Parameter	Correlation Coefficient
Named Storms	0.44***	Named Storm Days	0.57***
Hurricanes	0.42***	Hurricane Days	0.54***
Intense Hurricanes	0.63***	Intense Hurricane Days	0.70***
Int. Hur. (Bias Out)	0.63***	Int. Hur. Days (Bias Out)	0.65***
HDP	0.60***		

Detrending the rainfall index and the tropical cyclone activity does not significantly alter the correlations. The detrended analysis of June to July Western Sahel rainfall versus detrended intense hurricane days reveals a correlation coefficient of $r = 0.62$, slightly reduced from $r = 0.70$ in the original relationship. Removing the bias from the intense hurricane activity before detrending also causes a slight reduction in the correlation: detrended, bias-removed intense hurricane days correlate at $r = 0.59$, still with more than a third of the variance explained in a predictive relationship. It is surprising that such a high degree of the variance of seasonal intense hurricane days can be explained by June to July rainfall only.

Ranked rainfall values for the June to July Western Sahel Index are also useful for observational analysis. Table 7.4 ranks the rainfall data from the wettest to the driest for the 41 years of 1949 to 1989. The general trend to having wet regimes during the first two decades and dry regimes in the last twenty years is well reflected in this data. Only two years from the 1970’s and 1980’s are represented in the ten wettest years, while only one year in the 1950’s and 1960’s is included in the ten driest.

Table 7.5 shows the various tropical cyclone parameters stratified for the ten wettest and ten driest June to July periods in the Western Sahel. Although the total number of named storms shows only a three to two ratio for wet versus dry years, this difference increases with increasing cyclone intensity. For the intense hurricanes, there is a more than three to one ratio. Because of the overwhelming dependence of U.S. hurricane spawned destruction on intense hurricanes, the nearly eight to one ratio of damage from these

Table 7.4: June to July Western Sahel Index ranked by rainfall amounts expressed as relative mean standard deviations from 1949 to 1989.

Rank	Year	Index Value	Rank	Year	Index Value
1.	1955	1.43	22.	1962	-0.13
2.	1964	0.91	23.	1951	-0.17
3.	1961	0.88	24.	1988	-0.17
4.	1953	0.86	25.	1985	-0.27
5.	1989	0.85	26.	1968	-0.30
6.	1960	0.72	27.	1970	-0.30
7.	1954	0.62	28.	1971	-0.33
8.	1975	0.62	29.	1959	-0.33
9.	1952	0.60	30.	1982	-0.38
10.	1969	0.55	31.	1974	-0.43
11.	1967	0.41	32.	1966	-0.46
12.	1979	0.39	33.	1976	-0.46
13.	1950	0.34	34.	1984	-0.48
14.	1958	0.34	35.	1973	-0.51
15.	1978	0.15	36.	1987	-0.52
16.	1957	0.12	37.	1972	-0.76
17.	1956	0.05	38.	1977	-0.78
18.	1949	-0.01	39.	1983	-0.78
19.	1963	-0.02	40.	1986	-0.87
20.	1981	-0.08	41.	1980	-0.91
21.	1965	-0.12			

storms in wet years versus dry years follows. For U.S. East Coast hurricane destruction, these differences are extremely large (74 to 1). Figure 7.7 depicts the tracks of intense hurricanes for both wet and dry groupings.

Table 7.5: Summary of tropical cyclone parameters for the ten wettest June to July Western Sahel years and the ten driest years from 1949 to 1989. Damage is in millions of 1990 dollars. (Asterisks refer to significance level: 0.100 for '**', 0.025 for '***' and 0.005 for '****'.)

Tropical Cyclone Parameter	Wettest Years' Mean	Percent (%) of Normal	Driest Years' Mean	Percent (%) of Normal	Ratio Wet/ Dry	
Named Storms	11.0	118	7.6	82	1.45	***
Named Storm Days	59.5	127	36.0	77	1.65	***
Hurricanes	7.2	124	4.9	84	1.47	**
Hurricane Days	32.1	135	16.6	70	1.93	***
Intense Hurricanes	4.0	160	1.2	48	3.33	***
Intense Hurricane Days	11.0	190	2.0	34	5.50	***
HDP	109.2	146	45.7	61	2.39	***
US Landfalling:						
Named/Subtrop.	3.8	119	2.4	75	1.58	*
Hurricanes	2.3	143	1.1	68	2.09	**
Intense Hurricanes	1.1	180	0.2	33	5.50	***
Intense Gulf Coast	0.4	118	0.2	59	2.00	
Intense East Coast	0.7	241	0.0	0	∞	**
Hurricane Damage	\$4224	240	\$532	30	7.94	
' ' Gulf Coast	1099	124	399	45	2.75	
' ' East Coast	2380	324	38	4	74.47	***

An alternative method for evaluating the association between the June–July rainfall and tropical cyclone activity during 1949 to 1989 is with rank correlation tests. The correlation coefficient with intense hurricane days obtained using this method is $r = 0.69$. This number is essentially the same as that obtained ($r = 0.70$) for the linear correlation coefficient. The remaining relationships with other tropical cyclone parameters are likewise relatively unchanged in the rank correlation analysis.

7.4 Correlation with Seedling Index

A confirmation of the findings of Bunting *et al.* (1975) is seen in Figs. 7.8 and 7.9. The first figure presents the year to year variations of Western Sahel June to July rainfall versus the entire June to September rainy season. The two rainfall indices correlate at

$r = 0.81$. Obviously, these two indices are not independent as the June to July rainfall is included in the June to September total. While June and July are responsible for just 36% of the four month precipitation, on average, their contribution to the total variance of June to September Western Sahel rainfall is much larger. Figure 7.9 shows the scatter plot of June and July rainfall anomalies versus August and September rainfall anomalies. A strong association remains between these two rainfall indices.

A secondary investigation is necessary to understand how much of this early rainfall to late rainfall relationship is due to the concurrent downward trends in both rainfall indices. As stated earlier, the downward trend is much more discernible in the full June to September time period than in the early rainfall during June and July. Detrending the data somewhat reduces the correlations. For the June and July versus the June to September rainfall (dependent indices), the association drops from $r = 0.81$ to $r = 0.75$. For the June and July versus the August to September rainfall (independent indices), the correlation is lowered from $r = 0.60$ to $r = 0.44$.

Thus, it is apparent that there is a moderately strong predictive signal for the main portion of the rainy season found in the onset months of the monsoon. This predictive signal is only partially a result of the downward trend in the data.

7.5 Correlation with Gulf of Guinea Index

As stated in Chapter 6, the very strong association of August to November Gulf of Guinea rainfall to seasonal tropical cyclone activity almost a year later is hypothesized to be due to a positive feedback from the retreating monsoon during the fall into the following year's Sahel monsoon further north. Section 6.4 showed that Gulf of Guinea rainfall does correlate strongly to next year's June to September Seedling Index. This association was actually seen to increase in strength when detrending of both indices explained over two-thirds of the variance.

Another investigation examined how previous late year Gulf of Guinea rainfall relates to the early rainfall in the Sahel during June and July. Possibly, the first two months of the monsoon would be most affected by such a feedback. However, Fig. 7.10 does not confirm

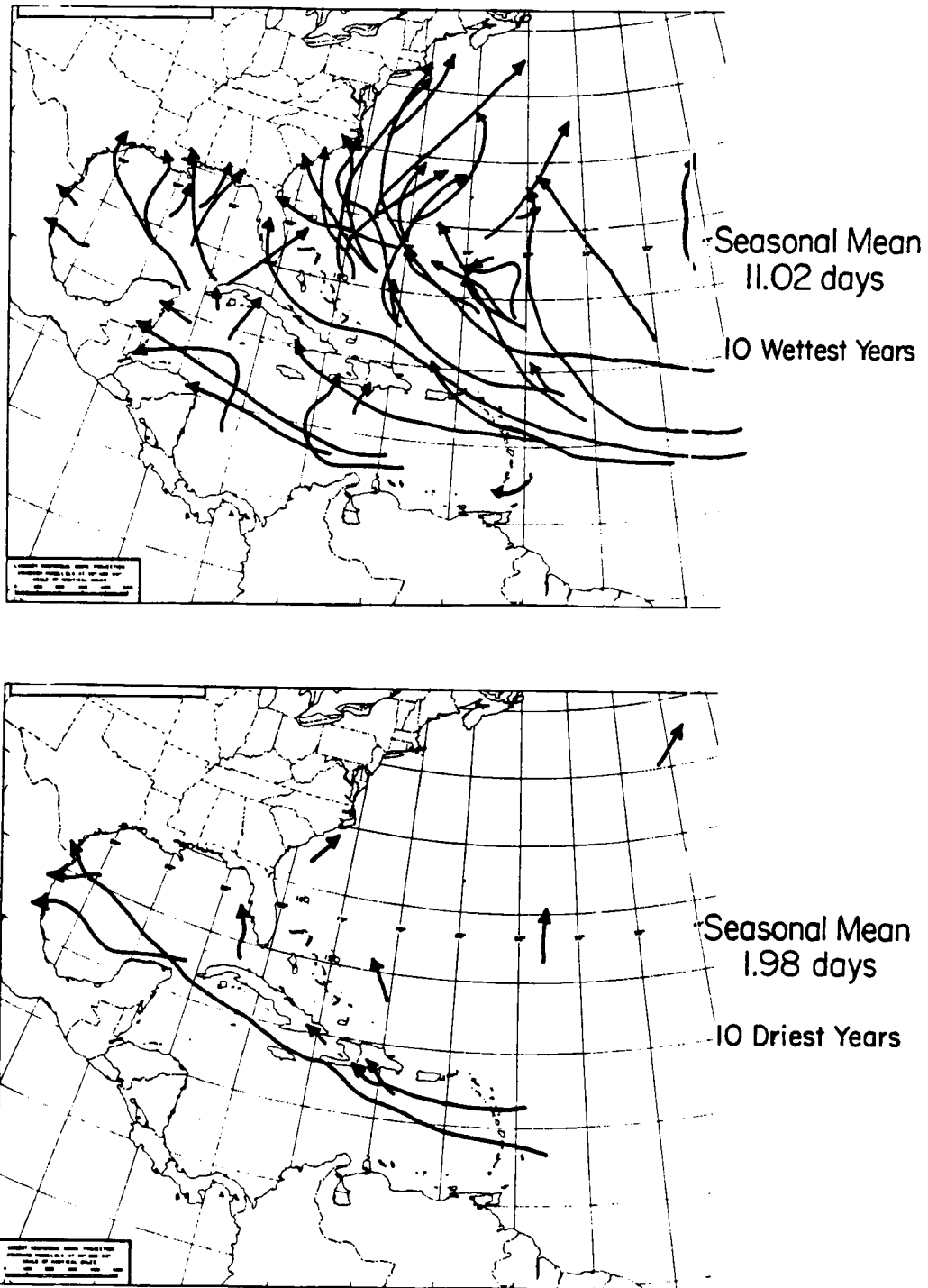


Figure 7.7: Intense hurricane tracks in the ten wettest (upper panel) versus the ten driest (bottom panel) Western Sahel June to July years between 1949 and 1989.

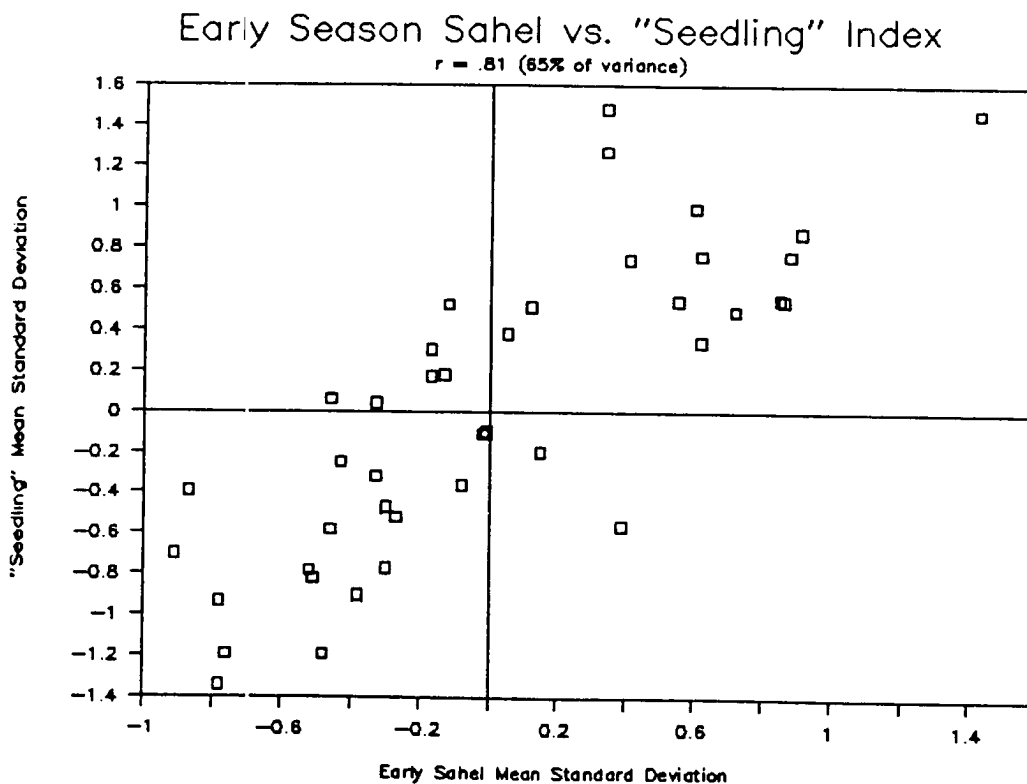


Figure 7.8: Scatter plot of Western Sahel June to July versus June to September Seedling Index rainfall anomalies for the years 1949 to 1989. The two dependent indices correlate at $r = 0.81$.

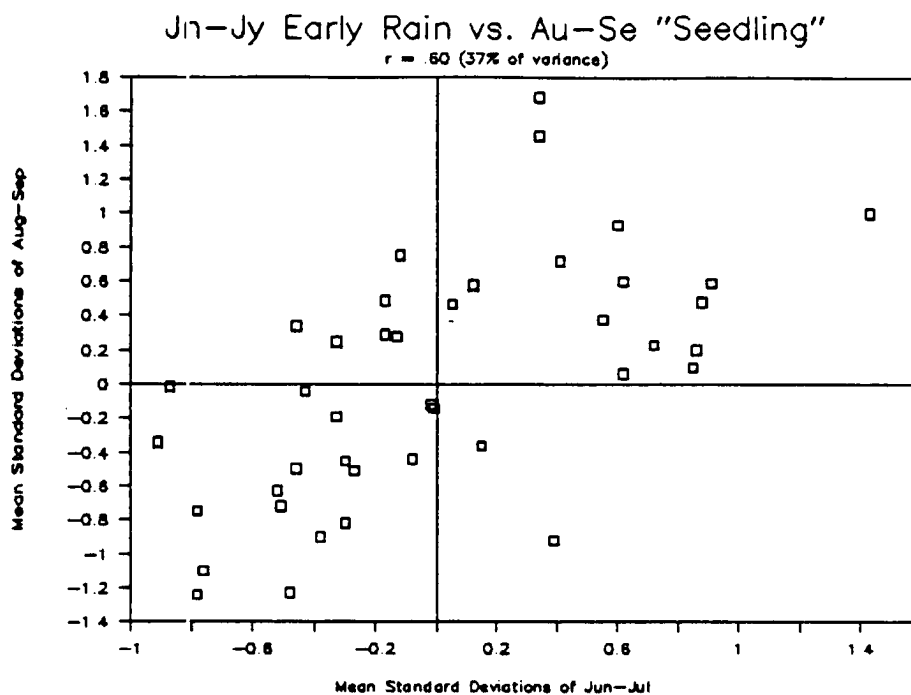


Figure 7.9: Scatter plot of Western Sahel June to July versus August to September rainfall anomalies for the years 1949 to 1989. The two independent indices correlate at $r = 0.60$.

this hypothesis. While a moderately strong relationship is observed, the correlation is not nearly as strong as that for the entire June to September rainy season. Detrending both the previous year Gulf of Guinea and the June and July Western Sahel rainfall time series before correlating only slightly reduces the association. Though not shown, the August to September Western Sahel rainfall also has a correlation of $r = 0.51$ with the prior year Gulf of Guinea rain.

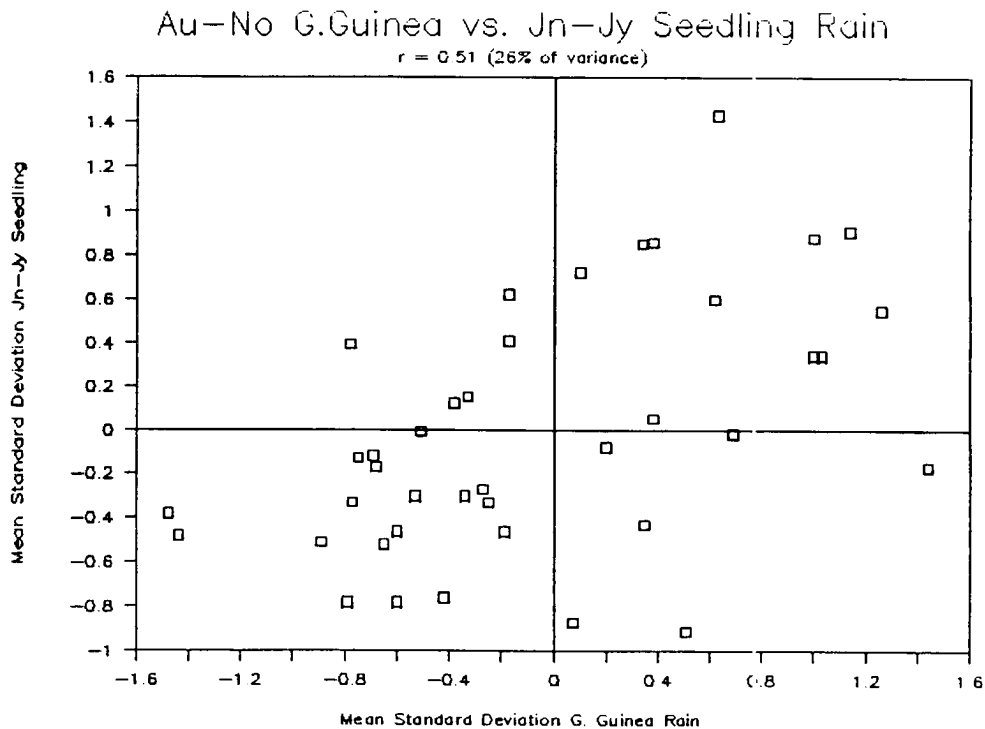


Figure 7.10: Scatter plot of August to November Gulf of Guinea Index rainfall anomalies (1948 to 1988) versus following year June to July Western Sahel Index rainfall anomalies (1949 to 1989). The two indices correlate at $r = 0.51$.

Apparently, the entire rainy season in the Sahel is correlated with the retreating monsoonal rainfall along the Gulf of Guinea during the year previous. A major uncertainty lingering in this relationship is the scarcity of data for some years in the 1980's. Fortunately, additional data sources (see Appendix B) have affirmed the strength of the predictive associations of these rainfall indices.

Chapter 8

EARLY SEASON COMBINATION RAINFALL INDEX

8.1 Development of the Index

Maximization of skill in 1 August forecasts for subsequent tropical cyclones and for the remainder of the monsoon rainy season in the Sahel is desirable. A multiple regression analysis was performed for the two predictive rainfall indices. Table 8.1 shows how the various combinations of the prior year August to November Gulf of Guinea Rainfall Index (Chapter 6) and the June to July Western Sahel Rainfall Index (Chapter 7) correlate with intense hurricane activity and with the June to September Seedling Index. The amount of variance explained is increased using a combination of both parameters, with an optimum obtained as a one third weighted Gulf of Guinea Index and two thirds weighted June–July Western Sahel Index. This combination of indices improves the amount of intense hurricane activity variance explained by an additional 10% over the best forecasts based on either index used separately. Also, the combination index improves variance explained for June to September Seedling Index rainfall by about 5%. Thus the optimum combination rainfall index, termed the “Early Season Combination Index” is specified as:

$$\begin{aligned} \text{Early Season Combination Index} &= (0.3) * \text{Previous Year Gulf of Guinea Index} \\ &+ (0.7) * \text{June to July Current Year Western Sahel Index} \end{aligned}$$

Figure 8.1 presents values for the yearly variations of the Early Season Combination Rainfall Index. While dry years predominate during the 1970's and 1980's and wet years are more prevalent during the previous 20 years. Yearly persistence is not nearly as strong as the June to September Seedling Index or with the June to July Western Sahel Index.

Table 8.1: Correlation coefficients for various combinations of the prior year August to November Gulf of Guinea Rainfall Index and the June to July Western Sahel Rainfall Index with intense hurricane days and with the June to September Seedling Rainfall Index. The asterisks indicate the best combination.

Gulf of Guinea Rainfall Contribution	Western Sahel Rainfall Contribution	r Intense Hurricane Days	r Seedling Index Rainfall
1.0	0.0	0.65	0.65
0.9	0.1	0.68	0.69
0.8	0.2	0.71	0.73
0.7	0.3	0.73	0.77
0.6	0.4	0.75	0.80
0.5	0.5	0.77	0.83
0.4	0.6	0.77	0.85
0.3*	0.7*	0.78	0.85
0.2	0.8	0.76	0.85
0.1	0.9	0.73	0.84
0.0	1.0	0.70	0.81

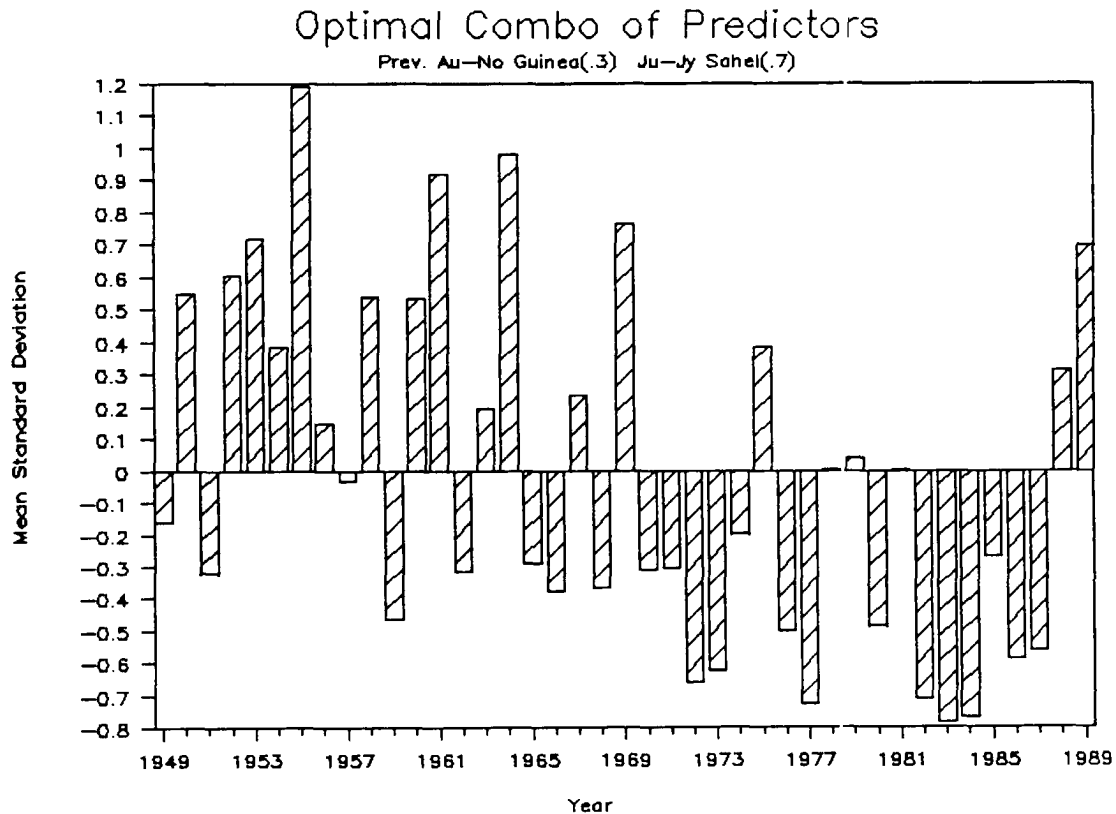


Figure 8.1: Annual values of the Early Season Combination Rainfall Index expressed as relative standard deviations above or below the mean. Data presented are from 1949 to 1989.

8.2 Correlation with Tropical Cyclones

Associations between this Combination Rainfall Index and Atlantic basin tropical cyclones are summarized in Table 8.2. Although the June to July Western Sahel Index is more strongly correlated with intense hurricanes, the Gulf of Guinea Index is better correlated with total named storm activity. If the Combination Rainfall Index were maximized for the latter parameter instead of for intense hurricane days, the relative contribution of the Gulf of Guinea Index would have been weighted more and the correlation with named storm activity would be slightly higher. With the current version of the Combination Index, a little more than one fourth of the variance of named storms is explained while more than half of the variance of intense hurricane days is explained. The scatter plot of the Combination Rainfall Index versus intense hurricane days is shown in Fig. 8.2.

Table 8.2: Correlation coefficients of the Early Season Combination Rainfall Index versus Atlantic basin tropical cyclone parameters for the years 1949 to 1989. (Asterisks refer to significance level: 0.100 for ‘*’, 0.025 for ‘**’ and 0.005 for ‘***’.)

Tropical Cyclone Parameter	Correlation Coefficient	Tropical Cyclone Parameter	Correlation Coefficient
Named Storms	0.52***	Named Storm Days	0.65***
Hurricanes	0.54***	Hurricane Days	0.63***
Intense Hurricanes	0.73***	Intense Hurricane Days	0.77***
Int. Hur. (Bias Out)	0.73***	Int. Hur. Days (Bias Out)	0.73***
HDP	0.69***		

Detrending both the Combination Rainfall Index and the intense hurricane activity prior to testing the correlation removes some of the strength of the association. The linear correlation coefficient of the detrended data is $r = 0.62$, down from $r = 0.77$ from the original analysis. Additionally, removing the bias found in the intense hurricane record before detrending also reduces the association to $r = 0.58$.

To further test this Combination Rainfall Index, ranked indices were created for the 41 years of data (Table 8.3). This step allows for rank correlations to be computed and for simple comparisons of the ten wettest years versus the ten driest years.

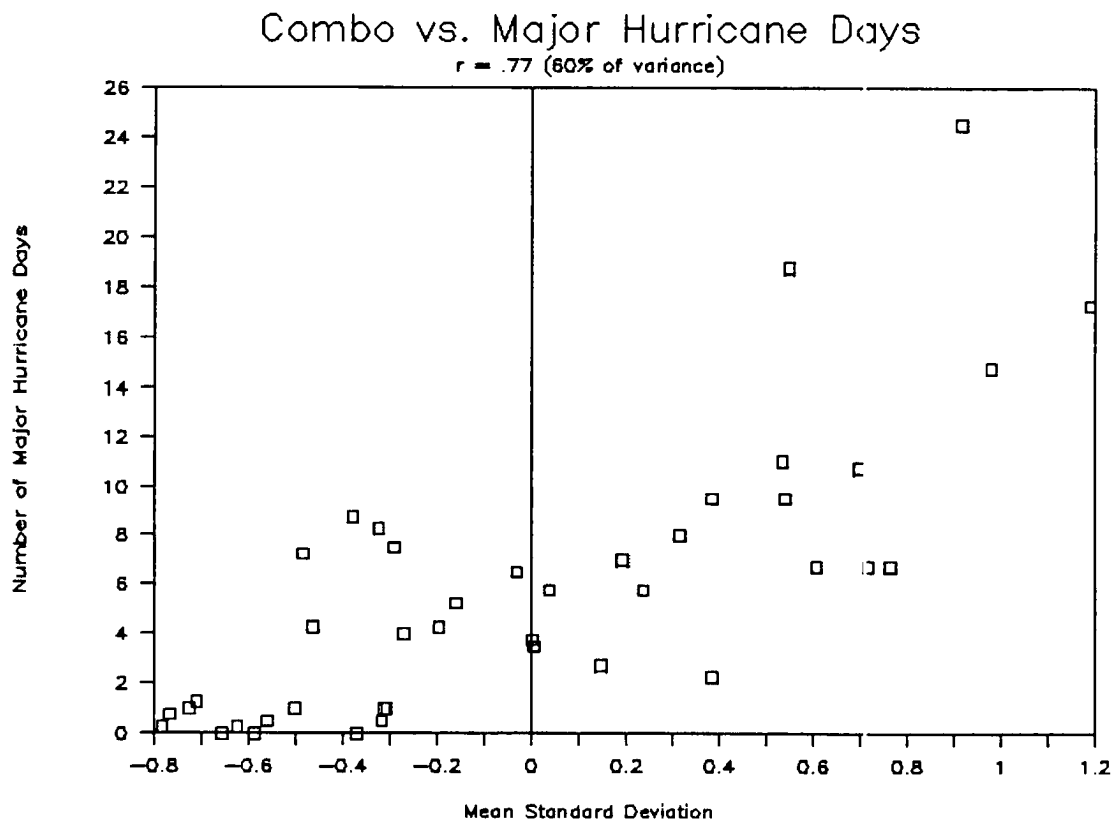


Figure 8.2: Scatter plot of values for the 1949 to 1989 Early Season Combination Rain-fall Index versus intense hurricane days. The two parameters have a linear correlation coefficient of $r = 0.77$.

Table 8.3: Early Season Combination Rainfall Index ranked from wettest (1) to driest (41) for the 41 years from 1949 to 1989.

Rank	Year	Index Value	Rank	Year	Index Value
1.	1955	1.19	22.	1974	-0.20
2.	1964	0.98	23.	1985	-0.27
3.	1961	0.92	24.	1965	-0.29
4.	1969	0.76	25.	1970	-0.31
5.	1953	0.72	26.	1971	-0.31
6.	1989	0.70	27.	1951	-0.32
7.	1952	0.61	28.	1962	-0.32
8.	1950	0.55	29.	1968	-0.37
9.	1958	0.54	30.	1966	-0.38
10.	1960	0.53	31.	1959	-0.46
11.	1954	0.38	32.	1980	-0.48
12.	1975	0.38	33.	1976	-0.50
13.	1988	0.31	34.	1987	-0.56
14.	1967	0.24	35.	1986	-0.59
15.	1963	0.19	36.	1973	-0.62
16.	1956	0.15	37.	1972	-0.66
17.	1979	0.04	38.	1982	-0.71
18.	1978	0.01	39.	1977	-0.73
19.	1981	0.00	40.	1984	-0.77
20.	1957	-0.03	41.	1983	-0.78
21.	1949	-0.16			

The rank correlation of the Combination Rainfall Index versus intense hurricane days correlates is $r = 0.76$, almost identical to $r = 0.77$ for the linear correlation coefficient. This result suggests that the association in the basic unranked data is fairly linear.

Wettest versus driest comparisons for a wide range of tropical cyclone parameters are shown in Table 8.4. As the strength of the cyclones is increased, the modulation of occurrence in relation to African rainfall becomes more pronounced. Note that the landfalling tropical cyclone statistics mirror the effect seen throughout the entire basin. Figure 8.3 shows a comparison of intense hurricane tracks in wet versus dry regimes. Activity in the Gulf of Mexico, as previously mentioned, seems to be less sensitive to African rainfall variations. The Gulf is in stark contrast to the Caribbean Sea and Atlantic Ocean regions which show very large differences in wet year versus dry year tropical cyclone activity.

Table 8.4: Summary of the variability of tropical cyclone parameters in the ten wettest and the ten driest Early Season Combination Rainfall Index years from 1949 to 1989. Damage is in millions of 1990 dollars. (Asterisks refer to significance level: 0.100 for '*', 0.025 for '**' and 0.005 for '**'.)

Tropical Cyclone Parameter	Wettest Years' Mean	Percent (%) of Normal	Driest Years' Mean	Percent (%) of Normal	Ratio Wet/ Dry	
Named Storms	11.4	123	7.3	78	1.56	***
Named Storm Days	66.2	142	31.4	67	2.11	***
Hurricanes	7.6	131	4.4	76	1.72	***
Hurricane Days	35.9	151	13.0	55	2.76	***
Intense Hurricanes	4.8	192	1.0	40	4.80	***
Intense Hurricane Days	12.6	217	1.0	17	12.60	***
HDP	125.2	167	34.9	47	3.59	***
US Landfalling:						
Named/Subtrop.	3.9	122	2.5	78	1.56	*
Hurricanes	2.3	143	1.0	62	2.30	**
Intense Hurricanes	0.9	148	0.2	33	4.50	**
Intense Gulf Coast	0.4	118	0.2	59	2.00	
Intense East Coast	0.5	172	0.0	0	∞	***
Hurricane Damage	\$3276	186	430	24	7.62	
' ' Gulf Coast	964	109	394	44	2.45	
' ' East Coast	2312	265	36	4	64.22	**

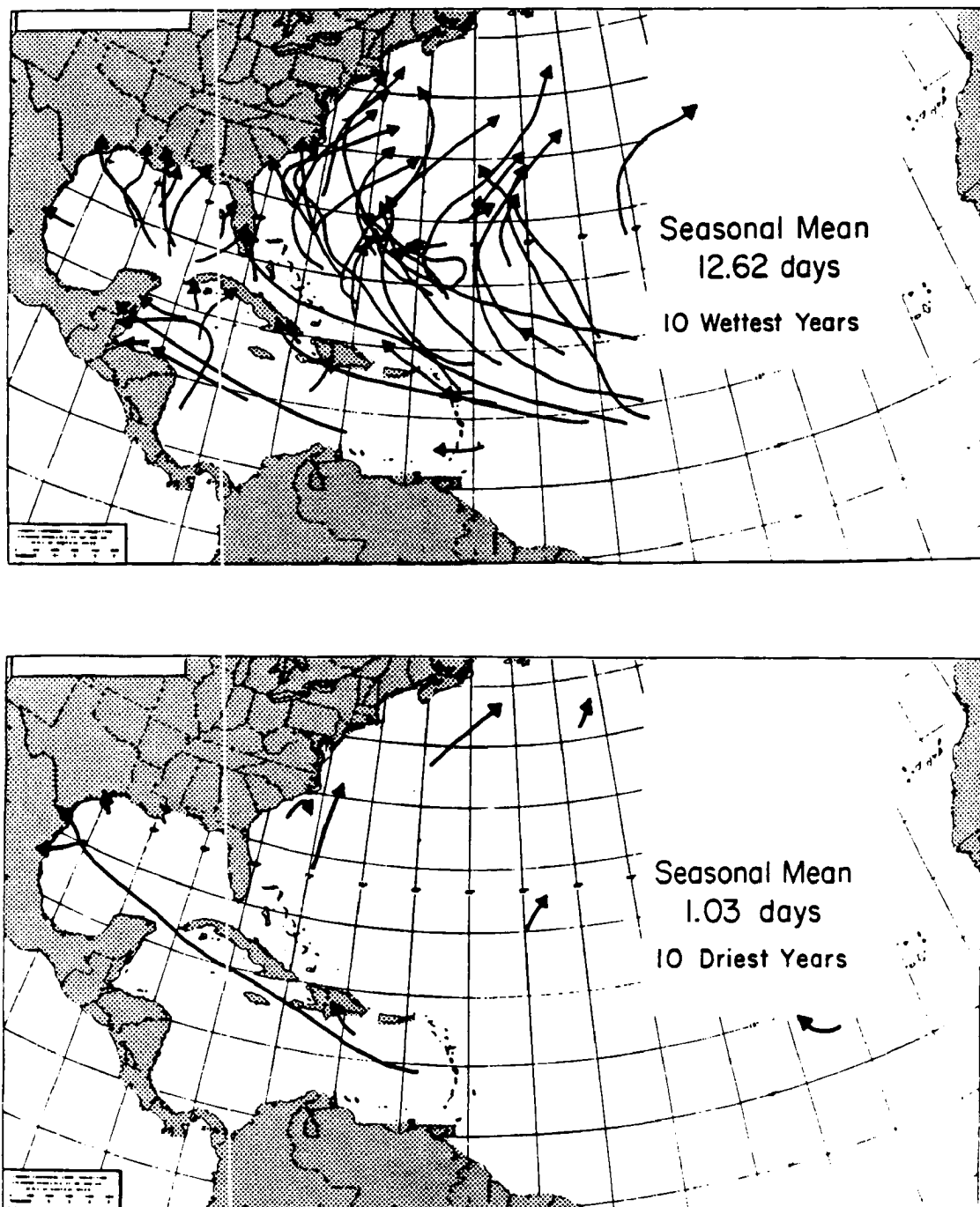


Figure 8.3: Intense hurricane tracks in the ten wettest (upper panel) versus the ten driest (bottom panel) Early Season Combination Rainfall Index years between 1949 to 1989.

8.3 Correlation with Seedling Index

The Early Season Combination Rainfall Index was created using a multiple regression technique to maximize the relationship with both intense hurricane activity and with the June to September Seedling Index. The correlation of the Combination Rainfall Index with the June to September Seedling Index is $r = 0.85$. A scatter plot is shown in Fig. 8.4. Hence, nearly three quarters of the variance in the June to September Western Sahel rainfall is explained by rainfall occurring before 1 August. A detrended analysis removes a substantial portion of the association, however, by lowering this correlation to $r = 0.67$.

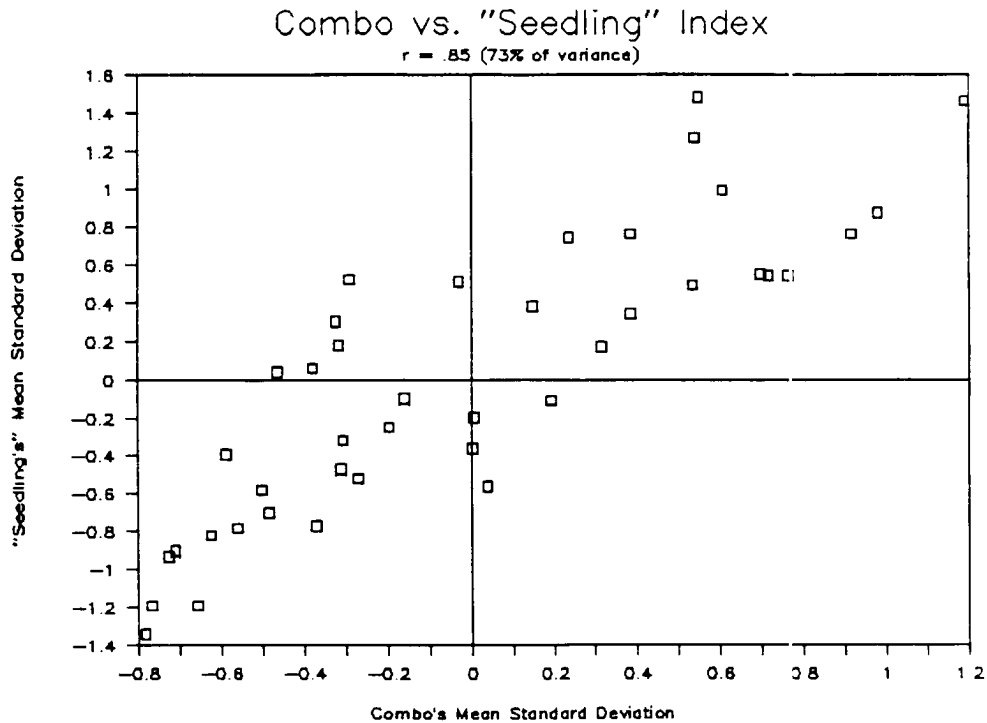


Figure 8.4: Scatter plot of Early Season Combination Rainfall Index (available by 1 August) versus June to September Seedling Index rainfall for the years 1949 to 1989. The two dependent indices correlate at $r = 0.85$.

An analysis of the Combination Rainfall Index versus August to September Western Sahel rainfall is shown as a scatter plot in Fig. 8.5. These two rainfall indices are now independent of one another in that no months of rainfall overlap one another. They correlate at a lower value of $r = 0.70$, but still explaining almost 50% of the variance in the main portion of the Sahel's rainy season. Detrending the two data series before correlating

has only a small reductive effect of reducing the correlation to $r = 0.65$. Thus the Early Season Combination Rainfall Index appears to have substantial skill in forecasting August and September rainfall in the Western Sahel, typically the rainiest months of the year.

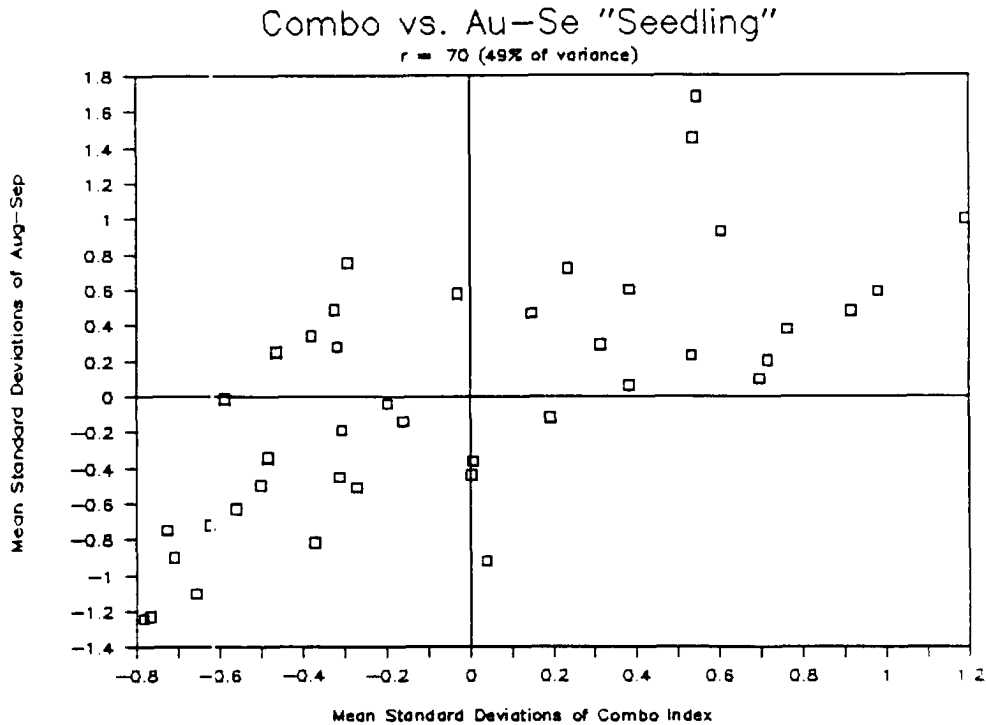


Figure 8.5: Scatter plot of Early Season Combination Rainfall Index (available by 1 August) versus August to September Index rainfall for the years 1949 to 1989. The two independent indices correlate at $r = 0.70$.

In summary, utilizing a multiple regression technique to combine the previous year Gulf of Guinea area rainfall with the June to July rainfall along the Western Sahel yields a useful predictive index. This Early Season Combination Rainfall Index shows considerable skill in predicting seasonal totals of Atlantic basin tropical cyclone activity, especially for the intense hurricane activity. It is noted again that more than 98 percent of all intense hurricane activity occurs after 1 August. In addition, useful predictive correlations are found for the Early Season Combination Rainfall Index versus the remaining two months of the Western Sahel rainy season.

Chapter 9

INDEPENDENT VERIFICATION

The importance of verifying statistical relationships with independent data cannot be overstated. That is, if one can obtain independent data of comparable quality. While showing that an association discovered in from one set of data also is present in an unrelated set does not prove that the association is real, it does provide important additional evidence of a physical connection.

An attempt is made to provide additional verification of the relationships developed in the 1949–89 data sets. Two verification methods are employed. First, the regression equations derived from the late 1940's through the 1980's data are used to forecast the 1990 Sahel rainfall and Atlantic basin tropical cyclone activity. Secondly, rainfall and tropical cyclone data from the 1920's to 1940's are analyzed to determine if similar results can be obtained from this independent information. As we shall see, the independent data substantiates some conclusions and is less definitive about other conclusions arrived at earlier.

9.1 Use of 1990 Data

The results of this research were recently used as a supplement to W.M. Gray's Atlantic basin seasonal tropical cyclone forecasts and verifications (Gray, 1989d, 1990a, 1990b, 1990d). Though the West African rainfall was just one of several variables considered for the forecasts, the 1990 Sahel rainfall and hurricane season provided an opportunity to test the earlier results.

What follows are the "forecasts" derived from regression equations for the Gulf of Guinea Index, the June to July Sahel Index, and the Early Season Combination Index.

These independent predictions were verified utilizing realtime tropical cyclone data from C. McAdie at NHC and realtime West African rainfall data from D. Miskus and R.J. Tinker at CAC.

9.1.1 1989 August to November Gulf of Guinea Rainfall

The 1989 August to November Gulf of Guinea rainfall value can be considered an independent data point as 1990 Sahel rainfall and 1990 tropical cyclone activity were not part of the developmental data base. Recall from Table 6.1 that the mean standard deviation at the 17 stations available in the Gulf of Guinea region was $\sigma = 0.12$ for 1989, slightly wetter than average.

Figure 9.1 presents two analyses of West African rainfall. Note that there are gaps in the analysis for the countries of Nigeria, Guinea, Central African Republic, Sudan, and Zaire and also throughout the largely uninhabited Sahara Desert. Fortunately, in the area of interest, along the Gulf of Guinea, there are enough stations to obtain an accurate regional measure of the rainfall anomalies. The top panel shows the absolute amount of precipitation in millimeters for the four month period.

Absolute amounts of rainfall do not allow for easy interpretation of anomalous precipitation. The bottom panel of Fig. 9.1 presents individual station rainfall anomalies for August to November 1989 expressed as relative standard deviations above or below normal. The values along the Gulf of Guinea south of 10°N are mixed, with both moderately positive and negative anomalies. No station in the area experienced an anomaly greater than one standard deviation.

Table 9.1 presents the regression equations and forecasted values for tropical cyclone activity and for Sahel rainfall. These results are based upon the rainfall to tropical cyclone associations described in Chapter 6. Note the large standard errors associated with the forecasts, a measure of the large uncertainties present. Figure 6.6 indicated that a rainfall anomaly value of $\sigma = 0.12$ dictated a range of intense hurricane days from 0.0 to 11.0 (10.75 with the intense hurricane bias removed). Hence, the late 1989 forecast of a near normal Sahel rainy season and a near normal tropical cyclone season was taken only as a rough

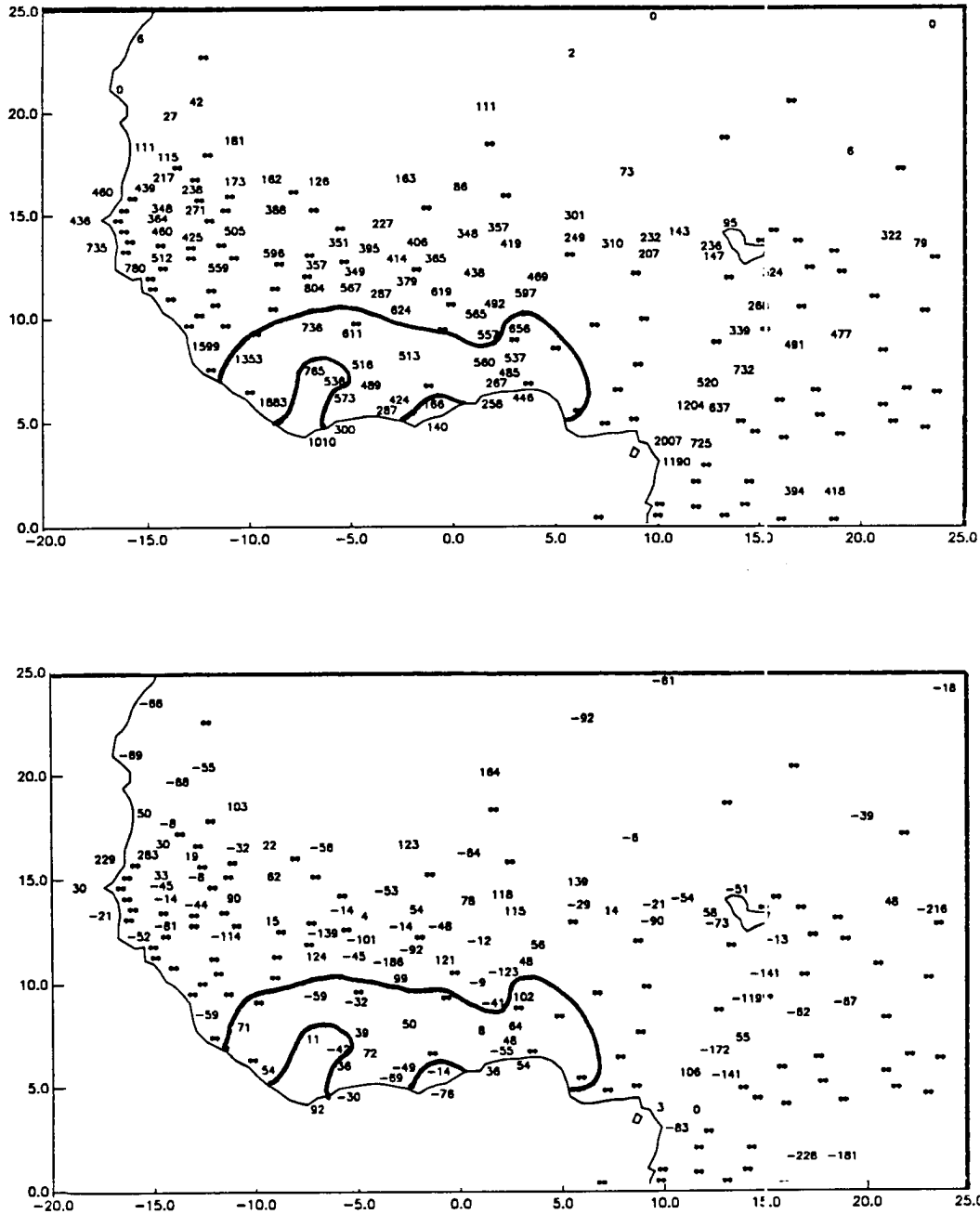


Figure 9.1: Analysis of 1989 August to November West African precipitation. The stations encircled by the boldface line are utilized in the August to November Gulf of Guinea Rainfall Index. The top panel shows the absolute rainfall amounts in mm. The bottom panel shows the rainfall expressed as the number of standard deviation above or below normal for each station—values are multiplied by 100, i.e. -141 means 1.41 standard deviations below the mean. Asterisks indicate no data available.

estimate. However, the near zero rainfall value for the Gulf of Guinea is substantially drier than the rainfall realized during these months for the previous two years ($\sigma = 1.44$ in 1987 and $\sigma = 0.34$ in 1988) and suggests less cyclone activity and drier Sahelian conditions that had occurred in 1988 and 1989.

Table 9.1: Regression equations and forecasted values (with standard errors) of 1990 seasonal Atlantic basin tropical cyclone activity and Sahelian rainfall (y) based upon the Gulf of Guinea Rainfall Index (x) relations for 1948 to 1988 (dependent data) and 1989 (independent data). Value of 1989 August to November Gulf of Guinea Index was $\sigma = 0.12$.

Parameter	Regression Equation	Forecasted Value	Climatological Value
Named Storms	$y = 9.45 + 2.028x$	9.7 ± 2.6	9.3
Named Storm Days	$y = 47.75 + 16.127x$	49.7 ± 16.3	46.7
Hurricanes	$y = 5.92 + 1.718x$	6.1 ± 1.8	5.9
Hurricane Days	$y = 24.43 + 11.338x$	25.8 ± 11.0	23.7
Int. Hurricanes (Bias Out)	$y = 2.31 + 1.443x$	2.5 ± 1.2	2.2
Int. Hur. Days (Bias Out)	$y = 5.08 + 3.970x$	5.6 ± 3.7	4.8
HDP	$y = 76.72 + 43.713x$	82.0 ± 38.3	75.5
Jun-Sep West Sahel Rain	$y = 0.06 + 0.775x$	0.14 ± 0.57	0.00

9.1.2 1990 June to July Western Sahel Rainfall

By the end of July, 1990 it had become apparent that the Sahel was headed for another severe drought year. Figure 9.2 documents the absolute and anomaly rainfall amounts for West Africa. Except for small portions of southeastern Mauritania, western Mali, and south central Niger, the entire Sahel region from Senegal to Ethiopia was experiencing dry conditions, one-half to two standard deviations below normal. The 25 available stations of the 38 station June to July Western Sahel Rainfall Index indicated a mean standard deviation of $\sigma = -0.53$, quite dry even with the near normal rainfall amounts seen in parts of Mauritania and Mali.

Table 9.2 presents the forecast regression equations derived from the end of July information for the upcoming seasonal tropical cyclone activity and for the remaining Sahel rainfall. Note that based on the negative anomaly for June and July rainfall, below normal tropical cyclone activity and August to September Sahelian rainfall are

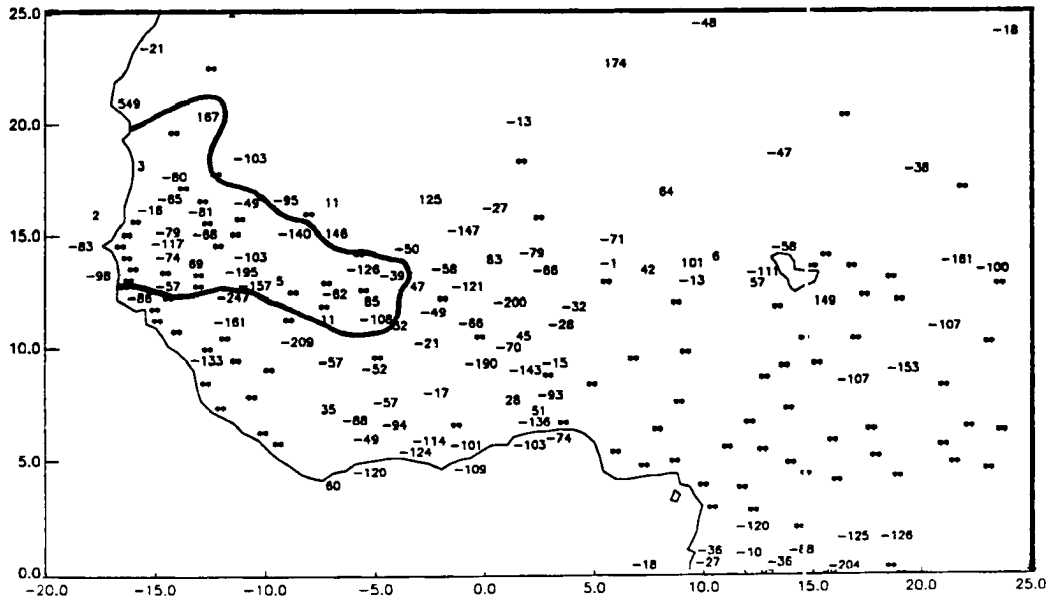
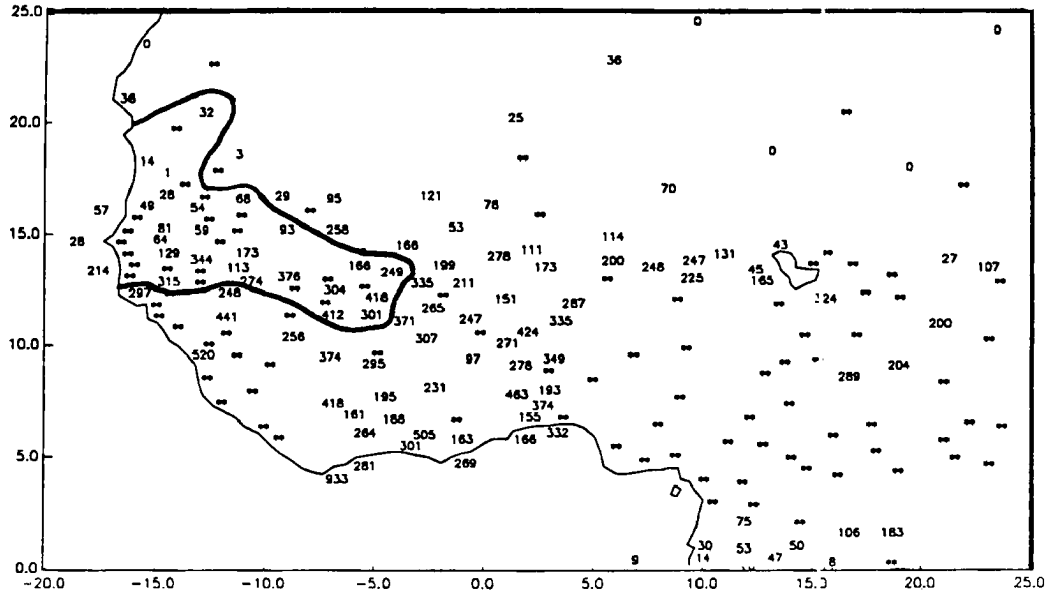


Figure 9.2: Same as Fig. 9.1 except for June to July 1990 rainfall. The boldface line encloses stations utilized in the June to July Western Sahel Rainfall Index.

predicted. The largest negative variations from mean climatological conditions were for intense hurricanes—57% of normal and for intense hurricane days—40% of normal.

Table 9.2: Regression equations and forecasted values (with standard errors) for 1990 seasonal Atlantic basin tropical cyclone activity and Sahelian rainfall (y) based upon the June to July Western Sahel Rainfall Index (x) relationships for 1949 to 1989 (dependent data) and 1990 (independent data). Value of 1990 June to July Western Sahel Index was $\sigma = -0.53$.

Parameter	Regression Equation	Forecasted Value	Climatological Value
Named Storms	$y = 9.30 + 2.232x$	8.1 ± 2.7	9.3
Named Storm Days	$y = 46.55 + 19.593x$	36.2 ± 16.6	46.7
Hurricanes	$y = 5.79 + 1.612x$	4.9 ± 2.0	5.9
Hurricane Days	$y = 23.60 + 12.782x$	16.8 ± 11.6	23.7
Int. Hurricanes (Bias Out)	$y = 2.21 + 1.687x$	1.3 ± 1.2	2.2
Int. Hur. Days (Bias Out)	$y = 4.78 + 5.331x$	2.0 ± 3.6	4.8
HDP	$y = 73.49 + 51.437x$	46.2 ± 40.0	75.5
Aug-Sep West Sahel Rain	$y = 0.01 + 0.742x$	-0.38 ± 0.56	0.00

9.1.3 1990 Early Season Combination Index

Addition of the June to July rainfall data for the Sahel to the previous late year rainfall data for the Gulf of Guinea produced a value of $\sigma = -0.31$ for the 1990 Early Season Rainfall Combination Index. This value was determined from the optimal weighting process (discussed in section 8.1) of 0.30 for the 1989 August to November Gulf of Guinea Rainfall value and 0.70 for the 1990 June to July Western Sahel Rainfall value.

As the early rains in the Western Sahel dominate the regression, the values for tropical cyclone activity and for August to September Sahel rainfall were thus predicted to be well below normal. Again, while the number of named storms (91% of normal) and hurricanes (88% of normal) were forecast to be only slightly reduced, it is the intense hurricanes (70% of normal) and the intense hurricane days (60% of normal) that the largest reductions were expected. Because of stronger correlations with the intense hurricanes, these forecasts are likely to be more skillful and thus should carry more reliability.

This information, which was available by 3 August, 1990, played a crucial role in reducing the forecasted magnitude of tropical cyclone numbers and intensities. Gray

Table 9.3: Regression equations and forecasted values (with standard errors) for 1990 seasonal Atlantic basin tropical cyclone activity and Sahelian rainfall (y) based upon the Early Season Combination Rainfall Index (x) values for 1949 to 1989 (dependent data) and 1990 (independent data). Value of 1990 combination index values was $\sigma = -0.31$.

Parameter	Regression Equation	Forecasted Value	Climatological Value
Named Storms	$y = 9.36 + 2.797x$	8.5 ± 2.6	9.3
Named Storm Days	$y = 47.35 + 23.680x$	40.0 ± 15.4	46.7
Hurricanes	$y = 5.84 + 2.154x$	5.2 ± 1.9	5.9
Hurricane Days	$y = 23.92 + 15.876x$	19.0 ± 10.7	23.7
Int. Hurricanes (Bias Out)	$y = 2.25 + 2.067x$	1.6 ± 1.1	2.2
Int. Hur. Days (Bias Out)	$y = 4.91 + 6.222x$	3.0 ± 3.2	4.8
HDP	$y = 74.79 + 62.882x$	55.3 ± 35.8	75.5
Aug-Sep West Sahel Rain	$y = 0.02 + 0.896x$	-0.26 ± 0.51	0.00

(1990b), in his seasonal forecast update, lowered his forecast number of hurricanes from 7 to 6, of hurricane days from 30 to 25, of intense hurricanes from 3 to 2, and issued, for the first time, a forecast of 5 intense hurricane days. To a large degree, Gray based this updated forecast on the negating effects of the early season West African rainfall signal (negative effect) whereas the stratospheric QBO phase and other forecast parameters were positive. While the original early June forecast (Gray, 1990a) had called for above average tropical cyclone activity, this new forecast was closer to the climatological mean.

9.1.4 Verification of Forecasts

Western Sahel Rainfall. Dry conditions in the Sahel observed during June and July of 1990 continued and worsened during the later months of the rainy season. The 1990 August to September rainfall anomaly value for the Western Sahel was a very dry $\sigma = -0.89$. Figure 9.3 presents the amounts of rainfall and anomalies (in standard deviations) above or below the mean during the four month period of June to September 1990. Observe from the anomaly diagram that virtually all of West Africa had below normal precipitation. This is especially true throughout the Sahel (approximately 11 to 20°N) where dry conditions of one to two or more standard deviations below normal are seen. The four month rainfall anomaly for the Western Sahel region was $\sigma = -0.95$.

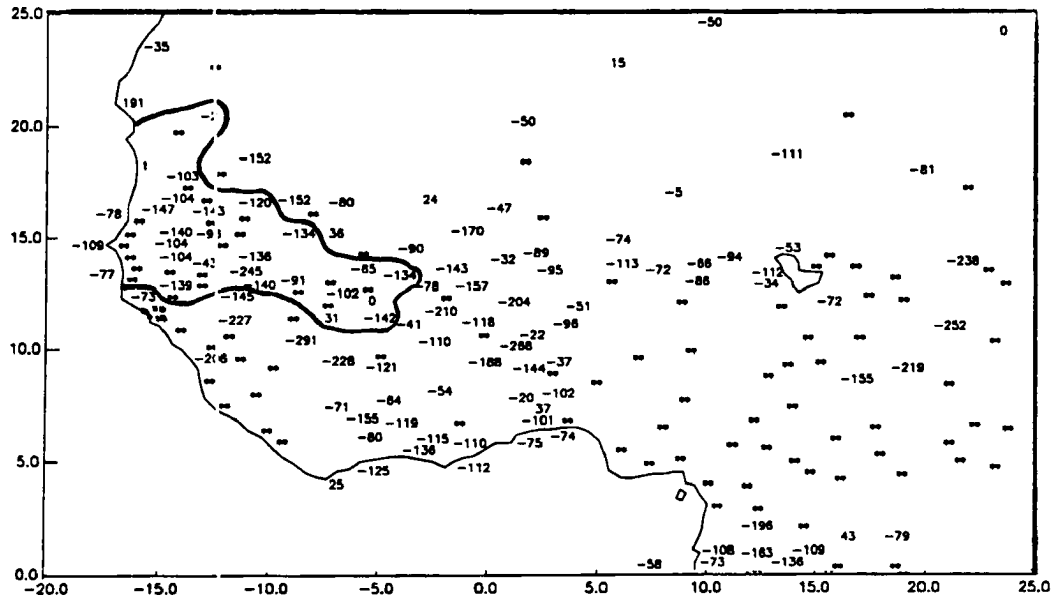
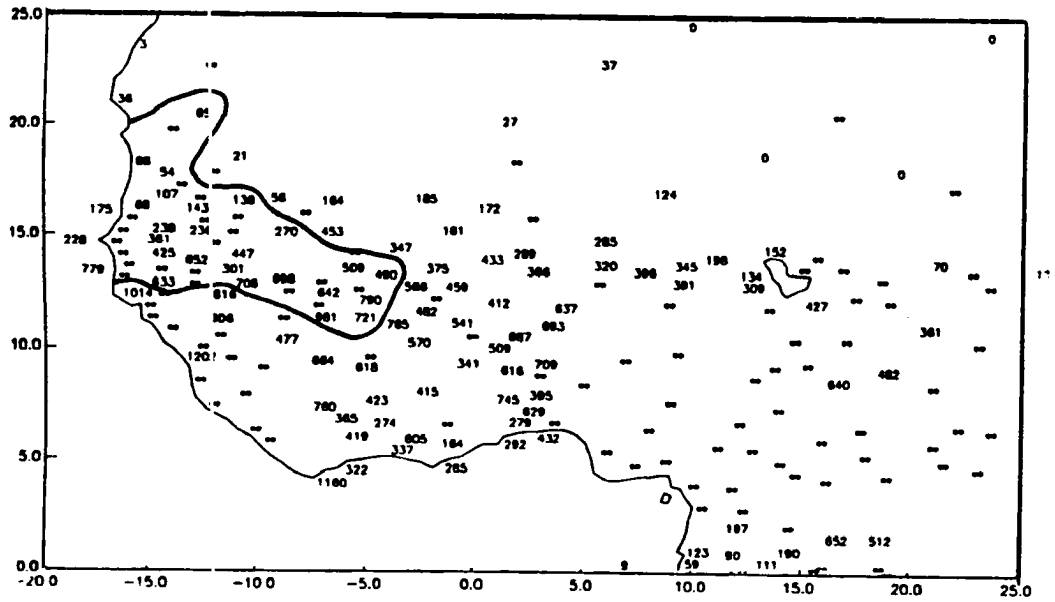


Figure 9.3: Same as Fig. 9.1 except for June to September 1990 rainfall. The boldface line encloses the stations utilized for the Seedling Rainfall Index.

While indications of near normal rainfall amounts from the previous year Gulf of Guinea data proved incorrect (but not beyond reasonable error limits—see Table 9.1), the June to July Western Sahel Index and the Early Season Combination Index did correctly suggest a below normal Sahel rainy season (see Tables 9.2 and 9.3). Figure 9.4 shows the scatter plot of 1949 to 1989 values of the Combination Index (available by 1 August) and the August to September Western Sahel Rainfall Index. Superimposed on this scatter plot is the best fit line and the independent data point representing the 1990 season. Whereas the predictor correctly anticipated the sign of the anomaly, it significantly underestimated its magnitude.

This 1990 test using independent data is encouraging for the possibility of forecasting the monsoonal rainfall in the Sahel. Prior knowledge of almost half of the likely rainfall variance during the main rainy months (August and September) may be possible. However, the Gulf of Guinea rainfall based forecast for the Sahel did not verify well in 1990, though no forecasting scheme can be adequately tested in just one year. The 1991 rainy season may become an excellent test of its use as a predictor: the 1990 August to November Gulf of Guinea anomaly was a very dry $\sigma = -0.70$.

1990 Atlantic Basin Tropical Cyclones. The tracks of 1990 Atlantic basin tropical cyclones of at least named storm strength are portrayed in Fig. 9.5. At first glance the basin appears to have had an active season. The fourteen named storms placed the season as one of the most active for named storms during the past 40 years. However, the weak intensity of the cyclones was such that Gray (1990d) characterized 1990 as “a year of many wimpy storms.”

Seasonal statistics for 1990 tropical cyclone activity are presented in Table 9.4. The “wimpy storms” label appears to be appropriate. Three tropical storms lasted less than two days each. Only three of the eight hurricanes survived as hurricanes for more than two days. Only one hurricane, Gustav, reached the intense hurricane threshold of 96 kt (50 m s^{-1}) and this for only one day.

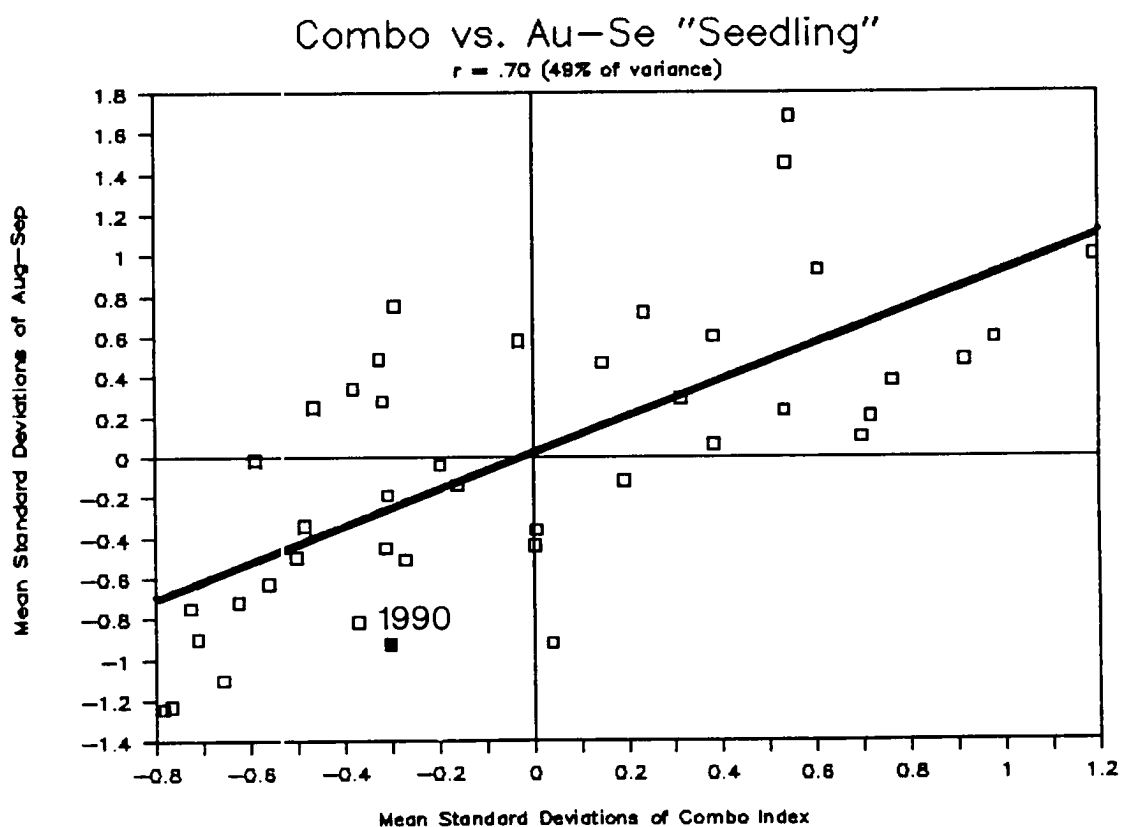


Figure 9.4: Scatter plot of the Early Season Combination Rainfall Index (available by 1 August) versus the August to September Western Sahel Rainfall Index. Superimposed upon the points is the best fit line. The point labeled '1990' is an independent data point.

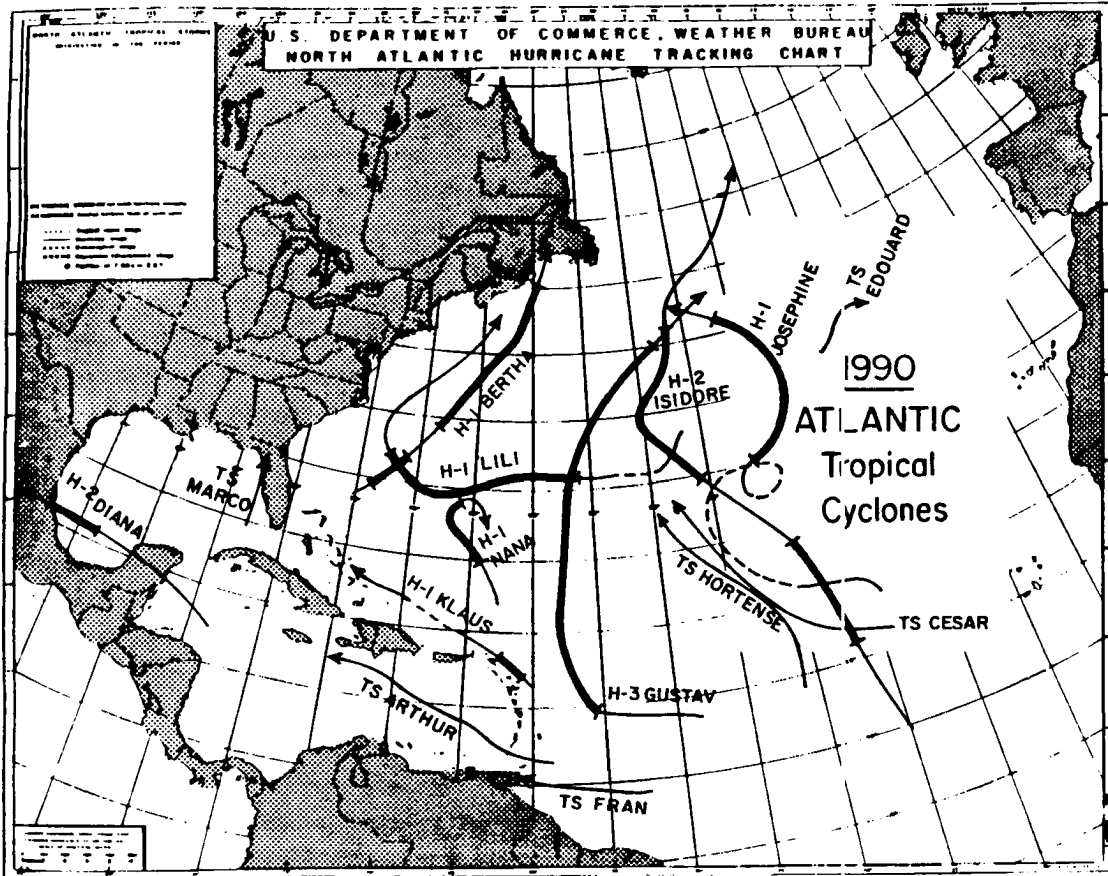


Figure 9.5: Track of the 1990 Atlantic basin named storms. The thin solid line refers to tropical storm strength, the thick solid line indicates hurricane strength, and the dashed line notes where the cyclone temporarily dipped below tropical storm intensity.

Table 9.4: Summary of information on 1990 Atlantic basin named tropical cyclones.

Storm Name and Category	Dates of Named Intensity	Named Storm Days	Hurr. Days	Intense Hurr. Days	HDP	Max Wind (kt)	Min Pressure (mb)
Arthur (TS)	7/24-27	2.75	—	—	—	60	995
Bertha (H1)	7/28-8/2	5.25	4.25	—	6.0	70	974
Cesar (TS)	8/1-5	4.50	—	—	—	45	1000
Diana (H2)	8/5-8	3.50	0.75	—	1.7	85	980
Edouard (TS)	8/3-10	1.75	—	—	—	40	1003
Fran (TS)	8/13-14	1.00	—	—	—	35	1007
Gustav (H3)	8/25-9/3	9.25	7.25	1.00	20.9	105	956
Hortense (TS)	8/26-30	3.75	—	—	—	55	993
Isidore (H2)	9/5-16	12.00	8.25	—	15.7	85	978
Josephine (H1)	9/24-25,10/1-6	5.25	1.50	—	2.9	75	980
Klaus (H1)	10/3-7	4.25	0.75	—	1.4	70	985
Lili (H1)	10/6-15	8.75	2.50	—	4.2	65	987
Marco (TS)	10/10-11	1.75	—	—	—	55	989
Nana (H1)	10/16-20	4.25	2.25	—	4.5	75	989

The question as to whether 1990 was an ‘active’ or a ‘calm’ hurricane season depends upon the definition utilized. Since the intense hurricanes cause over three-quarters of the U.S. tropical cyclone linked damage and the potential predictability for these cyclones is greater, use of intense hurricane days as the criteria to characterize the 1990 hurricane season would lead to a designation of a very inactive season. Another measure of intensity and duration of hurricanes, HDP, would also depict 1990 as being below normal.

As the rainfall indices are best associated with the strongest hurricanes but have a much weaker relationship with named storms, a mixed hurricane season like 1990 is possible—active with respect to the total number of systems but quite inactive with respect to intense cyclones. Other factors besides conditions associated with West African rainfall were favorable for named storm development in 1990 (Gray, 1990d).

Table 9.5 indicates that the number of 1990 named storms, named storm days, and hurricanes were more frequent than specified by climatology. The occurrence of hurricane days is close to the long term mean. The remaining parameters—intense hurricanes, intense hurricane days, and HDP were below normal with respect to climatology.

Table 9.5: Summary of forecasts and verification for Atlantic basin tropical cyclone activity during the 1990 season.

Tropical Cyclone Parameter	Gulf of Guinea Forecast	Jun-Jul W. Sahel Forecast	Combination Index Forecast	Verification	Climatology
Named Storms	9.7±2.6	8.1±2.7	8.5±2.6	14	9.3
Named Storm Days	49.7±16.3	36.2±16.6	40.0±15.4	68.0	46.7
Hurricanes	6.1±1.8	4.9±2.0	5.2±1.9	8	5.9
Hurricane Days	25.8±11.0	16.8±11.6	19.0±10.7	27.5	23.7
Intense Hurricanes	2.5±1.2	1.3±1.2	1.6±1.1	1	2.3
Int. Hur. Days	5.6±3.7	2.0±3.6	3.0±3.2	1.0	4.8
HDP	82.0±38.3	46.2±40.0	55.3±35.8	57.4	75.5

The forecast based on previous year Gulf of Guinea rainfall of near normal conditions was not accurate for intense hurricane activity. However, it did provide the best forecast for the first three parameters in Table 9.5, but was not an improvement over climatology. The forecasts based on the June to July Western Sahel Index and the Early Season Combination Index were similar, except that the June to July Western Sahel rainfall suggested less activity overall. For intense hurricanes, intense hurricane days, and HDP, both forecasts performed substantially better than climatology. Figure 9.6 presents a scatter plot of the Early Season Combination Index versus intense hurricane days with the 1990 data point superimposed.

The concurrent relationships between intense hurricane activity and June to September Western Sahel rainfall also verified quite well in 1990. Figure 9.7 presents a scatter plot of these two parameters with the 1949 to 1989 best fit line and the 1990 data point superimposed. If perfect foreknowledge of the Sahel rainfall had been available, the extremely dry value of $\sigma = -0.95$ would have dictated a forecast value of 0.5 intense hurricane days—just slightly lower than what actually occurred.

It would appear that forecasting seasonal tropical cyclone activity based West African rainfall anomalies has potential skill. The 1990 season was unusual in that the large number of total cyclones had a smaller than normal proportion of intense activity. Nevertheless, forecasts based on the June to July Western Sahel rainfall and the Early Season

Combo of Indices vs Intense Hur. Days

(BIAS OUT) $r = .73$ (53% of variance)

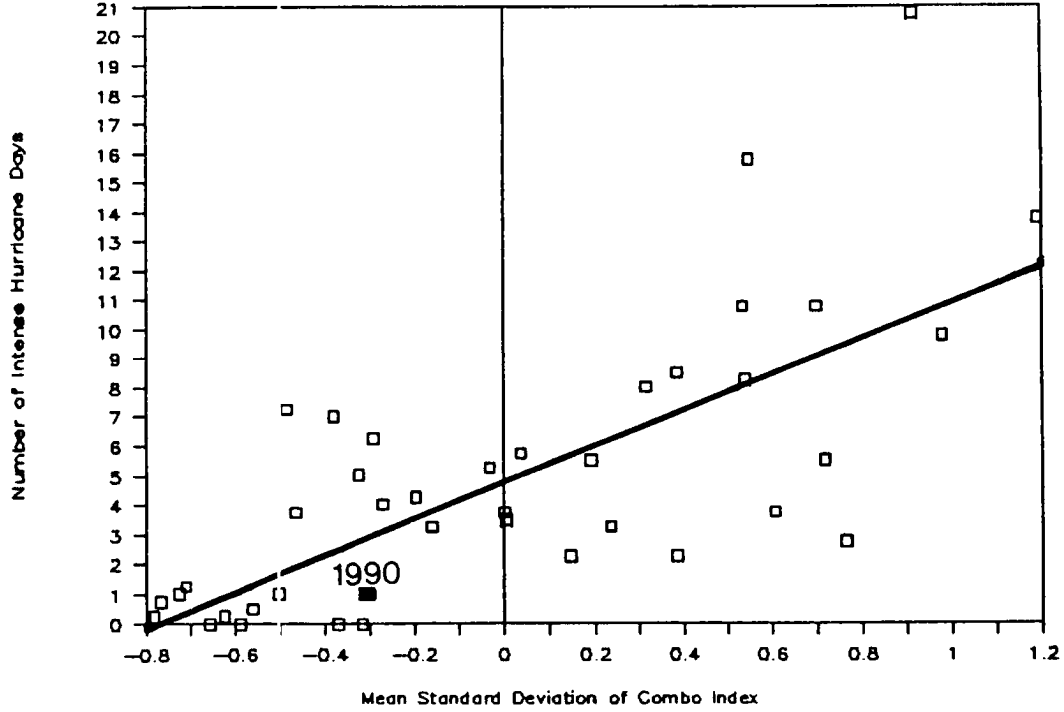


Figure 9.6: As in Fig. 9.4 except for Early Season Combination Rainfall Index versus Atlantic basin intense hurricane days.

"Seedling" vs. Intense Hurricane Days

(BIAS OUT) $r = .69$ (48% of variance)

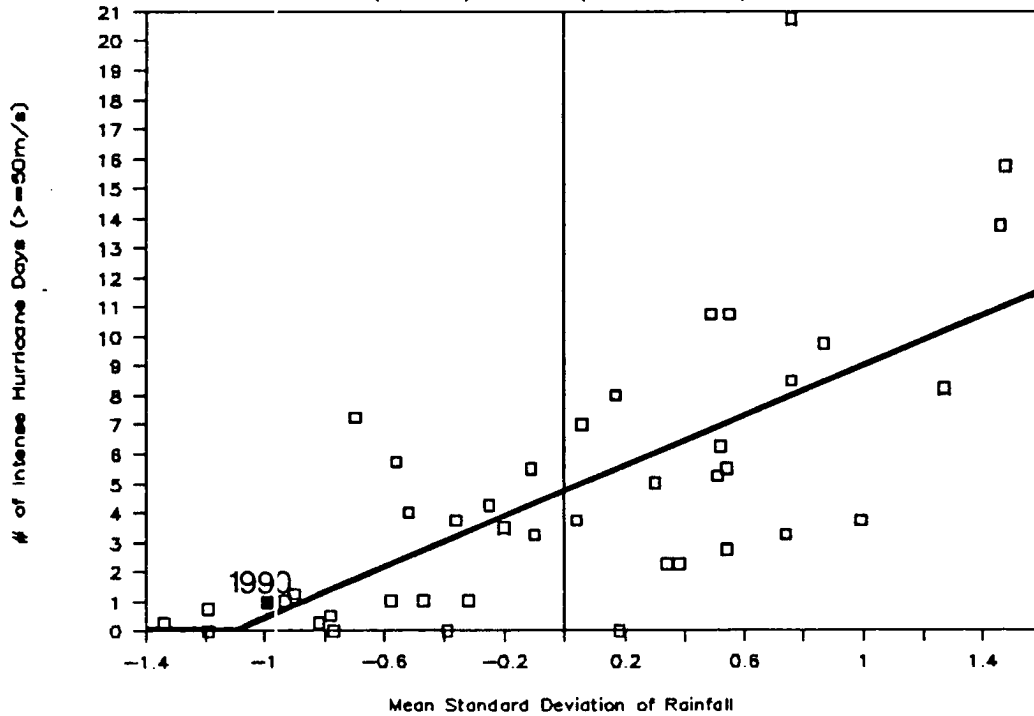


Figure 9.7: As in Fig. 9.4 except for June to September Western Sahel rainfall versus Atlantic basin intense hurricane days.

Combination Rainfall Index, however, showed quite an improvement over climatology for the intense hurricanes, intense hurricane days, and HDP. The August to November Gulf of Guinea rainfall data from the previous year displayed no skill as it forecast near normal conditions in a year which experienced below normal, normal, and above normal conditions depending on the parameter examined. The hurricane season of 1991 should provide a better test for this index in that, as previously discussed, the region near the Gulf of Guinea was substantially drier than normal ($\sigma = -0.70$) during August–November of 1990. This dryness should be a harbinger of an overall calm season, both in the number and strength of tropical cyclones during the fall of 1991.

9.2 Use of 1920's to 1940's Data

Due primarily to limitations on rainfall data availability, the years 1922 to 1948 were chosen for verification of the rainfall-tropical cyclone interrelationships. Consequently, for the Gulf of Guinea late season rainfall, the years 1921 to 1947 are utilized. Many West African rain gauge stations begun recording data in 1921. Assuming that the usable stations in this data set reflect the same rainfall variability characteristics as the larger data set of the more recent decades, then the rainfall to rainfall relationships should not have additional bias in the early decade data set.

There is, however, a large degradation of data quality for the Atlantic basin tropical cyclone information before the mid 1940's, was discussed in Chapter 2. This degradation is due to a lack of satellite and aircraft reconnaissance. This data problem likely causes a weakening of the rainfall to tropical cyclone relationships as more "noise" is introduced into the relationships. For this reason, only the U.S. landfalling tropical cyclone data during the wettest versus the driest years will be tested. Although these storms, while showing a much weaker year to year association with West African rainfall in the recent 1949–89 dependent data set, they provide the most reliable long term record of Atlantic basin tropical cyclone activity.

9.2.1 U.S. Landfalling Tropical Cyclones

Table 9.6 summarizes the yearly variations of tropical cyclones affecting the U.S. during the period 1922 to 1948. Note that, in general, this era had a larger mean for all intensities of landfalling tropical cyclones than observed in recent decades (see Table 3.4). However, the mean frequency of intense hurricanes striking the U.S. Gulf Coast was slightly lower.

Table 9.6: US landfalling tropical cyclone activity 1922 to 1948.

Year	Named/ Subtrop. Storms	Hurrs.	Intense Hurrs.	Gulf Intense Hurrs.	East Intense Hurrs.
1922	1	0	0	0	0
1923	4	1	0	0	0
1924	3	2	0	0	0
1925	2	1	0	0	0
1926	4	3	2	2	1
1927	1	0	0	0	0
1928	3	2	1	0	1
1929	2	2	1	0	1
1930	1	0	0	0	0
1931	2	0	0	0	0
1932	5	2	1	1	0
1933	7	5	3	1	2
1934	5	3	1	1	0
1935	2	2	1	0	1
1936	7	3	1	1	0
1937	4	0	0	0	0
1938	4	2	1	0	1
1939	3	1	0	0	0
1940	4	2	0	0	0
1941	4	2	1	1	0
1942	3	2	1	1	0
1943	4	1	0	0	0
1944	4	3	2	0	2
1945	4	3	1	0	1
1946	4	1	0	0	0
1947	7	3	1	0	1
1948	4	3	1	0	1
Mean	3.63	1.81	0.70	0.30	0.44
S.D.	1.64	1.22	0.76	0.53	0.63

9.2.2 June to September Seedling Index

Going back to 1922 reduces the number of rainfall stations available in the Western Sahel region from 38 to 18. Table 9.7 provides information concerning each station. Fortunately, in every year during this period at least 16 of the 18 possible stations had data and the spatial coverage is uniform and widespread throughout the area. The locations of the available stations, as well as others not yet operating, are shown in Fig. 9.8. The mean rainfall for the 18 stations was 600 mm. This value is almost identical to that for the 1949 to 1989 period (595 mm). However, since individual stations common to both periods show values 10 to 20% larger during the earlier period, there is a slight bias for the earlier period to have proportionally fewer southerly stations.

Table 9.7: The 18 stations used in the 1922 to 1948 June to September Seedling Index: CSU Rainfall Data Base identification number, station name and country, June to September mean and standard deviation (in mm), years of data in analysis, and correlation coefficients versus the Seedling Index.

Station	Rainfall Data			vs. Index
	Mean	SD	Years	r
0119 Niore Du Sahel, Mali	661.9	315.72	26	0.337
0123 Kayes, Mali	665.2	175.73	23	0.329
0126 Segou, Mali	632.9	128.62	21	0.857
0127 San, Mali	646.7	105.74	27	0.473
0131 Koutiala, Mali	806.7	128.92	27	0.112
0132 Bougouni, Mali	1063.9	277.73	27	0.029
0133 Sikasso, Mali	1068.5	201.46	27	0.211
0138 Atar, Mauritania	77.9	45.70	27	0.412
0142 Boutilimit, Mauritania	159.5	78.20	24	0.549
0146 Kiffa, Mauritania	312.1	120.96	27	0.702
0148 Saint Louis, Senegal	358.6	145.10	27	0.491
0149 Podor, Senegal	284.7	107.14	27	0.636
0151 Matam, Senegal	498.2	161.81	27	0.566
0152 Dakar/Yoff, Senegal	493.7	139.94	26	0.663
0154 Thies, Senegal	605.2	179.76	25	0.664
0155 Diourbel, Senegal	560.6	159.56	27	0.742
0157 Tambacounda, Senegal	810.3	177.97	25	0.311
0162 Bathurst/Yundum, Gambia	1095.8	260.09	19	0.344

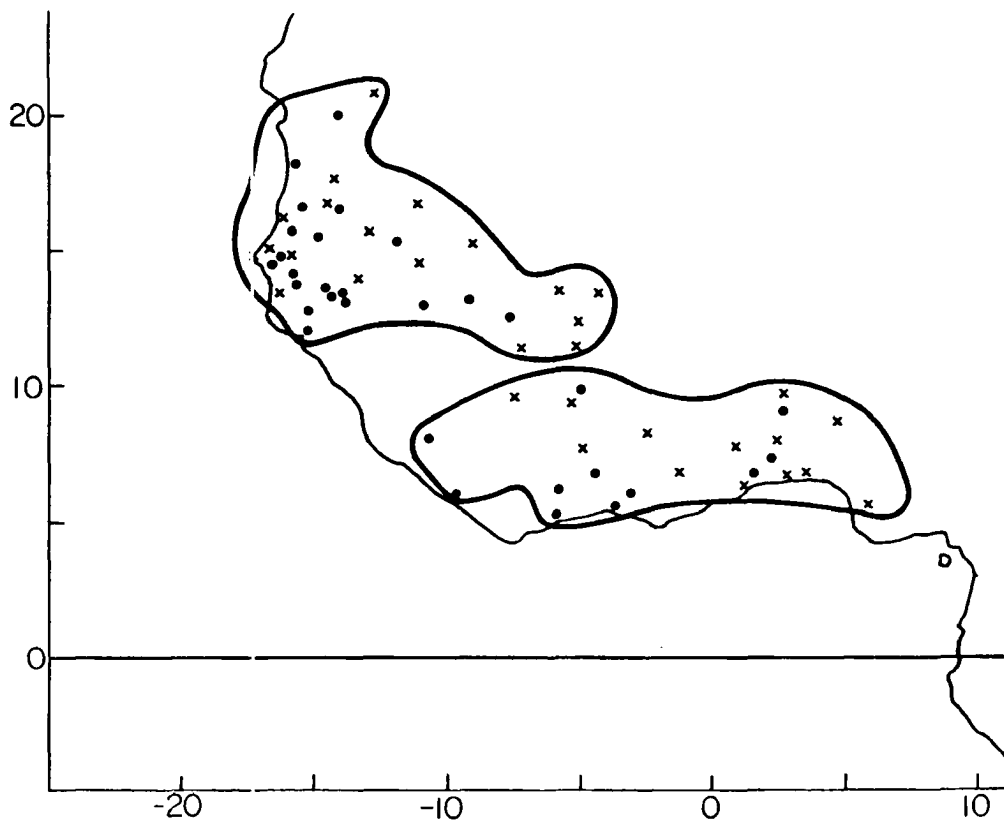


Figure 9.8: Location of rainfall stations which composed the June to September Seedling Index (northwestern region) and the Gulf of Guinea Index (southeastern region). Stations available for the 1922 to 1948 analysis (1921 to 1947 for the Gulf of Guinea) are indicated by 'X'.

The question arises as to whether this earlier rainfall data set can properly represent the June to September Seedling Index area. Testing the association for the years 1949 to 1989 with the 18 station index versus the entire 38 station index gives a linear correlation coefficient of $r = 0.98$, relating almost 97% of the variance between the two indices. Thus the use of this smaller subset should not induce a priori inconsistencies into the analysis.

Figure 9.9 presents the year to year rainfall anomaly values for the June to September Seedling Index during the period 1922 to 1948. A strong trend, so noticeable in the 1949 to 1989 analysis, does not occur during the earlier period. There is, however, some indication the 1940's were generally drier than normal whereas the late 1920's through the 1930's were somewhat wetter than normal. The year to year persistence of rainfall anomalies is much less of a factor during this period.

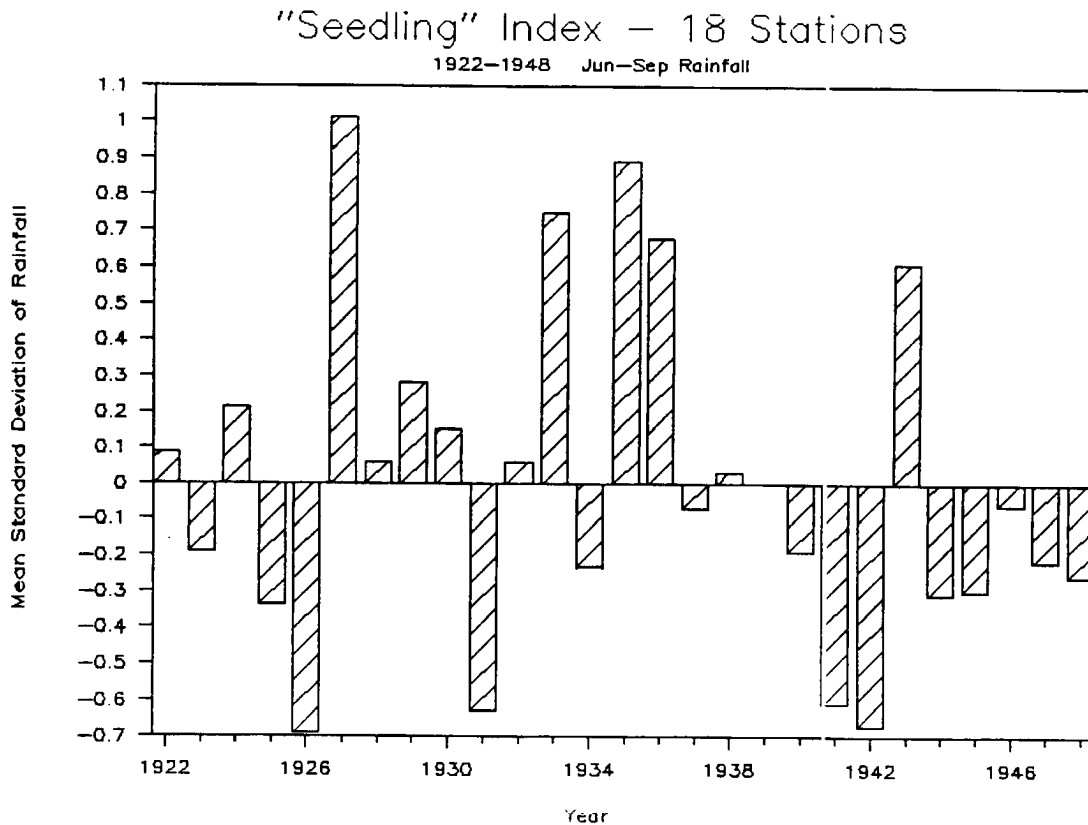


Figure 9.9: Rainfall anomalies expressed as mean standard deviations for the 18 station June to September Seedling Index of the Western Sahel in the period 1922 to 1948.

Table 9.8 summarizes the U.S. landfalling tropical cyclone statistics during the seven wettest and driest June to September Western Sahel seasons 1922 to 1948. While the

landfalling cyclones, especially the intense hurricanes along the US East Coast, show above normal activity during the wet years, the tropical cyclone activity is also above normal in the driest years as well. These results do not appear to provide verification of the concurrent relationship between June to September Western Sahel rainfall and Atlantic basin tropical cyclone activity.

Table 9.8: Summary of variability for U.S. landfalling tropical cyclones in the seven wettest and the seven driest Western Sahel years (as measured by the Seedling Index) from 1922 to 1948. (Asterisks refer to significance level: 0.100 for ‘*’, 0.025 for ‘**’ and 0.005 for ‘***’.)

Tropical Cyclones	Wettest Years' Mean	Percent (%) of Normal	Driest Years' Mean	Percent (%) of Normal	Ratio Wet/Dry
US Named Storms	3.6	99	3.3	91	1.09
US Hurricanes	2.0	110	2.0	110	1.00
US Intense Hurricanes	0.9	129	1.0	143	0.90
' Gulf Coast	0.3	100	0.6	200	0.50
' East Coast	0.6	136	0.6	136	1.00

9.2.3 August to November Gulf of Guinea Rainfall Index

As stated earlier, reliability of rainfall data is still quite good going back to 1921 in the West Africa region. Thus, for verification of the August to November Gulf of Guinea Rainfall Index, the years 1921 to 1947 will be utilized. Of the 24 Gulf of Guinea stations available for the original analysis of the period 1948–89, only 13 were operational by 1921. Each year from 1921 to 1947 had data for a minimum of at least 10 of the 13 stations. Specifics regarding these 13 stations are listed in Table 9.9 and location are shown in Fig. 9.8. Figure 9.8 demonstrates that the Gulf of Guinea region is reasonably well represented with some data gaps in Sierra Leone, Liberia, and southern Cote D'Ivoire. The lack of data from the southwestern portion of the region may increase the uncertainty in using this subset as representative of the whole region.

Representativeness is tested by comparing means and standard deviations for the whole set of 24 stations versus the 13 station subset. The subset has mean and standard deviation values of 597 mm and 172 mm for 1921 to 1947. These values are slightly lower

Table 9.9: The 13 stations used in the 1921 to 1947 Gulf of Guinea Index: CSU Rainfall Data Base identification number, station name and country, August to November rainfall mean and standard deviation (in mm), years of data in analysis, and correlation coefficients versus the Gulf of Guinea Rainfall Index.

Station	Rainfall Data			vs. Index
	Mean	SD	Years	r
0455 Ilorin, Nigeria	566.1	125.64	27	0.526
0459 Lagos/Ikeja, Nigeria	482.5	172.25	27	0.505
0460 Warri, Nigeria	1158.3	212.02	27	0.286
0467 Parakou, Benin	599.1	150.33	27	0.675
0469 Save, Benin	617.5	276.27	23	0.388
0471 Cotonou, Benin	310.2	129.39	23	0.755
0475 Atakpame, Togo	550.3	151.33	22	0.392
0477 Lome, Togo	198.8	110.51	23	0.423
0480 Kumasi, Ghana	546.3	134.64	23	0.737
0490 Odiene, Ivory Coast	901.4	210.09	25	0.335
0491 Korhogo, Ivory Coast	792.9	291.13	09	0.611
0493 Bondoukou, Ivory Coast	531.9	140.07	13	0.450
0495 Bouake, Ivory Coast	510.1	137.67	27	0.413

than the full 24 station values for 1948 to 1989. Individual stations common to both data periods also show no consistent trend from the earlier to the later period.

A secondary check was done to compare the subset time series versus that for the entire set for the same time period. Utilizing the period 1948 to 1989, the 13 station subset correlates with the entire 24 station set at $r = 0.96$, or about 93% of the variance explained between the two. Therefore, almost all of the variability seen in original Gulf of Guinea Index is reproduced in the 13 station subset.

Year to year rainfall anomalies portrayed in Fig. 9.10 show no discernible trend in the earlier 1921 to 1947 time period. Likewise only a small downward trend was seen in the later period Gulf of Guinea rainfall, even as the Sahel was experiencing a large decrease in precipitation.

The association with tropical cyclone activity during the earlier period is documented in Table 9.10. Though more activity is generally seen during the wet years than during the dry years, none of the differences are statistically significant. Even so, these results are suggestive but not conclusive regarding the validity of the original analysis.

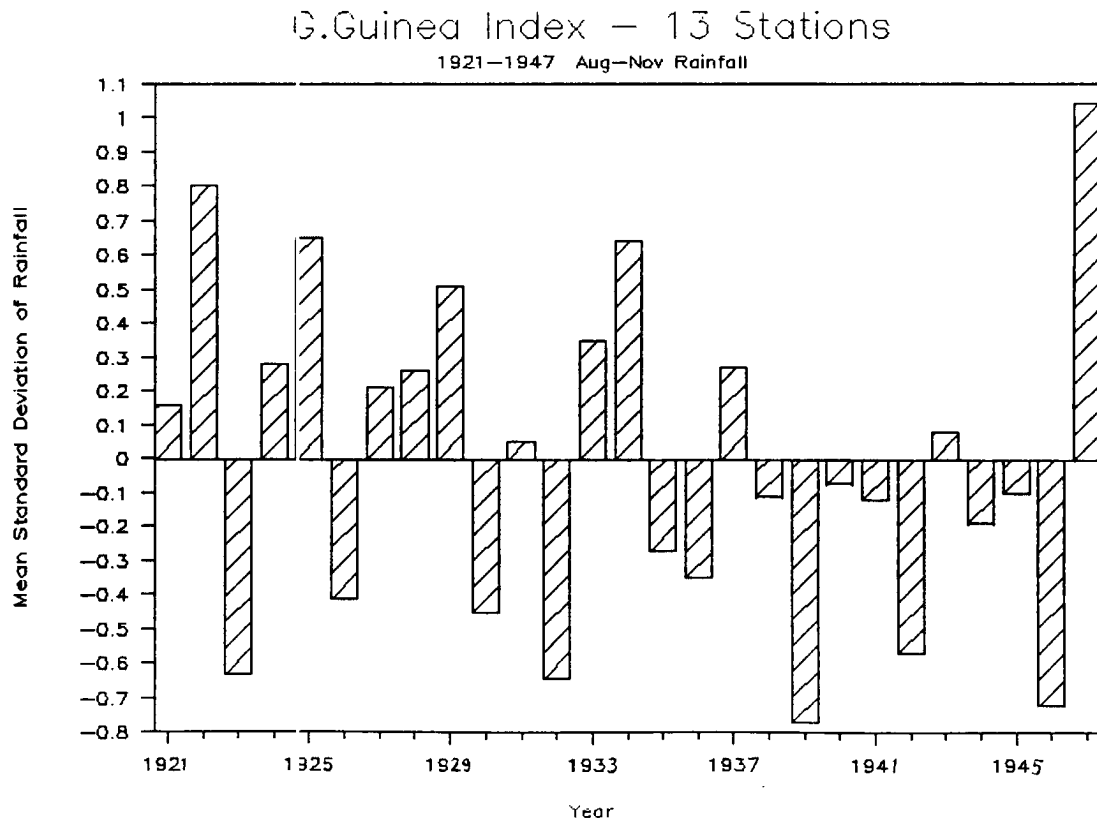


Figure 9.10: Rainfall anomalies expressed as mean standard deviations for the 13 station August to November Gulf of Guinea Index of rainfall for the period spanning 1921 to 1947.

Table 9.10: Summary of the variability of U.S. landfalling tropical cyclones during the years following the seven wettest and the seven driest August to November Gulf of Guinea years from 1921 to 1947. (Asterisks refer to significance level: 0.100 for ‘*’, 0.025 for ‘**’ and 0.005 for ‘***’.)

Tropical Cyclones	Wettest Years' Mean	Percent (%) of Normal	Driest Years' Mean	Percent (%) of Normal	Ratio Wet/Dry
US Named Storms	3.1	85	3.6	99	0.86
US Hurricanes	1.9	105	1.4	77	1.36
US Intense Hurricanes	0.7	100	0.4	57	1.75
' Gulf Coast	0.4	133	0.1	33	4.00
' East Coast	0.4	91	0.3	68	1.33

The Gulf of Guinea's late season rainfall during 1921 to 1947 has no correlation with the full June to September Western Sahel rainfall during the following year. Figure 9.11 shows a scatter plot of these two rainfall indices. The lack of association is surprising in that we had obtained a strong positive relationship of $r = 0.65$ for these parameters ($r = 0.83$ for detrended data) for 1948 to 1988. Rank correlation statistics for this earlier period Gulf of Guinea-Western Sahel rainfall association show a similar random result of $r = -0.18$. However, the June and July Sahel rainfall do show some correlation to previous year Gulf of Guinea rainfall. This association will be explored in the next section.

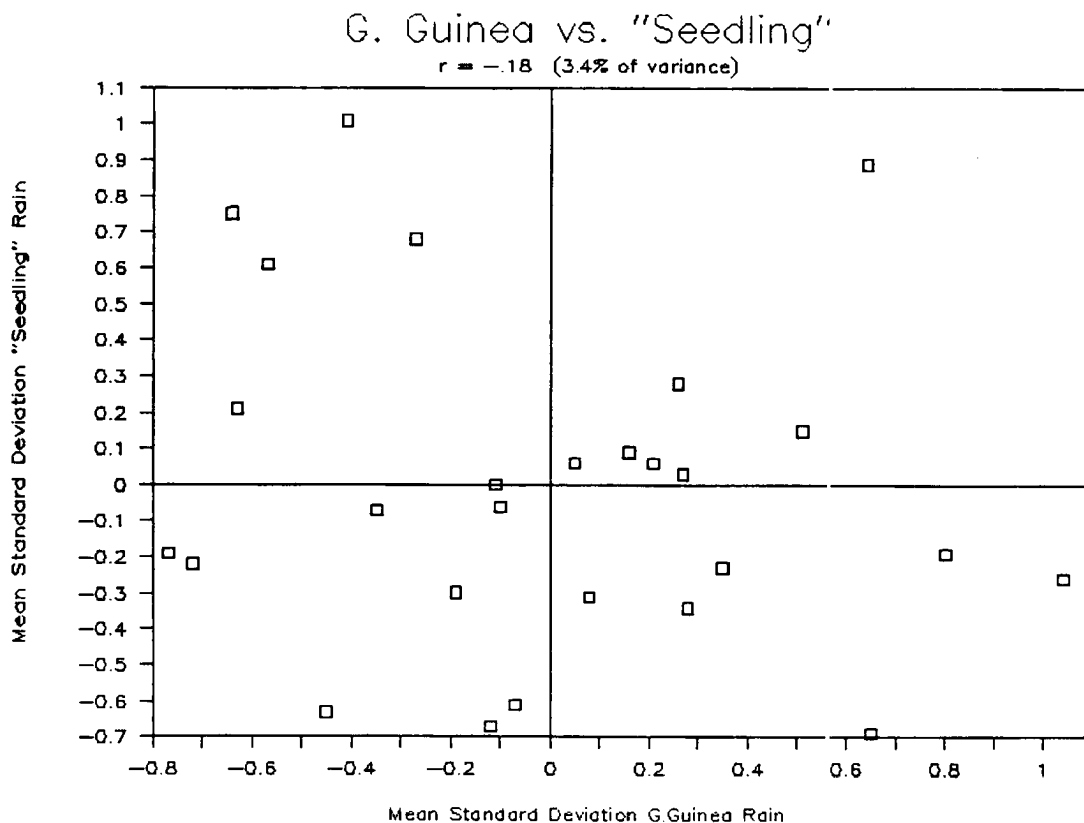


Figure 9.11: Scatter plot of August to November Gulf of Guinea Index rainfall anomalies (1921 to 1947) versus following year June to September Western Sahel Index rainfall anomalies (1922 to 1948). The two indices correlate at $r = -0.18$.

9.2.4 June to July Western Sahel Rainfall Index

The use of a reduced 18 station subset in the Western Sahel area (Fig. 9.8) for the early rainy season months of June and July carries the same caveats as does the entire

June to September Seedling Index rainfall. Specific data for individual stations are listed in Table 9.11.

While mean precipitation for the 18 stations from 1922 to 1948 (214 mm) is similar to that mean for the 38 station, individual index during the last few decades; stations common to both time periods show a 5 to 15% larger June–July mean during the earlier period. This slight bias is due to a smaller proportion of 18 stations located in the southern Seedling region. A further check of the applicability of the subset data to represent the entire 38 station index would be to compare the time series of the two for the same time period. Doing so reveals a linear correlation coefficient of $r = 0.97$, relating 94% of the variance between the two. It is likely then that this smaller data set adequately represents the characteristics of the June to July Western Sahel region contained in the full 38 station index.

Table 9.11: The 18 stations used in the June to July Western Sahel Rainfall Index for 1922 to 1948: CSU Rainfall Data Base identification number, station name and country, June to July mean and standard deviation (in mm), years of data in analysis, and correlation coefficients versus the June to July Rainfall Index.

Station	Rainfall Data			vs. Index r
	Mean	SD	Years	
0119 Nioro Du Sahel, Mali	256.1	134.27	26	0.406
0123 Kayes, Mali	258.8	89.84	23	0.302
0126 Segou, Mali	272.2	59.37	21	0.396
0127 San, Mali	288.0	65.87	27	0.395
0131 Koutiala, Mali	368.0	75.49	27	0.372
0132 Bougouni, Mali	443.9	161.59	27	0.094
0133 Sikasso, Mali	462.6	102.03	27	0.326
0138 Atar, Mauritania	16.0	23.60	27	0.210
0142 Boutilimit, Mauritania	41.9	35.79	24	0.437
0146 Kiffa, Mauritania	103.0	53.69	27	0.640
0148 Saint Louis, Senegal	62.9	48.25	27	0.575
0149 Podor, Senegal	74.8	55.43	27	0.712
0151 Matam, Senegal	175.9	92.24	27	0.682
0152 Dakar/Yoff, Senegal	93.3	62.03	26	0.656
0154 Thies, Senegal	126.6	76.46	27	0.734
0155 Diourbel, Senegal	171.1	87.22	27	0.612
0157 Tambacounda, Senegal	314.3	90.36	26	0.628
0162 Bathurst/Yundum, Gambia	330.1	177.28	19	0.357

The yearly anomalies for the two month early rainfall are depicted in Fig. 9.12. These mean standard deviations were constructed using data for at least 16 of the 18 possible stations available. There is a noticeable trend to wet conditions during the 1920's and mid 1930's with drier years from the late 1930's to the 1940's. This variability is similar to what was observed in the entire June to September rainy season. Unfortunately, the large anomaly in 1933—extremely wet for the two months of June and July—is twice the magnitude of the next largest anomaly. This extreme event tends to obscure the statistical relationships based on linear correlation coefficients. Therefore, analysis are presented for both the entire 27 year data set as well as with the 1933 value removed. Ranked statistical tests are also utilized to minimize the outlier effect on the associations.

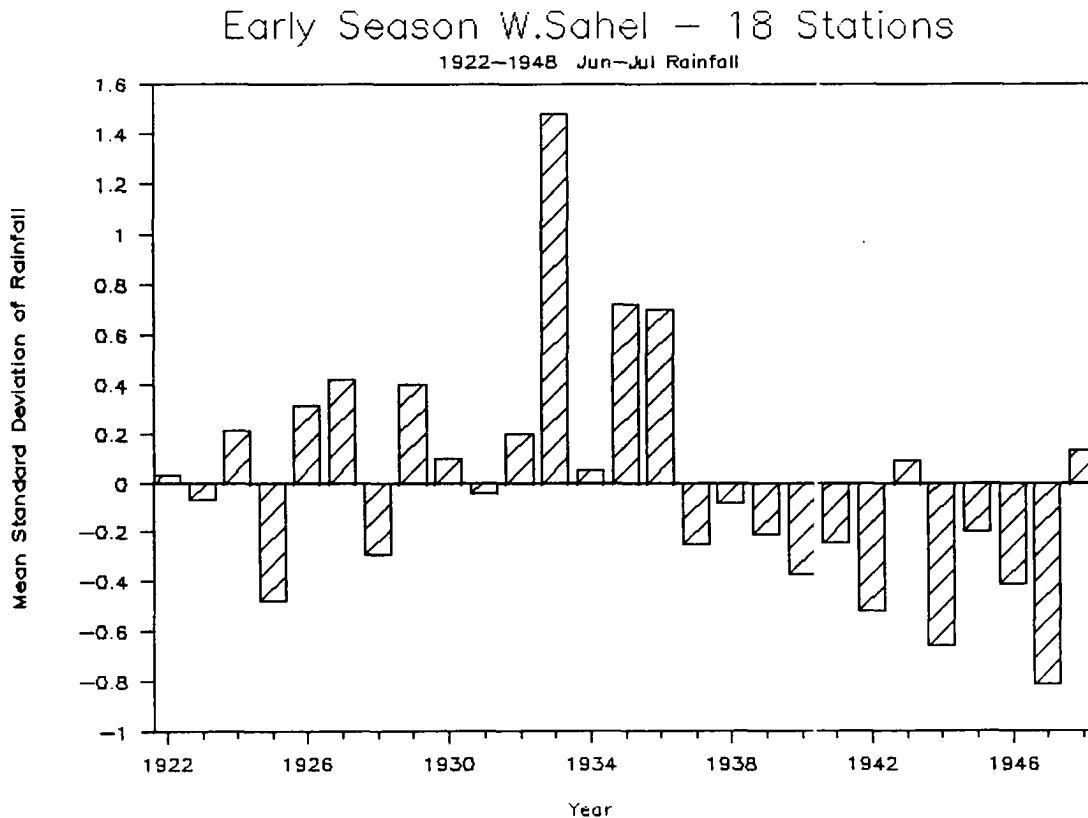


Figure 9.12: Rainfall anomalies expressed as mean standard deviations for the 18 station June to July Western Sahel Index of rainfall for the time period 1922 to 1948.

Table 9.12 compares the June and July Western Sahel Rainfall Index to US landfalling tropical cyclones during the earlier era. Once, again, there appears to be somewhat more

activity during the wet years than during the dry, but the differences are only marginally significant.

Table 9.12: Summary of the variability of U.S. landfalling tropical cyclones in the seven wettest and the seven driest June and July Western Sahel Rainfall Index from 1922 to 1948. (Asterisks refer to significance level: 0.100 for ‘*’, 0.025 for ‘**’ and 0.005 for ‘***’.)

Tropical Cyclones	Wettest Years' Mean	Percent (%) of Normal	Driest Years' Mean	Percent (%) of Normal	Ratio Wet/Dry
US Named Storms	3.7	102	3.9	107	0.95
US Hurricanes	2.4	133	2.0	110	1.20
US Intense Hurricanes	1.1	157	0.7	100	1.57
' ' Gulf Coast	0.6	200	0.1	33	6.00*
' ' East Coast	0.7	159	0.6	136	1.17

Figure 9.13 tests the inference that the early season rainfall is correlated with the primary August–September rainy season in the Sahel area. The figure shows a scatter plot analysis of the 18 station June and July Western Sahel rainfall versus the rainfall for the following August and September, using the same stations. The correlation between the two parameters, utilizing the entire data set, is a moderately strong $r = 0.22$ (significant to the 0.100 level). However, the relationship is enhanced by the removal of the outlier of 1933. With this data point removed, the correlation is increased to $r = 0.28$. Ranked correlation for the entire data set also confirm a moderately strong association $r = 0.30$. Thus this independent verification appears to provide some evidence that the relationship first uncovered by Bunting *et al.* in 1975 is stable and reliable.

The remaining relationship to be examined is the possible delayed feedback between the late year Gulf of Guinea area rainfall as the monsoon retreats southward with the rainfall in following year as the monsoon returns to the Sahel area during June and July. This relationship showed a value of $r = 0.51$ in the dependent (1949–89) data set. Figure 9.14 shows that for 1921–1948, the association is completely random with a correlation of nearly zero. However, removing the one large outlier from the analysis (i.e., 1932 Gulf of Guinea rainfall and 1933 Sahel rainfall) brings the correlation up to a significant (at three

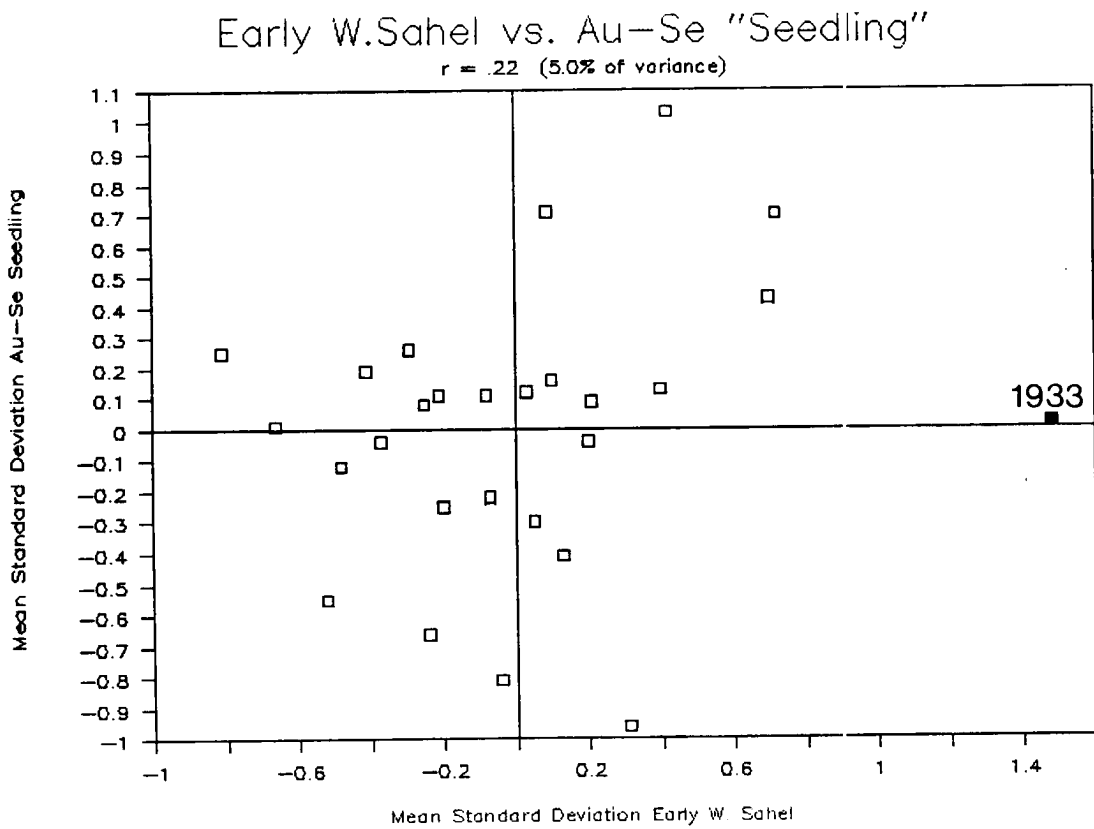


Figure 9.13: Scatter plot of Western Sahel June to July versus August to September Index rainfall anomalies for the years 1949 to 1989. The outlier value of 1933 is highlighted. The two indices correlate at $r = 0.22$.

0.100 level) $r = 0.28$. Additionally, a rank correlation of all the data provides a value of $r = 0.14$, possibly suggesting a confirmation of the positive association.

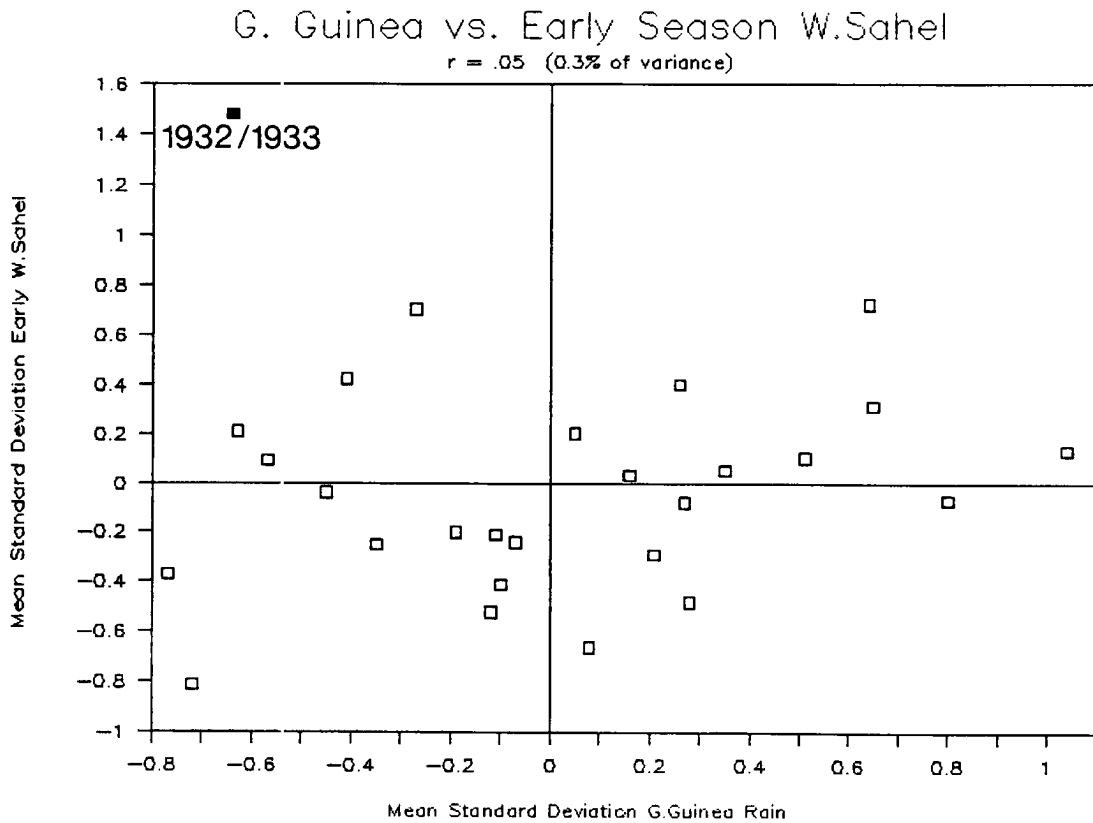


Figure 9.14: Scatter plot of August to November Gulf of Guinea Index rainfall anomalies (1921 to 1947) versus following year June to July Western Sahel Index rainfall anomalies (1922 to 1948). The outlier 1932/1933 data point is highlighted. The two indices correlate at $r = 0.05$.

Utilizing historic rainfall and tropical cyclone data sets, most of the conclusions reached in the dependent analysis have been supported in the independent data. The two relationships that could not be verified at all were the Gulf of Guinea late season rain with the subsequent June to September rainfall in the Sahel and the June to September Sahelian rainfall with tropical cyclone activity. Since there was a moderate association seen between the August to November Gulf of Guinea rainfall with the June to July Western Sahel rainfall, the lack of a signal with the entire rainy season must be due to a totally random association between the Gulf of Guinea late season rainfall with August and September Sahelian rain in the following year. This apparently is the case as the correlation (not shown) between the two is zero.

It is possible that since the 1940's, monsoon dynamics have altered so that the Gulf of Guinea rainfall in the previous year has played an increasing role in Sahel rainfall variations. Indeed, though a positive correlation is seen in the earlier time period Gulf of Guinea versus the June–July Sahel rainfall in the following year, it is weaker than that seen in the later time period ($r = 0.28$ versus $r = 0.51$). While some of this degradation can be attributed to differences in stations utilized, the loss of association must be due to some other additional source.

Another consideration is that the time period available for independent verification is only 27 years in length. This may be too short a record to provide enough variability for comparing wet and dry Sahel years versus hurricane activity. Indeed, to highlight any tropical cyclone differences in the rainfall regimes, the wettest quarter years are compared against the driest quarter years. This amounts to only seven versus seven years. Any outliers (such as the 1926 US landfalling hurricanes or the 1927 June to September Western Sahel rainfall) can obscure the longer term association.

However, additional research is currently attempting to study the hurricane–Sahel rainfall association back to 1899. This longer data set may provide enough independent data to permit adequate verification of the tropical cyclone–rainfall relationship.

Chapter 10

SUMMARY AND FUTURE RESEARCH POSSIBILITIES

Relationships between West African monsoonal rainfall and Atlantic basin tropical cyclones during the past four decades have been thoroughly examined. In regard to both intra and interannual variability of tropical cyclones, the most important differences occur for intense cyclones, the Saffir-Simpson category 3, 4, and 5 hurricanes. The incidence of these intense hurricanes has a more sharply peaked annual cycle than occurs for weaker tropical storms. Ninety-five percent of all intense hurricane activity occurs during the three months of August, September, and October. Although intense hurricanes, on average, strike the U.S. only twice in a three year period, they account for three-quarters of the tropical cyclone related damage and destruction.

Though not readily apparent in tropical storm and hurricane data, a large multi-decadal downward trend has occurred in both the number and duration of the most intense hurricanes. An earlier tendency to overestimate these hurricanes may have caused a portion of this observed trend, but as shown earlier, even with this bias removed, a strong decrease has occurred in recent years. The incidence of landfalling major hurricanes along the U.S. coastline during the last four decades has confirmed that the multidecadal variations in intense hurricane activity are real.

Gray (1987) made a substantiated connection between this downward trend in hurricane activity and variations of monsoon rainfall in Sahelian West Africa. This report was originally intended to simply document the relationships between seasonal tropical cyclone activity and West African rainfall. However, as research progressed, it became apparent that in addition to the expected concurrent Western Sahel-tropical cyclone relationship, important predictive signals were available in the rainfall data.

Two strong associations were observed that could serve as important forecasting tools for tropical cyclone activity. The first is a multimonth lag relation that appears in August to November rainfall along the Gulf of Guinea during the previous year. These months are in that portion of the annual rainfall cycle which experiences the ITCZ or monsoon trough passing southward as it retreats into the Southern Hemisphere. This monsoon retreat produces a second rainfall maxima south of 10°N during these months. This area is where the rainfall relationship to Sahel rainfall in the following year and to the following year's Atlantic basin tropical cyclones is strongest. Thus, there appears to be some form of positive feedback process linking the retreating monsoon to its onset during the following year.

The second finding was not as revolutionary in that Bunting *et al.* (1975) had confirmed the same phenomena 16 years ago; specifically, that early June–July rainfall in the Sahel can be used to forecast rainfall during the remainder of the season. For practical purposes, Bunting's scheme was not very useful because knowledge of the strength of the monsoon was not available until early August, well into the rainy season. Glantz (1977) suspects that even a forecast with a one year lead time could not be utilized by the inhabitants of the Sahel owing to a lack of resources and political instability in the affected area. However, in application to Atlantic basin tropical cyclones, especially intense hurricanes, this information proves to be a very useful excellent forecast of the seasonal amount of activity.

Figure 10.1 illustrates the idealized view of the predictive relationships uncovered in this research. The top panel illustrates the precursor signals seen in 'active' hurricane seasons. These are: abundant rainfall during August to November of the previous year along the Gulf of Guinea and during June and July in the Western Sahel. This is contrasted to 'calm' (with respect to intense hurricane activity) seasons: deficient rainfall amounts in the same locations.

Though these conclusions about potential forecast skill are verified in four decades of data, it is important to try to determine the physical mechanisms behind these as-

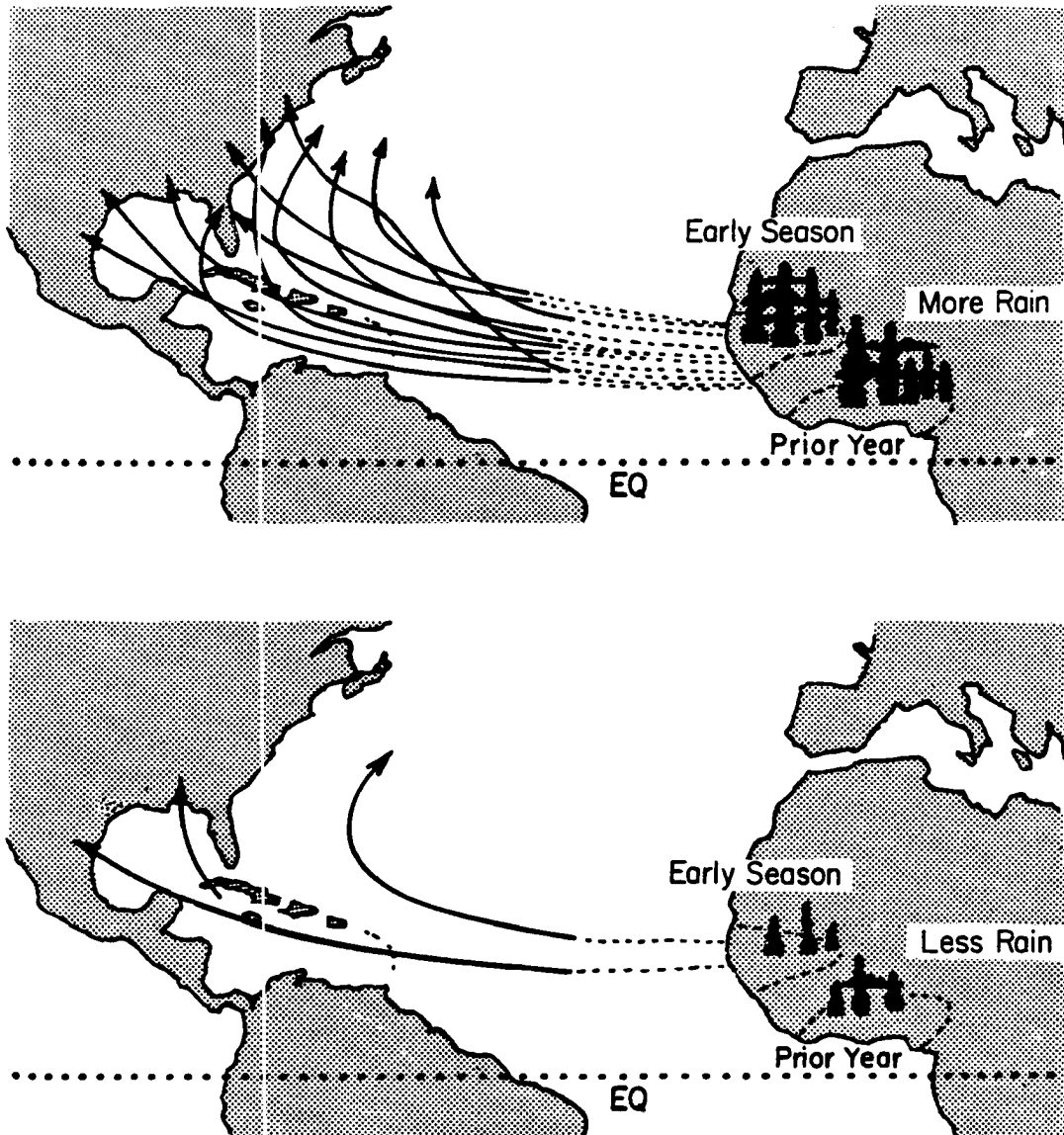


Figure 10.1: Idealized illustration of the differences in composite intense hurricane tracks during three years of high Early Season Combination Index rainfall amounts (upper panel) in contrast to a similar period of low rainfall amounts (bottom panel).

sociations. What physical processes are responsible for these rainfall–hurricane lag relationships? One basic assumption is that the predictive signals (the previous year Gulf of Guinea rainfall and the early season Western Sahel rainfall) are only indirectly related to hurricane activity; that they do not physically affect the tropical cyclone directly. Instead, these rainfall anomalies before 1 August are likely to be directly related to the later, primary rainy season in the Western Sahel.

The conditions associated with monsoon rainfall anomalies in August and September are believed to have a direct influence upon seasonal hurricane activity. As Kidson (1977) pointed out, dry years in the Sahel are accompanied by a weaker 200 mb easterly jet. This condition is complemented by the relationship, shown in Chapter 5, that Sahel rainfall has a rather strong negative correlation with 200 mb zonal wind anomalies in the Caribbean basin. Figure 10.2 depicts an idealized portrayal of the resulting 200 mb flow over the Atlantic basin in wet versus dry Sahel conditions. Vertical shear associated with upper tropospheric westerlies has long been known to inhibit tropical cyclone genesis and intensification (e.g., Gray, 1968).

Another plausible effect of the Western Sahel monsoon variations on tropical cyclone activity is through the modification of African–spawned easterly waves. These waves were shown by Riehl (1945) to act as the ‘seedling’ circulations for some tropical storms and hurricanes in the Atlantic basin. In that almost 90% of all intense hurricanes originate from easterly waves, it is not surprising that an association exists with African rainfall.

Since it has now been established that dry years in the Sahel correspond to inactive hurricane seasons, it is possible that: 1) the number of easterly waves per year is decreased (as suggested by Druryan, 1989), 2) that the mean latitude along which the waves travel westward is altered, or 3) that the amplitudes of the waves are diminished (also as suggested by Druryan). The first hypothesis appears not to be valid. Avila and Clark (1989) have shown that the number of waves originating over Africa is very stable. Yearly averages of 58 waves with a standard deviation of only 5 waves are observed. The second hypothesis is possible but not likely to affect tropical cyclone numbers and strengths unless

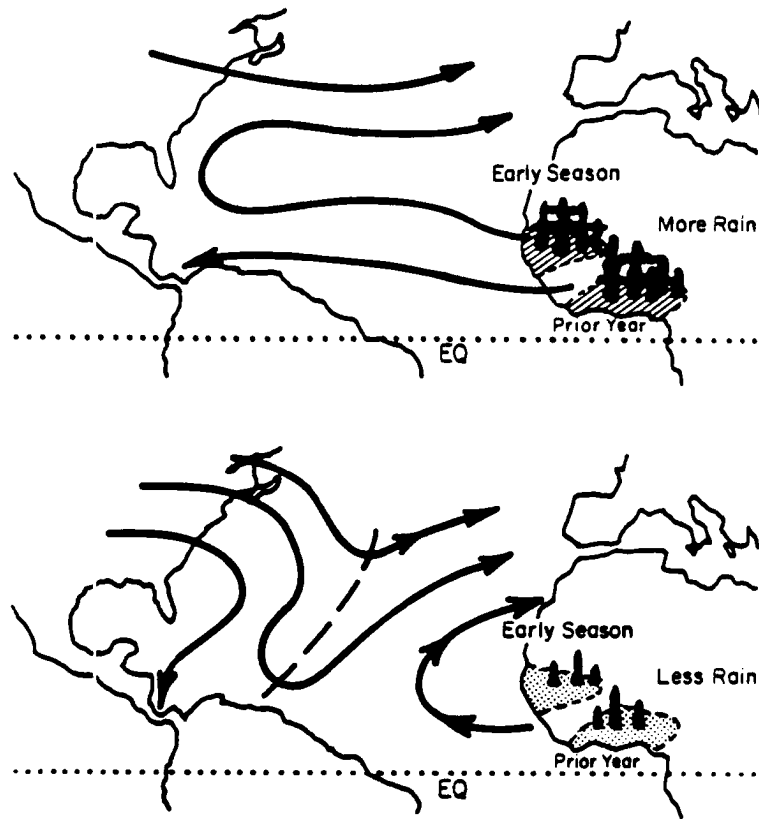


Figure 10.2: Idealized depiction of the 200 mb flow over the Atlantic basin during a year of abundant Western Sahel rainfall (upper panel) in contrast to a year of deficient rainfall (bottom panel).

the mean latitude is altered substantially. Personal communication from R. Zehr and L. Avila suggest that this does not occur.

Thus, the third hypothesis is the one needing most consideration. Figure 10.3 gives an idealized illustration of the variable strength of the easterly waves which propagate out of West Africa. It is suggested that in wet Western Sahel years (June to September) a number of easterly waves emanating from Africa have more concentrated convection and better internal organization (reflected in the streamlines at 700 m.b and surface pressure). In dry years, comparatively fewer easterly waves would show these properties.

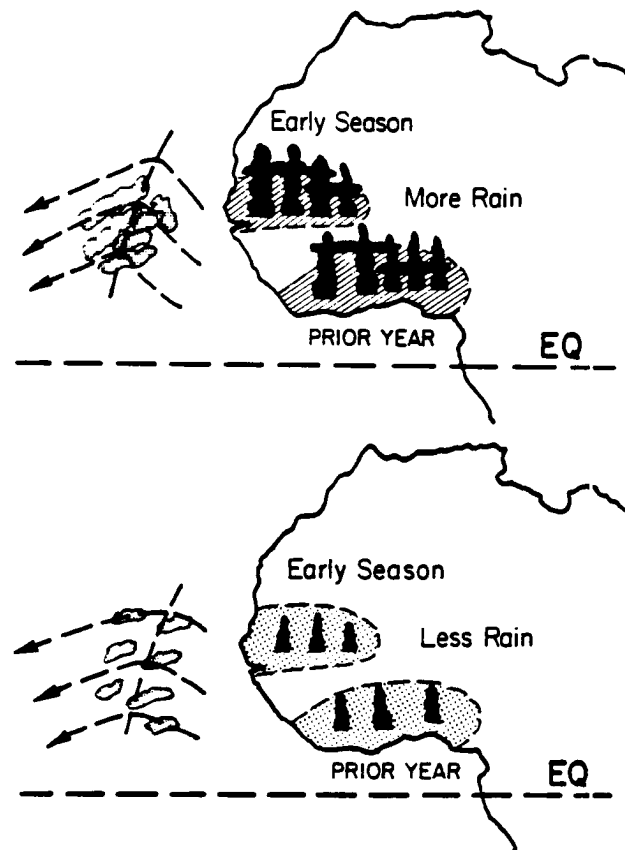


Figure 10.3: Idealized portrayal of the easterly wave variations that are suggested to occur when the Early Season Combination rainfall is above average (upper figure) and when the rainfall is below normal (bottom figure).

As the waves with their embedded squall lines are the major contributors to the monsoon rainfall, do weaker easterly waves cause the Sahel drought or, are weaker easterly

waves a result of the drought conditions? Perhaps there is a feedback between the two and no clear cause and effect. This question remains unanswered.

If changes in tropospheric vertical wind shear and easterly waves are the key to the rainfall–hurricane relationship, what accounts for the association between the various rainfall regimes? Specifically, what relates previous year August to November Gulf of Guinea (approximately 5 to 10°N) rainfall to the June to September Western Sahel (approximately 11 to 20°N) rainfall? Secondly, why do the early rain months of June and July in the Western Sahel relate so well to the following months of August and September?

It is suggested that the rainfall anomalies which occur along the Gulf of Guinea as the monsoon is retreating modulate anomalous storage of moisture either in the biosphere or as soil moisture. Excess moisture would then be available to be reincorporated as water vapor from evapotranspiration and evaporation when the monsoon returns the following summer. Thus, the late season Gulf of Guinea rainfall, if it is below normal, provides lower than normal moisture storage and less water vapor becomes available for the monsoon to be utilized as rainfall over the Sahel. Abundant rainfall along the Gulf of Guinea would lead to more storage than normal and then more water vapor flux into the monsoon in the following year.

Note that this concept does not account for the long term trends in the Sahel rainfall. In fact, as was shown, removal of the downward trend actually improved the correlation between the Gulf of Guinea and Western Sahel rainfall. It is very possible then that while another mechanism (e.g. global SST anomalies) is responsible for the large multidecadal downward trend, that Gulf of Guinea rain anomalies may account for much of these year to year variations. Although Nicholson (1981, 1986) has observed that decreased rainfall can occur throughout the entire West Africa subcontinent in some years, there are just as many years when the Gulf of Guinea region has a rainfall anomaly opposite that of the Sahel. It is the Gulf of Guinea's rainfall anomaly for the August to November period which provides a predictive signal that can account for about 40% of the variance in the following year's Western Sahel rainfall.

This physical explanation has some support in the literature. Oglesby and Erickson (1989) have shown the importance of soil moisture in modulating drought over the North American continent using the NCAR Community Climate Model. While the mechanisms of rain producing systems are much different from those over the Sahel, their results are likely to be applicable wherever land evaporation plays a significant role (10–30%) in comparison to water vapor advection in the formation of rainfall. Druyan and Koster (1989) present results from runs utilizing the Goddard Institute for Space Studies Climate Model II that also stress “the importance of recycling continental evaporate” in the production of Sahel precipitation.

The second hypothesis that the June and July Sahel rainfall influences the later month (August to September) rainfall in the same location, has already been shown in the study by Bunting *et al.* (1975). Their explanation of this association was that the early season rainfall (wet or dry) led to a “persistence” of conditions. This author agrees with the previous study but expands upon the idea.

The June-July to August-September rainfall association appears to be the result of two influences. The first is the more local effect of June and July Sahel precipitation feeding back onto short term future rainfall. This June-July rainfall is reincorporated back into the monsoon circulation as evaporate. The early rainfall has a large component that evaporates, in addition to being stored as soil moisture or advected away in river run off. This concept is supported by some early modeling work by Walker and Rowntree (1977) and by the more recent work by Rowell and Blondin (1990) who utilized the European Centre for Medium Range Weather Forecasts (ECMWF) operational forecasting model to study the effects of varying soil moisture on short term precipitation in the Sahel. Figure 10.4 shows a schematic of the two separate regions (Gulf of Guinea and Western Sahel) where the moisture flux is contributed to by anomalous amounts of evaporation and evapotranspiration.

The other “persistent” factor is that of the general strength and location of the monsoon circulation. Features that modulate the total convergence and rainfall in the

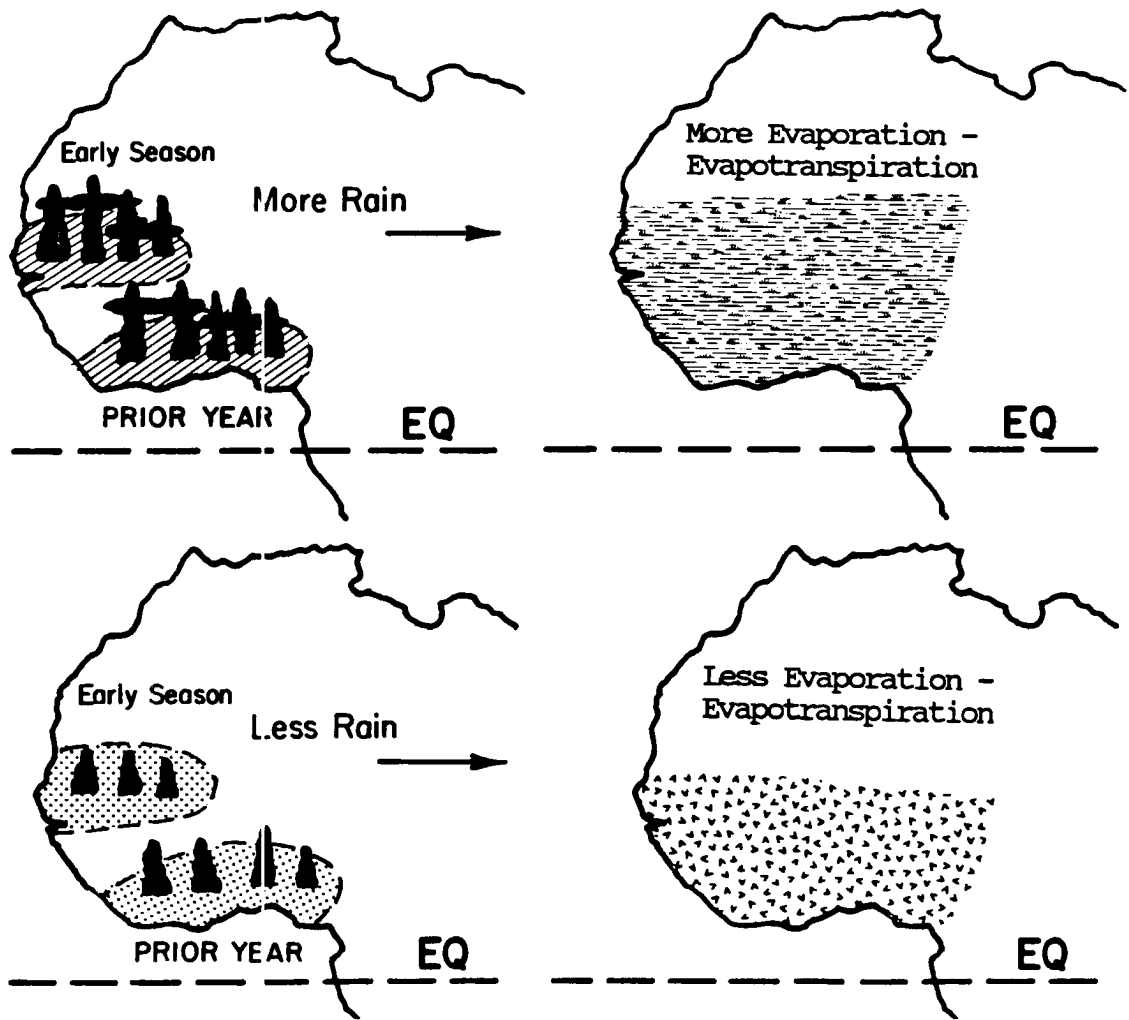


Figure 10.4: Schematic depicting the two regions where the monsoonal moisture flux is supplemented by anomalous evaporation and evapotranspiration induced by anomalous amounts of rainfall.

ITCZ (i.e. the intensity of the Hadley circulation) and the mean latitude of the monsoon trough are likely to be fairly persistent, once established. These features, besides the local effects of land surface moisture flux, have been suggested by Larib (1978a, 1978b) to be conditions of the Atlantic SST field. Researchers at the UK Met Office and at ECMWF have also identified global oceanic SST anomalies (Pacific, Indian as well as the Atlantic Ocean basins) that are associated with the modulating of Sahel rainfall (e.g. Folland *et al.* (1986) and Palmer (1986)).

Thus, while plausible physical explanations are presented, there is a great need to continue research in this area. This is especially true with regard to the recent discussion of the influences of Greenhouse Gas warming on tropical cyclone activity. The American Meteorological Society and the University Corporation for Atmospheric Research issued a joint statement (AMS Council and UCAR Board of Trustees, 1988) suggesting that a potential Greenhouse Gas impact was “a higher frequency and greater intensity of hurricanes.” Recent devastating storms with Hurricane Gilbert in 1988—the strongest storm ever measured in the western hemisphere (Willoughby *et al.*, 1989) and Hurricane Hugo in 1989—“the most costly hurricane in U.S. history” (Case and Mayfield, 1990) have only raised concerns higher.

This research, however, shows that the modulation of the intense hurricane activity in the Atlantic basin is codependent upon rainfall conditions in the Sahel. What is desired is additional work that will help clarify physical explanations for the statistical associations uncovered. Proposed research that should be undertaken include:

1. An examination of surface meteorological parameters (land/sea temperatures, sea level pressure, and zonal/meridional winds) and upper air data (zonal/meridional winds and height gradients) to specify conditions accompanying dry/calm years versus wet/active years. Special efforts would be made to identify predictive signals, particularly in the sea surface temperature data, for the tropical cyclones and the West African monsoon.

2. Analysis of interseasonal differences in spectral reflectance data from the NOAA-7 satellite's Advanced Very High Resolution Radiometer (AVHRR) will help assess the theory that there is a feedback from the Gulf of Guinea region rainfall into the biosphere. The AVHRR data has been applied to land-cover classification and monitoring of vegetative dynamics since NOAA-7's launch in 1982.
3. Utilizing the general circulation regimes identified with wet/active and dry/calm periods, effects on the amplification of easterly waves into tropical cyclones would be tested within a numerical model framework.

Thus a general framework of future research is mapped out using a variety of conventional observations, satellite data, and numerical modeling results that would bring a much greater understanding to the seasonal fluctuations of Atlantic basin tropical cyclone activity and Sahel rainfall.

It is essential that this knowledge be obtained so that residents of the Atlantic basin can better prepare for a return of the intense hurricane when, not if, the Sahel again experiences abundant rainfall. As Nicholson (1989) pointed out, there appears to have been many periods in the historical record wherein the Sahel experienced extreme drought (analogous to the current dryness), but then recovered to pre-drought conditions. While an extension of the current drought for several more decades is within the realm of possibilities, all prior severe dry periods in the past 3000 years had maximum durations of a few decades. Therefore, unless a major climatic change has taken place, the Sahel should be expected to return to near or above normal seasonal rainfall amounts in the not too distant future. Results from Chapter 5 suggest that if the switch to a wet regime in the Sahel does take place, the Atlantic basin, especially the Caribbean Islands and the U.S. East Coast/Florida, would likely experience four to five times as many intense hurricanes as have occurred over the last two decades.

The physical mechanisms of this surprising monsoon-tropical cyclone association are also needed before meaningful extrapolations can be made of Greenhouse warming effects on hurricane activity. Too much uncertainty exists as to the physical mechanism which

have governed the past variations of intense hurricane activity. We must first understand the past before we speculate on future changes.

ACKNOWLEDGEMENTS

The author is grateful for the African rainfall and Atlantic basin tropical data that has been supplied to our project for this research. These include the monthly rainfall data set from William Spangler and Roy Jenne of NCAR who incorporated the extensive collection originally compiled by Sharon Nicholson of Florida State University; Graham Farmer of the WMO's AID/Fews Project, Peter Lamb of the Illinois State Water Survey; Douglas Le Compte of the U.S. AID program; Dave Miskus and Richard Tinker of CAC; and E. Olukayode Oladipo of Ahmadu Bello University of Nigeria. Tropical cyclone data have been provided us through Colin McAdie, Lixion Avila, Harold Gerrish, Miles Lawrence, and Max Mayfield of the NHC.

The author had the privilege of attending the WMO's Symposium on "Meteorological Aspects of Tropical Droughts with Emphasis on Long-Range Forecasting" at Niamey, Niger in the spring of 1990. While there, I had many excellent discussions of the Sahel rainfall-tropical cyclone association with Stefan Hastenrath, Robert Livezey, Peter Lamb, Randy Pepler, Birama Diarra, Graham Farmer, Kevin Lane, Neal Ward, Yinka Adebayo, M.V. Sivakumar, Peter Hutchinson, Leonard Druyan, and Tim Palmer. My time was well spent as I gained a greater appreciation of the severity of Sahelian drought conditions, as well as for the people attempting to solve the mysteries of long term droughts. It was truly a wonderful experience.

Much valuable computer programming expertise was contributed by project members, Richard Taft, William Thorson, and Todd Massey. Barbara Brumit, Laneigh Walters, and Judy Sorbie-Dunn have provided important manuscript, data analysis, and figure drafting assistance. Additional valuable discussions were had with Professors Wayne Schubert, Roger Pielke, Duane Stevens, Dave Randall, Kenneth Berry, Paul Mielke and Edward

Prill; with Research Associates Paul Ciesielski and John Sheaffer (who also offered a detailed and helpful review of the manuscript); and with fellow Gray project students Steve Hodanish, Ray Zehr, Dan Mundell, Steve Hallin, John Knaff, and Mike Fitzpatrick here at CSU. Lloyd Shapiro and Stan Goldenberg at the Hurricane Research Division of NOAA also provided excellent suggestions and advice.

But most of all, thanks go out to my advisor, William Gray who proposed this research topic. His boundless enthusiasm for the seasonal predictability problem (actually for the entire field of tropical meteorology) has been the key to success for this project. He has taught me that much can still be learned in meteorology from an inquisitive and curious eye into the observations. May he always have legal pads and number two pencils to doodle with.

This research has been supported by the National Science Foundation Grant No. ATM-8814373 with supplementary support of the NOAA Climate Research Program Grant No. NA16RCO116-01 and the Office of the Federal Coordinator Grant No. NOAA NA85RAH05045 AMEND 2.

REFERENCES

- AMS Council and UCAR Board of Trustees, 1988: The changing atmosphere—challenges and opportunities. *Bull. Amer. Met. Soc.*, 69, 1434-1440.
- Avila, L. A., 1990: Atlantic tropical systems of 1989. *Mon. Wea. Rev.*, 118, 1178-1185.
- Avila, L. A. and G. B. Clark, 1989: Atlantic tropical systems of 1988. *Mon. Wea. Rev.*, 117, 2260-2265.
- Ballenzweig, E. M., 1959: Relation of long-period circulation anomalies to tropical storm formation and motion. *J. Meteor.*, 16, 121-139.
- Bunting, A. H., M. D. Dennett, J. Elston, and J. R. Milford, 1975: Seasonal rainfall forecasting in West Africa. *Nature*, 253, 622-623.
- Carlson, T. N. and J. D. Lee, 1978: Tropical Meteorology. Pennsylvania State University, Independent Study by Correspondence, University Park, Pennsylvania, 387 pp.
- Case, R. A., 1986: Atlantic hurricane season of 1985. *Mon. Wea. Rev.*, 114, 1390-1405.
- Case, R. A. and H. P. Gerrish, 1984: Atlantic hurricane season of 1983. *Mon. Wea. Rev.*, 112, 1083-1092.
- Case, R. A. and H. P. Gerrish, 1988: Atlantic hurricane season of 1987. *Mon. Wea. Rev.*, 116, 939-949.
- Case, R. A. and M. Mayfield, 1990: Atlantic hurricane season of 1989. *Mon. Wea. Rev.*, 118, 1165-1177.
- Clark, G. B., 1983: Atlantic hurricane season of 1982. *Mon. Wea. Rev.*, 111, 1071-1079.
- Davis, W. R., 1954: Hurricanes of 1954. *Mon. Wea. Rev.*, 82, 370-373.
- Druyan, L. M., 1989: Advances in the study of Subsaharan drought. *Int. J. Clim.*, 9, 77-90.
- Druyan, L. M. and R. D. Koster, 1989: Sources of Sahel precipitation for simulated drought and rainy seasons. *J. Climate*, 2, 1438-1446.
- Dunn, G. E., 1961: The hurricane season of 1960. *Mon. Wea. Rev.*, 89, 99-108.
- Dunn, G.E., W. R. Davis and P. L. Moore, 1955: Hurricanes of 1955. *Mon. Wea. Rev.*, 83, 315-326.

- Dunn, G. E., W. R. Davis and P. L. Moore, 1956: Hurricane season of 1956. *Mon. Wea. Rev.*, 84, 436-443.
- Dunn, G. E. and Staff, 1959: The hurricane season of 1959. *Mon. Wea. Rev.*, 87, 441-450.
- Dunn, G. E. and Staff, 1962: The hurricane season of 1961. *Mon. Wea. Rev.*, 90, 107-119.
- Dunn, G. E. and Staff, 1963: The hurricane season of 1962. *Mon. Wea. Rev.*, 91, 199-207.
- Dunn, G. E. and Staff, 1964: The hurricane season of 1963. *Mon. Wea. Rev.*, 92, 128-138.
- Dunn, G. E. and Staff, 1965: The hurricane season of 1964. *Mon. Wea. Rev.*, 93, 175-187.
- Dvorak, V. F., 1977: Tropical cyclone intensity analysis and forecasting from satellite imagery. *Mon. Wea. Rev.*, 103, 420-430.
- Dvorak, V. F., 1984: Tropical cyclone intensity analysis using satellite data. NOAA Technical Report NESDIS 11, U.S. Dept. of Comm., Washington, DC, 47 pp.
- Folland, C. K., T. N. Palmer and D. E. Parker, 1986: Sahel rainfall and worldwide sea temperatures, 1901-1985. *Nature*, 320, 602-607.
- Garriott, E. B., 1906: The West Indian hurricanes of September, 1906. *Mon. Wea. Rev.*, 34, 416-423.
- Glantz, M., 1977: The value of a long-range weather forecast for the West African Sahel. *Bull. Amer. Meteor. Soc.*, 58, 150-158.
- Gray, W. M., 1968: Global View of the Origin of Tropical Disturbances and Storms. *Mon. Wea. Rev.*, 96, 669-700.
- Gray, W. M., 1975: Tropical cyclone genesis. Dept. of Atmos. Sci. Paper No. 234, Colo. State Univ., Ft. Collins, CO, 121 pp.
- Gray, W. M., 1981: Recent advances in tropical cyclone research from rawinsonde composite analysis. World Meteorological Organization, Geneva, 407 pp.
- Gray, W. M., 1984a: Forecast of Atlantic seasonal hurricane activity for 1984. Colo. State Univ., Dept. of Atmos. Sci. Paper issued on 24 May 1984 Fort Collins, CO 80523, 34 pp.
- Gray, W. M., 1984b: Updated (as of 30 July 1984) Forecast of Atlantic Seasonal Hurricane Activity for 1984, Colo. State Univ. Dept. of Atmos. Sci. Paper, Fort Collins, CO 80523, 8 pp.
- Gray, W. M., 1984c: Atlantic seasonal hurricane frequency. Part I: El Niño and 30mb Quasi-Biennial Oscillation influences. *Mon. Wea. Rev.*, 112, 1649-1668.
- Gray, W. M., 1984d: Atlantic seasonal hurricane frequency. Part II: forecasting its variability. *Mon. Wea. Rev.*, 112, 1669-1683.
- Gray, W. M., 1987: Cyclic trends in hurricane destruction potential and discussion of factors which will be used in the 1987 seasonal forecast. 9th National Hurricane Conference, Orlando, FL, 3 April 1987, 29 pp.

- Gray, W. M., 1988a: Environmental influences on tropical cyclones. *Aust. Met. Mag.*, 36, 127-139.
- Gray, W. M., 1988b: Summary of 1988 Atlantic tropical cyclone activity and verification of author's seasonal forecast. Colo. State Univ., Dept. of Atmos. Sci. Paper issued on 28 November 1988, Fort Collins, CO 80523, 49 pp.
- Gray, W. M., 1989a: Background information for assessment of expected Atlantic hurricane activity for 1989. 11th National Hurricane Conference, Miami, FL, 7 April 1989, 41 pp.
- Gray, W. M., 1989b: Forecast of Atlantic seasonal hurricane activity for 1989. Colo. State Univ., Dept. of Atmos. Sci. Paper issued on 26 May 1989, Fort Collins, CO 80523, 41 pp.
- Gray, W. M., 1989c: Updated (as of 27 July 1989) forecast of Atlantic seasonal hurricane activity for 1989. Colo. State Univ., Dept. of Atmos. Sci. Paper, Fort Collins, CO 80523, 44 pp.
- Gray, W. M., 1989d: Summary of 1989 Atlantic tropical cyclone activity and seasonal forecast verification. Colo. State Univ., Dept. of Atmos. Sci. Paper issued on 20 November 1989, Fort Collins, CO 80523, 37 pp.
- Gray, W. M., 1990a: Forecast of Atlantic seasonal hurricane activity for 1990. Colo. State Univ., Dept. of Atmos. Sci. Paper issued on 5 June 1990, Fort Collins, CO 80523, 15 pp.
- Gray, W. M., 1990b: Updated forecast of Atlantic seasonal hurricane activity for 1990. Colo. State Univ., Dept. of Atmos. Sci. Paper issued on 3 August 1990, Fort Collins, CO 80523, 15 pp.
- Gray, W. M., 1990c: Strong association between West African rainfall and U.S. landfall of intense hurricanes. *Science*, 249, 1251-1256.
- Gray, W. M., 1990d: Summary of 1990 Atlantic tropical cyclone activity and seasonal forecast verification. Colo. State Univ., Dept. of Atmos. Sci. Paper issued on 28 November 1990, Fort Collins, CO 80523, 29 pp.
- Hastenrath, S., 1988: *Climate and Circulation of the Tropics*. Reidel, Dordrecht, Boston, Lancaster, Tokyo, Second Printing, 455 pp.
- Hastenrath, S., 1990: The relationship of highly reflective clouds to tropical climate anomalies. *J. Climate*, 3, 353-365.
- Hayward, D. F. and J. S. Oguntoyinbo, 1987: *The climatology of West Africa*. Barnes and Noble Books, Totowa, New Jersey, 217 pp.
- Hebert, P. J., 1976: Atlantic hurricane season of 1975. *Mon. Wea. Rev.*, 104, 453-465.
- Hebert, P. J., 1980: Atlantic hurricane season of 1979. *Mon. Wea. Rev.*, 106, 973-990.
- Hebert, P. J. and R. A. Case, 1990: The deadliest, costliest, and most intense United States hurricanes of this century (and other frequently requested hurricane facts). NOAA Technical Memorandum NWS NHC 31, Miami, FL, 31 pp.

- Hebert, P. J. and N. L. Frank, 1974: Atlantic hurricane season of 1973. *Mon. Wea. Rev.*, 102, 280-289.
- Hebert, P. J. and K. O. Poteat, 1975: A satellite classification technique for subtropical cyclones. NOAA Technical Memorandum NWS SR-83, Fort Worth, TX., 25 pp.
- Hebert, P. J. and G. Taylor, 1975: Hurricane experience levels of coastal county populations—Texas to Maine. Special Report, National Weather Service Community Preparedness Staff and Southern Region, 153 pp.
- Hope, J. R., 1975: Atlantic hurricane season of 1974. *Mon. Wea. Rev.*, 103, 285-293.
- Jarrell, J. D., 1987: *Impact of tropical cyclones (Chapter 5), A global view of tropical cyclones*. Edited by R.L. Elsberry, Office of Naval Research, 133-146.
- Jarvinen, B. R., C. J. Neumann and M. A. S. Davis, 1984: A tropical cyclone data tape for the North Atlantic basin, 1886-1983: Contents, limitations, and uses. NOAA Technical Memorandum NWS NHC 22, Miami, FL, 21 pp.
- Kraft, R. H., 1961: The hurricane's central pressure and highest wind. *Mar. Wea. Log*, 5, 155.
- Kraus, E. B., 1977: Subtropical droughts and cross-equatorial transports. *Mon. Wea. Rev.*, 105, 1009-1018.
- Lamb, P. J., 1978a: Case studies of tropical Atlantic surface circulation patterns during recent Subsaharan weather anomalies: 1967 and 1968. *Mon. Wea. Rev.*, 106, 482-491.
- Lamb, P. J., 1978b: Large-scale tropical Atlantic surface circulation patterns associated with Subsaharan weather anomalies. *Tellus*, 30, 240-251.
- Lamb, P. J., 1982: Persistence of Subsaharan drought. *Nature*, 299, 46-48.
- Lamb, P. J., 1985: Rainfall in Subsaharan West Africa during 1941-83. *Zeitschrift fur Gletscherkunde und Glazialgeologie*, 21, 131-139.
- Lamb, P. J., C. F. Ropelewski and D. H. Portis, 1990: Real-time monitoring of Subsaharan rainy season. Extended Abstracts of Papers Presented at the Third WMO Symposium on Meteorological Aspects of Tropical Droughts with Emphasis on Long-Range Forecasting, WMO/TD - No. 353, 163-166.
- Lawrence, M. B., 1977: Atlantic hurricane season of 1976. *Mon. Wea. Rev.*, 105, 497-507.
- Lawrence, M. B., 1978: Atlantic hurricane season of 1977. *Mon. Wea. Rev.*, 106, 534-545.
- Lawrence, M. B., 1979: Atlantic hurricane season of 1978. *Mon. Wea. Rev.*, 107, 477-491.
- Lawrence, M. B., 1987: Atlantic hurricane season of 1986. *Mon. Wea. Rev.*, 115, 2155-2160.
- Lawrence, M. B. and G. B. Clark 1985: Atlantic hurricane season of 1984. *Mon. Wea. Rev.*, 113, 1228-1237.

- Lawrence, M. B. and J. M. Gross, 1989: Atlantic hurricane season of 1988. *Mon. Wea. Rev.*, 117, 2248-2259.
- Lawrence, M. B. and J. M. Pelissier, 1981: Atlantic hurricane season of 1980. *Mon. Wea. Rev.*, 109, 1567-1582.
- Lawrence, M. B. and J. M. Pelissier, 1982: Atlantic hurricane season of 1981. *Mon. Wea. Rev.*, 110, 852-866.
- Moore, P. L. and Staff, 1957: The hurricane season of 1957. *Mon. Wea. Rev.*, 85, 401-408.
- Namias, J., 1955: Secular fluctuations in vulnerability to tropical cyclones in and off New England. *Mon. Wea. Rev.*, 83, 155-162.
- Neumann, C. J., B. E. Jarvinen, A. C. Pike and J. D. Elms, 1987: Tropical cyclones of the North Atlantic Ocean, 1871-1986. National Climatic Data Center in cooperation with the National Hurricane Center, Coral Gables, FL 186 pp.
- Nicholson, S. E., 1979: Revised rainfall series for the West African subtropics. *Mon. Wea. Rev.*, 107, 620-623.
- Nicholson, S. E., 1981: Rainfall and atmospheric circulation during drought and wetter periods in West Africa. *Mon. Wea. Rev.*, 109, 2191-2208.
- Nicholson, S. E., 1983: The spatial coherence of African rainfall anomalies: Interhemispheric teleconnections. *J. Climat. Appl. Meteor.*, 25, 1365-1381.
- Nicholson, S. E., 1986: Long-term changes in African rainfall. *Weather*, 44, 46-56.
- Norton, G., 1951: Hurricanes of the 1950 season. *Mon. Wea. Rev.*, 79, 8-15.
- Norton, G., 1952: Hurricanes of 1951. *Mon. Wea. Rev.*, 80, 1-4.
- Norton, G., 1953a: Hurricanes of 1952. *Mon. Wea. Rev.*, 81, 12-15.
- Norton, G., 1953b: Hurricanes of 1953. *Mon. Wea. Rev.*, 81, 388-391.
- Oglesby, R. J. and D. J. Erickson, III, 1989: Soil moisture and the persistence of North American drought. *J. Climate*, 2, 1362-1380.
- Palmer, T. N., 1986: Influence of the Atlantic, Pacific, and Indian Oceans on Sahel rainfall. *Nature*, 322, 251-253.
- Quinn, W. H., D. O. Zopf, K. S. Short and R. T. W. Kuo Yang, 1978: Historical trends and statistics of the Southern Oscillation, El Niño, and Indonesian droughts. *Fish. Bull.*, 76, 663-678.
- Ray, C. L., 1935: Relation of tropical cyclone frequency to summer pressures and ocean surface-water temperatures. *Mon. Wea. Rev.*, 63, 10-12.
- Riehl, H., 1945: Waves in the easterlies and the polar front in the tropics. Misc. Rept., No. 17, Dept. Meteorology, University of Chicago, 79 pp.

- Rowell, D. P. and C. Blondin, 1990: The influence of soil wetness distribution on short-range rainfall forecasting in the West African Sahel. *Quart. J. Roy. Meteor. Soc.*, 116, 1471-1485.
- Shapiro, L. J., 1982: Hurricane climate fluctuations. Part II: Relation to large-scale circulation. *Mon. Wea. Rev.*, 110, 1014-1023.
- Shapiro, L. J., 1989: The relationship of the quasi-biennial oscillation to Atlantic tropical storm activity. *Mon. Wea. Rev.*, 117, 1545-1552.
- Shinoda, M., 1989: Annual rainfall variability and its interhemispheric coherence in the semi-arid region of tropical Africa: Data updated to 1987. *J. Meteor. Soc. Japan*, 67, 555-564.
- Simpson, R. H., 1974: The hurricane disaster potential scale. *Weatherwise*, 27, 169-186.
- Simpson, R. H., N. Frank, D. Shideler and H. M. Johnson, 1968: Atlantic tropical disturbances, 1967. *Mon. Wea. Rev.*, 96, 251-259.
- Simpson, R.H. and P. J. Hebert, 1973: Atlantic hurricane season of 1972. *Mon. Wea. Rev.*, 101, 323-333.
- Simpson, R. H. and J. R. Hope, 1972: Atlantic hurricane season of 1971. *Mon. Wea. Rev.*, 100, 257-267.
- Simpson, R. H. and J. M. Pelissier, 1971: Atlantic hurricane season of 1970. *Mon. Wea. Rev.*, 99, 269-277.
- Simpson, R. H., A. L. Sugg, and Staff, 1970: The Atlantic hurricane season of 1969. *Mon. Wea. Rev.*, 98, 293-306.
- Spiegler, D. B., 1971: The unnamed Atlantic tropical storms of 1970. *Mon. Wea. Rev.*, 99, 966-976.
- Spiegel, M. R., 1988: *Statistics-Schaums Outline Series*. Second Edition, McGraw-Hill, Inc., New York, NY, 504 pp.
- Spiegler, D. B., 1972: Cyclone categories and definitions: Some proposed revisions. *Bull. Amer. Meteor. Soc.*, 53, 1174-1178.
- Staff—USWB, 1958: The hurricane season of 1958. *Mon. Wea. Rev.*, 86, 477-485.
- Sugg, A. L., 1966: The hurricane season of 1965. *Mon. Wea. Rev.*, 94, 183-191.
- Sugg, A. L., 1967: The hurricane season of 1966. *Mon. Wea. Rev.*, 95, 131-142.
- Sugg, A. L. and P. J. Hebert, 1969: The Atlantic hurricane season of 1968. *Mon. Wea. Rev.*, 97, 225-239.
- Sugg, A. L. and J. M. Pelissier, 1968: The hurricane season of 1967. *Mon. Wea. Rev.*, 96, 242-250.
- US Department of Commerce, USWB, 1959: World Weather Records, 1941-1950, Washington, D.C.

- US Department of Commerce, Environmental Data Services, 1966: World Weather Records, 1951-1960, Washington, D.C.
- US Department of Commerce, NOAA, NCDC, National Environmental Satellite, Data, and Information Service, 1971-1983, 1989, 1990: Monthly Climatic Data for the World, Asheville, NC, 24-36, 42, 43, No. 1-12.
- US Department of Commerce, NOAA, Federal Coordinator for Meteorological Services and Supporting Research, 1977: National Hurricane Operations Plan, FCM 77-2, Washington, D.C., 104 pp.
- US Department of Commerce, NOAA, Environmental Data and Information Service, 1982: World Weather Records, 1961-1970, Washington, D.C.
- US Department of Commerce, NOAA, Federal Coordinator for Meteorological Services and Supporting Research, 1990a: National Hurricane Operations Plan, FCM-P12-1990, Washington, D.C., 128pp.
- US Department of Commerce, NOAA, NWS, NMC, 1990b: Climate Diagnostics Bulletin, 90, Camp Springs, Maryland.
- US Department of Commerce, NOAA, NWS, NMC, CAC, 1990c: Weekly Climate Bulletin, 90, Washington, D.C.
- Walker, J. and P. R. Rowntree, 1977: The effect of soil moisture on circulation and rainfall in a tropical model. *Quart. J. Roy. Meteor. Soc.*, 103, 29-46.
- Weare, B. C., 1986: An extension of an El Niño index. *Mon. Wea. Rev.*, 114, 644-647.
- Willoughby, H. E., J. M. Masters and C. W. Landsea, 1989: A record minimum sea level pressure observed in hurricane Gilbert. *Mon. Wea. Rev.*, 117, 2824-2828.
- Wright, P. B., 1984: Relationships between indices of the Southern Oscillation. *Mon. Wea. Rev.*, 112, 1913-1919.
- Zoch, R. T., 1949: North Atlantic hurricanes and tropical disturbances of 1949. *Mon. Wea. Rev.*, 77, 339-342.
- (Gray 1984a, 1984b, 1987, 1988b, 1989a, 1989b, 1989c, 1989d, 1990a, 1990b, 1990d available upon request from the author's office.)

Appendix A

AFRICAN RAINFALL STATION: BACKGROUND

The CSU Rainfall Data Base is composed primarily of monthly precipitation data for stations in the African continent and surrounding islands. As described in Chapter 2, the data originated from the WMSSC tapes, with various supplements which have extended the data through 1990 and to include additional non-standard stations.

The following pages document the 751 stations for which analyses were performed. Included for each station is the CSU Rainfall Data Base identification number, station name and country, latitude and longitude, original data source and number, first year of data, last year of data, and number of years (whole or partial) of available data. The sources are keyed as follows:

- W - WMSSC data set,
- A - AID data set,
- L - Lamb data set,
- N - Nigerian data set,
- C - CAC data set.

ID	Station	Lat	Lon	Orig ID	First Yr	Last Yr	Num Yrs
0001	CORVO /AZORES/	39.7N	31.1W	W085030	1961	1970	10
0002	HORTA /AZORES/	38.5N	28.7W	W085050	1902	1981	80
0003	HORTA /AZORES/	38.9N	28.6W	W085060	1981	1989	9
0004	LAJES /AZORES/	38.8N	27.1W	W085090	1951	1970	20
0005	PONTA DELGADA /AZORES/	37.8N	25.7W	W085130	1894	1989	96
0005	- ALSO W085120						
0007	SANTA MARIA /AZORES/	37.0N	25.2W	W085150	1961	1989	25
0008	FUNCHAL /MADEIRA/	32.7N	16.8W	W085210	1880	1990	104
0009	FUNCHAL /MADEIRA/	32.6N	16.9W	W085220	1981	1989	9
0010	PORTO SANTO /MADEIRA/	33.1N	16.4W	W085240	1940	1990	33
0011	CABO CARVOEIRO, PORTUGAL	39.4N	9.4W	W085300	1961	1990	12
0012	LISBOA, PORTUGAL	38.7N	9.1W	W085350	1981	1988	8
0013	LISBOA, PORTUGAL	38.8N	9.1W	W085360	1864	1981	118
0014	SINTRA/GRANJA, PORTUGAL	38.8N	9.3W	W085377	1939	1960	22
0015	SAGRES, PORTUGAL	37.0N	9.0W	W085380	1961	1990	12
0016	VIANA DO CASTELO, PORTUGAL	41.7N	8.8W	W085430	1961	1990	12
0017	PORTO/PEDRAS RUBAS, PORTUGAL	41.2N	8.7W	W085450	1961	1990	23
0018	PORTO/SERRA DO PILAR, PORTUGAL	41.1N	8.6W	W085460	1981	1988	8
0019	COIMBRA, PORTUGAL	40.2N	8.4W	W085490	1961	1990	17
0020	FARO, PORTUGAL	37.0N	8.0W	W085540	1961	1990	17
0021	EVORA, PORTUGAL	38.6N	7.9W	W085570	1961	1990	12
0022	BEJA, PORTUGAL	38.0N	7.9W	W085620	1961	1990	17
0023	VILA REAL, PORTUGAL	41.3N	7.7W	W085660	1961	1990	12
0024	PENHAS DOURADAS, PORTUGAL	40.4N	7.6W	W085680	1961	1990	17
0025	PORTALEGRE, PORTUGAL	39.3N	7.4W	W085710	1961	1990	12
0026	BRAGANCA, PORTUGAL	41.8N	6.8W	W085750	1961	1990	17
0027	MINDELO /CAPE VERDE/	16.9N	25.0W	W085830	1921	1990	43
0028	PRAIA /CAPE VERDE/	14.9N	23.5W	W085890	1921	1960	33
0029	SAL /CAPE VERDE/	16.7N	23.0W	W085940	1951	1990	32
0030	MONTE IZANA /CANARY/	28.3N	16.5W	W600100	1951	1990	30
0031	TENERIFE/LOS RODEOS /CANARY/	28.5N	16.3W	W600150	1885	1990	89
0032	SANTA CRUZ DE TENERIFE /CANARY	28.5N	16.3W	W600200	1925	1990	66
0033	LAS PALMAS/GANDO /CANARY/	27.9N	15.4W	W600300	1941	1990	50
0034	FUERTEVENTURA /CANARY/	28.5N	13.9W	W600350	1952	1990	19
0035	SIDI IFNI, MOROCCO	29.4N	10.2W	W600600	1951	1990	26
0036	VILLA CISNEROS, WESTERN SAHARA	23.7N	15.9W	W600960	1951	1990	32
0036	- AD DAKHLA, WESTERN SAHARA						
0037	KENITRA II, MOROCCO	34.3N	6.6W	W601190	1951	1960	10
0038	FES/CITY, MOROCCO	34.0N	5.0W	W601400	1951	1961	11
0039	MEKNES, MOROCCO	33.9N	5.5W	W601500	1961	1990	30
0040	CASABLANCA, MOROCCO	33.6N	7.7W	W601550	1902	1990	87
0041	KASBA TADLA, MOROCCO	32.6N	6.3W	W601900	1961	1990	20
0042	MARRAKECH, MOROCCO	31.6N	8.0W	W602300	1900	1990	87
0043	AGADIR, MOROCCO	30.4N	9.6W	W602500	1931	1990	60
0044	OUARZAZATE, MOROCCO	30.9N	6.9W	W602650	1961	1990	30
0045	JIJEL, ALGERIA	36.8N	5.8E	W603510	1987	1990	4
0046	SKIKDA, ALGERIA	36.9N	7.0E	W603550	1966	1990	19
0047	ANNABA, ALGERIA	36.8N	7.8E	W603600	1963	1990	22
0047	- BONE, ALGERIA						
0048	EL KALA, ALGERIA	36.9N	8.5E	W603670	1987	1989	3
0049	ALGER/DAR EL BEIDA, ALGERIA	36.7N	3.3E	W603900	1951	1990	35
0050	CAP CARBON, ALGERIA	36.8N	5.1E	W604000	1951	1960	10
0051	BEJAIA, ALGERIA	36.7N	5.1E	W604020	1969	1990	16
0052	CONSTANTINE, ALGERIA	36.3N	6.6E	W604190	1837	1990	137
0053	CHLEF, ALGERIA	36.2N	1.3E	W604250	1981	1990	10
0053	- AL ASNAM, ALGERIA						
0054	MILIANA, ALGERIA	36.3N	2.2E	W604300	1951	1990	22
0055	BORDJ BOU ARRERIDJ, ALGERIA	36.1N	4.8E	W604440	1981	1990	10
0056	SETIF, ALGERIA	36.2N	5.4E	W604450	1981	1990	10
0057	MOSTAGANEM, ALGERIA	35.9N	0.1E	W604570	1982	1989	8
0058	M'SILA, ALGERIA	35.7N	4.5E	W604670	1982	1990	9

0059	TEBESSA, ALGERIA	35.4N	8.1E	W604750	1951	1990	22
0060	ORAN/ES SENIA, ALGERIA	35.6N	0.6W	W604900	1924	1990	61
0061	MASCARA GRISS, ALGERIA	35.3N	0.2E	W605070	1987	1988	2
0062	TIARET, ALGERIA	35.3N	1.4E	W605110	1987	1990	4
0063	BOU SAADA, ALGERIA	35.3N	4.2E	W605150	1987	1990	4
0064	BENI SAF, ALGERIA	35.3N	1.4E	W605180	1981	1990	10
0065	MAGHNA, ALGERIA	34.8N	1.8W	W605220	1981	1989	9
0066	BISKRA, ALGERIA	34.8N	5.7E	W605250	1932	1990	50
0067	TLEMCEN, ALGERIA	34.9N	1.3W	W605300	1922	1985	49
0068	TLEMCEN(ZENATA), ALGERIA	35.0N	1.5E	W605310	1982	1990	9
0069	DJELFA, ALGERIA	34.7N	3.3E	W605350	1875	1990	94
0070	EL KHEITER, ALGERIA	34.2N	0.1E	W605400	1983	1989	7
0071	LAGHOUAT, ALGERIA	33.8N	2.9E	W605450	1900	1989	80
0072	MECHERIA, ALGERIA	33.5N	0.3W	W605490	1981	1990	10
0073	EL BAYADH, ALGERIA	33.7N	1.0E	W605500	1981	1990	10
0074	TOUGGOURT, ALGERIA	33.1N	6.1E	W605550	1981	1990	10
0075	EL OUED-GUEMAR, ALGERIA	33.5N	6.8E	W605590	1970	1990	13
0076	AIN SEFRA, ALGERIA	32.8N	0.6W	W605600	1982	1990	9
0077	GHARDAIA/NOUMERATE, ALGERIA	32.4N	3.8E	W605660	1970	1990	16
0078	BECHAR, ALGERIA	31.6N	2.3W	W605710	1906	1990	80
0078	- COLOMB-BECHAR, ALGERIA						
0079	OUARGLA, ALGERIA	31.9N	5.4E	W605800	1902	1986	66
0080	HASSI-MESSAOUD, ALGERIA	31.7N	6.2E	W605810	1968	1990	17
0081	EL GOLEA, ALGERIA	30.6N	2.9E	W605900	1909	1990	76
0082	BENI ABBES, ALGERIA	30.1N	2.2W	W606000	1931	1969	33
0083	BENI ABBES, ALGERIA	30.1N	2.2W	W606020	1981	1990	10
0084	TIMIMOUN, ALGERIA	29.3N	0.3E	W606070	1939	1990	41
0085	IN AMENAS, ALGERIA	28.1N	9.6E	W606110	1963	1990	23
0086	ADRAR, ALGERIA	27.9N	0.3W	W606200	1906	1990	74
0087	AOULEF, ALGERIA	27.0N	1.1E	W606250	1931	1962	32
0088	IN SALAH, ALGERIA	27.2N	2.5E	W606300	1964	1990	22
0089	ILLIZI, ALGERIA	26.5N	8.4E	W606400	1961	1990	6
0089	- FORT POLIGNAC, ALGERIA						
0090	REGGANE, ALGERIA	26.7N	0.3E	W606460	1963	1963	1
0091	TINDOUF VILLE, ALGERIA	27.7N	8.1W	W606550	1963	1966	3
0092	TINDOUF, ALGERIA	27.7N	8.1W	W606560	1935	1989	47
0093	DJANET, ALGERIA	24.6N	9.5E	W606700	1925	1990	57
0094	OUALLEN, ALGERIA	24.6N	1.3E	W606750	1931	1962	32
0095	TAMANRASSET, ALGERIA	22.8N	5.5E	W606800	1951	1990	35
0096	TUNIS/CARTHAGE, TUNISIA	36.8N	10.2E	W607150	1895	1990	94
0096	- TUNIS/EL AOUIA, TUNISIA						
0097	JENDOUBA, TUNISIA	36.5N	8.8E	W607250	1964	1990	21
0097	- SOUK EL ARBA, TUNISIA						
0098	KAIROUAN, TUNISIA	35.7N	10.1E	W607350	1964	1990	21
0099	GAFSA, TUNISIA	34.4N	8.8E	W607450	1902	1990	83
0100	GABES, TUNISIA	33.9N	10.1E	W607650	1951	1990	34
0101	BILMA, NIGER	18.7N	12.9E	W610170	1923	1990	68
0102	AGADECZ, NIGER	17.0N	8.0E	W610240	1921	1990	70
0102	- ALSO A061024, L000009						
0103	TILLABERI, NIGER	14.2N	1.5E	W610360	1951	1990	40
0103	- ALSO A061036						
0104	TAHOUA, NIGER	14.9N	5.3E	W610430	1921	1990	70
0104	- ALSO A061043						
0105	GOURE, NIGER	14.0N	10.3E	W610450	1951	1990	40
0105	- ALSO A061045						
0106	NGUIGMI, NIGER	14.3N	13.1E	W610490	1921	1990	70
0106	- ALSO A061049						
0107	NIAMEY-AIRPORT, NIGER	13.5N	2.2E	W610520	1905	1990	86
0107	- ALSO A061052, L000011						
0108	BIRNI N'KONNI, NIGER	13.8N	5.3E	W610750	1941	1990	50
0108	- ALSO A061075, L000010						
0109	MARADI, NIGER	13.5N	7.1E	W610800	1931	1990	59
0109	- ALSO A061080						

0110	DIFFA, NIGER	13.4N	12.8E	W610850	1951	1990	39
0110	- ALSO A061085						
0111	ZINDER-AERO, NIGER	13.8N	9.0E	W610900	1905	1990	86
0111	- ALSO A061090, L000012						
0112	MAGARIA, NIGER	13.0N	8.9E	W610910	1951	1990	40
0112	- ALSO A061091						
0113	MAINE SOROA, NIGER	13.2N	12.0E	W610960	1951	1990	40
0113	- ALSO A061096						
0114	GAYA, NIGER	11.9N	3.5E	W610990	1951	1990	40
0114	- ALSO A061099						
0115	TESSALIT, MALI	20.2N	1.0E	W612020	1947	1990	44
0115	- ALSO A061202						
0116	KIDAL, MALI	18.4N	1.4E	W612140	1923	1990	68
0117	TOMBOUCTOU, MALI	16.7N	3.0W	W612230	1897	1990	82
0117	- ALSO A061223, L000006						
0118	GAO, MALI	16.3N	0.1W	W612260	1919	1990	72
0118	- ALSO A061226, L000003						
0119	NIORO DU SAHEL, MALI	15.2N	9.6W	W612300	1919	1990	72
0119	- ALSO A061230						
0120	NARA, MALI	15.2N	7.3W	W612330	1921	1990	64
0120	- ALSO A061233						
0121	HOMBORI, MALI	15.3N	1.7W	W612400	1920	1990	61
0121	- ALSO A061240						
0122	MENAKA, MALI	15.9N	2.4E	W612500	1923	1990	68
0122	- ALSO A061250						
0123	KAYES, MALI	14.4N	11.4W	W612570	1896	1990	87
0123	- ALSO A061257, L000004						
0124	MOPTI, MALI	14.5N	4.1W	W612650	1921	1990	70
0124	- ALSO A061265, L000005						
0125	KITA, MALI	13.1N	9.5W	W612700	1931	1990	60
0125	- ALSO A061270						
0126	SEGOU, MALI	13.4N	6.3W	W612720	1907	1990	82
0126	- ALSO A061272						
0127	SAN, MALI	13.3N	4.9W	W612770	1921	1990	70
0127	- ALSO A061277						
0128	KENIEBA, MALI	12.9N	11.2W	W612850	1951	1990	40
0128	- ALSO A061285						
0129	BAMAKO, MALI	12.6N	8.0W	W612900	1919	1989	56
0130	BAMAKO/SENOU, MALI	12.5N	8.0W	W612910	1941	1990	50
0130	- ALSO A061291						
0131	KOUTIALA, MALI	12.4N	5.5W	W612930	1921	1990	70
0131	- ALSO A061293						
0132	BOUGOUNI, MALI	11.4N	7.5W	W612960	1921	1990	70
0132	- ALSO A061296						
0133	SIKASSO, MALI	11.4N	5.7W	W612970	1907	1990	78
0133	- ALSO A061297						
0134	BIR MOGHREIN, MAURITANIA	25.2N	11.6W	W614010	1942	1990	45
0134	- FORT TRINQUET, MAURITANIA						
0134	- ALSO A061401						
0135	FDERIK, MAURITANIA	22.7N	12.7W	W614030	1938	1982	45
0135	- FT GOURAUD						
0135	- ALSO A061403						
0136	ZOUERATE, MAURITANIA	22.8N	12.5W	W614040	1984	1990	7
0137	NOUADHIBOU, MAURITANIA	20.9N	17.0W	W614150	1905	1990	79
0137	- PT ETIENNE, MAURITANIA						
0138	ATAR, MAURITANIA	20.5N	13.1W	W614210	1921	1990	70
0138	- ALSO A061421						
0139	AKJOUJT, MAURITANIA	19.8N	14.4W	W614370	1931	1990	60
0139	- ALSO A061437						
0140	NOUAKCHOTT, MAURITANIA	18.1N	16.0W	W614420	1930	1990	61
0140	- ALSO A061442, L000008						
0141	TIDJIKJA, MAURITANIA	18.6N	11.4W	W614500	1921	1990	69
0141	- ALSO A061450						

0142	BOUTILIMIT, MAURITANIA	17.5N	14.7W	W614610	1921	1990	68
0142	- ALSO A061461						
0143	ROSSO, MAURITANIA	16.5N	15.8W	W614890	1951	1990	40
0143	- ALSO A061489						
0144	KAEDI, MAURITANIA	16.2N	13.5W	W614920	1951	1990	40
0144	- ALSO A061492						
0145	NEMA, MAURITANIA	16.6N	7.3W	W614970	1922	1990	69
0145	- ALSO A061497, L000007						
0146	KIFFA, MAURITANIA	16.6N	11.4W	W614980	1922	1990	69
0146	- ALSO A061498						
0147	AIOUN EL ATROUSS, MAURITANIA	16.7N	9.6W	W614990	1951	1990	40
0147	- ALSO A061499						
0148	SAINT LOUIS, SENEGAL	16.1N	16.5W	W616000	1854	1990	137
0148	- ALSO A061600, L000017						
0149	PODOR, SENEGAL	16.6N	14.9W	W616120	1918	1990	73
0149	- ALSO A061612, L000016						
0150	LINGUERE, SENEGAL	15.4N	15.1W	W616270	1933	1990	58
0150	- ALSO A061627						
0151	MATAM, SENEGAL	15.6N	13.3W	W616300	1918	1990	73
0151	- ALSO A061630						
0152	DAKAR/YOFF, SENEGAL	14.7N	17.5W	W616410	1898	1990	92
0152	- ALSO A061641, L000015						
0153	DAKAR-OUAKAM, SENEGAL	14.7N	17.4W	W616420	1961	1961	1
0154	THIES, SENEGAL	14.8N	17.0W	W616540	1918	1987	70
0154	- ALSO A380075						
0155	DIORBEL, SENEGAL	14.7N	16.2W	W616660	1919	1990	72
0155	- ALSO A061666						
0156	KAOLACK, SENEGAL	14.1N	16.1W	W616790	1951	1990	40
0156	- ALSO A061679						
0157	TAMBACOUNDA, SENEGAL	13.8N	13.7W	W616870	1920	1990	71
0157	- ALSO A061687, L000018						
0158	ZIGUINCHOR, SENEGAL	12.6N	16.3W	W616950	1951	1990	40
0158	- ALSO A061695						
0159	CAP-SKIRBING, SENEGAL	12.4N	16.8W	W616970	1982	1990	8
0159	- ALSO A061697						
0160	KOLDA, SENEGAL	12.9N	15.0W	W616980	1951	1990	40
0160	- ALSO A061698						
0161	KEDOUGOU, SENEGAL	12.6N	12.2W	W616990	1918	1990	72
0161	- ALSO A061699						
0162	BATHURST/YUNDUM, GAMBIA	13.4N	16.7W	W617010	1884	1990	99
0162	- BANJUL/YUNDUM, GAMBIA						
0162	- ALSO A061701, L000001						
0163	BISSAU AIRPORT, GUINEA-BISSAU	11.9N	15.7W	W617660	1941	1989	49
0163	- ALSO L000014						
0164	BOLAMA, GUINEA-BISSAU	11.6N	15.5W	W617690	1910	1989	61
0165	BAFATA, GUINEA-BISSAU	12.2N	14.7W	W617810	1983	1990	5
0166	LABE, GUINEA	11.3N	12.3W	W618090	1923	1990	61
0167	SIGUIRI, GUINEA	11.4N	9.2W	W618110	1922	1984	58
0168	BOKE, GUINEA	10.9N	14.3W	W618160	1922	1990	63
0169	KINDIA, GUINEA	10.1N	12.9W	W618180	1922	1985	63
0170	MAMOU, GUINEA	10.4N	12.1W	W618200	1922	1983	60
0171	KANKAN, GUINEA	10.4N	9.3W	W618290	1921	1990	65
0172	CONAKRY/GBESSIA, GUINEA	9.6N	13.6W	W618320	1905	1990	73
0173	FARANAH/BADALA, GUINEA	10.0N	10.8W	W618330	1976	1981	5
0174	KISSIDOUGOU, GUINEA	9.2N	10.1W	W618340	1921	1981	57
0175	MACENTA, GUINEA	8.5N	9.5W	W618470	1964	1982	12
0176	NZEREKORE, GUINEA	7.7N	8.8W	W618490	1964	1990	18
0177	LUNGI, SIERRA LEONE	8.6N	13.2W	W618560	1875	1990	115
0178	BONTHE, SIERRA LEONE	7.5N	12.5W	W618660	1951	1989	36
0179	NJALA, SIERRA LEONE	8.1N	12.1W	W618780	1982	1989	8
0180	BO, SIERRA LEONE	8.0N	11.8W	W618810	1968	1988	20
0181	KABALA, SIERRA LEONE	9.6N	11.6W	W618860	1955	1989	33
0182	DARU, SIERRA LEONE	8.0N	10.9W	W618910	1951	1989	39

0182	- SEGBWEMA, SIERRA LEONE							
0183	ASCENSION IS.	7.9S	14.4W	W619000	1923	1976	54	
0184	HUTTS GATE, ST. HELENA IS.	16.0S	5.7W	W619010	1892	1990	99	
0185	BOTTOMS WOOD, ST. HELENA IS.	16.0S	5.7W	W619070				
0186	SAO TOME ISLAND	0.4N	6.7E	W619310	1939	1990	39	
0187	PRINCIPE ISLAND	1.7N	7.4E	W619340	1961	1970	10	
0188	DIEGO GARCIA /CHAGOS ARCH./	7.3S	72.4E	W619670	1951	1990	32	
0189	ILES GLORIEUSES	11.6S	47.3E	W619680	1956	1990	35	
0190	ILE JUAN DE NOVA	17.1S	42.7E	W619700	1973	1990	18	
0191	ILE EUROPA	22.4S	40.4E	W619720	1951	1990	40	
0192	AGALEGA ISLAND	10.4S	56.8E	W619740	1951	1990	40	
0193	SERGE-FROLOW, ILE THOMELIN	15.9S	54.5E	W619760	1955	1990	36	
0194	ST. DENIS/GILLOT, REUNION IS.	20.9S	55.5E	W619800	1951	1990	40	
0195	ST. PIERRE, REUNION ISLAND	21.3S	55.5E	W619840	1951	1988	25	
0196	ST. BRANDON, ST. RAPHAEL IS.	16.5S	59.6E	W619860	1951	1990	40	
0197	RODRIGUES ISLAND	19.7S	63.4E	W619880	1951	1990	40	
0198	PLAISANCE /MAURITIUS/	20.4S	57.7E	W619900	1951	1990	40	
0199	PAMPLEMOUSSES /MAURITIUS/	20.1S	57.6E	W619930	1910	1960	51	
0200	ILE NOUVELLE-AMSTERDAM	37.8S	77.5E	W619960	1951	1990	40	
0200	- MARTIN DE VIVIES, AMSTERDAM IS.							
0201	ILES CROZET (AMOS)	46.5S	51.0E	W619970	1973	1990	17	
0201	- ALFRED FAURE, CROZET IS.							
0202	PRT-AUX-FRANCAIS, KERGUELEN I	49.3S	70.2E	W619980	1951	1990	40	
0203	NALUT, LIBYA	31.9N	11.0E	W620020	1925	1990	42	
0204	BENI ULID, LIBYA	31.8N	14.0E	W620037	1951	1960	10	
0205	MIZDA, LIBYA	31.5N	13.0E	W620057	1951	1960	10	
0206	ZUARA, LIBYA	32.9N	12.1E	W620070	1951	1990	35	
0207	GARIAN, LIBYA	32.2N	13.0E	W620087	1951	1960	10	
0208	HOMS/LA VALDAGNO, LIBYA	32.6N	14.2E	W620097	1951	1960	10	
0209	TRIPOLI INTL. AP, LIBYA	32.7N	13.2E	W620100	1879	1990	109	
0209	- TRIPOLI/IDRIS, LIBYA							
0210	MISURATA, LIBYA	32.4N	15.1E	W620160	1925	1990	61	
0211	TUMMINA/CRISPI, LIBYA	32.2N	15.1E	W620177	1951	1960	10	
0212	SIRTE, LIBYA	31.2N	16.6E	W620190	1926	1990	54	
0213	BENINA, LIBYA	32.1N	20.3E	W620530	1945	1990	45	
0214	AGEDABIA, LIBYA	30.7N	20.2E	W620550	1954	1990	17	
0215	SHAHAT, LIBYA	32.8N	21.9E	W620560	1945	1990	23	
0216	DERNA, LIBYA	32.7N	22.6E	W620590	1913	1990	54	
0217	TOBRUQ, LIBYA	32.1N	23.9E	W620620	1915	1990	55	
0218	EL ADEM/NASSER, LIBYA	31.9N	23.9E	W620630	1945	1984	35	
0219	SEBHA, LIBYA	27.0N	14.4E	W621240	1930	1990	53	
0220	HON, LIBYA	29.1N	16.0E	W621310	1954	1990	32	
0221	GIALO, LIBYA	29.0N	21.6E	W621610	1964	1990	26	
0222	KUFRA, LIBYA	24.2N	23.3E	W622710	1933	1990	57	
0223	SALLOUM, EGYPT	31.5N	25.2E	W623000	1951	1990	32	
0224	SIDI BARRANI, EGYPT	31.6N	26.0E	W623030	1909	1970	47	
0225	MERSA MATRUH, EGYPT	31.3N	27.2E	W623060	1905	1990	74	
0226	ALEXANDRIA/NOUZHA, EGYPT	31.2N	30.0E	W623180	1901	1990	85	
0227	KOM EL NADURA, EGYPT	31.2N	29.9E	W623197	1868	1957	90	
0228	PORT SAID/EL GAMIL, EGYPT	31.3N	32.2E	W623330	1896	1987	87	
0229	GHAZZA EGYPT UAR	31.5N	34.5E	W623380	1953	1967	12	
0230	CAIRO, EGYPT	30.1N	31.4E	W623660	1903	1990	79	
0231	ABBASSIA/CAIRO HQ, EGYPT	30.1N	31.3E	W623710	1887	1960	43	
0232	HELWAN, EGYPT	29.9N	31.3E	W623780	1904	1989	83	
0233	EL MINYA, EGYPT	28.1N	30.7E	W623870	1934	1990	50	
0234	MANQABAD/ASYUT, EGYPT	27.2N	31.1E	W623930	1951	1990	32	
0235	QENA, EGYPT	26.2N	32.7E	W624020	1935	1963	26	
0236	LUXOR, EGYPT	25.7N	32.7E	W624050	1941	1990	43	
0237	ASWAN, EGYPT	24.0N	32.8E	W624140	1935	1990	51	
0238	SIWA (EAST), EGYPT	29.2N	25.5E	W624170	1920	1990	62	
0239	BAHARIA, EGYPT	28.3N	28.9E	W624200	1951	1990	30	
0240	DAKHLA, EGYPT	25.5N	29.0E	W624320	1932	1990	52	
0241	KHARGA, EGYPT	25.5N	30.5E	W624350	1926	1990	56	

0242	ISMAILIA, EGYPT	30.6N	32.3E	W624410	1900	1987	59
0243	HURGHADA, EGYPT	27.2N	33.8E	W624620	1951	1990	33
0244	WADI HALFA, SUDAN	21.8N	31.3E	W626000	1937	1990	38
0245	ABU HAMED, SUDAN	19.5N	33.3E	W626400	1909	1990	71
0246	PORT SUDAN, SUDAN	19.6N	37.2E	W626410	1906	1990	85
0247	DONGOLA, SUDAN	19.2N	30.5E	W626500	1945	1990	46
0248	KARIMA, SUDAN	18.6N	31.9E	W626600	1951	1990	29
0249	GEBEIT, SUDAN	19.0N	36.8E	W626610	1951	1975	25
0250	TOKAR, SUDAN	18.4N	37.7E	W626710	1913	1975	63
0251	ATBARA, SUDAN	17.7N	34.0E	W626800	1907	1990	76
0252	SHENDI, SUDAN	16.7N	33.4E	W627000	1951	1975	25
0253	KHARTOUM, SUDAN	15.6N	32.6E	W627210	1899	1990	92
0254	KASSALA, SUDAN	15.5N	36.4E	W627300	1901	1990	79
0255	HALFA EL GEDIDA, SUDAN	15.3N	35.6E	W627330	1971	1975	5
0256	ED DUEIM, SUDAN	14.0N	32.3E	W627500	1951	1987	26
0257	WAD MEDANI, SUDAN	14.4N	33.5E	W627510	1951	1990	29
0258	GEDAREF, SUDAN	14.0N	35.4E	W627520	1965	1990	14
0259	EL FASHER, SUDAN	13.6N	25.3E	W627600	1913	1990	73
0260	SENNAR, SUDAN	13.6N	33.6E	W627620	1981	1990	8
0261	GENEINA, SUDAN	13.5N	22.5E	W627700	1929	1990	49
0262	EL OBEID, SUDAN	13.2N	30.2E	W627710	1902	1990	89
0263	KOSTI, SUDAN	13.2N	32.7E	W627720	1909	1990	73
0264	ZALINGEI, SUDAN	12.9N	23.3E	W627800	1929	1975	44
0265	EN NAHUD, SUDAN	12.7N	28.4E	W627810	1912	1990	67
0266	TOZI/ABU NAAMA, SUDAN	12.5N	34.0E	W627950	1952	1990	21
0267	ABU NAAMA, SUDAN	12.7N	34.1E	W627957	1963	1990	11
0268	DAMAZINE, SUDAN	11.8N	34.4E	W628050	1962	1990	29
0269	KADUGLI, SUDAN	11.0N	29.7E	W628100	1987	1990	4
0270	MALAKAL, SUDAN	9.6N	31.7E	W628400	1909	1990	81
0271	WAU, SUDAN	7.7N	28.0E	W628800	1904	1986	83
0272	WAU, SUDAN	7.7N	28.0E	W628807	1967	1967	1
0273	JUBA, SUDAN	4.9N	31.6E	W629410	1901	1989	89
0274	AGORDAT, ETHIOPIA	15.6N	37.9E	W630130	1922	1974	40
0275	ASMARA, ETHIOPIA	15.3N	38.9E	W630210	1903	1990	88
0276	MASSAWA, ETHIOPIA	15.6N	39.5E	W630230	1885	1986	74
0277	ASSAB, ETHIOPIA	13.1N	42.7E	W630430	1963	1990	6
0278	DJIBOUTI CITY, DJIBOUTI	11.6N	43.2E	W631250	1901	1990	88
0279	BOSASO, SOMALIA	11.3N	49.2E	W632100	1934	1960	21
0280	GARDO, SOMALIA	9.5N	49.1E	W632250	1954	1978	25
0281	GALCAIO, SOMALIA	6.9N	47.3E	W632300	1933	1960	28
0282	MOGADISHU, SOMALIA	2.0N	45.4E	W632600	1911	1990	78
0282	- MUODISHU, SOMALIA						
0283	CHISIMAI, SOMALIA	0.4S	42.5E	W632700	1894	1982	56
0283	- KISMAYU, SOMALIA						
0284	MAKALE, ETHIOPIA	13.5N	39.5E	W633300	1973	1974	2
0285	GONDAR, ETHIOPIA	12.5N	37.4E	W633310	1952	1990	36
0286	BAHAR DAR, ETHIOPIA	11.6N	37.4E	W633320	1967	1990	16
0287	DESSIE/COMBOLCHA, ETHIOPIA	11.1N	39.7E	W633330	1952	1990	34
0288	DEBRE MARCOS, ETHIOPIA	10.4N	37.7E	W633340	1964	1990	17
0289	LEKEMTI, ETHIOPIA	9.1N	36.6E	W633400	1972	1990	5
0290	JIMA, ETHIOPIA	7.7N	36.8E	W634020	1964	1990	27
0291	GORE, ETHIOPIA	8.3N	35.6E	W634030	1914	1990	69
0292	ADDIS ABABA, ETHIOPIA	9.0N	38.8E	W634500	1898	1990	92
0293	HARAR MEDA, ETHIOPIA	8.7N	39.0E	W634510	1971	1990	11
0294	AWASH, ETHIOPIA	9.0N	40.2E	W634530	1952	1990	17
0295	AWASSA,, ETHIOPIA	7.1N	38.5E	W634600	1973	1990	4
0296	DIRE DAWA, ETHIOPIA	9.6N	41.9E	W634710	1964	1990	27
0297	JIGGIGA, ETHIOPIA	9.3N	42.7E	W634730	1967	1990	12
0298	GOBA, ETHIOPIA	7.0N	40.0E	W634740	1967	1990	10
0299	GABRE DARE, ETHIOPIA	6.8N	44.3E	W634750	1975	1977	3
0300	GODE, ETHIOPIA	5.1N	44.6E	W634780	1971	1990	11
0301	NEGHELLI, ETHIOPIA	5.3N	39.8E	W635330	1975	1990	14
0302	LODWAR, KENYA	3.1N	35.6E	W636120	1920	1990	64

0303	MOYALE, KENYA	3.5N	39.1E	W636190	1915	1990	72
0304	MANDERA, KENYA	4.0N	41.9E	W636240	1951	1990	35
0305	GULU, UGANDA	2.8N	32.3E	W636300	1911	1977	67
0306	WAJIR, KENYA	1.8N	40.1E	W636710	1918	1990	54
0307	ELDORET, KENYA	0.5N	35.3E	W636860	1976	1990	15
0308	ENTEbbe AP, UGANDA	0.1N	32.5E	W637050	1896	1990	83
0309	KAMPALA, UGANDA	0.3N	32.6E	W637067	1931	1954	24
0310	GARISSA, KENYA	0.5S	39.6E	W637230	1931	1990	60
0311	NAIROBI/KABETE, KENYA	1.3S	36.8E	W637390	1929	1963	35
0312	NAIROBI AIRPORT, KENYA	1.3S	36.9E	W637400	1951	1990	40
0313	NAIROBI/DAGORETTI, KENYA	1.3S	36.8E	W637410	1955	1990	23
0314	MWANZA, TANZANIA	2.5S	32.9E	W637560	1902	1990	72
0315	MALINDI, KENYA	3.2S	40.1E	W637990	1892	1990	95
0316	MOMBASA, KENYA	4.0S	39.6E	W638200	1890	1990	95
0317	TABORA AIRPORT, TANZANIA	5.1S	32.8E	W638320	1894	1990	79
0318	DODOMA, TANZANIA	6.2S	35.8E	W638620	1922	1990	63
0319	KISAUNI, ZANZIBAR IS.	6.2S	39.2E	W638700	1892	1990	71
0320	DAR ES SALAAM AP, TANZANIA	6.9S	39.2E	W638940	1893	1990	87
0321	SONGEA, TANZANIA	10.7S	35.6E	W639620	1908	1990	68
0322	MTWARA, TANZANIA	10.3S	40.2E	W639710	1976	1990	13
0323	MAHE /SEYCHELLES/	4.7S	55.5E	W639800	1891	1990	81
0323	- SEYCHELLES INTL AIRPORT						
0324	MBANDAKA, ZAIRE	0.0N	18.3E	W640050	1951	1990	24
0325	LISALA, ZAIRE	2.3N	21.6E	W640140	1952	1971	15
0326	LIBENGE, ZAIRE	3.6N	18.6E	W640150	1951	1971	18
0327	BUMBA, ZAIRE	2.2N	22.6E	W640160	1952	1960	8
0328	BASOKO, ZAIRE	1.3N	23.6E	W640180	1951	1960	10
0329	BUTA, ZAIRE	2.8N	24.8E	W640340	1951	1969	17
0330	KISANGANI, ZAIRE	0.5N	25.2E	W640400	1951	1990	23
0331	ISIRO, ZAIRE	2.8N	27.7E	W640620	1951	1971	19
0332	BUTEMBO, ZAIRE	0.1N	29.3E	W640720	1952	1990	11
0333	WATSA, ZAIRE	3.1N	29.5E	W640740	1951	1960	10
0334	IRUMU, ZAIRE	1.5N	29.9E	W640750	1928	1957	28
0335	BUNIA, ZAIRE	1.5N	30.2E	W640760	1961	1971	8
0336	BANNINGVILLE, ZAIRE	3.3S	17.4E	W641080	1963	1990	12
0336	- BANDUNDU, ZAIRE						
0337	INONGO, ZAIRE	2.0S	18.3E	W641150	1951	1990	23
0338	BOENDE, ZAIRE	0.2S	20.9E	W641260	1930	1971	34
0339	LODJA, ZAIRE	3.5S	23.5E	W641460	1952	1971	18
0340	KINDU, ZAIRE	3.0S	25.9E	W641550	1951	1970	17
0341	USUMBURA, BURUNDI	3.3S	29.3E	W641780	1951	1960	10
0342	BUKAVU, ZAIRE	2.5S	28.9E	W641800	1951	1971	19
0343	GOMA, ZAIRE	1.7S	29.2E	W641840	1952	1989	16
0344	MOANDA, ZAIRE	6.0S	12.4E	W642010	1963	1971	3
0345	BANANA, ZAIRE	6.0S	12.4E	W642020	1951	1960	10
0346	KITONA, ZAIRE	5.9S	12.4E	W642030	1963	1970	4
0347	MATADI, ZAIRE	5.8S	13.4E	W642070	1963	1983	10
0348	KINSHASA/N'DJILI, ZAIRE	4.4S	15.4E	W642100	1931	1990	51
0349	ZAIRE	4.3S	15.3E	W642107	1961	1961	1
0350	KIKWIT, ZAIRE	5.0S	18.8E	W642220	1932	1990	47
0351	PORT FRANCOU, ZAIRE	4.3S	20.6E	W642240	1951	1990	15
0351	- ILEBO, ZAIRE						
0352	LULUABOURG, ZAIRE	5.9S	22.4E	W642350	1908	1990	43
0352	- KANANGA, ZAIRE						
0353	LUSAMBO, ZAIRE	5.0S	23.4E	W642460	1951	1990	16
0354	MBUJI-MAYI, ZAIRE	6.2S	23.6E	W642470	1963	1987	10
0355	KONGOLO, ZAIRE	5.4S	27.0E	W642760	1927	1973	38
0356	MANONO, ZAIRE	7.3S	27.4E	W642820	1951	1983	20
0357	KALEMIE, ZAIRE	5.9S	29.2E	W642850	1952	1969	14
0358	KAMINA BASE, ZAIRE	8.6S	25.3E	W643150	1952	1966	12
0359	MITWABA, ZAIRE	8.6S	27.3E	W643480	1951	1960	10
0360	LUBUMBASHI-LUANO, ZAIRE	11.7S	27.5E	W643600	1912	1983	63
0360	- ELISABETHVILLE, ZAIRE						

0361	KIGALI, RWANDA	2.0S	30.1E	W643870	1971	1990	10
0362	BUJUMBURA, BURUNDI	3.3S	29.3E	W643900	1965	1990	14
0363	POINTE-NOIRE, CONGO	4.8S	11.9E	W644000	1929	1990	60
0364	DOLISIE, CONGO	4.2S	12.7E	W644010	1941	1990	49
0364	- LOUBOMO, CONGO						
0365	MOUYONDZI, CONGO	4.0S	13.9E	W644020	1951	1990	36
0366	MAKABANA, CONGO	3.5S	12.6E	W644030	1963	1990	25
0367	SIBITI, CONGO	3.7S	13.4E	W644050	1951	1990	36
0368	BRAZZAVILLE/MAYA-MAYA, CONGO	4.3S	15.3E	W644500	1941	1990	47
0369	MPOUYA, CONGO	2.6S	16.2E	W644520	1951	1990	33
0370	DJAMBALA, CONGO	2.5S	14.8E	W644530	1941	1990	45
0371	GAMBOMA, CONGO	1.9S	15.9E	W644540	1951	1990	31
0372	MAKOUA, CONGO	0.0S	15.7E	W644560	1952	1990	31
0373	FORT ROUSSET, CONGO	0.5S	15.9E	W644567	1936	1972	36
0374	OUESSO, CONGO	1.6N	16.1E	W644580	1951	1990	36
0375	IMPFONDO, CONGO	1.6N	18.1E	W644590	1932	1990	51
0376	SOUANKE, CONGO	2.1N	14.1E	W644600	1951	1982	28
0377	LIBREVILLE, GABON	0.5N	9.4E	W645000	1901	1990	69
0378	PORT GENTIL, GABON	0.7S	8.8E	W645010	1937	1990	53
0379	MAYUMBA, GABON	3.4S	10.7E	W645030	1901	1990	59
0380	COCOBACH, GABON	1.0N	9.6E	W645040	1951	1990	38
0381	TCHIBANGA, GABON	2.9S	11.0E	W645070	1952	1990	37
0382	BITAM, GABON	2.1N	11.5E	W645100	1951	1990	38
0383	MEKAMBO, GABON	1.0N	13.9E	W645450	1951	1990	36
0384	MOUILA, GABON	1.9S	11.0E	W645500	1951	1990	39
0385	LAMBARENE, GABON	0.7S	10.2E	W645510	1951	1990	39
0386	MITZIC, GABON	0.8N	11.5E	W645520	1951	1990	39
0387	FRANCEVILLE, GABON	1.6S	13.6E	W645530	1936	1972	37
0388	OYEM/HEVEA, GABON	1.7N	11.7E	W645550	1951	1960	10
0389	MAKOKOU, GABON	0.6N	12.9E	W645560	1951	1990	38
0390	LASTOURSVILLE, GABON	0.8S	12.7E	W645600	1951	1990	39
0391	MOANDA, GABON	1.5S	13.3E	W645650	1961	1990	29
0392	BERBERATI, CENTRAL AFRICAN REP	4.2N	15.8E	W646000	1945	1990	45
0393	BOUAR, CENTRAL AFRICAN REP	6.0N	15.6E	W646010	1951	1990	39
0394	BOUCA, CENTRAL AFRICAN REP	6.5N	18.3E	W646030	1951	1967	17
0395	BOSSEMBELE, CENTRAL AFRICAN REP	5.3N	17.6E	W646050	1951	1990	39
0396	BOSSANGOA, CENTRAL AFRICAN REP	6.5N	17.4E	W646100	1923	1990	63
0397	BANGUI, CENTRAL AFRICAN REP	4.4N	18.5E	W646500	1903	1990	70
0398	N'DELE, CENTRAL AFRICAN REP	8.4N	20.7E	W646540	1923	1990	63
0399	BRIA, CENTRAL AFRICAN REP	6.5N	22.0E	W646550	1941	1990	49
0400	BANGASSOU, CENTRAL AFRICAN REP	4.7N	22.8E	W646560	1941	1989	48
0401	BIRAO, CENTRAL AFRICAN REP	10.3N	22.8E	W646580	1939	1990	51
0402	OBO, CENTRAL AFRICAN REP	5.4N	26.5E	W646590	1951	1989	38
0403	BAMBARI, CENTRAL AFRICAN REP	5.8N	20.7E	W646600	1931	1990	60
0404	YALINGA, CENTRAL AFRICAN REP	6.5N	23.3E	W646610	1951	1990	39
0405	ALINDAO, CENTRAL AFRICAN REP	5.0N	21.2E	W646620	1951	1990	39
0406	FORT LAMY, CHAD	12.1N	15.0E	W647000	1907	1990	57
0406	- N'DJAMENA, CHAD						
0406	- ALSO A064700						
0407	MAO, CHAD	14.1N	15.3E	W647010	1940	1987	39
0407	- ALSO A064701						
0408	BOL, CHAD	13.4N	14.7E	W647020	1903	1987	50
0408	- ALSO A064702						
0409	ZOUAR, CHAD	20.5N	16.2E	W647040	1944	1970	27
0410	BOUSSO, CHAD	10.5N	16.7E	W647050	1943	1987	42
0410	- ALSO A064705						
0411	MOUNDOU, CHAD	8.6N	16.1E	W647060	1931	1990	58
0411	- ALSO A064706						
0412	BOKORO, CHAD	12.4N	17.1E	W647080	1945	1987	38
0412	- ALSO A064708						
0413	PALA, CHAD	9.4N	14.9E	W647090	1945	1987	38
0413	- ALSO A064709						
0414	BARDAI, CHAD	21.3N	17.0E	W647200	1961	1966	6

0415	FORT-ARCHAMBAULT, CHAD	9.2N	18.4E	W647500	1931	1990	53
0415	- SARH, CHAD						
0415	- ALSO A064750						
0416	ATI, CHAD	13.2N	18.3E	W647510	1936	1989	46
0416	- ALSO A064751						
0417	FAYA-LARGEAU, CHAD	18.0N	19.2E	W647530	1933	1990	47
0418	AM-TIMAN, CHAD	11.0N	20.3E	W647540	1946	1990	39
0418	- ALSO A064754						
0419	ABECHE, CHAD	13.9N	20.9E	W647560	1935	1990	49
0419	- ALSO A064756						
0420	FADA, CHAD	17.2N	21.6E	W647570	1934	1972	39
0421	MONGO, CHAD	12.2N	18.7E	W647580	1949	1987	38
0421	- ALSO A064758						
0422	MAROUA-SALAK, CAMEROON	10.5N	14.3E	W648510	1954	1990	34
0423	KAELE, CAMEROON	10.1N	14.5E	W648530	1951	1960	10
0424	GAROUA, CAMEROON	9.3N	13.4E	W648600	1907	1990	70
0425	POLI, CAMEROON	8.5N	13.3E	W648610	1951	1960	10
0426	NGAOUNDERE, CAMEROON	7.4N	13.6E	W648700	1928	1990	63
0427	BANYO, CAMEROON	6.8N	11.8E	W648800	1909	1990	46
0428	TIBATI, CAMEROON	6.5N	12.6E	W648810	1951	1960	10
0429	MEIGANGA, CAMEROON	6.5N	14.4E	W648820	1951	1990	19
0430	MAMFE, CAMEROON	5.7N	9.3E	W648900	1969	1990	13
0431	KOUNDJA, CAMEROON	5.7N	10.8E	W648930	1951	1990	35
0432	YOKO, CAMEROON	5.6N	12.4E	W649000	1932	1990	52
0433	BETARE OYA, CAMEROON	5.6N	14.1E	W649010	1951	1990	14
0434	DOUALA OBS., CAMEROON	4.0N	9.7E	W649100	1888	1990	88
0435	DOUALA R. S., CAMEROON	4.0N	9.7E	W649107	1972	1975	3
0436	NKONGSAMBA, CAMEROON	5.0N	9.9E	W649110	1951	1990	18
0437	NGAMBE, CAMEROON	4.3N	10.6E	W649130	1951	1960	10
0438	BAFIA, CAMEROON	4.7N	11.3E	W649200	1951	1990	17
0439	NANGA-EBOKO, CAMEROON	4.7N	12.4E	W649220	1951	1960	10
0440	BERTOUA, CAMEROON	4.6N	13.7E	W649300	1932	1973	41
0441	BATOURI, CAMEROON	4.5N	14.4E	W649310	1951	1990	32
0442	EDEA, CAMEROON	3.8N	10.1E	W649410	1951	1960	10
0443	ESEKA, CAMEROON	3.6N	10.7E	W649420	1951	1960	10
0444	YAOUNDE, CAMEROON	3.8N	11.5E	W649500	1889	1990	67
0445	AKONOLINGA, CAMEROON	3.8N	12.2E	W649520	1951	1960	10
0446	ABONG-MBANG, CAMEROON	4.0N	13.2E	W649600	1951	1990	17
0447	LOMIE, CAMEROON	3.2N	13.6E	W649610	1951	1990	14
0448	YOKADOUMA, CAMEROON	3.5N	15.1E	W649620	1951	1960	10
0449	KRIBI, CAMEROON	3.0N	9.9E	W649710	1951	1990	32
0450	EBOLWA, CAMEROON	2.9N	11.2E	W649720	1951	1960	10
0451	SANGMELIMA, CAMEROON	2.9N	12.0E	W649740	1934	1973	40
0452	SOKOTO, NIGERIA	13.0N	5.3E	W650100	1907	1987	81
0452	- ALSO N650100						
0453	KANO, NIGERIA	12.1N	8.5E	W650460	1905	1988	84
0453	- ALSO L000013, N650460						
0454	MAIDUGURI, NIGERIA	11.9N	13.1E	W650820	1909	1987	78
0454	- ALSO N650820						
0455	ILORIN, NIGERIA	8.5N	4.6E	W651010	1906	1987	82
0455	- ALSO N651010						
0456	MINNA, NIGERIA	9.6N	6.5E	W651230	1916	1988	73
0456	- ALSO N651230						
0457	JOS, NIGERIA	9.9N	8.9E	W651340	1922	1988	66
0457	- ALSO N651340						
0458	YOLA, NIGERIA	9.2N	12.5E	W651670	1906	1984	78
0458	- ALSO N651670						
0459	LAGOS/IKEJA, NIGERIA	6.6N	3.3E	W652010	1892	1987	96
0459	- ALSO N652010						
0460	WARRI, NIGERIA	5.5N	5.7E	W652360	1907	1987	81
0460	- ALSO N652360						
0461	PORT HARCOURT, NIGERIA	4.9N	7.0E	W652500	1948	1984	37
0461	- ALSO N652500						

0462	ENUGU, NIGERIA	6.5N	7.6E	W652570	1916	1988	68
0462	- ALSO N652570						
0463	CALABAR, NIGERIA	5.0N	8.4E	W652640	1895	1988	93
0463	- ALSO N652640						
0464	MAKURDI, NIGERIA	7.7N	8.6E	W652710	1943	1987	43
0464	- ALSO N652710						
0465	KANDI, BENIN	11.1N	2.9E	W653060	1921	1990	70
0466	NATITINGOU, BENIN	10.3N	1.4E	W653190	1921	1990	70
0467	PARAKOU, BENIN	9.4N	2.6E	W653300	1921	1990	70
0468	TCHAOUROU, BENIN	8.9N	2.6E	W653330	1941	1965	25
0469	SAVE, BENIN	8.0N	2.4E	W653350	1921	1990	70
0470	BOHICON, BENIN	7.2N	2.1E	W653380	1951	1990	40
0471	COTONOU, BENIN	6.4N	2.4E	W653440	1910	1990	74
0472	DAPAN, TOGO	10.9N	0.3E	W653510	1981	1990	9
0472	- DAPAONG, TOGO						
0473	MANGO, TOGO	10.4N	0.5E	W653520	1905	1990	71
0474	SOKODE, TOGO	9.0N	1.1E	W653610	1901	1990	76
0475	ATAKPAME, TOGO	7.6N	1.1E	W653760	1899	1990	76
0476	TABLIGBO, TOGO	6.6N	1.5E	W653800	1961	1990	25
0477	LOME, TOGO	6.2N	1.3E	W653870	1900	1990	81
0478	GAMBAGA, GHANA	10.5N	0.5W	W654027	1899	1972	68
0479	TAMALE, GHANA	9.4N	0.9W	W654180	1907	1990	70
0480	KUMASI, GHANA	6.7N	1.6W	W654420	1921	1990	62
0481	TAKORADI, GHANA	4.9N	1.8W	W654670	1939	1990	39
0482	ACCRA, GHANA	5.6N	0.2W	W654720	1888	1990	90
0483	DORI, BURKINA FASO	14.0N	0.0W	W655010	1920	1990	71
0483	- ALSO A065501						
0484	OUAHIGOUYA, BURKINA FASO	13.6N	2.4W	W655020	1920	1990	71
0484	- ALSO A065502						
0485	OUAGADOUGOU, BURKINA FASO	12.4N	1.5W	W655030	1902	1990	89
0485	- ALSO A065503, L000020						
0486	FADA N'GOURMA, BURKINA FASO	12.1N	0.4E	W655070	1920	1990	71
0486	- ALSO A065507						
0487	BOBO DILOULASSO, BURKINA FASO	11.2N	4.3W	W655100	1907	1990	82
0487	- ALSO A065510, L000019						
0488	BOROMO, BURKINA FASO	11.7N	2.9W	W655160	1922	1990	69
0488	- ALSO A065516						
0489	GAOUA, BURKINA FASO	10.3N	3.2W	W655220	1921	1990	70
0489	- ALSO A065522						
0490	ODIENNE, IVORY COAST	9.5N	7.6W	W655280	1921	1990	70
0491	KORHOGO, IVORY COAST	9.4N	5.6W	W655360	1905	1990	61
0492	FERKESSEDOUGOU, IVORY COAST	9.6N	5.2W	W655390	1927	1973	45
0493	BONDOUKOU, IVORY COAST	8.1N	2.8W	W655450	1919	1990	63
0494	MAN, IVORY COAST	7.4N	7.5W	W655480	1923	1990	65
0495	BOUAKE, IVORY COAST	7.7N	5.1W	W655550	1908	1990	81
0496	GAGNOA, IVORY COAST	6.1N	6.0W	W655570	1923	1990	66
0497	DALOA, IVORY COAST	6.9N	6.5W	W655600	1919	1990	67
0498	DIMBOKRO, IVORY COAST	6.7N	4.7W	W655620	1922	1990	67
0499	YAMCUSSOUKRO, IVORY COAST	6.9N	5.4W	W655630	1979	1990	12
0500	ABIDJAN, IVORY COAST	5.3N	3.9W	W655780	1926	1990	62
0501	ADIAKE, IVORY COAST	5.3N	3.3W	W655850	1951	1990	38
0502	TABOU, IVORY COAST	4.4N	7.4W	W655920	1919	1990	68
0503	SAN PEDRO, IVORY COAST	4.8N	6.8W	W655940	1979	1990	12
0504	SASSANDRA, IVORY COAST	5.0N	6.1W	W655990	1922	1990	67
0505	HARBEL, LIBERIA	6.4N	10.4W	W656507	1936	1973	38
0506	ROBERTS FIELD, LIBERIA	6.3N	10.4W	W656600	1951	1990	40
0507	CABINDA, ANGOLA	5.6S	12.2E	W661040	1913	1972	38
0508	AMBRIZETE, ANGOLA	7.3S	12.9E	W661300	1914	1972	31
0509	CARMONA, ANGOLA	7.6S	15.0E	W661400	1947	1981	29
0510	DUNDO, ANGOLA	7.4S	20.8E	W661520	1933	1972	36
0511	LUANDA, ANGOLA	8.9S	13.2E	W661600	1901	1985	83
0512	MALANGE, ANGOLA	9.6S	16.4E	W662150	1951	1986	33
0513	HENRIQUE DE CARVALHO, ANGOLA	9.7S	20.4E	W662260	1947	1975	27

0514	PORTO AMBOIM, ANGOLA	10.7S	13.8E	W662400	1922	1979	33
0515	CELA, ANGOLA	11.4S	15.1E	W662700	1951	1972	22
0516	LUSO, ANGOLA	11.8S	19.9E	W662850	1937	1985	39
0517	LOBITO, ANGOLA	12.4S	13.5E	W663050	1911	1972	49
0518	BENGUELA, ANGOLA	12.6S	13.4E	W663100	1911	1982	42
0519	NOVA LISBOA, ANGOLA	12.8S	15.8E	W663180	1940	1982	37
0520	SILVA PORTO, ANGOLA	12.4S	17.0E	W663250	1930	1972	26
0521	SA DA BANDEIRA, ANGOLA	14.9S	13.6E	W663900	1913	1975	45
0522	SERPA PINTO, ANGOLA	14.7S	17.7E	W664100	1940	1975	36
0523	MOCAMEDES, ANGOLA	15.2S	12.2E	W664220	1914	1985	61
0524	MAVINGA, ANGOLA	15.8S	20.4E	W664470	1953	1975	23
0525	VILA PEREIRA D ECA, ANGOLA	17.1S	15.7E	W664907	1928	1972	42
0526	MORONI, GRANDE-COMORE IS.	11.7S	43.2E	W670010	1951	1983	32
0527	OUANI, ANJOUAN IS.	12.1S	44.4E	W670040	1967	1983	16
0528	DZAOUZI/PAMANZI, MAYOTTE IS.	12.8S	45.3E	W670050	1951	1989	35
0529	DIEGO-SUAREZ, MADAGASCAR	12.4S	49.3E	W670090	1941	1989	49
0530	FASCENE/NOSSI-BE, MADAGASCAR	13.3S	48.3E	W670120	1951	1960	10
0531	ANALALAVA, MADAGASCAR	14.6S	47.8E	W670190	1951	1989	26
0532	ANTALAHA, MADAGASCAR	15.0S	50.3E	W670250	1951	1989	26
0533	MAJUNGA, MADAGASCAR	15.7S	46.4E	W670270	1951	1989	26
0534	MAINTIRANO, MADAGASCAR	18.1S	44.0E	W670730	1951	1989	26
0535	TANANARIVE/IVATO, MADAGASCAR	18.8S	47.5E	W670830	1890	1989	98
0535	- ANTANANARIVO/IVATO, MADAGASCAR						
0536	TANANARIVE, MADAGASCAR	18.9S	47.5E	W670850	1890	1973	84
0537	TAMATAVE, MADAGASCAR	18.1S	49.4E	W670950	1951	1989	39
0538	FIANARANTSOA, MADAGASCAR	21.6S	47.1E	W671370	1969	1970	2
0539	MANANJARY, MADAGASCAR	21.2S	48.4E	W671430	1951	1989	26
0540	TULEAR, MADAGASCAR	23.4S	43.7E	W671610	1951	1989	39
0541	FORT-DAUPHIN, MADAGASCAR	25.0S	47.0E	W671970	1941	1989	36
0542	PORTO AMELIA, MOZAMBIQUE	13.0S	40.5E	W672150	1916	1989	58
0542	- PEMBA, MOZAMBIQUE						
0543	VILA CABRAL, MOZAMBIQUE	13.3S	35.3E	W672170	1934	1989	56
0543	- LICHINGA, MOZAMBIQUE						
0544	NAMPULA, MOZAMBIQUE	15.1S	39.3E	W672300	1924	1974	31
0545	NAMPULA, MOZAMBIQUE	15.1S	39.3E	W672370	1971	1989	19
0546	MOSSURIL, MOZAMBIQUE	15.0S	40.7E	W672407	1951	1955	5
0547	LUMBO, MOZAMBIQUE	15.0S	40.7E	W672410	1956	1969	14
0548	MOSSURIL, MOZAMBIQUE	14.9S	40.6E	W672470	1913	1970	48
0549	TETE, MOZAMBIQUE	16.2S	33.6E	W672610	1907	1989	67
0550	QUELIMANE, MOZAMBIQUE	17.9S	36.9E	W672830	1907	1989	80
0551	BEIRA/SACADURA CABRAL, MOZAMB.	19.8S	34.9E	W672970	1913	1989	77
0552	INHAMBANE, MOZAMBIQUE	23.9S	35.4E	W673230	1909	1989	81
0553	LOURENCO MARQUES, MOZAMBIQUE	26.0S	32.6E	W673390	1891	1978	80
0554	LOURENCO MARQUES/COUNTINHO	25.9S	32.6E	W673410	1910	1989	80
0554	- MAPUTO/MAVALANE, MOZAMBIQUE						
0555	KASAMA, ZAMBIA	10.2S	31.2E	W674750	1925	1989	65
0556	NDOLA, ZAMBIA	13.0S	28.7E	W675610	1912	1974	63
0557	FORT JAMESON, ZAMBIA	13.6S	32.6E	W675810	1903	1974	72
0558	KAMUZU INT ARPT, MALAWI	13.8S	33.8E	W675860	1982	1989	8
0559	LILONGWE, MALAWI	14.0S	33.7E	W675870	1920	1982	63
0560	MONGU, ZAMBIA	15.3S	23.2E	W676330	1904	1989	86
0561	LUSAKA, ZAMBIA	15.4S	28.2E	W676510	1917	1974	58
0562	LUSAKA, ZAMBIA	15.4S	28.3E	W676610	1917	1960	44
0563	BROKEN HILL, ZAMBIA	14.4S	28.5E	W676630	1910	1989	80
0563	- KABWE, ZAMBIA						
0564	CHILEKA, MALAWI	15.7S	35.0E	W676930	1939	1986	48
0565	ZOMBA, MALAWI	15.4S	35.3E	W676970	1893	1973	81
0566	LIVINGSTONE, ZAMBIA	17.8S	25.8E	W677430	1904	1989	86
0567	HARARE (BELVEDERE), ZIMBABWE	17.8S	31.0E	W677740	1896	1985	81
0567	- SALISBURY OBS., ZIMBABWE						
0568	SALISBURY/KUTSAGA OBS., ZIMB.	17.9S	31.1E	W677750	1898	1989	92
0568	- HARARE/KUTSAGA, ZIMBABWE						
0569	BULAWAYO/GOETZ OBS., ZIMBABWE	20.2S	28.6E	W679640	1897	1989	93

0570	CHIPINGA, ZIMBABWE	20.2S	32.6E	W679830	1912	1986	75
0571	GROOTFONTEIN, NAMIBIA	19.6S	18.1E	W680140	1898	1985	81
0572	GHANZI, BOTSWANA	21.7S	21.7E	W680240	1987	1989	3
0573	MAUN, BOTSWANA	20.0S	23.4E	W680320	1921	1989	63
0574	WINDHOEK/J G STRYDOM, NAMIBIA	22.6S	17.1E	W681100	1891	1985	94
0575	J.G.STRIJDOM/WINDHOKW, NAMIBIA	22.5S	17.5E	W681120	1966	1987	22
0576	MAHALAPYE, BOTSWANA	23.1S	26.8E	W681480	1917	1980	64
0577	PIETERSBURG, SOUTH AFRICA	23.9S	29.5E	W681740	1904	1989	81
0578	MAFEKING, SOUTH AFRICA	25.9S	25.6E	W682420	1901	1974	54
0579	PRETORIA, SOUTH AFRICA	25.7S	28.2E	W682620	1910	1989	75
0580	PRETORIA (IRENE), SOUTH AFRICA	25.9S	28.2E	W682630	1983	1989	2
0581	KEETMANSHOOP, NAMIBIA	26.6S	18.1E	W683120	1893	1987	87
0582	JAN SMUTS JOHANNESBURG, S AFR	26.1S	28.2E	W683680	1951	1989	39
0583	JOHANNESBURG/JOUBERT, S AFRICA	26.2S	28.1E	W683697	1889	1960	72
0584	ALEXANDER BAY, SOUTH AFRICA	28.6S	16.5E	W684060	1930	1987	58
0585	UPINGTON, SOUTH AFRICA	28.4S	21.3E	W684240	1900	1989	80
0586	KIMBERLEY, SOUTH AFRICA	28.8S	24.8E	W684380	1877	1989	113
0587	BLOEMFONTEIN/JBM HERTZOG, S AF	29.1S	26.3E	W684420	1903	1989	82
0588	BETHLEHEM AIRPORT, S AFRICA	28.3S	28.3E	W684610	1987	1989	3
0589	LADYSMITH, SOUTH AFRICA	28.6S	29.8E	W684760	1987	1989	3
0590	ESTCOURT, SOUTH AFRICA	29.0S	29.9E	W684780	1895	1973	79
0591	OKIEP, SOUTH AFRICA	29.6S	17.9E	W685120	1882	1960	79
0592	ALIWAL NORTH, SOUTH AFRICA	30.7S	26.7E	W685460	1883	1972	81
0593	DURBAN/LOUIS BOTHA, S AFRICA	30.0S	31.0E	W685880	1873	1989	117
0594	BEAUFORT WEST, SOUTH AFRICA	32.3S	22.7E	W687280	1900	1987	70
0595	CAPE TOWN/D.F. MALAN, S AFRICA	34.0S	18.6E	W688160	1951	1989	39
0596	CAPE TOWNE/ROYAL OBS, S AFRICA	33.9S	18.5E	W688177	1841	1973	133
0597	GEORGE, SOUTH AFRICA	34.0S	22.4E	W688280	1900	1989	63
0597	- GEORGE AIRPORT, S AFRICA						
0598	PORT ELIZABETH, SOUTH AFRICA	34.0S	25.6E	W688420	1867	1989	123
0599	EAST LONDON, SOUTH AFRICA	33.0S	27.8E	W688580	1900	1989	82
0600	TRISTAN DA CUNHA	37.1S	12.3W	W689020	1942	1961	19
0601	GOUGH ISLAND	40.4S	9.9W	W689060	1955	1989	35
0602	MARION ISLAND	46.9S	37.9E	W689940	1943	1989	42
0603	SARIA, BURKINA FASO	12.3N	2.2W	A200065	1951	1987	31
0604	BAZEGA, BURKINA FASO	*	*	A200152	1980	1987	8
0605	BEREGADOUGOU, BURKINA FASO	*	*	A200153	1974	1986	13
0606	DEDOUGOU, BURKINA FASO	12.5N	3.4W	A065505	1951	1990	39
0607	PO, BURKINA FASO	11.2N	1.2W	A065518	1951	1990	40
0608	MOUSSORO, CHAD	13.7N	16.5E	A064707	1951	1987	30
0609	NAUDE, GAMBIA	*	*	A150008	1971	1986	16
0610	JIBANACK, GAMBIA	*	*	A150015	1971	1986	16
0611	BANSANG, GAMBIA	13.4N	14.7W	A150024	1951	1986	34
0612	BAKENDIK, GAMBIA	*	*	A150041	1971	1986	15
0613	BANJUL/HALF DIE, GAMBIA	13.4N	16.7W	A061711	1951	1987	31
0614	KEREWAN, GAMBIA	13.5N	16.2W	A061712	1971	1987	14
0615	GEORGETOWN, GAMBIA	13.5N	14.8W	A061721	1951	1989	33
0616	SAPU, GAMBIA	*	*	A061722	1974	1987	14
0617	BASSE MET, GAMBIA	13.4N	14.3W	A061731	1951	1990	35
0618	JENOI MET, GAMBIA	*	*	A061741	1951	1987	33
0619	BAMAKO VILLE, MALI	*	*	A270007	1941	1989	49
0619	- ALSO L000002						
0620	NIONO, MALI	14.3N	6.0W	A270067	1951	1987	37
0621	KATITOUGOU, MALI	12.6N	7.5W	A270114	1951	1987	36
0622	N'TARLA, MALI	12.7N	5.8W	A270121	1966	1987	22
0623	SOTUTA, MALI	12.4N	7.6W	A270130	1951	1987	31
0624	MAHIRA, MALI	*	*	A270185	1978	1986	9
0625	MOUDJERIA, MAURITANIA	17.9N	12.5W	A300018	1951	1986	36
0626	ALEG, MAURITANIA	17.0N	14.0W	A300023	1951	1987	37
0627	BOGHE, MAURITANIA	16.5N	14.3W	A300028	1951	1987	37
0628	N'BOUT, MAURITANIA	16.0N	12.6W	A300034	1951	1987	30
0629	KANKOSSA, MAURITANIA	15.9N	11.5W	A300035	1953	1987	27
0630	SELIBABY, MAURITANIA	15.2N	12.2W	A300037	1951	1987	37

0631	TIMBEDRA, MAURITANIA	16.3N	8.3W	A300052	1951	1976	26
0632	LOUGA, SENEGAL	15.6N	16.2W	A380051	1951	1987	36
0633	BAKEL, SENEGAL	14.9N	12.4W	A380072	1951	1987	37
0634	GHAT, LIBYA	25.1N	10.1E	C622120	1982	1990	8
0635	MBOUR, SENEGAL	14.4N	16.9W	A380090	1951	1986	36
0636	NIRO DU RIP, SENEGAL	13.9N	15.9W	A380114	1951	1987	36
0637	VELINGARA CASAMANCE, SENEGAL	13.2N	14.1W	A380118	1951	1987	36
0638	SEDHIOU, SENEGAL	12.7N	15.5W	A380129	1951	1986	36
0639	BAMBAY MET, SENEGAL	14.7N	16.5W	A061650	1951	1987	37
0640	PORTUGAL	38.8N	9.1W	C085790	1989	1990	2
0641	HIERRO /CANARY/	27.8N	17.9W	C600010	1981	1990	10
0642	LA PALMA /CANARY/	28.6N	17.8W	C600050	1981	1990	10
0643	PUNTA ANAGA /CANARY/	28.6N	16.1W	C600250	1981	1990	10
0644	ARRECIFE /CANARY/	29.0N	13.6W	C600400	1981	1990	10
0645	TANGIER AIRPORT, MOROCCO	35.7N	5.9W	C601010	1981	1990	10
0646	LARACHE, MOROCCO	35.2N	6.1W	C601050	1981	1990	10
0647	AL HOCEIMA, MOROCCO	35.2N	3.9W	C601070	1981	1990	10
0648	OUJDA, MOROCCO	34.8W	2.0W	C601150	1981	1990	10
0649	TAZA, MOROCCO	34.2N	4.0W	C601270	1981	1990	10
0650	RABAT-SALE, MOROCCO	34.1N	6.8W	C601350	1981	1990	10
0651	FES-SAIS, MOROCCO	33.9N	5.0W	C601410	1981	1990	10
0652	CASABLANCA/NOUASSE, MOROCCO	33.4N	7.6W	C601560	1981	1990	10
0653	SAFI, MOROCCO	32.3N	9.2W	C601850	1981	1990	10
0654	BENI, MOROCCO	32.4N	6.4W	C601910	1981	1990	10
0655	MIDELT, MOROCCO	32.7N	4.7W	C601950	1982	1990	9
0656	ERRACHIDIA, MOROCCO	32.0N	4.4W	C602100	1981	1990	10
0657	ESSAOUIRA, MOROCCO	31.5N	9.8W	C602200	1981	1990	10
0658	TAN TAN, MOROCCO	28.5N	11.2W	C602850	1982	1990	8
0659	TETUAN/SANIA RAMEL, MOROCCO	35.6N	5.3W	C603180	1981	1990	10
0660	MELILLA (SPAIN), MOROCCO	35.3N	3.0W	C603380	1981	1990	10
0661	NADOR, MOROCCO	35.2N	2.9W	C603400	1981	1990	10
0662	BATNA, ALGERIA	35.6N	6.2E	C604680	1981	1990	10
0663	MASCARA, ALGERIA	35.6N	0.3E	C605060	1982	1990	8
0664	TABARKA, TUNISIA	36.9N	8.8E	C607100	1981	1990	10
0665	BIZERTE, TUNISIA	37.2N	9.8E	C607140	1981	1990	10
0666	KELIBIA, TUNISIA	37.1N	11.0E	C607200	1981	1990	10
0667	TUNISIA	36.4N	10.7E	C607280	1989	1990	2
0668	SILIANA, TUNISIA	36.1N	9.4E	C607340	1981	1990	8
0669	THALA, TUNISIA	35.6N	8.7E	C607380	1981	1990	10
0670	MONASTIR, TUNISIA	35.8N	10.8E	C607400	1981	1990	10
0671	SIDI BOUZID, TUNISIA	35.0N	9.5E	C607480	1981	1990	10
0672	SFAX, TUNISIA	34.7N	10.7E	C607500	1981	1990	10
0673	TOZEUR, TUNISIA	33.9N	8.2E	C607600	1981	1990	10
0674	DJERBA, TUNISIA	33.9N	10.8E	C607690	1981	1990	10
0675	MEDENINE, TUNISIA	33.4N	11.0E	C607700	1981	1990	10
0676	REMADA, TUNISIA	32.3N	10.4E	C607750	1981	1990	10
0677	EL BORMA, TUNISIA	31.7N	9.2E	C607800	1983	1990	8
0678	LIBYA	32.1N	12.5E	C620080	1989	1990	2
0679	GHADAMES, LIBYA	30.1N	9.5E	C621030	1981	1990	10
0680	GARIAT-EL-SHARGHIA, LIBYA	30.4N	13.6E	C621200	1981	1990	10
0681	GIARABUB, LIBYA	29.8N	24.5E	C621760	1981	1990	10
0682	TAZERBO, LIBYA	25.7N	21.1E	C622590	1981	1990	10
0683	EGYPT	31.3N	32.2E	C623320	1989	1990	2
0684	EGYPT	31.1N	33.8E	C623370	1989	1990	2
0685	EGYPT	30.6N	32.2E	C624400	1989	1990	2
0686	KOSSEIR, EGYPT	26.1N	34.3E	C624650	1981	1990	10
0687	SUDAN	12.0N	24.9E	C627900	1989	1990	2
0688	SOMALIA	8.0N	48.5E	C632270	1989	1990	2
0689	BARDERA, SOMALIA	2.4N	42.3E	C632500	1981	1990	5
0690	ETHIOPIA	6.1N	37.7E	C635000	1989	1990	2
0691	MARSABIT, KENYA	2.3N	37.9E	C636410	1981	1990	10
0692	KITALE, KENYA	1.0N	35.0E	C636610	1981	1990	10
0693	KENYA	0.3N	34.8E	C636870	1989	1990	2

0694	MERU, KENYA	0.1N	37.6E	C636950	1981	1990	10
0695	CAMEROON	6.0N	10.2E	C648920	1989	1990	2
0696	TIKO, CAMEROON	4.1N	9.4E	C649120	1982	1990	6
0697	TOGO	9.8N	1.1E	C653550	1989	1990	2
0698	LAMA-KARA, TOGO	9.6N	1.2E	C653570	1981	1990	10
0699	GHANA	10.0N	2.5W	C654040	1990	1990	1
0700	GHANA	6.6N	0.5E	C654530	1989	1990	2
0701	GHANA	5.9N	1.0W	C654570	1989	1990	2
0702	SUDAN	11.3N	27.8E	C628090	1989	1990	2
0703	GHANA	6.2N	2.3W	C654450	1990	1990	1
0704	GHANA	5.2N	1.1W	C654690	1989	1990	2
0705	GHANA	9.0N	2.5W	C654160	1989	1990	2
0706	IN-GUEZZAM, ALGERIA	19.5N	5.8E	W606900	1989	1990	2
0707	CEUTA (SPAIN), MOROCCO	35.9N	5.3W	C603200	1981	1990	10
0708	ASCENSION IS.	8.0S	14.4W	C619020	1989	1990	2
0709	MAURITIUS IS.	20.3S	57.5E	C619950	1989	1990	2
0710	UGANDA	0.2N	30.1E	C636740	1990	1990	1
0711	KISUMU, KENYA	0.1S	34.8E	C637080	1981	1990	10
0712	KENYA	0.7S	34.7E	C637090	1989	1990	2
0713	KENYA	0.4S	35.4E	C637100	1989	1990	2
0714	NAKURU, KENYA	0.3S	36.1E	C637140	1981	1990	10
0715	NYERI, KENYA	0.5S	37.0E	C637170	1981	1990	10
0716	EMBU, KENYA	0.5S	37.5E	C637200	1981	1990	10
0717	TANZANIA	1.3S	31.8E	C637290	1989	1990	2
0718	MUSOMA, TANZANIA	1.5S	33.8E	C637330	1983	1990	8
0719	KENYA	1.1S	35.8E	C637370	1989	1990	2
0720	KENYA	1.3S	36.8E	C637420	1989	1990	2
0721	MAKINDU, KENYA	2.3S	37.8E	C637660	1981	1990	10
0722	KENYA	2.3S	40.9E	C637720	1989	1990	2
0723	TANZANIA	3.3S	36.6E	C637890	1989	1990	2
0724	TANZANIA	3.4S	37.3E	C637900	1989	1990	2
0725	KILIMANJARO ARPT., TANZANIA	3.4S	37.1E	C637910	1981	1990	9
0726	VOI, KENYA	3.4S	38.6E	C637930	1981	1990	10
0727	TANZANIA	4.9S	29.6E	C638010	1989	1990	2
0728	TANZANIA	4.1S	37.7E	C638160	1989	1990	2
0729	TANGA, TANZANIA	5.1S	39.1E	C638440	1981	1990	7
0730	PEMBA ISLAND	5.1S	39.6E	C638450	1989	1990	2
0731	MOROGORO, TANZANIA	6.8S	37.7E	C638660	1981	1990	7
0732	TANZANIA	7.7S	35.8E	C638870	1989	1990	2
0733	MBEYA, TANZANIA	8.9S	33.5E	C639320	1982	1990	9
0734	SEYCHELLES ISLANDS	9.4S	46.5E	C639950	1989	1990	2
0735	ZAIRE	6.4S	20.8E	C642280	1989	1990	2
0736	RWANDA	2.5S	28.9E	C643800	1989	1990	2
0737	RWANDA	1.7S	29.3E	C643810	1989	1990	2
0738	RWANDA	1.5S	29.6E	C643830	1989	1990	2
0739	RWANDA	2.6S	29.7E	C643840	1989	1990	2
0740	BURUNDI	2.8S	30.3E	C643970	1990	1990	1
0741	EL AAIUN, WESTERN SAHARA	27.2N	13.2W	C600330	1981	1981	1
0742	KENITRA, MOROCCO	34.3N	6.6W	C601200	1981	1989	3
0743	EL ARISH, EGYPT	31.1N	33.8E	C623360	1983	1983	1
0744	STATION NO. 6, SUDAN	20.8N	32.5E	C626200	1981	1981	1
0745	HARGEISA, SOMALIA	9.5N	44.1E	C631700	1983	1985	2
0746	BURAO, SOMALIA	9.5N	45.6E	C631750	1983	1983	1
0747	BELET UEN, SOMALIA	4.7N	45.2E	C632400	1983	1986	4
0748	INGA, ZAIRE	5.5S	13.6E	C642060	1982	1982	1
0749	GHANA	8.8N	2.1W	C654320	1990	1990	1
0750	GHANA	6.1N	0.2W	C654590	1990	1990	1
0751	GHANA	5.8N	0.6E	C654750	1990	1990	1

Appendix B

REVISED RAINFALL INDICES

With the addition of CAC historical data, more complete Nigerian rainfall data (essential for the Gulf of Guinea Index), and the 1990 rainfall values, an update of the various indices was appropriate. The following are the most complete rainfall information available in the CSU Rainfall Data Base as of August 1991.

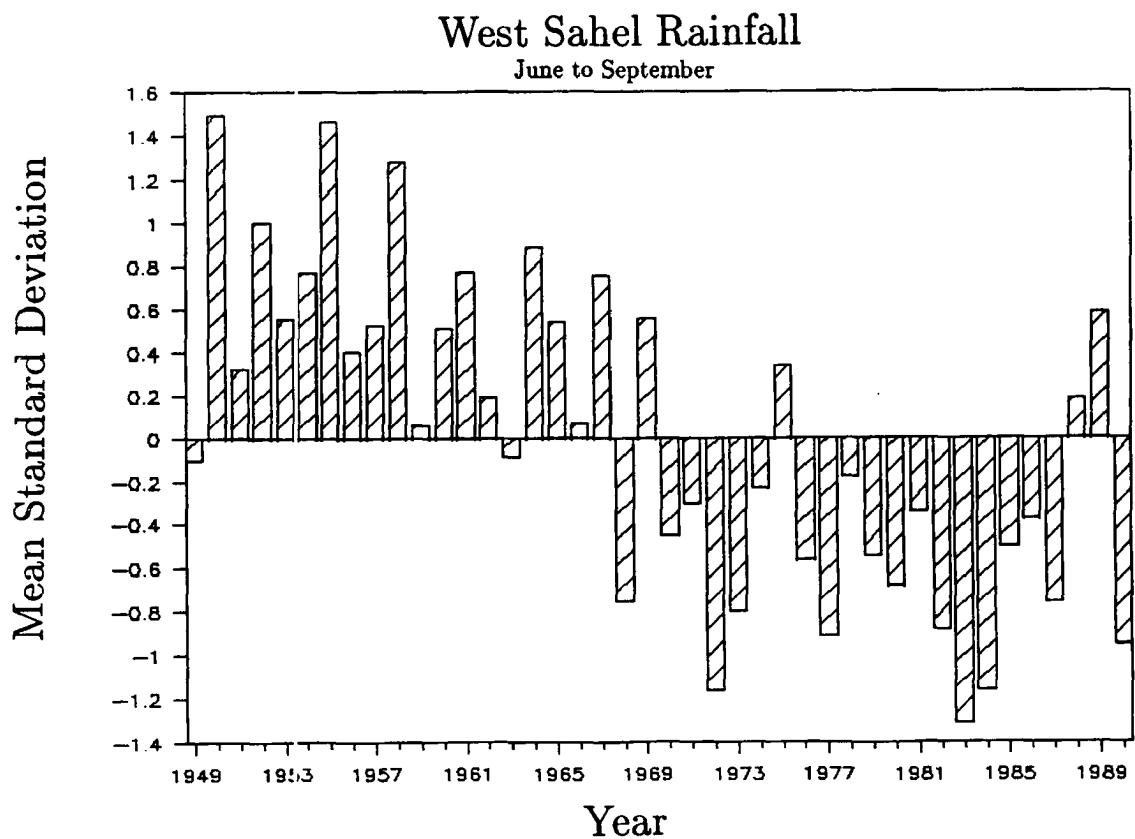


Figure B.1: Mean standard deviations of rainfall for the 38 station June to September Seedling Index of the Western Sahel. Data are presented from 1949 to 1990.

Table B.1: Mean standard deviations and data availability (out of a possible 38 stations per year) for the June to September Seedling Index.

Year	Standard Deviation	Number of Stations	Year	Standard Deviation	Number of Stations
1949	-0.10	24	1970	-0.45	37
1950	1.49	24	1971	-0.30	37
1951	0.32	37	1972	-1.16	38
1952	1.00	37	1973	-0.80	38
1953	0.55	38	1974	-0.23	38
1954	0.77	38	1975	0.34	38
1955	1.46	38	1976	-0.56	38
1956	0.40	38	1977	-0.91	37
1957	0.52	38	1978	-0.18	38
1958	1.28	37	1979	-0.54	38
1959	0.06	36	1980	-0.68	37
1960	0.51	35	1981	-0.34	37
1961	0.77	38	1982	-0.88	37
1962	0.19	37	1983	-1.31	37
1963	-0.09	38	1984	-1.16	37
1964	0.88	38	1985	-0.50	37
1965	0.54	37	1986	-0.37	37
1966	0.07	38	1987	-0.76	26
1967	0.75	37	1988	0.18	26
1968	-0.75	37	1989	0.58	25
1969	0.55	37	1990	-0.95	25

Table B.2: Regression equations and correlation coefficients (for both the previous value using 1949 to 1989, data and the new value using 1949 to 1990) of June to September Seedling Index rainfall (x) versus Atlantic basin tropical cyclone parameters (y). (Asterisks refer to significance level: 0.100 for '**', 0.025 for '***' and 0.005 for '****'.)

Tropical Cyclone Parameter	Correlation Coefficient (old value)	Correlation Coefficient (new value)	Regression Equation (new value)	Standard Error (New Value)
Named Storms	0.41	0.35**	$y = 9.42 + 1.406 x$	± 2.8
Named Storm Days	0.62	0.56***	$y = 47.12 + 15.052 x$	16.7
Hurricanes	0.52	0.47***	$y = 5.85 + 1.404 x$	2.0
Hurricane Days	0.69	0.67***	$y = 23.73 + 12.192 x$	10.1
Int. Hur. (Bias Out)	0.68	0.68***	$y = 2.18 + 1.420 x$	1.1
Int. Hur. Days (Bias Out)	0.69	0.70***	$y = 4.71 + 4.399 x$	3.3
HDP	0.72	0.73***	$y = 73.21 + 47.936 x$	33.8

Table B.3: June to September Seedling Index, ranked by rainfall amounts in mean standard deviations, for 1949 to 1990.

Rank	Year	Index Value	Rank	Year	Index Value
1.	1950	1.49	22.	1963	-0.09
2.	1955	1.46	23.	1949	-0.10
3.	1958	1.28	24.	1978	-0.18
4.	1952	1.00	25.	1974	-0.23
5.	1964	0.88	26.	1971	-0.30
6.	1954	0.77	27.	1981	-0.34
7.	1961	0.77	28.	1986	-0.37
8.	1967	0.75	29.	1970	-0.45
9.	1989	0.58	30.	1985	-0.50
10.	1969	0.55	31.	1979	-0.54
11.	1953	0.55	32.	1976	-0.56
12.	1965	0.54	33.	1980	-0.68
13.	1957	0.52	34.	1968	-0.75
14.	1960	0.51	35.	1987	-0.76
15.	1956	0.40	36.	1973	-0.80
16.	1975	0.34	37.	1982	-0.88
17.	1951	0.32	38.	1977	-0.91
18.	1962	0.19	39.	1990	-0.95
19.	1988	0.18	40.	1972	-1.16
20.	1966	0.07	41.	1984	-1.16
21.	1959	0.06	42.	1983	-1.31

Table B.4: Summary of the variability of tropical cyclone parameters during the ten wettest Western Sahel years (as measured by the June to September Seedling Index) and the ten driest years from 1949 to 1990. (Asterisks refer to significance level: 0.100 for '*', 0.025 for '**' and 0.005 for '***'.)

Tropical Cyclone Parameter	Wettest Years' Mean	Percent (%) of Normal	Driest Years' Mean	Percent (%) of Normal	Ratio Wet/ Dry
Trop./Subtropical	3.4	86	3.8	96	0.89
Named Storms	11.2	120	7.7	83	1.45***
Named Storm Days	67.0	143	34.0	73	1.97***
Hurricanes	8.0	138	4.6	79	1.74***
Hurricane Days	39.1	165	13.2	55	2.96***
Intense Hurricanes	4.5	180	0.9	36	5.00***
Intense Hurricane Days	12.4	214	1.2	21	10.33***
HDP	131.2	175	33.9	45	3.87***
US Landfalling:					
Named/Subtrop.	3.4	106	2.1	66	1.62*
Hurricanes	2.1	130	0.7	43	3.00**
Intense Hurricanes	1.2	197	0.2	33	6.00***
' ' Gulf Coast	0.5	147	0.2	59	2.50*
' ' East Coast	0.7	241	0.0	0	∞ **
Hurricane Damage	\$3934	223	407	23	9.67***
' ' Gulf Coast	1058	119	394	44	2.69
' ' East Coast	2876	329	13	1	221.23***

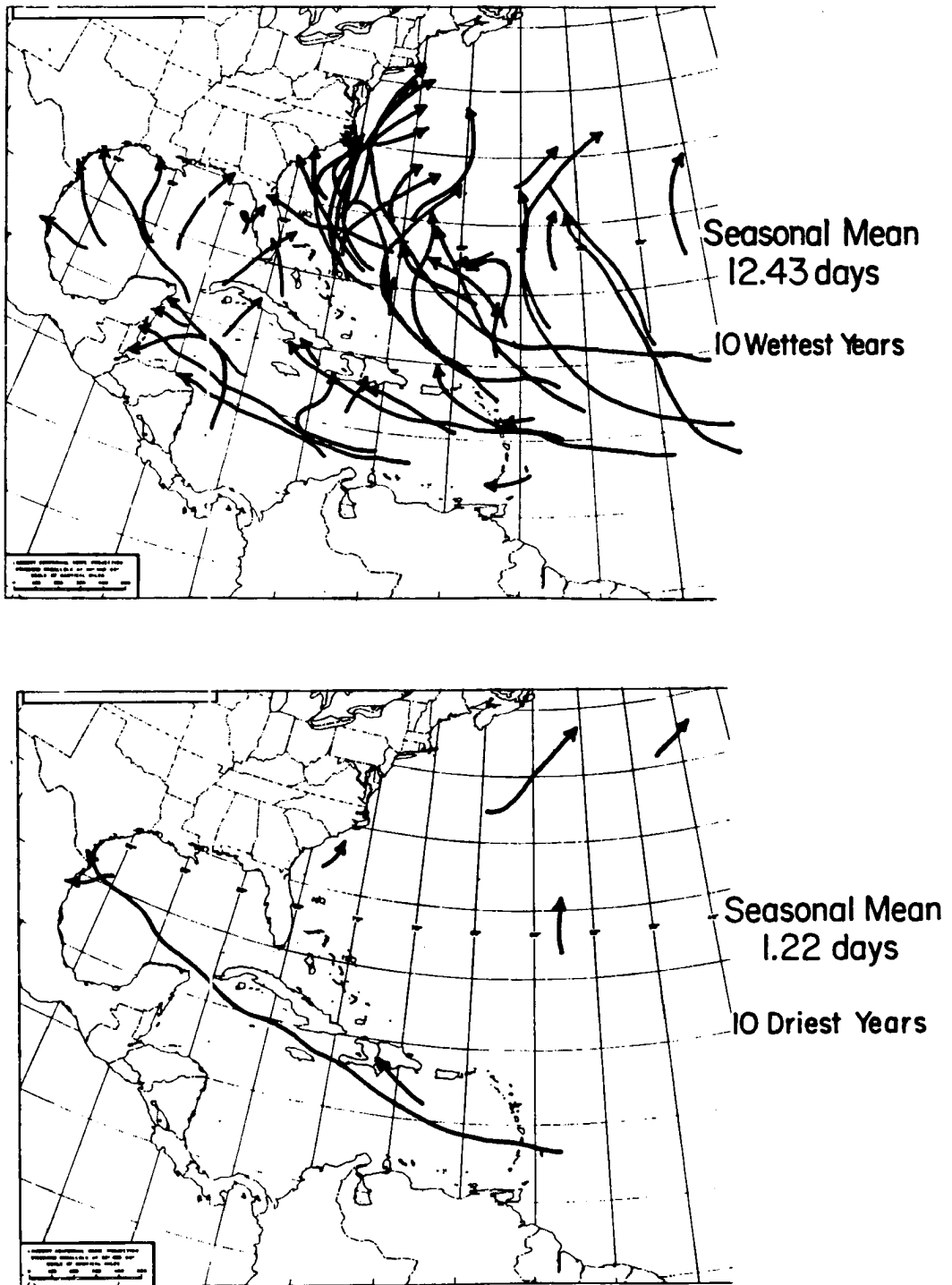


Figure B.2: Intense hurricane tracks during the ten wettest (upper panel) versus the ten driest (bottom panel) June to September Western Sahel years from 1949 to 1990.

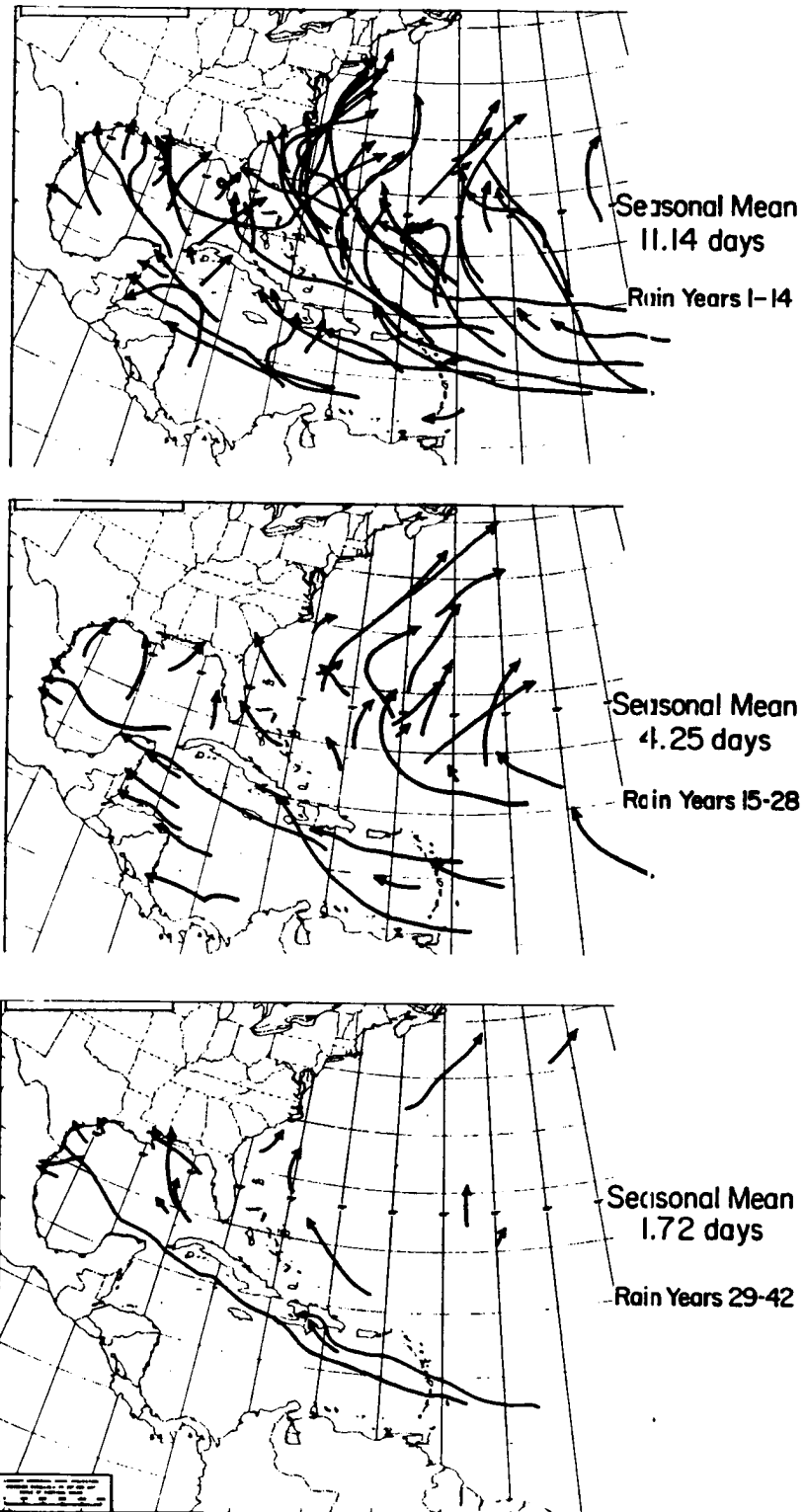


Figure B.3: Intense hurricane tracks during the fourteen wettest (upper panel), the fourteen near normal (middle panel), and the fourteen driest (bottom panel) June to September Western Sahel years from 1949 to 1990.

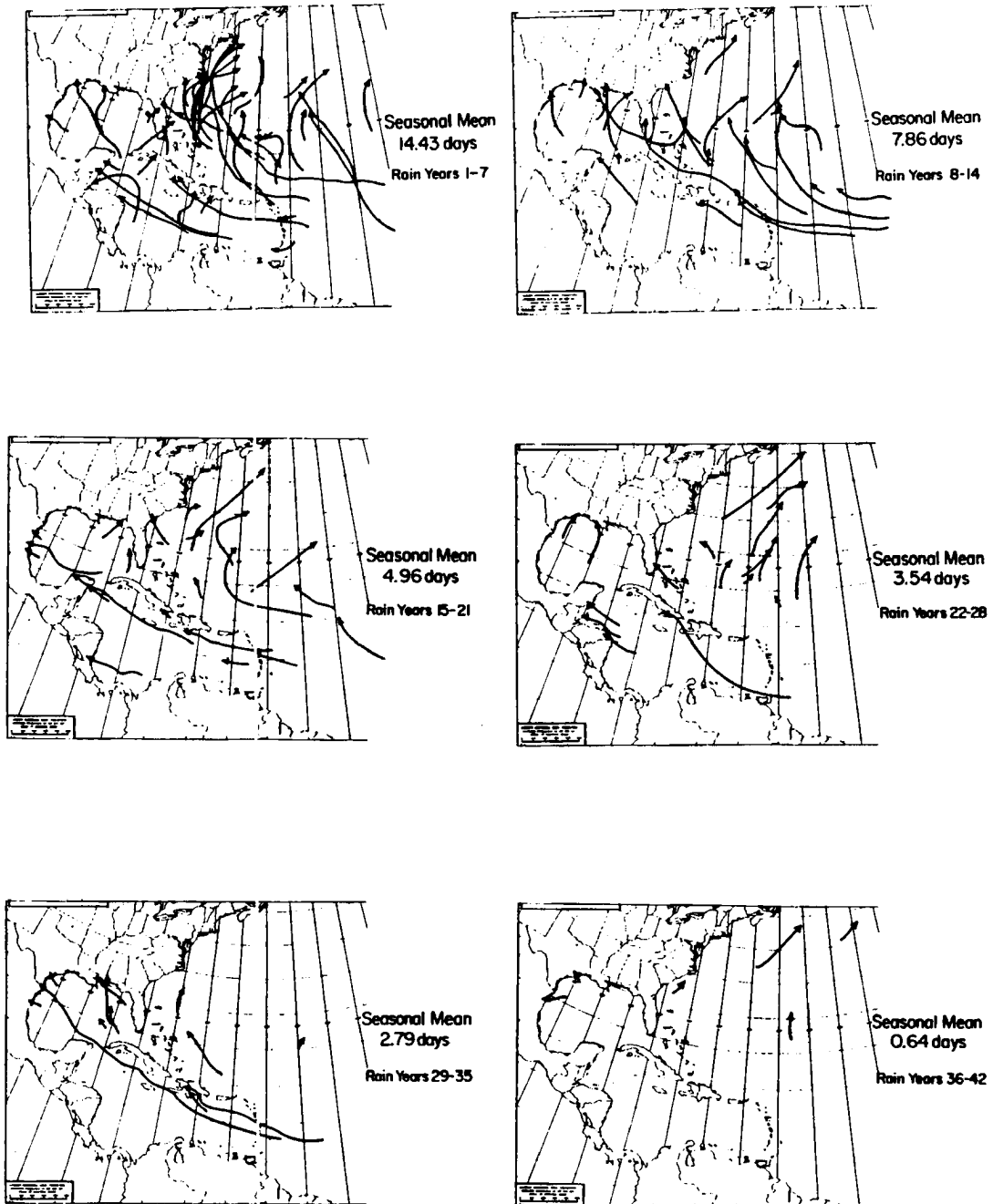


Figure B.4: Intense hurricane tracks for 6 seven-year groupings, based upon ranking of the June to September Western Sahel rainfall. The top left panel depicts the seven wettest years, the bottom right panel depicts the seven driest years.

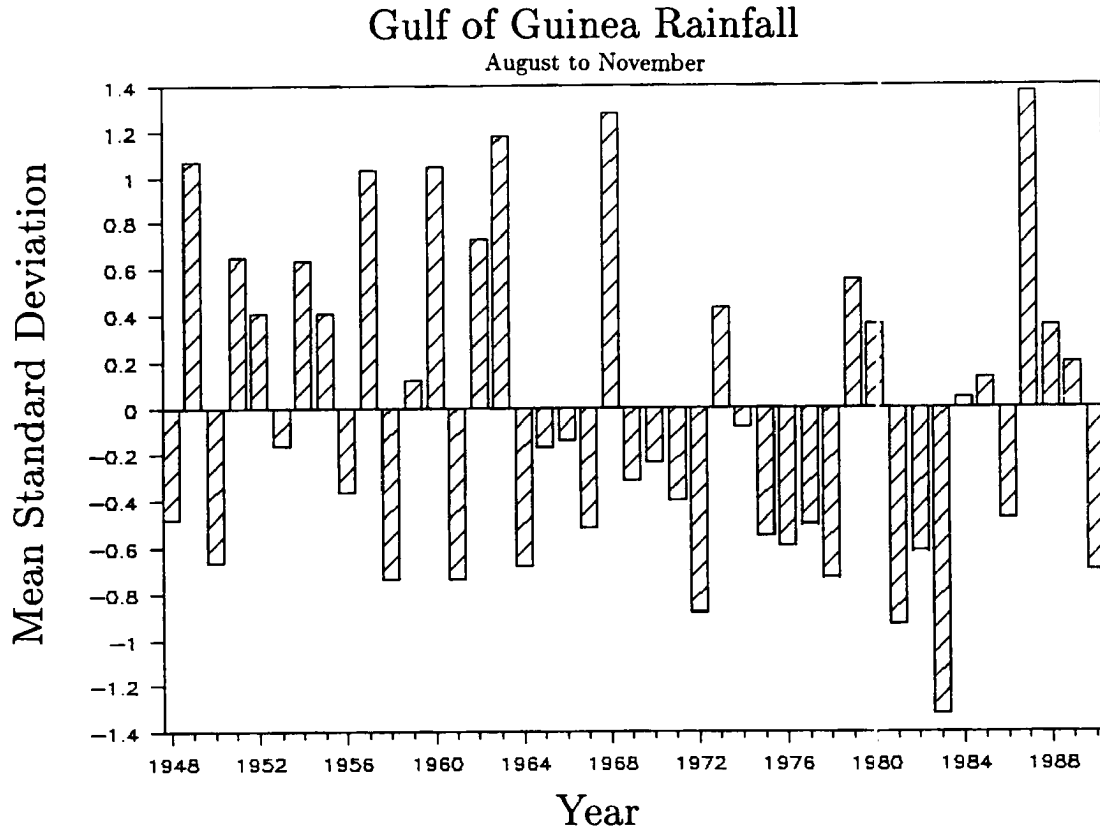


Figure B.5: Mean standard deviations of rainfall for the 24 station August to November Gulf of Guinea Index of rainfall. Data are presented for 1948 to 1990.

Table B.5: Mean standard deviations and data availability (out of a possible 24 stations) for the August to November Gulf of Guinea Index.

Year	Standard Deviation	Number of Stations	Year	Standard Deviation	Number of Stations
1948	-0.48	19	1970	-0.23	22
1949	1.07	19	1971	-0.40	22
1950	-0.66	19	1972	-0.88	21
1951	0.65	23	1973	0.43	21
1952	0.41	23	1974	-0.08	20
1953	-0.16	23	1975	-0.55	12
1954	0.64	23	1976	-0.59	17
1955	0.41	23	1977	-0.50	19
1956	-0.36	23	1978	-0.73	18
1957	1.03	23	1979	0.55	17
1958	-0.74	23	1980	0.36	18
1959	0.12	15	1981	-0.93	5
1960	1.05	15	1982	-0.61	16
1961	-0.74	21	1983	-1.32	17
1962	0.73	22	1984	0.04	10
1963	1.18	24	1985	0.13	15
1964	-0.68	23	1986	-0.48	12
1965	-0.17	14	1987	1.37	11
1966	-0.14	19	1988	0.35	9
1967	-0.51	21	1989	0.19	18
1968	1.28	21	1990	-0.70	17
1969	-0.31	18			

Table B.6: Regression equations and correlation coefficients (for both the previous value using 1948 to 1988 data and for the new value using 1948 to 1989) of August to November Gulf of Guinea Index rainfall (x) versus following year Atlantic basin tropical cyclone parameters and June to September Western Sahel Rainfall (y). (Asterisks refer to significance level: 0.100 for '*', 0.025 for '**' and 0.005 for '***'.)

Tropical Cyclone Parameter	Correlation Coefficient (old value)	Correlation Coefficient (new value)	Regression Equation (new value)	Standard Error (New Value)
Named Storms	0.50	0.48***	$y = 9.44 + 2.087 x$	± 2.7
Named Storm Days	0.58	0.58***	$y = 47.29 + 16.843 x$	16.5
Hurricanes	0.56	0.55***	$y = 5.87 + 1.779 x$	1.8
Hurricane Days	0.60	0.59***	$y = 23.86 + 11.624 x$	11.0
Int. Hur. (Bias Out)	0.68	0.68***	$y = 2.20 + 1.526 x$	1.1
Int. Hur. Days (Bias Out)	0.61	0.60***	$y = 4.75 + 4.074 x$	3.8
HDP	0.64	0.63***	$y = 73.71 + 44.790 x$	38.3
June-Sept W. Sahel Rainfall	0.65	0.60***	$y = 0.01 + 0.651 x$	0.60

Table B.7: August to November Gulf of Guinea Index, ranked by rainfall amounts in terms of mean standard deviations from 1948 to 1990. The 1990 value (asterisked) has not been utilized in the ten wettest versus ten driest years comparisons.

Rank	Year	Index Value	Rank	Year	Index Value
1.	1987	1.37	22.	1953	-0.16
2.	1968	1.28	23.	1965	-0.17
3.	1963	1.18	24.	1970	-0.23
4.	1949	1.07	25.	1969	-0.31
5.	1960	1.05	26.	1956	-0.36
6.	1957	1.03	27.	1971	-0.40
7.	1962	0.73	28.	1948	-0.48
8.	1951	0.65	29.	1986	-0.48
9.	1954	0.64	30.	1977	-0.50
10.	1979	0.55	31.	1967	-0.51
11.	1973	0.43	32.	1975	-0.55
12.	1952	0.41	33.	1976	-0.59
13.	1955	0.41	34.	1982	-0.61
14.	1980	0.36	35.	1950	-0.66
15.	1988	0.35	36.	1964	-0.68
16.	1989	0.19	37.	*1990*	-0.70
17.	1985	0.13	38.	1978	-0.73
18.	1959	0.12	39.	1958	-0.74
19.	1984	0.04	40.	1961	-0.74
20.	1974	-0.08	41.	1972	-0.88
21.	1966	-0.14	42.	1981	-0.93
			43.	1983	-1.32

Table B.8: Summary of the variability of subsequent year tropical cyclone parameters for the ten wettest August to November Gulf of Guinea years and for the ten driest years from 1948 to 1989. Damage is in millions of 1990 dollars. (Asterisks refer to significance level: 0.100 for '**', 0.025 for '***' and 0.005 for '****'.)

Tropical Cyclone Parameter	Wettest Years' Mean	Percent (%) of Normal	Driest Years' Mean	Percent (%) of Normal	Ratio Wet/ Dry
Named Storms	11.6	125	7.7	83	1.51****
Named Storm Days	66.1	142	37.6	81	1.76****
Hurricanes	8.0	138	4.6	79	1.74****
Hurricane Days	39.0	165	17.7	75	2.20****
Intense Hurricanes	4.7	188	1.8	72	2.61****
Intense Hurricane Days	12.0	207	3.0	52	4.00****
HDP	132.1	176	50.5	67	2.62****
US Landfalling:					
Named/Subtrop.	3.1	97	2.9	91	1.07
Hurricanes	1.9	118	0.9	56	2.00*
Intense Hurricanes	0.8	131	0.4	66	2.00
' ' Gulf Coast	0.3	88	0.3	88	1.00
' ' East Coast	0.5	172	0.2	69	2.50
Hurricane Damage	\$2277	129	\$1675	95	1.35
' ' Gulf Coast	1010	114	1510	170	0.67
' ' East Coast	1267	145	165	19	7.68

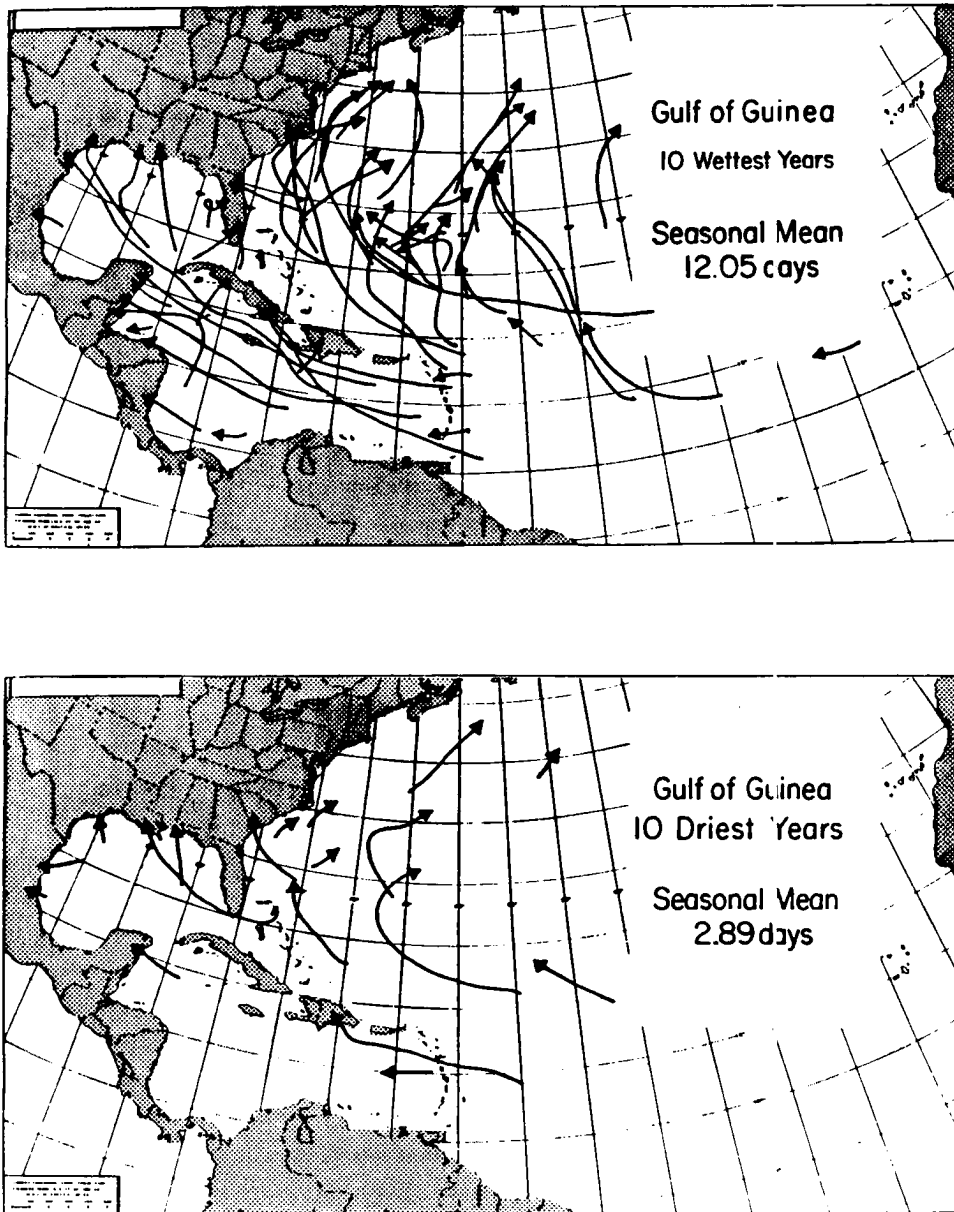


Figure B.6: Intense hurricane tracks in the years following the ten wettest (upper panel) versus the ten driest (bottom panel) August to November Gulf of Guinea years from 1948 to 1989.

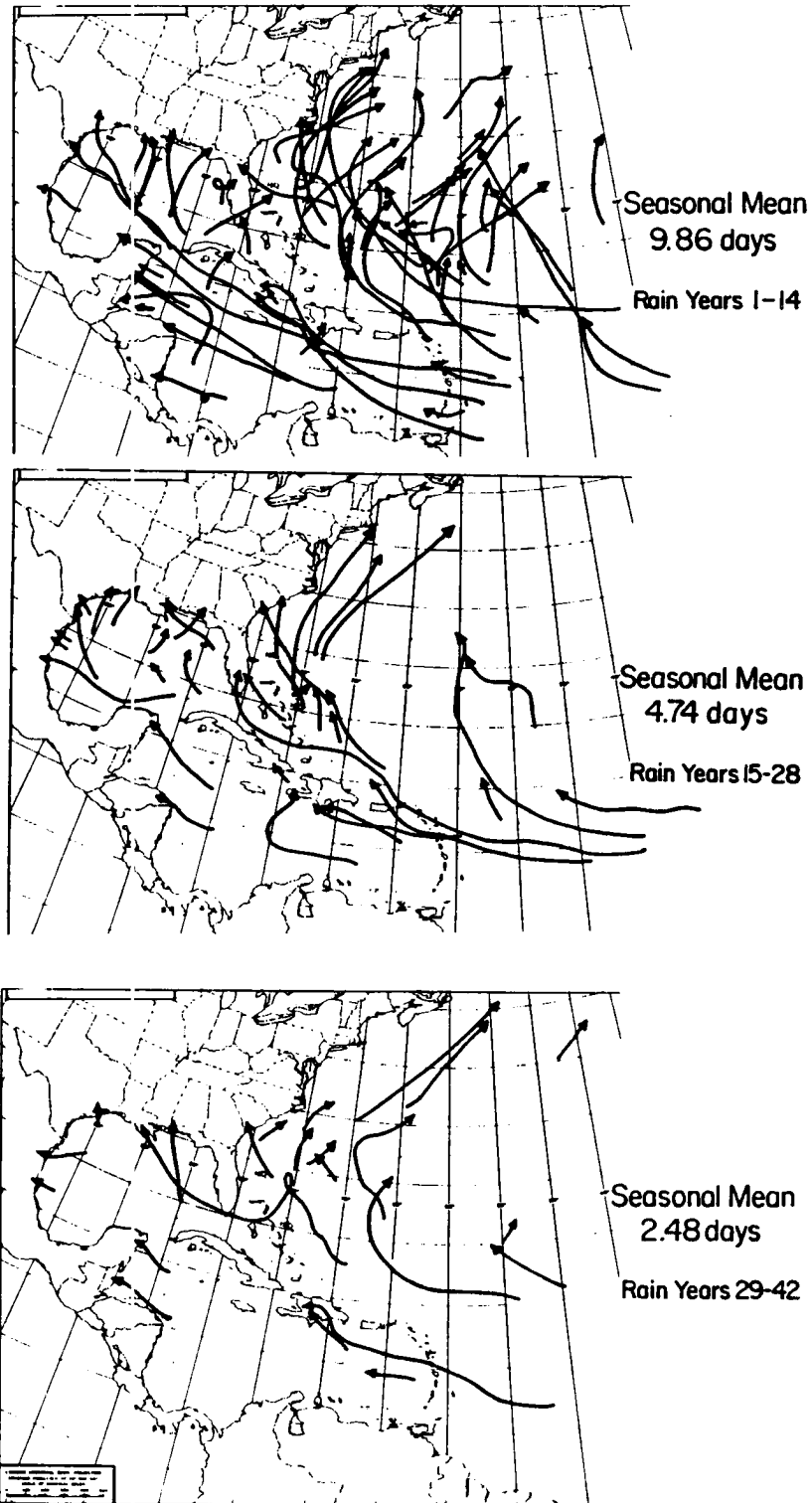


Figure B.7: Intense hurricane tracks in the years following the fourteen wettest (upper panel), the fourteen near normal (middle panel), and the fourteen driest (bottom panel) August to November Gulf of Guinea years from 1948 to 1989.

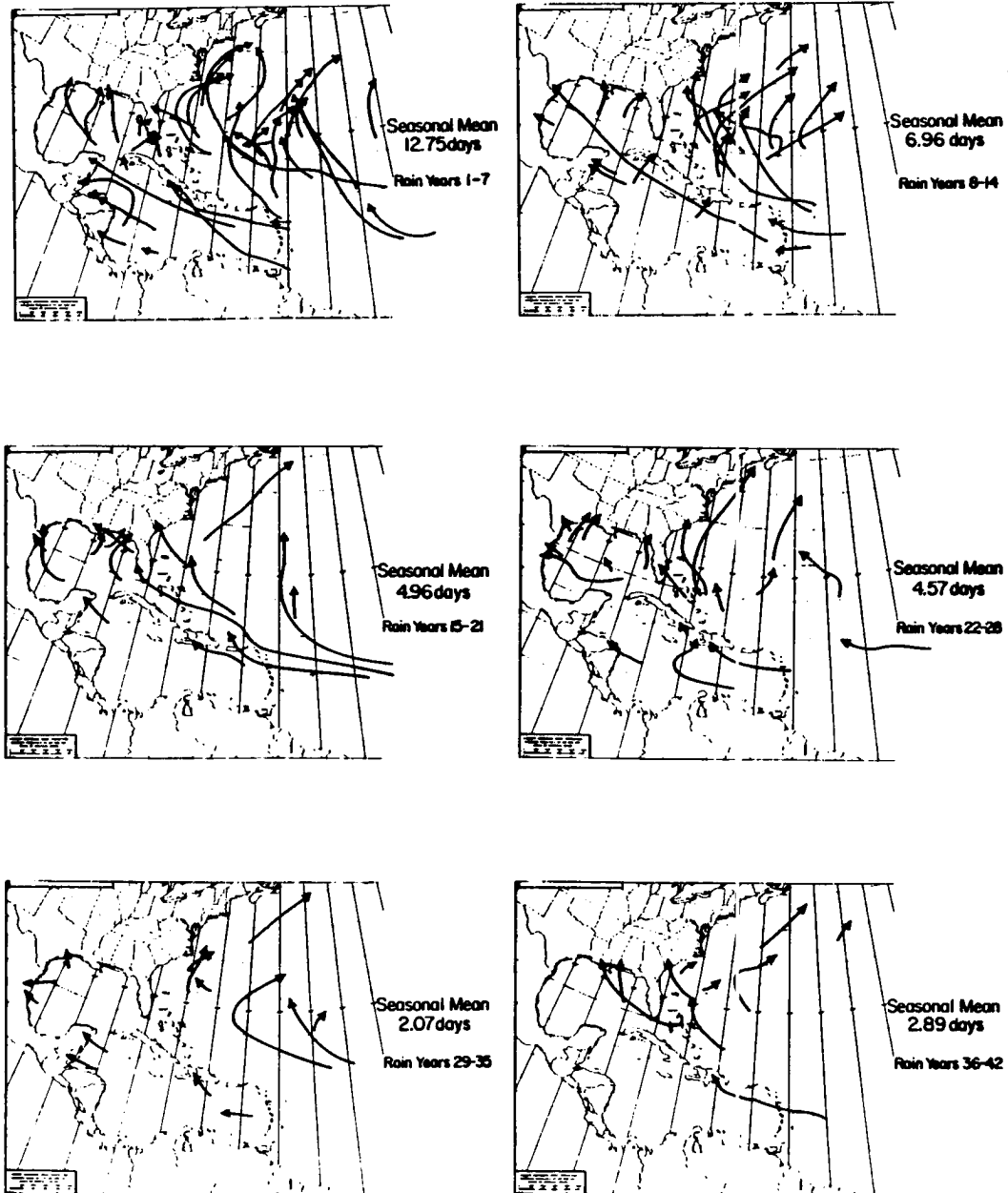


Figure B.8: Intense hurricane tracks for 6 seven year groupings based upon the previous year August to November Gulf of Guinea rainfall amounts. The upper left panel depicts the seven wettest years, the bottom right shows the seven driest years.

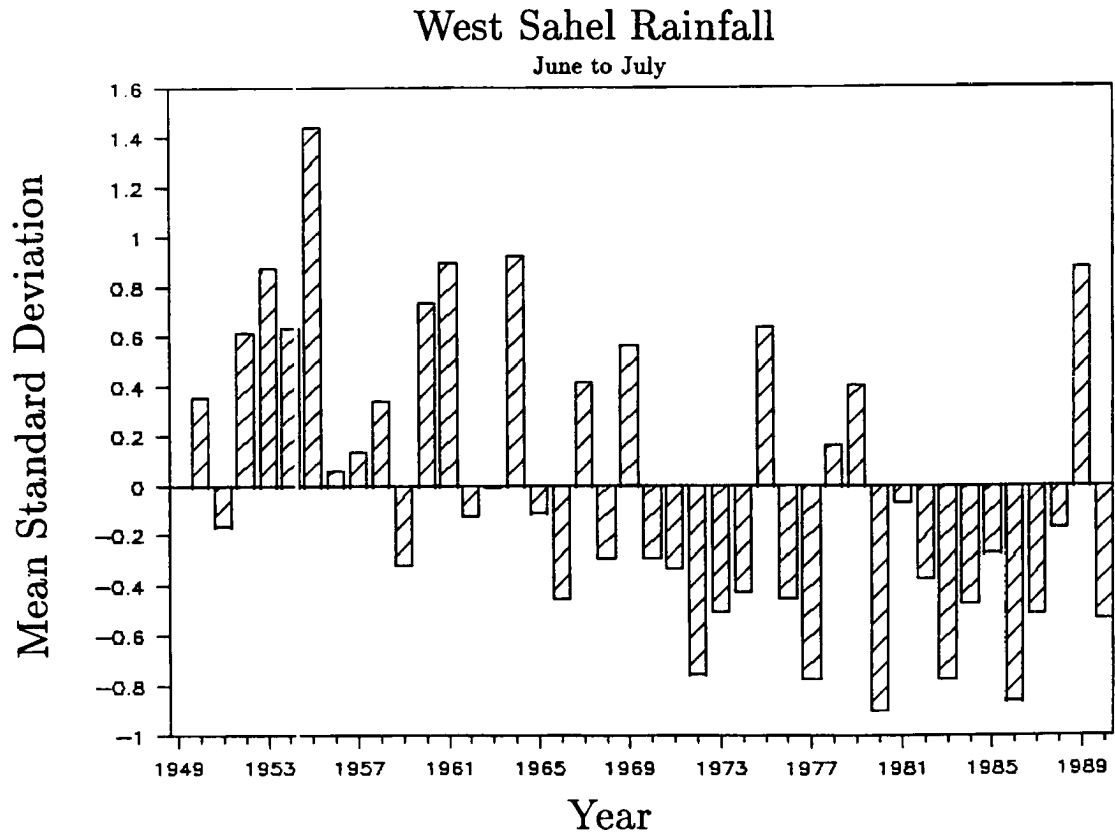


Figure B.9: Mean standard deviation of rainfall for the 38 station June to July Western Sahel Index. Data presented are from 1949 to 1990.

Table B.9: Mean standard deviations and data availability (out of a possible 38 stations per year) for the June to July Western Sahel Index.

Year	Standard Deviation	Number of Stations	Year	Standard Deviation	Number of Stations
1949	0.00	24	1970	-0.29	37
1950	0.35	24	1971	-0.33	37
1951	-0.16	38	1972	-0.75	38
1952	0.61	37	1973	-0.50	38
1953	0.87	38	1974	-0.42	38
1954	0.63	38	1975	0.63	38
1955	1.44	38	1976	-0.45	38
1956	0.06	38	1977	-0.77	37
1957	0.13	38	1978	0.16	38
1958	0.34	37	1979	0.40	38
1959	-0.32	36	1980	-0.90	38
1960	0.73	35	1981	-0.07	37
1961	0.89	38	1982	-0.37	37
1962	-0.12	37	1983	-0.77	37
1963	-0.01	38	1984	-0.47	37
1964	0.92	38	1985	-0.27	37
1965	-0.11	37	1986	-0.86	37
1966	-0.45	38	1987	-0.51	34
1967	0.41	37	1988	-0.17	26
1968	-0.29	37	1989	0.87	25
1969	0.56	37	1990	-0.53	25

Table B.10: Regression equations and correlation coefficients (for both the previous value using 1949 to 1989 data and for the new value using 1949 to 1990) of June to July Western Sahel Index rainfall (x) versus Atlantic basin tropical cyclone parameters and August to September Western Sahel Rainfall (y). (Asterisks refer to significance level: 0.100 for '**', 0.025 for '**' and 0.005 for '***'.)

Tropical Cyclone Parameter	Correlation Coefficient (old value)	Correlation Coefficient (new value)	Regression Equation (new value)	Standard Errors (New Value)
Named Storms	0.44	0.38**	$y = 9.424 + 1.990 x$	± 2.8
Named Storm Days	0.57	0.52***	$y = 47.14 + 18.279 x$	17.2
Hurricanes	0.42	0.39**	$y = 5.85 + 1.487 x$	2.0
Hurricane Days	0.54	0.52***	$y = 23.75 + 12.306 x$	11.6
Int. Hur. (Bias Out)	0.63	0.63***	$y = 2.19 + 1.696 x$	1.2
Int. Hur. Days (Bias Out)	0.65	0.66***	$y = 4.71 + 5.364 x$	3.5
HDP	0.60	0.60***	$y = 73.30 + 50.916 x$	39.5
Aug-Sept W. Sahel Rainfall	0.60	0.62***	$y = 0.00 + 0.760 x$	0.56

Table B.11: June to July Western Sahel Index, ranked by rainfall amounts in terms of mean standard deviations from 1949 to 1990.

Rank	Year	Index Value	Rank	Year	Index Value
1.	1955	1.44	22.	1962	-0.12
2.	1964	0.92	23.	1951	-0.16
3.	1961	0.89	24.	1988	-0.17
4.	1953	0.87	25.	1985	-0.27
5.	1989	0.87	26.	1968	-0.29
6.	1960	0.73	27.	1970	-0.29
7.	1954	0.63	28.	1959	-0.32
8.	1975	0.63	29.	1971	-0.33
9.	1952	0.61	30.	1982	-0.37
10.	1969	0.56	31.	1974	-0.42
11.	1967	0.41	32.	1976	-0.45
12.	1979	0.40	33.	1966	-0.45
13.	1950	0.35	34.	1984	-0.47
14.	1958	0.34	35.	1973	-0.50
15.	1978	0.16	36.	1987	-0.51
16.	1957	0.13	37.	1990	-0.53
17.	1956	0.06	38.	1972	-0.75
18.	1949	0.00	39.	1977	-0.77
19.	1963	-0.01	40.	1983	-0.77
20.	1981	-0.07	41.	1986	-0.86
21.	1965	-0.11	42.	1980	-0.90

Table B.12: Summary of the variability of the same-year tropical cyclone parameters during the ten wettest June to July Western Sahel years and for the ten driest years from 1949 to 1990. Damage is in millions of 1990 dollars. (Asterisks refer to significance level: 0.100 for '*', 0.025 for '**' and 0.005 for '***'.)

Tropical Cyclone Parameter	Wettest Years' Mean	Percent (%) of Normal	Driest Years' Mean	Percent (%) of Normal	Ratio Wet/ Dry
Named Storms	11.0	118	8.2	88	1.34**
Named Storm Days	59.5	127	38.3	82	1.55**
Hurricanes	7.2	124	5.1	88	1.41**
Hurricane Days	32.1	135	16.8	71	1.91**
Intense Hurricanes	4.0	160	1.1	44	3.64***
Intense Hurricane Days	11.0	190	1.8	34	6.11***
HDP	109.2	146	44.9	60	2.43***
US Landfalling:					
Named/Subtrop.	3.8	119	1.9	59	2.00**
Hurricanes	2.3	143	1.0	62	2.30**
Intense Hurricanes	1.1	180	0.2	33	5.50***
' ' Gulf Coast	0.4	118	0.2	59	2.00
' ' East Coast	0.7	241	0.0	0	∞ **
Hurricane Damage	\$3929	223	\$413	23	9.51***
' ' Gulf Coast	1099	124	399	45	2.75
' ' East Coast	2830	324	12	1	235.83***

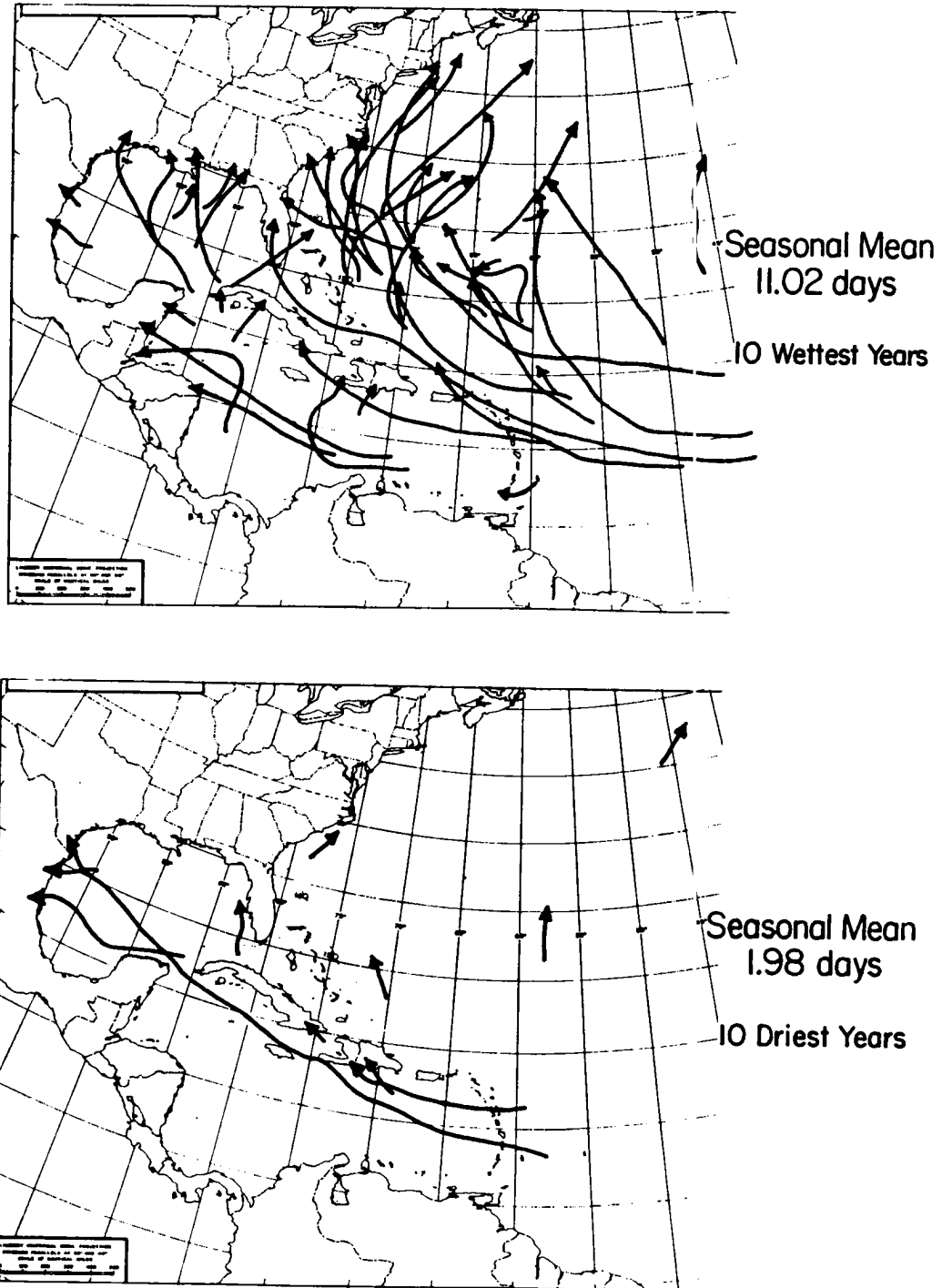


Figure B.10: Intense hurricane tracks during the ten wettest (upper panel) versus the ten driest (bottom panel) June to July Western Sahel rainfall years between 1949 and 1990.

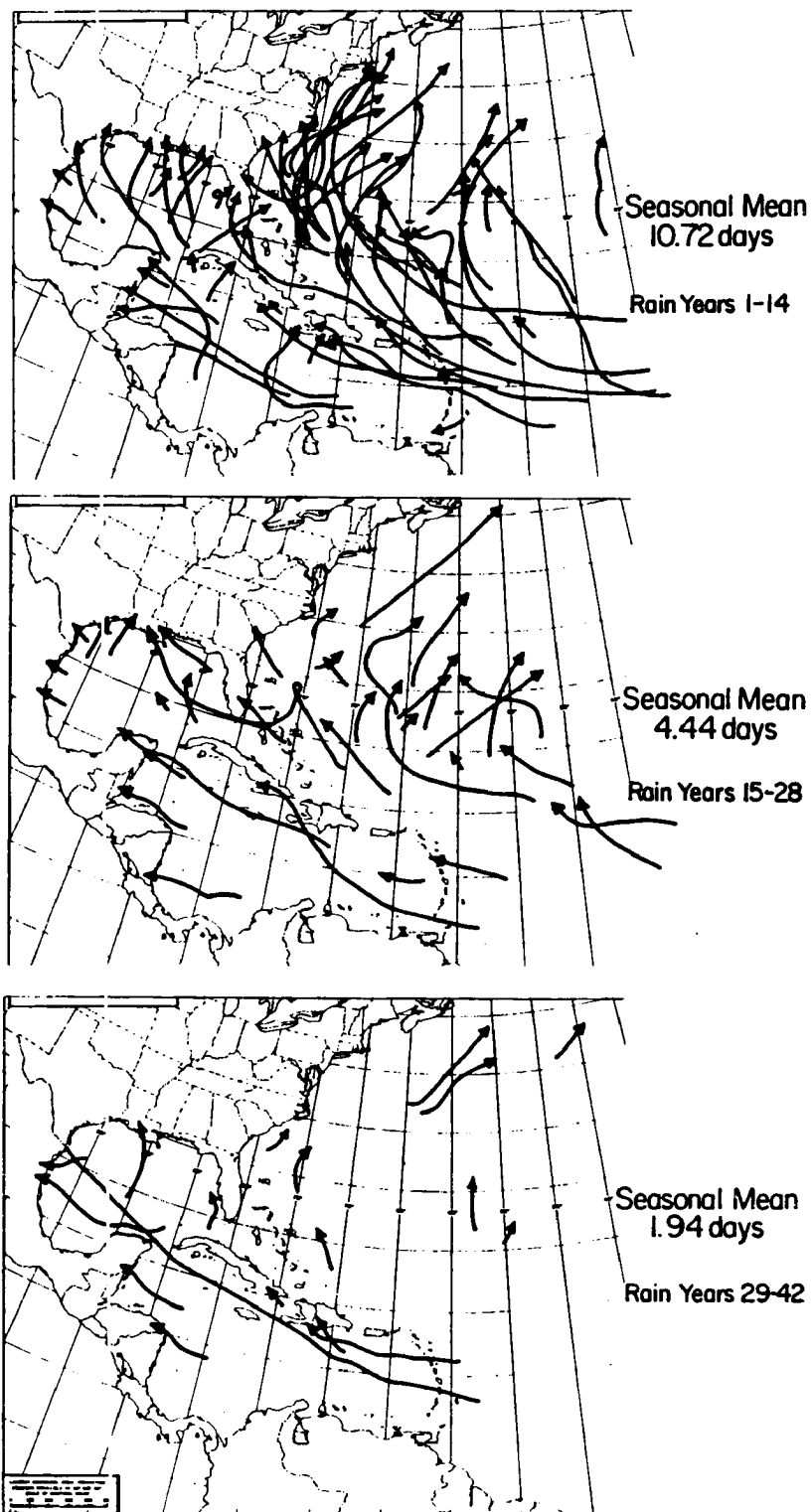


Figure B.11: Intense hurricane tracks during the fourteen wettest (upper panel), the fourteen near normal (middle panel), and the fourteen driest (bottom panel) June to July Western Sahel rainfall years between 1949 and 1990.

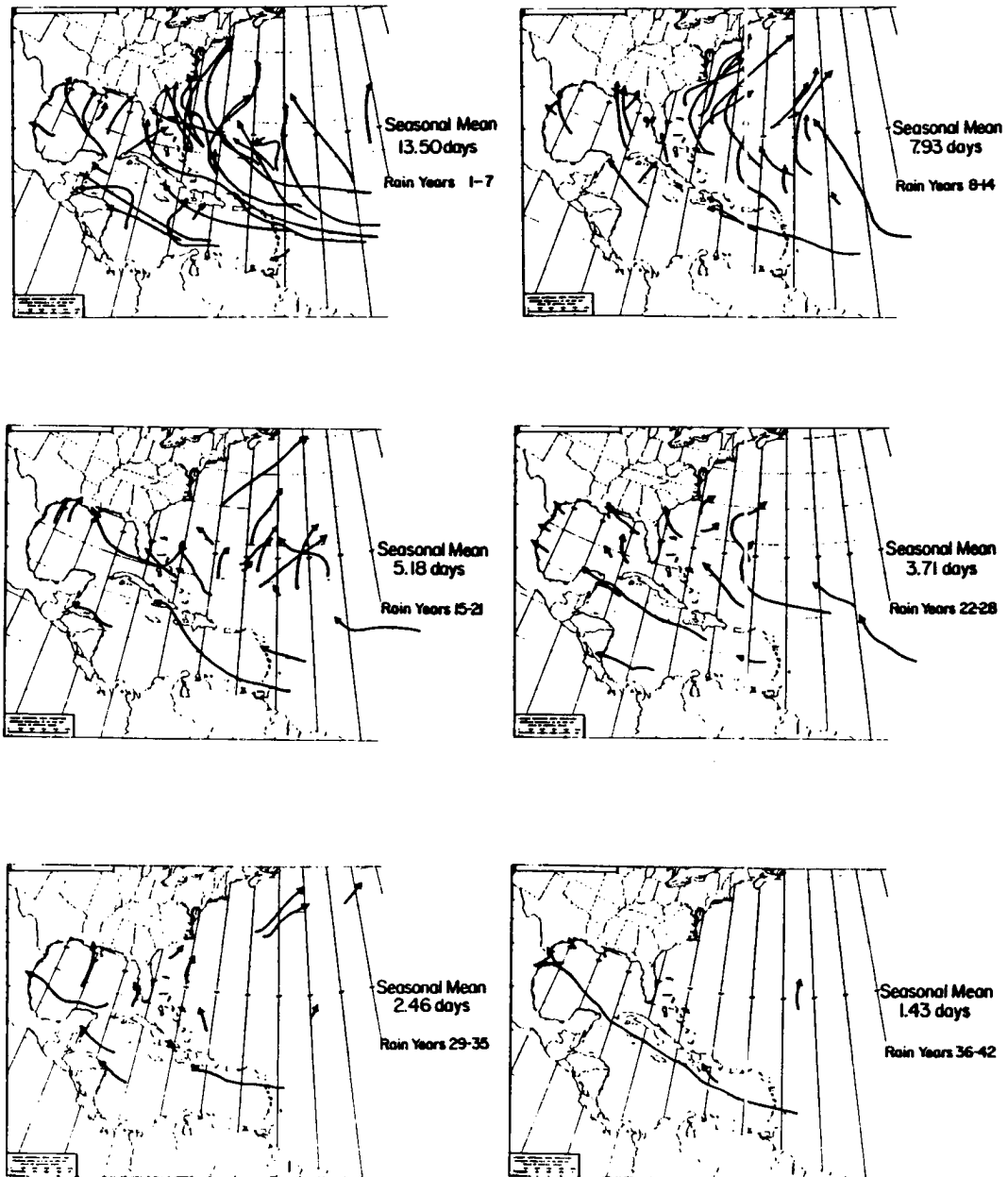


Figure B.12: Intense hurricane tracks for 6 seven year groupings of the June to July Western Sahel rainfall amounts. The upper left panel depicts the seven wettest years; the bottom right shows the seven driest years.

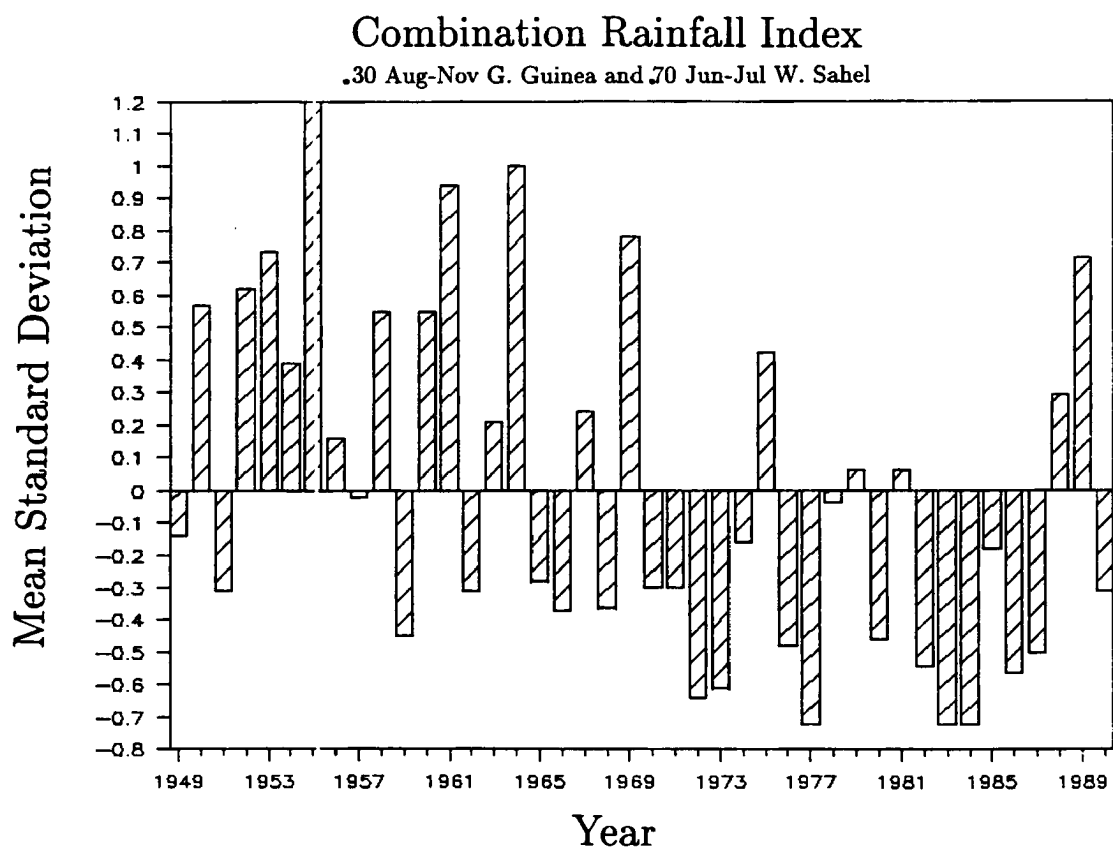


Figure B.13: Mean standard deviation of the Early Season Combination Rainfall Index. Data are presented for 1949 to 1990.

Table B.13: Regression equations and correlation coefficients (for both the previous value using 1949 to 1989 data, and for the new value using 1949 to 1990) of the Early Season Combination Rainfall Index (x) versus Atlantic basin tropical cyclone parameters and August to September Western Sahel Rainfall (y). (Asterisks refer to significance level: 0.100 for '*', 0.025 for '**' and 0.005 for '**').)

Tropical Cyclone Parameter	Correlation Coefficient (old value)	Correlation Coefficient (new value)	Regression Equation (new value)	Standard Errors (New Value)
Named Storms	0.52	0.47***	$y = 9.43 + 2.658 x$	± 2.7
Named Storm Days	0.65	0.62***	$y = 47.20 + 23.275 x$	15.8
Hurricanes	0.54	0.51***	$y = 5.86 + 2.097 x$	1.9
Hurricane Days	0.63	0.62***	$y = 23.79 + 15.793 x$	10.7
Int. Hur. (Bias Out)	0.73	0.74***	$y = 2.19 + 2.138 x$	1.0
Int. Hur. Days (Bias Out)	0.73	0.73***	$y = 4.73 + 6.386 x$	3.2
HDP	0.69	0.69***	$y = 73.43 + 63.691 x$	35.5
Aug-Sept W. Sahel Rainfall	0.70	0.69***	$y = 0.01 + 0.913 x$	0.51

Table B.14: Early Season Combination Rainfall Index ranked from wettest to driest for the 42 years from 1949 to 1990.

Rank	Year	Index Value	Rank	Year	Index Value
1.	1955	1.20	22.	1974	-0.16
2.	1964	1.00	23.	1985	-0.18
3.	1961	0.94	24.	1965	-0.28
4.	1969	0.78	25.	1970	-0.30
5.	1953	0.73	26.	1971	-0.30
6.	1989	0.71	27.	1951	-0.31
7.	1952	0.62	28.	1990	-0.31
8.	1950	0.57	29.	1962	-0.31
9.	1958	0.55	30.	1968	-0.36
10.	1960	0.55	31.	1966	-0.37
11.	1975	0.42	32.	1959	-0.45
12.	1954	0.39	33.	1980	-0.46
13.	1988	0.29	34.	1976	-0.48
14.	1967	0.24	35.	1987	-0.50
15.	1963	0.21	36.	1982	-0.54
16.	1956	0.16	37.	1986	-0.56
17.	1979	0.06	38.	1973	-0.61
18.	1981	0.06	39.	1972	-0.64
19.	1957	-0.02	40.	1977	-0.72
20.	1978	-0.04	41.	1983	-0.72
21.	1949	-0.14	42.	1984	-0.72

Table B.15: Summary of the variability of tropical cyclone parameters during the ten wettest and the ten driest Early Season Combination Rainfall Index years, from 1949 to 1990. Damage is in millions of 1990 dollars. (Asterisks refer to significance level: 0.100 for '*', 0.025 for '**' and 0.005 for '**'.')

Tropical Cyclone Parameter	Wettest Years' Mean	Percent (%) of Normal	Driest Years' Mean	Percent (%) of Normal	Ratio Wet/ Dry	
Named Storms	11.4	123	7.3	78	1.56	***
Named Storm Days	66.2	142	31.4	67	2.11	***
Hurricanes	7.6	131	4.4	76	1.72	***
Hurricane Days	35.9	151	13.0	55	2.76	***
Intense Hurricanes	4.8	192	1.0	40	4.80	***
Intense Hurricane Days	12.6	217	1.0	17	12.60	***
HDP	125.2	167	34.9	47	3.59	***
US Landfalling:						
Named/Subtrop.	3.9	122	2.5	78	1.56	*
Hurricanes	2.3	143	1.0	62	2.30	**
Intense Hurricanes	0.9	148	0.2	33	4.50	**
' ' Gulf Coast	0.4	118	0.2	59	2.00	
' ' East Coast	0.5	172	0.0	0	∞	*
Hurricane Damage	\$3276	186	430	24	7.62	**
' ' Gulf Coast	964	109	394	44	2.45	
' ' East Coast	2312	265	36	4	64.22	**

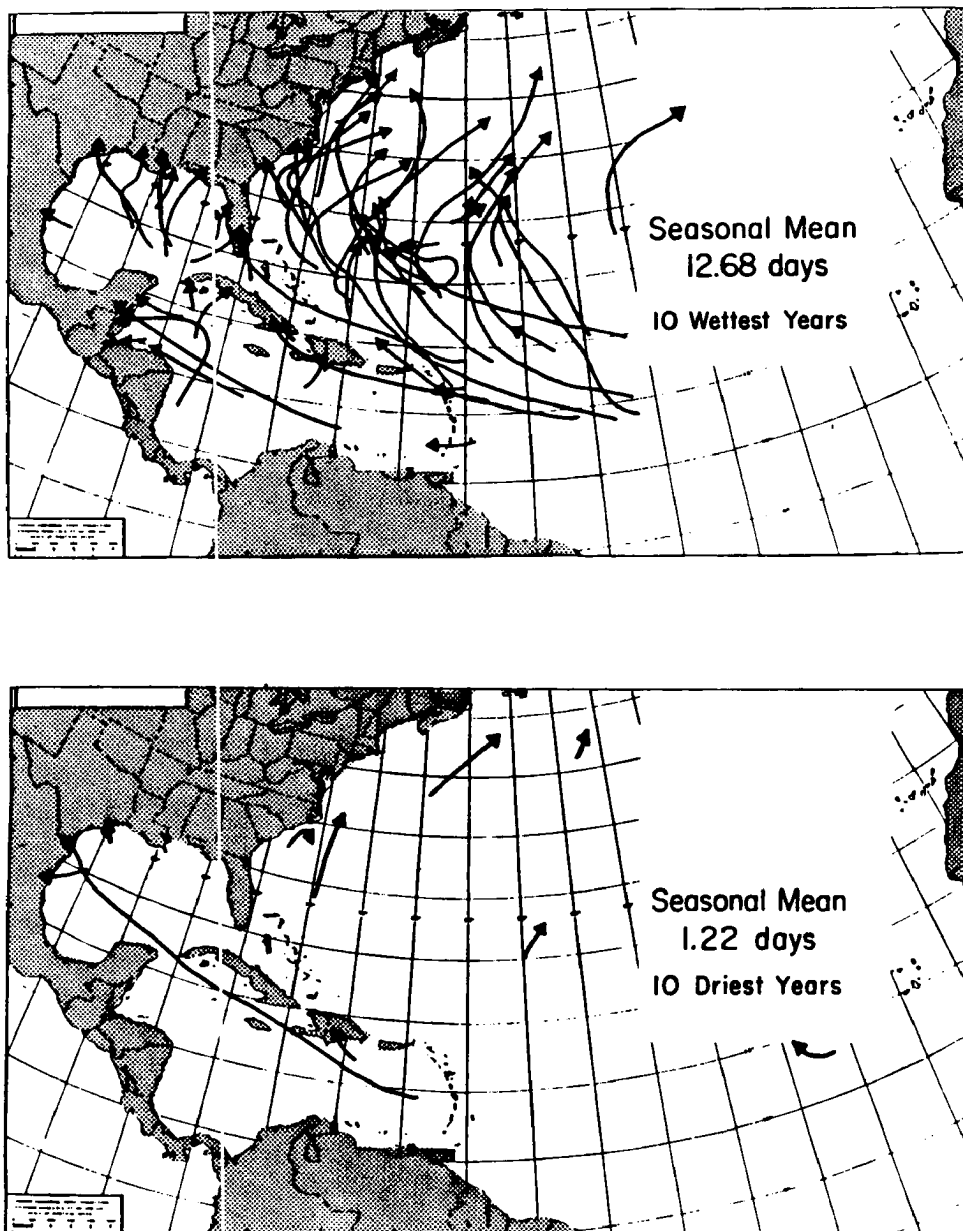


Figure B.14: Intense hurricane tracks during the ten wettest (upper panel) versus the ten driest (bottom panel) Early Season Combination Rainfall Index years between 1949 and 1990.

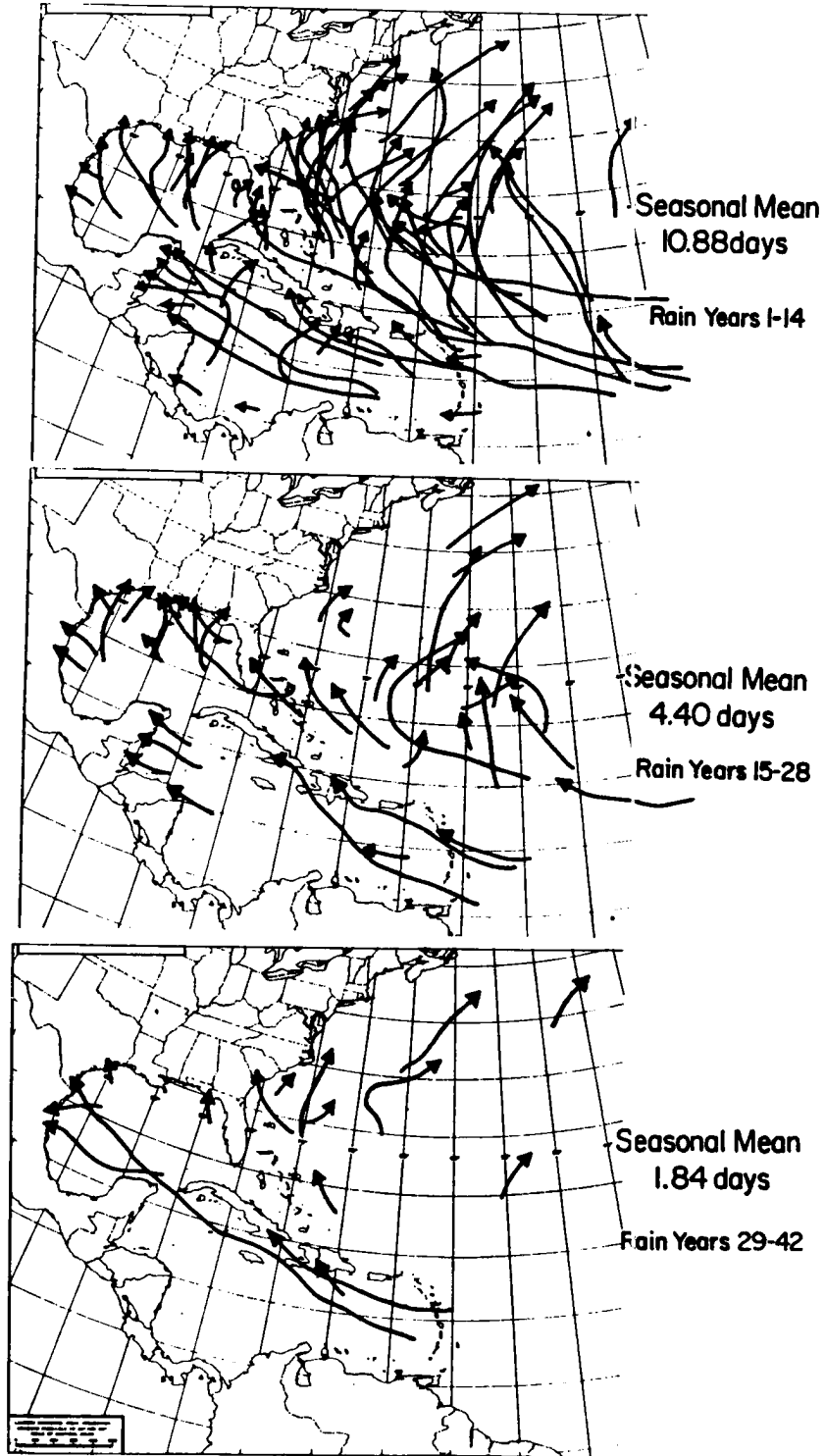


Figure B.15: Intense hurricane tracks during the fourteen wettest (upper panel), the fourteen near normal (middle panel), and the fourteen driest (bottom panel) Early Season Combination Rainfall Index years between 1949 and 1990.

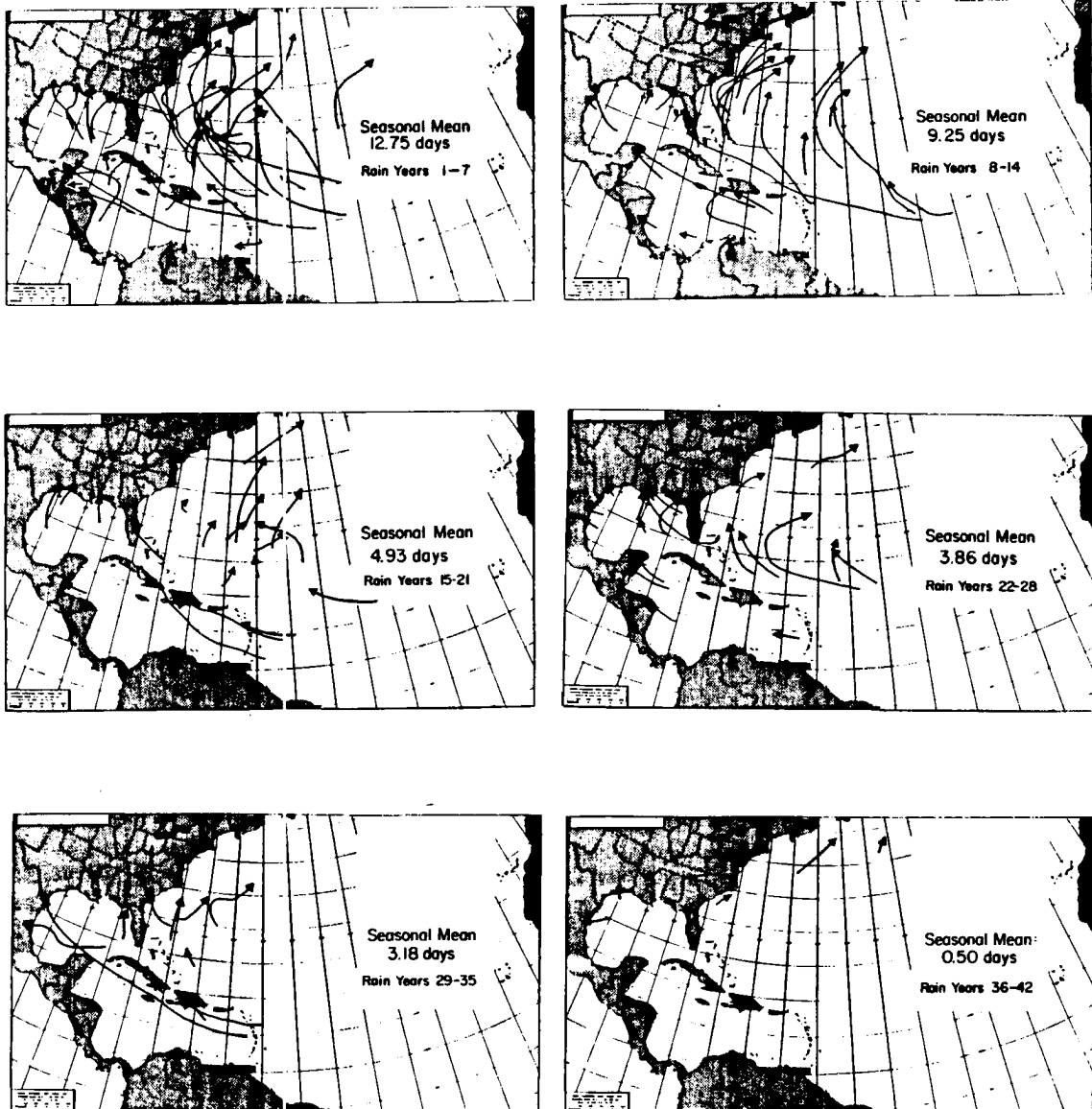


Figure B.16: Intense hurricane tracks for 6 seven year groupings based on the Early Season Combination Index rainfall amounts. The upper left panel depicts the seven wettest years, the bottom right shows the seven driest years.

Table B.16: Mean standard deviations of rainfall and data availability (out of a possible 38 stations per year) for the August to September Western Sahel Index.

Year	Standard Deviation	Number of Stations	Year	Standard Deviation	Number of Stations
1949	-0.13	24	1970	-0.44	37
1950	1.69	24	1971	-0.18	37
1951	0.51	37	1972	-1.08	38
1952	0.94	37	1973	-0.71	38
1953	0.22	38	1974	-0.02	38
1954	0.61	38	1975	0.07	38
1955	1.01	38	1976	-0.48	38
1956	0.49	38	1977	-0.73	37
1957	0.59	38	1978	-0.34	38
1958	1.45	37	1979	-0.91	38
1959	0.27	36	1980	-0.33	37
1960	0.24	36	1981	-0.42	37
1961	0.49	38	1982	-0.88	37
1962	0.29	37	1983	-1.21	37
1963	-0.11	38	1984	-1.21	37
1964	0.60	38	1985	-0.50	37
1965	0.77	37	1986	0.01	37
1966	0.35	38	1987	-0.61	26
1967	0.73	37	1988	0.31	26
1968	-0.81	37	1989	0.18	25
1969	0.39	37	1990	-0.89	26

Table B.17: August to September Western Sahel Index ranked by rainfall amounts in mean standard deviations for 1949 to 1990.

Rank	Year	Index Value	Rank	Year	Index Value
1.	1950	1.69	22.	1986	0.01
2.	1958	1.45	23.	1974	-0.02
3.	1955	1.01	24.	1963	-0.11
4.	1952	0.94	25.	1949	-0.13
5.	1965	0.77	26.	1971	-0.18
6.	1967	0.73	27.	1980	-0.33
7.	1954	0.61	28.	1978	-0.34
8.	1964	0.60	29.	1981	-0.42
9.	1957	0.59	30.	1970	-0.44
10.	1951	0.51	31.	1976	-0.48
11.	1956	0.49	32.	1985	-0.50
12.	1961	0.49	33.	1987	-0.60
13.	1969	0.39	34.	1973	-0.71
14.	1966	0.35	35.	1977	-0.73
15.	1988	0.31	36.	1968	-0.81
16.	1962	0.29	37.	1982	-0.88
17.	1959	0.27	38.	1990	-0.89
18.	1960	0.24	39.	1979	-0.91
19.	1953	0.22	40.	1972	-1.08
20.	1989	0.18	41.	1983	-1.21
21.	1975	0.07	42.	1984	-1.21

Table B.18: Mean standard deviations of rainfall and data availability (out of a possible 38 stations) for individual months of May to October in the Western Sahel.

Year	May		Jun		Jul		Aug		Sep		Oct	
	Index	Stations	Index	Stations	Index	Stations	Index	Stations	Index	Stations	Index	Stations
1949	0.02	24	-0.10	24	0.01	24	0.59	24	-0.98	24	-0.33	24
1950	0.37	24	0.09	24	0.35	24	1.52	24	0.91	24	0.64	24
1951	1.77	38	-0.08	38	-0.11	38	0.29	38	0.53	37	2.97	37
1952	1.37	38	0.02	38	0.72	37	-0.27	37	1.86	37	0.57	37
1953	-0.01	38	0.16	38	0.94	38	0.11	38	0.29	38	0.44	38
1954	-0.17	38	0.39	38	0.53	38	0.98	38	-0.20	38	-0.33	38
1955	0.49	38	0.94	38	1.25	38	0.72	38	0.80	38	-0.09	38
1956	-0.03	38	0.07	38	0.01	38	0.07	38	0.68	38	-0.02	38
1957	-0.13	38	0.37	38	-0.08	38	0.38	38	0.56	38	1.13	38
1958	-0.13	37	0.70	37	-0.00	37	2.18	37	-0.25	37	-0.07	38
1959	0.33	37	-0.03	37	-0.32	36	0.44	36	-0.09	36	-0.60	36
1960	0.18	35	0.20	35	0.79	36	-0.02	36	0.41	36	-0.43	35
1961	-0.21	38	0.41	38	0.83	38	0.23	38	0.52	38	-0.60	38
1962	-0.13	37	0.07	37	-0.16	37	0.82	37	-0.51	37	0.29	37
1963	-0.36	38	-0.29	38	0.18	38	-0.01	38	-0.14	38	1.34	38
1964	0.62	38	0.41	38	0.79	38	0.59	38	0.26	38	-0.58	38
1965	-0.30	37	0.35	37	-0.30	37	0.44	37	0.75	37	-0.04	37
1966	-0.09	38	0.59	38	-0.86	38	-0.29	38	0.99	38	1.91	38
1967	-0.17	38	0.43	38	0.26	37	0.26	38	0.89	37	0.34	37
1968	-0.29	37	-0.26	37	-0.21	37	-0.85	37	-0.27	37	-0.43	37
1969	-0.26	37	-0.55	37	0.94	37	0.51	37	0.06	37	1.01	37
1970	0.09	37	-0.41	37	-0.11	37	-0.27	37	-0.40	37	-0.67	37
1971	-0.39	37	-0.36	37	-0.20	37	0.09	37	-0.40	37	-0.67	37
1972	-0.19	38	-0.09	38	-0.80	38	-0.80	38	-0.81	38	-0.16	38
1973	-0.11	38	-0.21	38	-0.50	38	-0.16	38	-0.94	38	-0.64	38
1974	-0.42	38	-0.69	38	-0.15	38	0.27	38	-0.37	38	-0.47	38
1975	-0.16	38	-0.57	38	1.05	38	-0.16	38	0.33	38	-0.41	38
1976	0.40	38	-0.44	38	-0.28	38	-0.48	38	-0.19	38	0.48	38
1977	-0.26	37	-0.57	37	-0.57	37	-0.97	37	0.00	37	-0.55	37
1978	-0.02	38	-0.19	38	0.23	38	-0.49	38	0.04	38	0.06	37
1979	0.46	38	1.18	38	-0.15	38	-0.62	38	-0.76	38	-0.04	38
1980	-0.40	38	-0.58	38	-0.76	38	-0.26	37	-0.22	37	-0.64	38
1981	0.35	37	-0.26	37	0.12	37	-0.17	37	-0.49	37	-0.38	37
1982	-0.09	37	-0.49	37	-0.21	37	-0.44	37	-0.94	38	-0.10	37
1983	-0.17	37	-0.04	37	-0.85	37	-0.95	37	-0.85	37	-0.76	37
1984	0.06	37	0.44	37	-0.85	37	-1.14	37	-0.59	37	-0.41	37
1985	-0.60	37	-0.38	37	-0.08	37	-0.42	37	-0.32	37	-0.72	37
1986	-0.03	37	-0.51	37	-0.70	37	-0.49	37	0.63	37	-0.37	32
1987	-0.41	34	-0.18	35	-0.53	34	-0.60	33	-0.27	26	0.02	23
1988	-0.34	25	-0.12	26	-0.06	26	0.21	26	0.18	26	-0.65	26
1989	-0.62	25	1.26	26	0.12	25	0.54	25	-0.48	26	-0.11	26
1990	-0.43	26	-0.52	26	-0.35	25	-0.71	26	-0.55	26	-0.23	24

PROJECT REPORTS FROM W. M. GRAY'S FEDERALLY SUPPORTED RESEARCH
(SINCE 1967)

CSU Dept. of
Atmos. Sci.

<u>Report No.</u>	<u>Report Title, Author, Date, Agency Support</u>
104	The Mutual Variation of Wind, Shear and Baroclinicity in the Cumulus Convective Atmosphere of the Hurricane (69 pp.). W. M. Gray. February 1967. NSF Support.
114	Global View of the Origin of Tropical Disturbances and Storms (105 pp.). W. M. Gray. October 1967. NSF Support.
116	A Statistical Study of the Frictional Wind Veering in the Planetary Boundary Layer (57 pp.). B. Mendenhall. December 1967. NSF and ESSA Support.
124	Investigation of the Importance of Cumulus Convection and ventilation in Early Tropical Storm Development (88 pp.). R. Lopez. June 1968. ESSA Satellite Lab. Support.
Unnumbered	Role of Angular Momentum Transports in Tropical Storm Dissipation over Tropical Oceans (46 pp.). R. F. Wachtmann. December 1968. NSF and ESSA Support.
Unnumbered	Monthly Climatological Wind Fields Associated with Tropical Storm Genesis in the West Indies (34 pp.). J. W. Sartor. December 1968. NSF Support.
140	Characteristics of the Tornado Environment as Deduced from Proximity Soundings (55 pp.). T. G. Wills. June 1969. NOAA and NSF Support.
161	Statistical Analysis of Trade Wind Cloud Clusters in the Western North Pacific (80 pp.). K. Williams. June 1970. ESSA Satellite Lab. Support.
—	A Climatology of Tropical Cyclones and Disturbances of the Western Pacific with a Suggested Theory for Their Genesis/Maintenance (225 pp.). W. M. Gray. NAVWEARSCHFAC Tech. Paper No. 19-70. November 1970. (Available from US Navy, Monterey, CA). US Navy Support.
179	A diagnostic Study of the Planetary Boundary Layer over the Oceans (95 pp.). W. M. Gray. February 1972. Navy and NSF Support.
182	The Structure and Dynamics of the Hurricane's Inner Core Area (105 pp.). D. J. Shea. April 1972. NOAA and NSF Support.
188	Cumulus Convection and Larger-scale Circulations, Part I: A Parametric Model of Cumulus Convection (100 pp.). R. E. Lopez. June 1972. NSF Support.
189	Cumulus Convection and Larger-scale Circulations, Part II: Cumulus and Meso-scale Interactions (63 pp.). R. E. Lopez. June 1972. NSF Support.
190	Cumulus Convection and Larger-scale Circulations, Part III: Broad-scale and Meso-scale Considerations (80 pp.). W. M. Gray. July 1972. NOAA-NESS Support.
195	Characteristics of Carbon Black Dust as a Tropospheric Heat Source for Weather Modification (55 pp.). W. M. Frank. January 1973. NSF Support.
196	Feasibility of Beneficial Hurricane Modification by Carbon Black Seeding (130 pp.). W. M. Gray. April 1973. NOAA Support.
199	Variability of Planetary Boundary Layer Winds (157 pp.). L. R. Hoxit. May 1973. NSF Support.
200	Hurricane Spawned Tornadoes (57 pp.). D. J. Novlan. May 1973. NOAA and NSF Support.

CSU Dept. of
Atmos. Sci.

<u>Report No.</u>	<u>Report Title, Author, Date, Agency Support</u>
212	A Study of Tornado Proximity Data and an Observationally Derived Model of Tornado Genesis (101 pp.). R. Maddox. November 1973. NOAA Support.
219	Analysis of Satellite Observed Tropical Cloud Clusters (91 pp.). E. Ruprecht and W. M. Gray. May 1974. NOAA/NESS Support.
224	Precipitation Characteristics in the Northeast Brazil Dry Region (56 pp.). R. P. L. Ramos. May 1974. NSF Support.
225	Weather Modification through Carbon Dust Absorption of Solar Energy (190 pp.). W. M. Gray, W. M. Frank, M. L. Corrin, and C. A. Stokes. July 1974.
234	Tropical Cyclone Genesis (121 pp.). W. M. Gray. March 1975. NSF Support.
—	Tropical Cyclone Genesis in the Western North Pacific (66 pp.). W. M. Gray. March 1975. US Navy Environmental Prediction Research Facility Report. Tech. Paper No. 16-75. (Available from the US Navy, Monterey, CA). Navy Support.
241	Tropical Cyclone Motion and Surrounding Parameter Relationships (105 pp.). J. E. George. December 1975. NOAA Support.
243	Diurnal Variation of Oceanic Deep Cumulus Convection. Paper I: Observational Evidence, Paper II: Physical Hypothesis (106 pp.). R. W. Jacobson, Jr. and W. M. Gray. February 1976. NOAA-NESS Support.
257	Data Summary of NOAA's Hurricanes Inner-Core Radial Leg Flight Penetrations 1957-1967, and 1969 (245 pp.). W. M. Gray and D. J. Shea. October 1976. NSF and NOAA Support.
258	The Structure and Energetics of the Tropical Cyclone (180 pp.). W. M. Frank. October 1976. NOAA-NHEML, NOAA-NESS and NSF Support.
259	Typhoon Genesis and Pre-typhoon Cloud Clusters (79 pp.). R. M. Zehr. November 1976. NSF Support.
Unnumbered	Severe Thunderstorm Wind Gusts (81 pp.). G. W. Walters. December 1976. NSF Support.
262	Diurnal Variation of the Tropospheric Energy Budget (141 pp.). G. S. Foltz. November 1976. NSF Support.
274	Comparison of Developing and Non-developing Tropical Disturbances (81 pp.). S. L. Erickson. July 1977. US Army Support.
—	Tropical Cyclone Research by Data Compositing (79 pp.). W. M. Gray and W. M. Frank. July 1977. US Navy Environmental Prediction Research Facility Report. Tech. Paper No. 77-01. (Available from the US Navy, Monterey, CA). Navy Support.
277	Tropical Cyclone Cloud and Intensity Relationships (154 pp.). C. P. Arnold. November 1977. US Army and NHEML Support.
297	Diagnostic Analyses of the GATE A/B-scale Area at Individual Time Periods (102 pp.). W. M. Frank. November 1978. NSF Support.
298	Diurnal Variability in the GATE Region (80 pp.). J. M. Dewart. November 1978. NSF Support.
299	Mass Divergence in Tropical Weather Systems, Paper I: Diurnal Variation; Paper II: Large-scale Controls on Convection (109 pp.). J. L. McBride and W. M. Gray. November 1978. NOAA-NHEML Support.

CSU Dept. of
Atmos. Sci.

<u>Report No.</u>	<u>Report Title, Author, Date, Agency Support</u>
—	New Results of Tropical Cyclone Research from Observational Analysis (108 pp.). W. M. Gray and W. M. Frank. June 1978. US Navy Environmental Prediction Research Facility Report. Tech. Paper No. 78-01. (Available from the US Navy, Monterey, CA). Navy Support.
305	Convection Induced Temperature Change in GATE (128 pp.). P. G. Grube. February 1979. NSF Support.
308	Observational Analysis of Tropical Cyclone Formation (230 pp.). J. L. McBride. April 1979. NOAA-NHEML, NSF and NEPRF Support.
—	Tropical Cyclone Origin, Movement and Intensity Characteristics Based on Data Compositing Techniques (124 pp.). W. M. Gray. August 1979. US Navy Environmental Prediction Research Facility Report. Tech. Paper No. CR-79-06. (Available from the US Navy, Monterey, CA). Navy Support.
—	Further Analysis of Tropical Cyclone Characteristics from Rawinsonde Compositing Techniques (129 pp.). W. M. Gray. March 1981. US Navy Environmental Prediction Research Facility Report. Tech. Paper No. CR-81-02. (Available from the US Navy, Monterey, CA). Navy Support.
333	Tropical Cyclone Intensity Change—A Quantitative Forecasting Scheme. K. M. Dropco. May 1981. NOAA Support.
—	Recent Advances in Tropical Cyclone Research from Rawinsonde Composite Analysis (407 pp.). WMO Publication. W. M. Gray. 1981.
340	The Role of the General Circulation in Tropical Cyclone Genesis (230 pp.). G. Love. April 1982. NSF Support.
341	Cumulus Momentum Transports in Tropical Cyclones (78 pp.). C. S. Lee. May 1982. ONR Support.
343	Tropical Cyclone Movement and Surrounding Flow Relationships (68 pp.). J. C. L. Chan and W. M. Gray. May 1982. ONR Support.
346	Environmental Circulations Associated with Tropical Cyclones Experiencing Fast, Slow and Looping Motions (273 pp.). J. Xu and W. M. Gray. May 1982. NOAA and NSF Support.
348	Tropical Cyclone Motion: Environmental Interaction Plus a Beta Effect (47 pp.). G. J. Holland. May 1982. ONR Support.
—	Tropical Cyclone and Related Meteorological Data Sets Available at CSU and Their Utilization (186 pp.). W. M. Gray, E. Buzzell, G. Burton and Other Project Personnel. February 1982. NSF, ONR, NOAA, and NEPRF Support.
352	A Comparison of Large and Small Tropical Cyclones (75 pp.). R. T. Merrill. July 1982. NOAA and NSF Support.
358	On the Physical Processes Responsible for Tropical Cyclone Motion (200 pp.). Johnny C. L. Chan. November 1982. NSF, NOAA/NHRL and NEPRF Support.
363	Tropical Cyclones in the Australian/Southwest Pacific Region (264 pp.). Greg J. Holland. March 1983. NSF, NOAA/NHRL and Australian Government Support.
370	Atlantic Seasonal Hurricane Frequency, Part I: El Nino and 30 mb QBO Influences; Part II: Forecasting Its Variability (105 pp.). W. M. Gray. July 1983. NSF Support.

CSU Dept. of
Atmos. Sci.

<u>Report No.</u>	<u>Report Title, Author, Date, Agency Support</u>
379	A Statistical Method for One- to Three-Day Tropical Cyclone Track Prediction (201 pp). Clifford R. Matsumoto. December, 1984. NSF/NOAA and NEPRF support.
—	Varying Structure and Intensity Change Characteristics of Four Western North Pacific Tropical Cyclones. (100 pp.). Cecilia A. Askue and W. M. Gray. October 1984. US Navy Environmental Prediction Research Facility Report No. CR 84-08. (Available from the US Navy, Monterey, CA). Navy Support.
—	Characteristics of North Indian Ocean Tropical Cyclone Activity. (108 pp.). Cheng-Shang Lee and W. M. Gray. December 1984. US Navy Environmental Prediction Research Facility Report No. CR 84-11. (Available from the US Navy, Monterey, CA). Navy Support.
391	Typhoon Structural Variability. (77 pp.). Candis L. Weatherford. October, 1985. NSF/NOAA Support.
392	Global View of the Upper Level Outflow Patterns Associated with Tropical Cyclone Intensity Change During FGGE. (126 pp.). L. Chen and W. Gray. October, 1985. NASA support.
394	Environmental Influences on Hurricane Intensification. (156 pp.). Robert T. Merrill. December, 1985. NSF/NOAA Support.
403	An Observational Study of Tropical Cloud Cluster Evolution and Cyclogenesis in the Western North Pacific. (250 pp.). Cheng-Shang Lee. September, 1986. NSF/NOAA support.
—	Factors Influencing Tropical Cyclone Genesis as Determined from Aircraft Investigative Flights into Developing and Non-Developing Tropical Disturbances in the Western North Pacific. Michael Middlebrooke. October, 1986 (70 pp.). NSF/NOAA support.
—	Recent Colorado State University Tropical Cyclone Research of Interest to Forecasters. (115 pp.). William M. Gray. June, 1987. US Navy Environmental Prediction Research Facility Contractor Report CR 87-10. Available from US Navy, Monterey, CA. Navy support.
428	Tropical Cyclone Observation and Forecasting With and With and Without Aircraft Reconnaissance. (105 pp.) Joel D. Martin. May, 1988. USAF, NWS, ONR support.
429	Investigation of Tropical Cyclone Genesis and Development Using Low-level Aircraft Flight Data. (94 pp.) Michael G. Middlebrooke. May, 1988. USAF, NSF support.
436	Environmental and convective influence on tropical cyclone development vs. non-development. (105 pp.) Patrick A. Lunney. December, 1988.
446	The structural evolution of typhoons. (198 pp.). Candis Weatherford. September, 1989. NSF/NOAA and ONR Support
457	Relationships between tropical cyclone deep convection and the radial extent of damaging winds. (109 pp.) Daniel N. Shoemaker. October, 1989. AFGL Support.
468	Associations between West Pacific equatorial zonal winds and East Pacific SST anomalies. (103 pp.) Christopher C. Collimore. May, 1990. NSF Support.

CSU Dept. of
Atmos. Sci.

Report No. Report Title, Author, Date, Agency Support

480 An observational analysis of tropical cyclone recurvature. (124 pp.).

Stephen J. Hodanish. May, 1991. ONR Support.

— West African monsoonal rainfall and intense hurricane associations.

Christopher W. Landsea. October, 1991. NSF Support.